

NATIONAL INSTITUTE FOR FUSION SCIENCE

Intensity Ratios of Emission Lines from 0V Ions for Temperature and Density Diagnostics

T. Kato, J. Lang and K.E. Berrington

(Received — Sep. 8, 1989)

NIFS-DATA-2

Mar. 1990

RESEARCH REPORT NIFS-DATA Series

This report was prepared as a preprint of compilation of evaluated atomic, molecular, plasma-wall interaction, or nuclear data for fusion research, performed as a collaboration research of the Data and Planning Center, the National Institute for Fusion Science (NIFS) of Japan. This document is intended for future publication in a journal or data book after some rearrangements of its contents.

Inquiries about copyright and reproduction should be addressed to the Research Information Center, National Institute for Fusion Science, Nagoya 464-01, Japan.

NAGOYA, JAPAN

**Intensity Ratios of Emission Lines from 0V Ions
for Temperature and Density Diagnostics**

T. Kato, J. Lang and K.E. Berrington

(Received — Sep. 8, 1989)

NIFS-DATA-2

Mar. 1990

Intensity Ratios of Emission Lines from OV Ions
for Temperature and Density Diagnostics

T. Kato, J. Lang¹⁾ and K.E. Berrington²⁾

National Institute for Fusion Science, Nagoya 464-01, Japan

Permanent address

- 1) Space Science Department, Rutherford Appleton Laboratory,
Chilton, Didcot, Oxon OX11 0QX, U. K.
- 2) Department of Applied Mathematics and Theoretical Physics,
The Queen's University, Belfast, BT7 1NN, Northern Ireland,
U.K.

Abstract

Intensity ratios of emission lines from OV ions are calculated for use in temperature and density diagnostics. The dependence on temperature and density of the intensity ratios is shown in graphs. The excitation rate coefficients among $n = 2$ and $n = 3$ levels are fitted to an analytical formula and the fitting parameters are tabulated. The rate coefficients are shown graphically.

Keywords

OV ion, line emission, intensity ratio, temperature and density diagnostics, excitation rate coefficients, inner sub-shell ionization

CONTENT

Introduction

Atomic Data

Energy Levels

Transition Probabilities

Excitation Rate Coefficients by Electron Impact

Ionization and Recombination

Population Density

Line Intensity Ratios

Conclusions

Explanation of Table

Explanation of Figures

Table I. Fit Parameters for the Recommended Rate Coefficients

Figures

I. Line Intensity Ratios vs. Temperature

II. Line Intensity Ratios vs. Density

III. Recommended Excitation Rate Coefficients

1. Introduction

Spectral line emissions of OV ions have been measured from the solar transition region^{1,2} and from laboratory plasmas such as from tokamaks.^{3,4,5,6} Theoretical calculations have been done to interpret line intensities.^{7,8,9} We present here the calculation of the intensity ratios of emission lines using new data for electron impact excitation calculated by Berrington and Kingston¹⁰ by the R-matrix method including 26 states($2s^2$, $2 \times 2s2p$, $3 \times 2p^2$, $2 \times 2s3s$, $2 \times 2s3p$, $2 \times 2s3d$, $2 \times 2p3s$, $6 \times 2p3p$, $6 \times 2p3d$). We include in our calculation the ionization and recombination processes from/to excited levels which are important in a transient plasma.

2. Atomic Data

i) Energy Levels

The levels of the $2s^2$, $2s2p$, $2p^2$, $2s3s$, $2s3p$ and $2s3d$ configurations for OV¹¹(20 levels) and the n=2 levels for OIV¹² (6 states) and OVI¹³ (2 states) ions are considered in our model. They are listed in Table 1. For OIV and OV ions the fine

structure levels are combined to one state for the calculation of the population densities as indicated in Table 1 by arabic numerals. For OV Fig. 1 shows the relevant part of the energy level diagram.

i i) Transition Probabilities

The data for transition probabilities among $n = 2$ and $n = 3$ levels are taken from ref. 14 for OV. For OIV and OVI ions, the data from ref. 15 and from ref. 16, respectively, are used.

i ii) Excitation rate coefficients by electron impact

Effective collision strengths γ have been calculated using the R-matrix method including 26 states by Berrington and Kingston¹⁰ in the electron temperature range from $3 \times 10^4 \text{ K} < T_e < 1.3 \times 10^6 \text{ K}$. These data are fitted to an empirical formula for collision strength Ω as given in refs. 17 and 18 as follows,

$$\Omega = a_1 + a_2/X + a_3/X^2 + a_4/X^3 + a_5 \ln X , \quad (1)$$

where X is the energy of the incident electron in units of transition energy, $X = E/\Delta E$. The effective collision strength is defined as

$$\gamma = y e^y \int_1^\infty \Omega e^{-yX} dX , \quad (2)$$

and can be written

$$\gamma = y \{ (a_1/y + a_3) + a_4(1-y)/2 + e^y E_1(y) (a_2 - a_3 y + a_4 y^2/2 + a_5/y) \} , \quad (3)$$

where

$$E_1(y) = \int_y^\infty e^{-t}/t dt , \quad (4)$$

and $y = \Delta E/T_e$. The parameter a_5 in eq.(1) is derived from the Bethe limit as $a_5 = 4w_i f_{ij}/\Delta E$ for the allowed transitions where w_i is the statistical weight of the lower level i , f_{ij} is the absorption oscillator strength from level i to j and ΔE the excitation energy in Rydbergs units.

For the fine structure transitions where the transition energy is very small compared to the electron temperature, the effective collision strengths are fitted by the following formula

$$\log \gamma = b_1 + b_2/TL + b_3/TL^2 + b_4/TL^3 , \quad (5)$$

where $TL = \log T(\text{K})$ and T indicates the electron temperature in degrees Kelvin.

The excitation rate coefficients can then be calculated using the formula (with T_e in eV units),

$$R = 8.01 \times 10^{-8} e^{-y} \gamma / (w_i T_e^{1/2}) \quad \text{cm}^3 \text{s}^{-1} . \quad (6)$$

The derived parameters a_i and b_i ($i = 1 - 5$) are listed in Table I and the calculated rate coefficients are given as in Fig.III. The evaluated values in ref.17 are plotted by dashed lines for comparison. The excitation rate coefficients for the $2s^2 - 2p^2$ (3P , 1D and 1S) transitions differ from those in ref. 17 by 30 - 100 %. The excitation rate coefficient for $2s^2$ 1S - $2s3p$ 1P is larger by 40 % at 20 eV compared to that calculated by Mann(as quated in Ref.17) using the Distorted Wave method, but agrees well at temperatures higher than 80 eV. For the $2s^2$ 1S - $2s3s$ 1S and $2s3d$ 1D transitions, the new data are smaller by about 50 % and 30 %, respectively, as shown in Fig. III.

The validity range of the given rate coefficients is 3×10^4 K $< T_e < 1.3 \times 10^6$ K. It is risky to simple extend the formulas outside of their validity range. Extrapolation is permissible to some extent, but its accuracy depends on the transition. Since the parameters are derived to fit the effective collision strength γ , the collision strength Ω , calculated from the fit parameters, has no real meaning.

For OIV and OVI ions, the data recommended in ref.17 are used.

iv) Ionization and recombination

The ionization process from ground and metastable levels becomes important when the electron temperature T_e is higher than the equilibrium temperature T_z (Ref.5). The ionization rate coefficients are calculated by the Lotz formula¹⁹, dividing through by statistical weights as in ref.9.

The recombination process is also included in our calculation for excited levels as well as for the ground level. The data from ref.20 are used for the ground state and are extrapolated for excited levels. Actually the recombination process has no effect in our calculation.

3. Population density

The population densities are calculated for the 20 levels shown in Table 1 under the assumption that all transitions considered are optically thin. All the possible ionization and recombination processes from other ionic levels and/or to other ionic levels are taken into account. The rate equations for the

population densities including ionization and recombination processes are described in ref.9.

Be-like OV ions have metastable levels $2s2p\ ^3P_{0,1,2}$ for which the population density is comparable to the ground level for an electron density n_e greater than 10^{12} cm^{-3} as shown in Fig.2. The populations of these levels relative to that of the ground level tend to be constant for $n_e > 10^{13} \text{ cm}^{-3}$ because of the small value of the transition probability from $2s2p\ ^3P$ to the $2s^2\ ^1S$ ground level. The calculated values of the populations at 20 eV agree well (within 10%) with those calculated by Keenan et al.⁸

Ionization processes from OV $2s2p\ ^3P$ to OVI 2s or 2p decrease the population of $2s2p\ ^3P$, whereas those from OIV $2s^22p$ to OV $2s2p\ ^3P$ and from OIV $2s2p^2$ to OV $2s2p\ ^3P$ increase it. Ionization from OIV $2s^22p$ populates also the ground level of OV $2s^2\ ^1S$. Ionization rate coefficients are compared to excitation rate coefficients in Fig.3. It is shown that for the $2s2p\ ^3P$ the ionization rate coefficient exceeds the excitation one when the temperature range is above 100 eV. This effect is not important in an ionization equilibrium plasma where the electron temperature is as low as 20 - 30 eV. In an ionizing plasma at higher temperature such as in a tokamak or a solar flare, this effect becomes important. The population of $2s2p\ ^3P$ relative to $2s^2\ ^1S$ is decreased by about 60% by the inclusion of the ionization process from OV as shown in Fig.2 for $T_e = 100 \text{ eV}$ by the dashed curve. Then taking into account the ionization from OIV ions to all the levels of OV ions assuming $n(\text{OIV}) = n(\text{OV})$, where $n(\text{OIV})$ represents the density of OIV ions, the relative population of $2s2p\ ^3P$ increases by 50% for $T_e = 100 \text{ eV}$ as shown in Fig.2 by a dashed - dotted curve. The recombination process is not important for plasmas of $T_e > 5 \text{ eV}$, but would be effective in a strongly recombining plasma at low temperatures.

The populations of the triplet levels are mainly excited from the metastable levels $2s2p\ ^3P$ for $n_e > 10^{10} \text{ cm}^{-3}$ where the population of the metastable levels are comparable to that of the ground level, since the excitation rate coefficients from the $2s^2\ ^1S$ ground level to the triplet levels are small. At densities $10^{10} < n_e < 10^{12} \text{ cm}^{-3}$, the population densities of such levels

are approximately proportional to n_e^{-2} , while at higher densities where the populations of the metastable levels are determined only by collisional processes, this changes to a linear dependence. Then the ratio of the intensity of a line excited from the metastable levels to a line excited from the ground level is density dependent at $10^{10} < n_e < 10^{13} \text{ cm}^{-3}$.

The temperature dependence of the excitation rate coefficients to $n = 3$ levels from the ground or metastable levels is different from those to $n = 2$ levels because of the difference in the excitation energies. This result is used for temperature diagnostics.

We have included proton excitation which is comparable to the electron excitation between fine structure transitions for $2s2p\ ^3P$ and $2p^2\ ^3P$ levels²¹, because the effect in the populations is found to be large in high temperature and low density regions; the population of $2s2p\ ^3P_2$ decreases by 35 % at $T_e = 100 \text{ eV}$ and $n_e = 10^9 \text{ cm}^{-3}$. But the effect is within 10 % for $n_e > 10^{11} \text{ cm}^{-3}$ and negligibly small for $n_e > 10^{12} \text{ cm}^{-3}$. At temperature lower than 50 eV the effect is also wthin 10%.

4. Line intensity ratios

We present in this section the line intensity ratios of OV ions for density and temperature diagnostics. The spectral lines emitted from OV ions related to our calculations are listed in Table 2(taken from Ref.11) whose visible wavelengths are those in the air.

As we have discussed in the previous section, the metastable $2s2p\ ^3P$ levels and other triplet levels have varying electron density dependence and this is utilised for density diagnostics by the line ratio method. The most commonly used line ratio for density diagnostics is $I(760.45, 760.23, 762.00, 761.13, 758.68, 759.44) / I(629.73)$ $2s2p\ ^3P - 2p^2\ ^3P$ /. This intensity ratio is plotted in Fig. 4 as a function of electron density for $T_e = 20$ and 100 eV . The intensity ratio $I(1218) / I(629.73)$ $2s^2\ ^1S - 2s2p\ ^3P$ is also plotted in Fig.4. The density dependent intensity ratios $I(192.90) / I(629.73)$ $2s2p\ ^3P_2 - 2s3d\ ^3D_{2,3}$ /, $I(248.46) / I(629.73)$ $2s2p\ ^1P - 2s3s\ ^1S$ /, $I(215.25) / I(629.73)$ $2s2p\ ^3P_2 - 2s3s\ ^3S_1$ /

$I(220.35 \text{ } 2s2p \text{ } ^1P - 2s3d \text{ } ^1D)$, $I(192.80 \text{ } 2s2p \text{ } ^3P_{0,1} - 2s3d \text{ } ^3D_{1,2})/I(220.35)$ are shown in Fig.5. The above calculations do not include any ionization processes to allow a comparison of our calculations with others who do not include ionization processes. In Fig.4, the intensity ratio for $I(760)/I(630)$ is compared with those by Doyle et al.¹ and by Finkenthal et al.³ The results in ref.3 give agreement to within 10 % but those of ref.1 are smaller by more than 40 % at $n_e = 10^{12} \text{ cm}^{-3}$. Both works used R-matrix calculations for electron excitation rate coefficients.^{7, 8} We have found differences between our calculations and those by Widing et al.² for triplet lines (see Fig.5); their values are smaller than ours by 50 % and 70 % for $I(192.90)/I(248.46)$ and $I(192.80)/I(220.35)$ at $n_e = 10^9 \text{ cm}^{-3}$, although the rate coefficients used are not that different. However at densities higher than 10^{11} cm^{-3} , the agreement is good, within 10 % as shown in Fig.5. The calculations by Huang et al.⁴ agree with our calculations to within 30 %.

Our calculations including ionization and recombination processes are presented in Figs.I and II. The line intensities for multiplets are summed up for the triplet system, except when the wavelength is written to be full precision of its value in Table 2, in which case it is calculated only for one line.

The ratios of lines from levels excited from the same levels are a sensitive function of temperature when the difference in their excitation energy is greater than the electron temperature. In Fig.I, the ratios of $I(172)/I(630)$, $I(193)/I(760)$ and $I(220)/I(248)$ are shown for $n_e = 10^9$ (solid line), 10^{11} (dashed-dotted line) and 10^{13} cm^{-3} (dashed line) as a function of electron temperature for $n(\text{OIV}) = 0.0$. The dotted line shows the result for $n_e = 10^{13} \text{ cm}^{-3}$ assuming $n(\text{OIV}) = n(\text{OV})$. The contribution of the ionization from OIV ions is negligible in this case. When the cross sections have different energy dependence even though the excitation energies are nearly the same, the line ratio is also sensitive to the electron temperature. In this case the ratio is also density dependent as shown in Fig.I for $I(215)/I(220)$, $I(215)/I(193)$ and $I(220)/I(193)$.

The intensity ratios in the singlet system such as $I(220)/I(172)$ and $I(220)/I(248)$ exhibit small density and temperature dependence as shown in Fig.II. The intensity ratios for $T_e = 20$ eV (solid line), 40 eV (dashed dotted line) and 100 eV (dashed line) are shown as a function of the electron density assuming $n(OIV) = 0.0$. For the case of $n(OIV) = n(OV)$ for $T_e = 100$ eV, the ratios are also plotted as dotted lines. These ratios can be used to cross check the spectrometer sensitivity calibration. (It can be noted that on the scale of these figures, the dashed and the dotted lines nearly coincide.)

Density dependent line ratios involving the triplet system are also shown in Fig. II. Plots are given for the followings; $I(760)/I(630)$, $I(1218)/I(630)$, $I(193)/I(248)$, $I(193)/I(220)$, $I(215)/I(220)$, $I(193)/I(172)$, $I(215)/I(193)$, $I(271)/I(215)$, $I(2781.01)/I(193)$, $I(2781.01)/I(215)$, $I(760.45)/I(630)$ and $I(270.98)/I(215)$. As indicated by the truncations of the wavelength values the intensities are for the multiplet for the triplet transition except for the last four sets, where particular single lines are being represented.

5. Conclusions

The ionization process from the metastable OV $2s2p\ ^3P$ state to the OVI 2s and 2p states decreases the relative population to the ground state $n(2s2p\ ^3P)/n(2s^2\ ^1S)$ as the temperature increases; 10 %, 40% and 60 % at $T_e = 50$ eV, 80 eV and 100 eV, respectively. On the other hand the ionization from OIV ions to OV $2s2p\ ^3P$ increases the relative population of the metastable state by 10%, 30% and 50% at $T_e = 50$ eV, 80 eV and 100 eV for the ion density $n(OIV) = n(OV)$.

The changes in population caused by the inclusion of ionization processes can thus be substantial and are important in an ionizing plasma such as a tokamak where the temperature is comparatively higher than that for ionization equilibrium. Proton excitation is also important for high temperature and low density plasmas.

The detailed analysis of measurements obtained from the tokamaks will be published in a separate paper.

Acknowledgements

The authors thank Mr.N.Yamada for making graphs and tables of rate coefficients and Dr.K.Masai for useful comments.

References

- 1) J.G.Doyle, P.L.Dufton, F.P.Keenan and A.E. Kingston, Solar Physics, **89**, 243(1983)
- 2) K.G.Widing, J.G.Doyle, P.L.Dufton and A.E.Kingston, Ap.J. **257**, 913(1982)
- 3) M.Finkenthal, T.L.Yu,S.Lippmann, L.K.Huang, H.W.Moos, B.C.Stratton, A.K.Bhatia, R.D.Bengston, W.L.Hodge, P.E.Philips, J.L.Porter, T.R.Price, T.L.Rhodes, B.Richards, C.P.Ritz and W.L.Rowan, Ap.J. **313**, 920(1987)
- 4) L.K.Huang, S.Lippmann, B.C.Stratton and H.W.Moos, Phys. Rev. A, **37**, 3927(1988)
- 5) T.Kato, K.Masai and K.Sato, Phys. Letters, **108A**, 259(1985)
- 6) Y.Ogawa, K.Masai, T.Watari, R.Akiyama, R.Ando, J.Fujita, Y.Hamada, S.Hirokura, K.Ida, K.Kadata, E.Kako, O.Kanako, K.Kawahata, Y.Kawasumi, S.Kitagawa, T.Kuroda, K.Matsuoka, A.Mohri, S.Morita, A.Nishizawa, N.Noda, I.Ogawa, K.Ohkubo, Y.Oka, S.Okajima, T.Ozaki, M.Sasao, K.Sato, K.N.Sato, S.Tanahashi, Y.Taniguchi, K.Toi, H.Yamada, IPPJ-903 (1989), Nucl. Fusion, **29**, 1873(1989)
- 7) P.L.Dufton, K.A.Berrington, P.G.Burke and A.E.Kingston, Astron. & Astrophys. **62**, 111(1978)
- 8) F.P.Keenan, K.A. Berrington, P.G.Burke, A.E.Kingston and P.L.Dufton, Mon. Not. R. astr. Soc. **207**, 459(1984)
- 9) T.Kato, K.Masai and J.Mizuno, J.Phys.Soc. Japan, **52**, 3019(1983)
" (Errata), J.Phys.Soc. Japan, **54**, 3203(1985)
- 10) K.A.Berrington and A.E.Kingston,(1989) in preparation
- 11) C.E.Moore,NSRDS-NBS3, Sec.9(1980)
- 12) " Sec.10(1982)
- 13) " Sec.8(1979)
- 14) A. Hibbert, J.Phys. B, **13**, 1721(1980)
- 15) D.R.Flower and H.Nussbaumer, Astron. & Astrophys. **45**, 145(1975)
- 16) W.L.Wiese, M.W.Smith and B.M.Glennon, NSRDS-NBS 4 Vol.1(1966)
G.A. Martin, W.L.Wiese, J. Phys. Chem. Ref. Data, **5**, 537(1976)
- 17) Y.Itikawa, S. Hara, T.Kato, S.Nakazaki, M.S. Pindzola and D.H. Crandall, Atomic Data & Nucl. Data Tables, **33**(1985) 149
- 18) T.Kato and S.Nakazaki, ADNDT, **42**, 313 (1989)

- 19) W.Lotz, Ap. J. Suppl. **14**, 207(1967)
- 20) S.M.V.Aldrovandi and D.Pequignot, Astron. & Astrophys. **251**, 137(1973)
- 21) J.G.Doyle, A.E.Kingston and R.H.Reid, Astron. & Astrophys. **90**, 97 (1980)

Table 1
Energy levels of OV

level No.	Configuration	J	Energy (cm ⁻¹)	(eV)
1	2s ² ¹ S	0	0	0
2	2s2p ³ P	0	81942.5	10.16
3		1	82078.6	10.18
4		2	82385.3	10.21
5	2s2p ¹ P	1	158797.1	19.69
6	2p ² ³ P	0	213462.5	26.47
7		1	213618.2	26.49
8		2	213887.0	26.52
9	¹ D	2	231721.4	28.73
10	¹ S	0	287910.3	35.70
11	2s3s ³ S	1	546972.7	67.82
12	¹ S	0	561276.4	69.59
13	2s3p ¹ P	1	580824.9	72.01
14	³ P	0	582806.4	72.26
15		1	582843.1	72.26
16		2	582920.3	72.27
17	2s3d ³ D	1	600748.9	74.48
18		2	600758.9	74.49
19		3	600779.2	74.49
20	¹ D	2	612615.6	75.96

Energy levels of OIV				Energy levels of OVI			
1	2s ² 2p ² P	1/2	0 (cm ⁻¹)	1	2s ² S	1/2	0.0(cm ⁻¹)
		3/2	385.9	2	2p ² P	1/2	96375.
2	2s2p ² ⁴ P	1/2	71439.8			3/2	96907.5
		3/2	71570.1				
		5/2	71755.5				
3	2s2p ² ² D	5/2	126936.3				
		3/2	126950.2				
4	2s2p ² ² S	1/2	164366.4				
5	2s2p ² ² P	1/2	180480.8				
		3/2	180724.2				
6	2p ³ ⁴ S	3/2	231537.5				

Table II
Prominent emission lines from OV ions

Wavelength(A)(Ref. 11)	Transition
172.17	$2s^2 \ ^1S$ - $2s3p \ ^1P$
192.8	$2s2p \ ^3P_0,1$ - $2s3d \ ^3D_{1,2}$
192.9	" 3P_2 - " $^3D_{2,3}$
215.245	$2s2p \ ^3P_2$ - $2s3s \ ^3S_1$
215.103	" 3P_1 - " 3S_1
215.040	" 3P_0 - " 3S_1
220.35	$2s2p \ ^1P_1$ - $2s3d \ ^1D_2$
248.46	$2s2p \ ^1P$ - $2s3s \ ^1S$
270.98	$2p^2 \ ^3P_2$ - $2s3p \ ^3P_2$
286.45	$2p^2 \ ^1D$ - $2s3p \ ^1P$
629.73	$2s^2 \ ^1S$ - $2s2p \ ^1P$
760.45	$2s2p \ ^3P_2$ - $2p^2 \ ^3P_2$
760.23	$2s2p \ ^3P_1$ - $2p^2 \ ^3P_1$
762.00	$2s2p \ ^3P_2$ - $2p^2 \ ^3P_1$
761.13	$2s2p \ ^3P_1$ - $2p^2 \ ^3P_0$
758.68	$2s2p \ ^3P_1$ - $2p^2 \ ^3P_2$
759.44	$2s2p \ ^3P_0$ - $2p^2 \ ^3P_1$
774.52	$2s2p \ ^1P$ - $2p^2 \ ^1S$
1218.34	$2s^2 \ ^1S$ - $2s2p \ ^3P_1$
1371.29	$2s2p \ ^1P$ - $2p^2 \ ^1D$
2781.01(air)	$2s3s \ ^3S_1$ - $2s3p \ ^3P_2$
2786.99(air)	$2s3s \ ^3S_1$ - $2s3p \ ^3P_1$
2789.85(air)	$2s3s \ ^3S_1$ - $2s3p \ ^3P_0$
5114.07(air)	$2s3s \ ^1S$ - $2s3p \ ^1P$
5597.91 -	$2s3p \ ^3P$ - $2s3d \ ^3D$
5607.41(air)	

Figure captions

Fig.1 Schematic energy level diagram for OV. The term designations are shown across the top of the figure; the level numbers are same as those in Table 1; the wavelengths are approximate values in Å.

Fig.2 Population density of the metastable level $2s2p\ ^3P_1$ for $T_e = 20$ and 100 eV as a function of electron density. Solid, dashed and dash - dotted curves indicate the results without ionization processes ($T_e = 20$ and 100 eV), with ionization from OV to OVI ions ($T_e = 100$ eV) and with ionization both from OV to OVI and OIV to OV ions ($T_e = 100$ eV), respectively. The values from Keenan et al.⁸ for 20 eV are shown by triangles.

Fig.3 Rate coefficients for excitation, recombination (α) and ionization processes (S). The dotted portions extending the solid lines represent the extrapolated values from ref.10.

Fig.4 Density dependent line ratios for $I(760)/I(630)$, $I(1218)/I(630)$ without ionization processes for $T_e = 20$ (solid line) and 100 eV (dashed line). The calculated results from ref.1 (dotted line) and ref.3 (dashed dotted line) for 22 eV are also shown.

Fig.5 Density dependent line ratios for $I(192.90\text{\AA})/I(248.46\text{\AA})$, $I(215.25\text{\AA})/I(220.35\text{\AA})$ and $I(192.80\text{\AA})/I(220.35\text{\AA})$ for $T_e = 20$ eV (solid line) and 100 eV (dashed line) without ionization processes. Dashed dotted lines are results from ref.2 for $T_e = 17$ eV.

Fig. 1

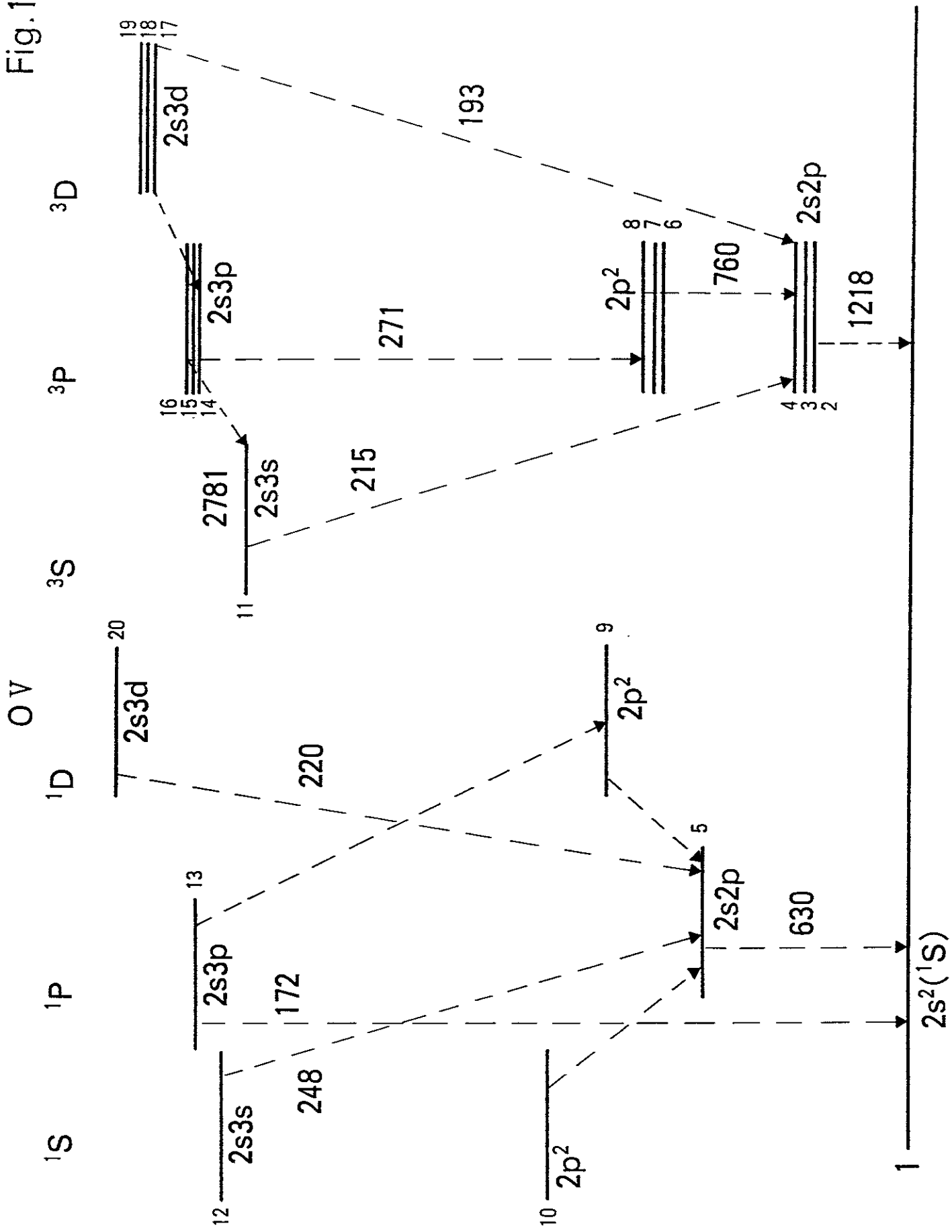


Fig.2

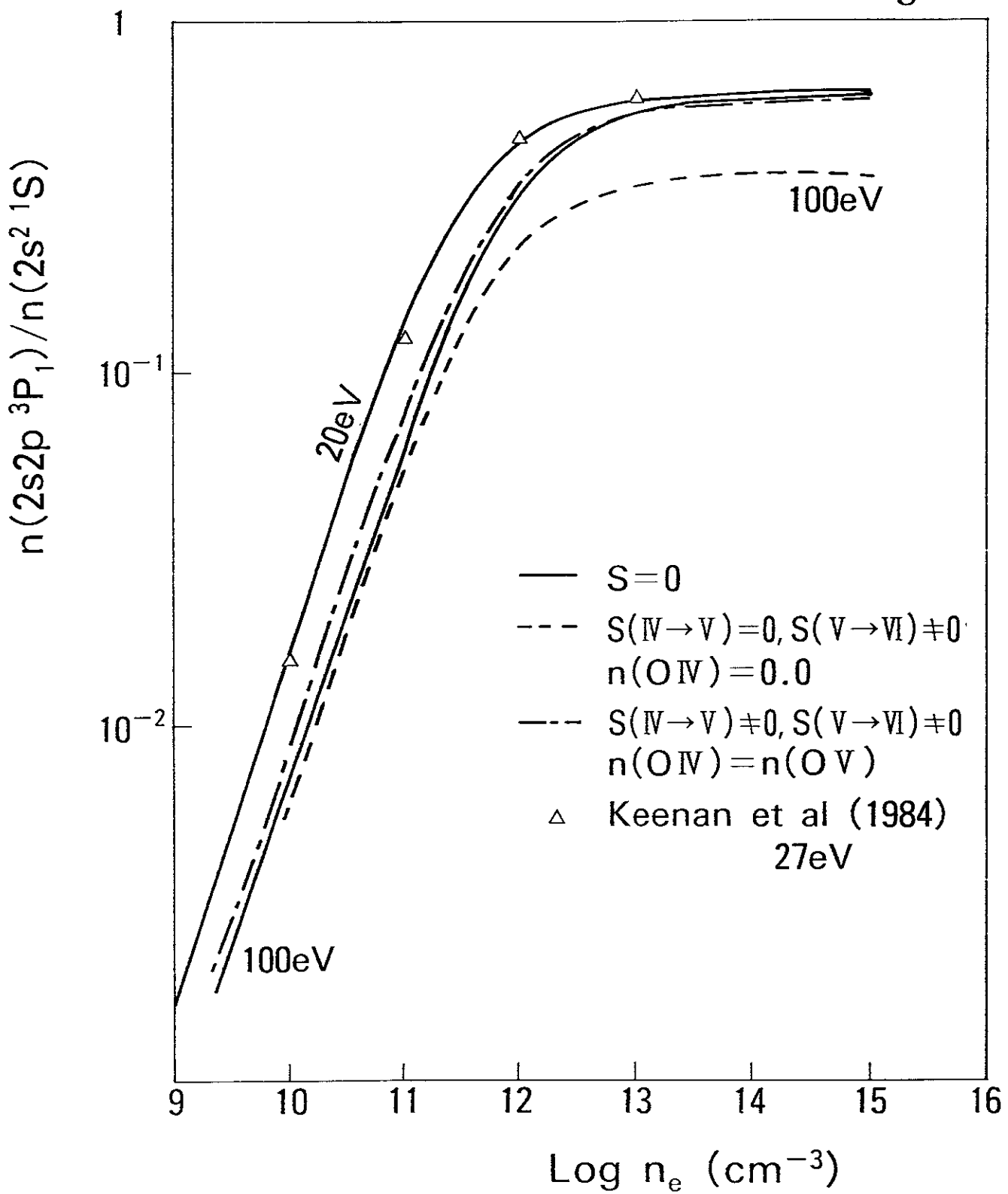


Fig.3

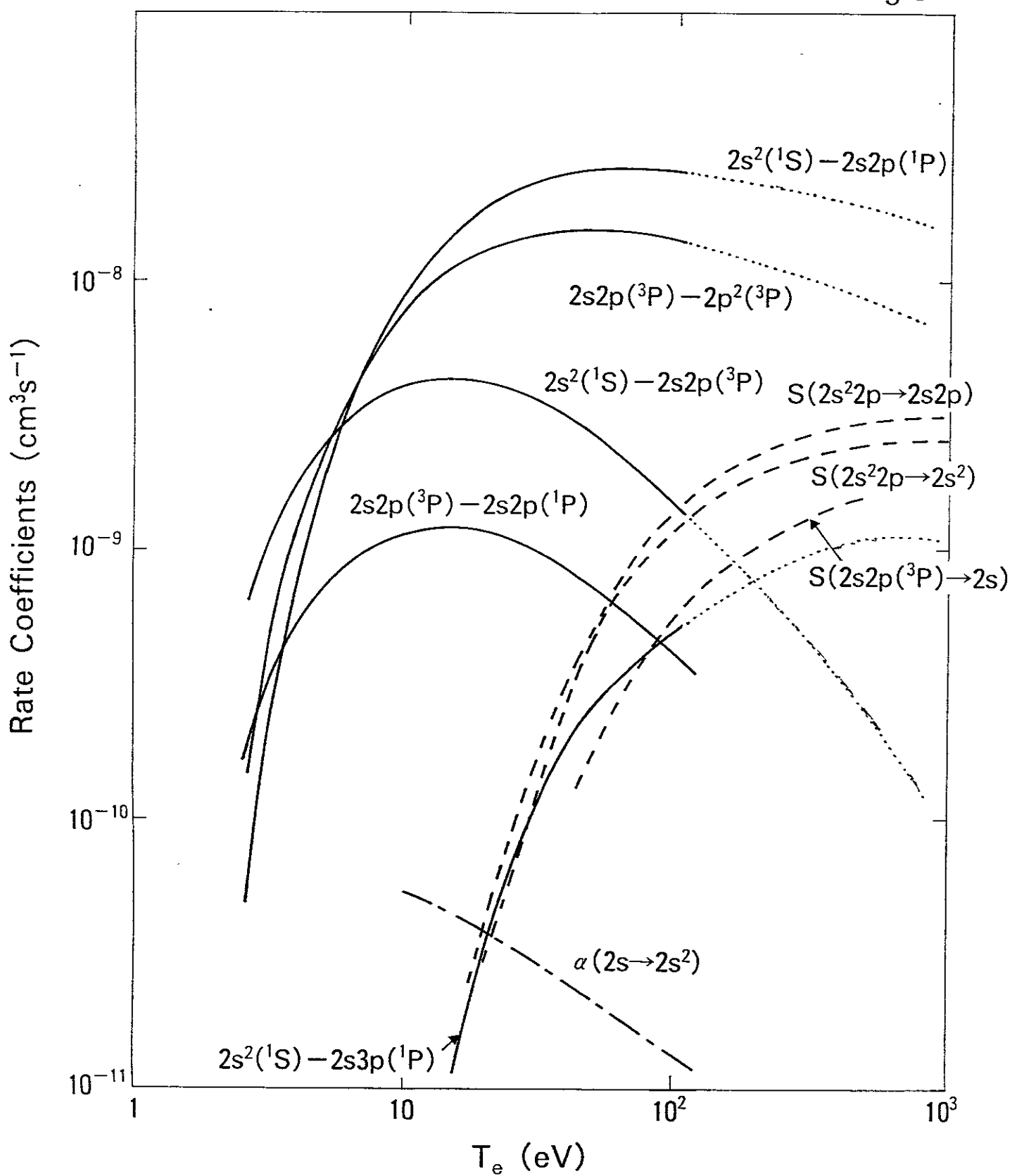


Fig.4

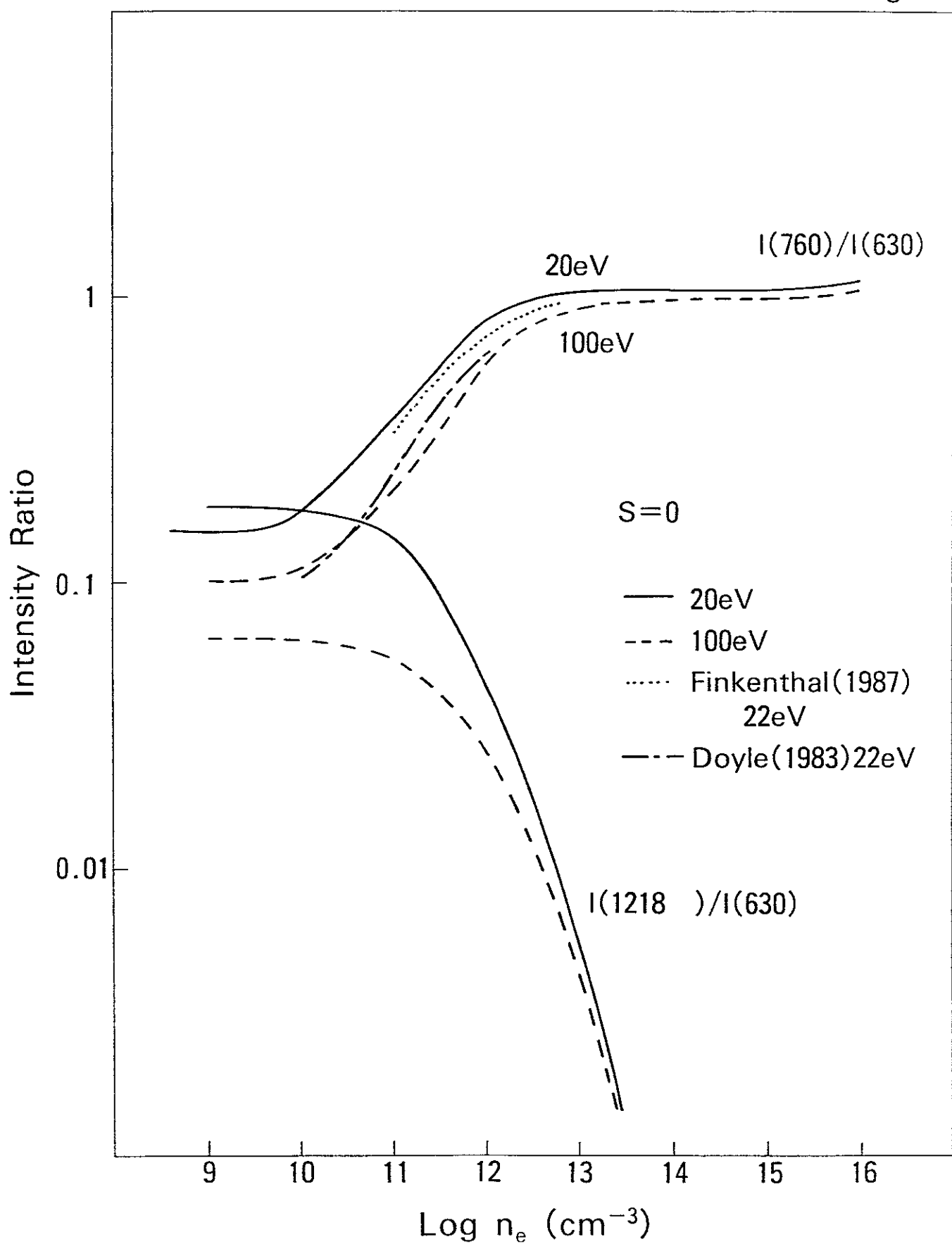
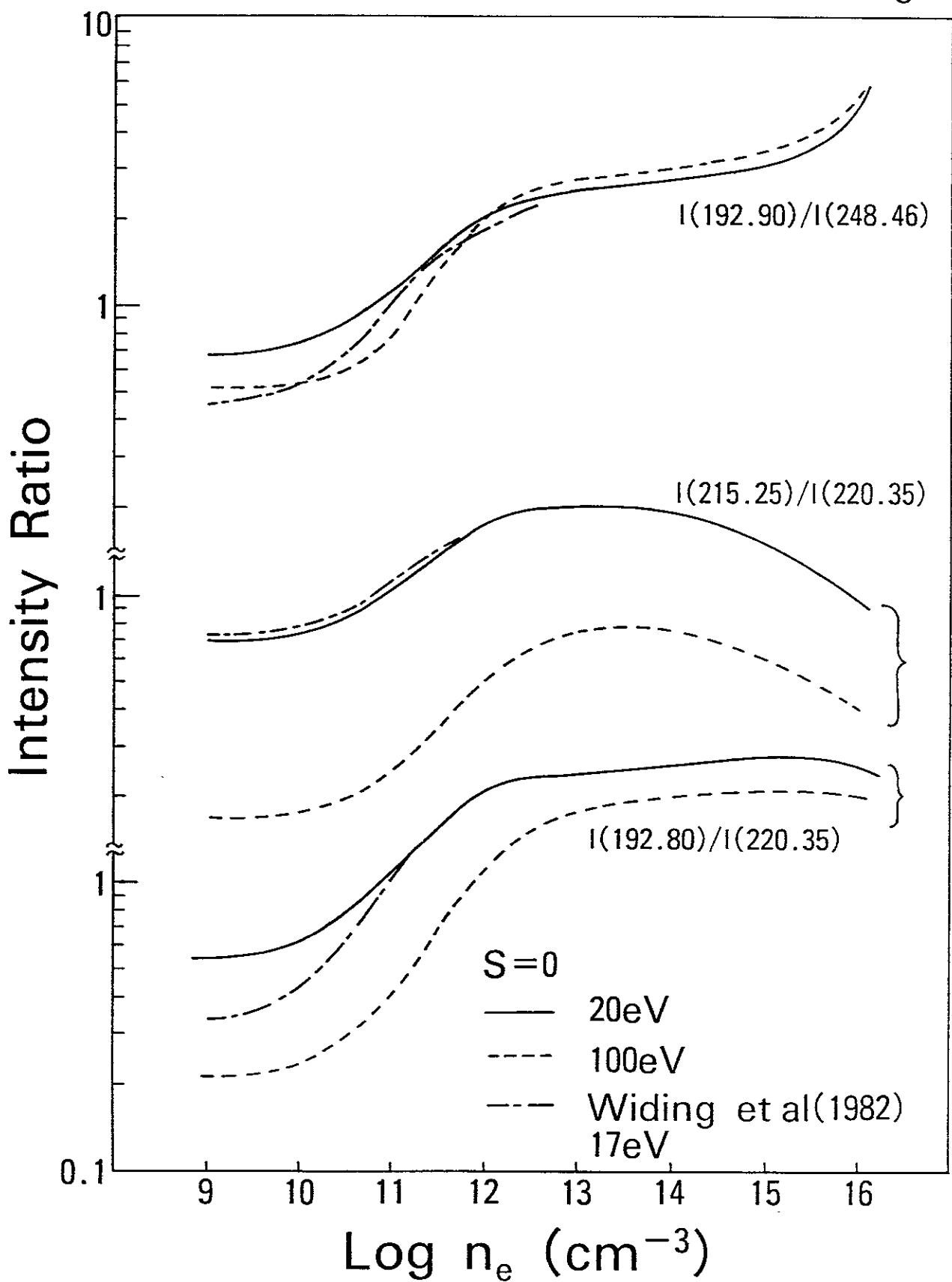


Fig.5



Appendix

Explanation of Tables

Table I. Fit parameters for the Recommended Rate Coefficients

Fit parameters are tabulated for each excitation process of OV. Transitions between energy terms are listed first, followed by transition between the triplet fine structure levels. The notation $2s^2 \ ^1S - 2s2p \ ^3P$, for example, means the excitation from the lower state $2s^2 \ ^1S$ to the upper triplet term $2s2p \ ^3P$, while $2s2p \ ^3P_0 - 2p^2 \ ^3P_2$ indicates a transition between fine structure levels.

ΔE	Excitation energy in eV
a_1, a_2, a_3, a_4, a_5	Fit parameters in Eq.(3) ($\Delta E \neq 0$)
b_1, b_2, b_3, b_4	Fit parameters in Eq.(5) for transitions between fine structure levels belonging to the same term ($\Delta E = 0$).

Table I

	$\Delta E(\text{eV})$	a_1	a_2	a_3	a_4	a_5
$2s^2 \ ^1S - 2s2p \ ^3P$	1.02E+01	-2.52E-02	2.07E+00	-3.71E+00	2.49E+00	0.0
$2s^2 \ ^1S - 2s2p \ ^1P$	2.06E+01	1.66E+00	6.65E-01	2.75E-01	0.0	1.40E+00
$2s^2 \ ^1S - 2p^2 \ ^3P$	2.66E+01	-8.40E-05	1.44E-02	4.82E-02	-5.63E-02	0.0
$2s^2 \ ^1S - 2p^2 \ ^1D$	2.96E+01	1.06E-02	4.25E-01	-4.85E-01	1.54E-01	0.0
$2s^2 \ ^1S - 2p^2 \ ^1S$	3.69E+01	-6.91E-04	9.27E-02	-6.46E-03	-6.44E-02	0.0
$2s^2 \ ^1S - 2s3s \ ^3S$	6.78E+01	-8.79E-03	1.73E-01	-5.98E-01	5.58E-01	0.0
$2s^2 \ ^1S - 2s3s \ ^1S$	6.96E+01	3.12E-02	1.32E+00	-2.87E+00	1.75E+00	0.0
$2s^2 \ ^1S - 2s3p \ ^1P$	7.20E+01	-2.08E-01	1.19E-01	1.71E-01	0.0	2.95E-01
$2s^2 \ ^1S - 2s3p \ ^3P$	7.22E+01	1.08E-03	3.55E-02	-7.44E-02	1.30E-01	0.0
$2s^2 \ ^1S - 2s3d \ ^3D$	7.46E+01	2.50E-03	3.10E-02	1.08E-01	-8.69E-03	0.0
$2s^2 \ ^1S - 2s3d \ ^1D$	7.64E+01	4.51E-01	-4.31E-01	2.59E-02	6.76E-02	0.0
$2s2p \ ^3P - 2s2p \ ^1P$	1.04E+01	1.04E-02	3.87E+00	-6.00E+00	4.23E+00	0.0
$2s2p \ ^3P - 2p^2 \ ^3P$	1.64E+01	2.55E+01	-3.91E+01	4.37E+01	-1.73E+01	0.0
$2s2p \ ^3P - 2p^2 \ ^1D$	1.94E+01	-4.21E-02	2.39E+00	-2.85E+00	8.74E-01	0.0
$2s2p \ ^3P - 2p^2 \ ^1S$	2.67E+01	-1.14E-03	2.60E-02	5.92E-01	-5.87E-01	0.0
$2s2p \ ^3P - 2s3s \ ^3S$	5.76E+01	1.37E+00	4.72E+04	-4.72E+04	0.0	4.61E-02
$2s2p \ ^3P - 2s3s \ ^1S$	5.94E+01	7.81E-03	3.05E-01	-1.62E+00	1.74E+00	0.0

$\Delta E(\text{eV})$	a_1	a_2	a_3	a_4	a_5	
$2s2p \ ^3P - 2s3p \ ^1P$	$6.19E+01$	$-2.42E-02$	$6.73E-01$	$-2.06E+00$	$1.89E+00$	0.0
$2s2p \ ^3P - 2s3p \ ^3P$	$6.20E+01$	$-6.99E-01$	$1.71E+01$	$-3.74E+01$	$2.40E+01$	0.0
$2s2p \ ^3P - 2s3d \ ^3D$	$6.44E+01$	$8.11E+00$	$-1.24E+01$	$7.63E+00$	0.0	$5.38E-01$
$2s2p \ ^3P - 2s3d \ ^1D$	$6.62E+01$	$-1.01E-03$	$1.12E-01$	$-1.30E-01$	$5.01E-01$	0.0
$2s2p \ ^1P - 2p^2 \ ^3P$	$6.04E+00$	$-5.62E-02$	$3.91E+00$	$-1.05E+01$	$8.77E+00$	0.0
$2s2p \ ^1P - 2p^2 \ ^1D$	$8.98E+00$	$9.62E+00$	$-1.00E+01$	$9.38E+00$	0.0	$1.94E+00$
$2s2p \ ^1P - 2p^2 \ ^1S$	$1.63E+01$	$4.61E+00$	$-5.66E+00$	$3.70E+00$	0.0	$2.06E-01$
$2s2p \ ^1P - 2s3s \ ^3S$	$4.73E+01$	$-1.06E-02$	$2.59E-01$	$-1.07E+00$	$1.24E+00$	0.0
$2s2p \ ^1P - 2s3s \ ^1S$	$4.90E+01$	$1.80E-01$	$-1.06E-02$	$1.31E-02$	0.0	$4.71E-02$
$2s2p \ ^1P - 2s3p \ ^1P$	$5.15E+01$	$4.60E-02$	$2.02E+00$	$-5.34E+00$	$3.95E+00$	0.0
$2s2p \ ^1P - 2s3p \ ^3P$	$5.16E+01$	$-2.54E-04$	$2.13E-01$	$-7.59E-01$	$1.08E+00$	0.0
$2s2p \ ^1P - 2s3d \ ^3D$	$5.40E+01$	$-4.02E-03$	$5.46E-01$	$-1.42E+00$	$1.65E+00$	0.0
$2s2p \ ^1P - 2s3d \ ^1D$	$5.58E+01$	$2.37E+00$	$-3.34E+00$	$2.04E+00$	0.0	$5.41E-01$
$2p^2 \ ^3P - 2p^2 \ ^1D$	$2.94E+00$	$6.18E-02$	$1.99E+01$	$-6.37E+01$	$5.16E+01$	0.0
$2p^2 \ ^3P - 2p^2 \ ^1S$	$1.03E+01$	$-2.12E-02$	$1.20E+00$	$-1.61E+00$	$5.52E-01$	0.0
$2p^2 \ ^3P - 2s3s \ ^3S$	$4.12E+01$	$-4.04E-03$	$1.60E-01$	$-8.83E-01$	$1.17E+00$	0.0
$2p^2 \ ^3P - 2s3s \ ^1S$	$4.30E+01$	$-2.45E-03$	$8.44E-02$	$-4.51E-01$	$5.44E-01$	0.0

$\Delta E(\text{eV})$	a_1	a_2	a_3	a_4	a_5	
$2p^2 \ ^3P - 2s3p \ ^1P$	4.54E+01	-2.75E-02	9.65E-01	-4.07E+00	4.05E+00	0.0
$2p^2 \ ^3P - 2s3p \ ^3P$	4.56E+01	-8.76E-02	2.00E+00	-8.27E+00	8.87E+00	0.0
$2p^2 \ ^3P - 2s3d \ ^3D$	4.80E+01	1.98E-01	3.56E-01	-5.08E+00	7.16E+00	0.0
$2p^2 \ ^3P - 2s3d \ ^1D$	4.97E+01	-1.74E-02	4.20E-01	-1.82E+00	1.99E+00	0.0
$2p^2 \ ^1D - 2p^2 \ ^1S$	7.36E+00	3.92E-01	-1.83E-01	5.00E-02	1.33E-02	0.0
$2p^2 \ ^1D - 2s3s \ ^3S$	3.83E+01	-7.35E-03	2.56E-01	-1.30E+00	1.61E+00	0.0
$2p^2 \ ^1D - 2s3s \ ^1S$	4.00E+01	-1.13E-04	6.19E-01	-2.51E+00	2.49E+00	0.0
$2p^2 \ ^1D - 2s3p \ ^1P$	4.25E+01	6.64E-01	-2.55E+00	2.70E+00	0.0	2.30E-02
$2p^2 \ ^1D - 2s3p \ ^3P$	4.27E+01	-1.44E-02	4.80E-01	-2.32E+00	2.74E+00	0.0
$2p^2 \ ^1D - 2s3d \ ^3D$	4.50E+01	-2.06E-02	6.31E-01	-3.00E+00	3.46E+00	0.0
$2p^2 \ ^1D - 2s3d \ ^1D$	4.68E+01	2.24E-01	-8.46E-03	-1.21E+00	2.18E+00	0.0
$2p^2 \ ^1S - 2s3s \ ^3S$	3.09E+01	-1.73E-04	2.13E-02	-1.68E-01	3.10E-01	0.0
$2p^2 \ ^1S - 2s3s \ ^1S$	3.27E+01	1.25E-03	2.35E-02	-2.27E-02	1.03E-01	0.0
$2p^2 \ ^1S - 2s3p \ ^1P$	3.51E+01	1.55E-01	-8.50E-01	9.99E-01	0.0	1.11E-02
$2p^2 \ ^1S - 2s3p \ ^3P$	3.53E+01	-4.76E-03	1.59E-01	-7.33E-01	8.54E-01	0.0
$2p^2 \ ^1S - 2s3d \ ^3D$	3.77E+01	-3.13E-03	1.06E-01	-5.13E-01	6.59E-01	0.0
$2p^2 \ ^1S - 2s3d \ ^1D$	3.94E+01	5.86E-02	8.49E-02	-3.65E-01	4.97E-01	0.0

	ΔE (eV)	a_1	a_2	a_3	a_4	a_5
2s3s ⁰ S - 2s3s ¹ S	1.77E+00	2.98E-02	8.25E-02	5.45E+00	-3.94E+00	0.0
2s3s ⁰ S - 2s3p ¹ P	4.22E+00	-1.03E-02	1.18E+00	-2.33E+00	2.78E+00	0.0
2s3s ⁰ S - 2s3p ⁰ P	4.39E+00	3.18E+01	-4.96E+01	7.07E+01	0.0	1.63E+01
2s3s ⁰ S - 2s3d ⁰ D	6.76E+00	6.64E+00	-6.92E+00	1.20E+01	-5.69E+00	0.0
2s3s ⁰ S - 2s3d ¹ D	8.53E+00	3.54E-03	6.17E-01	-1.29E-01	1.59E-01	0.0
2s3s ¹ S - 2s3p ¹ P	2.45E+00	1.17E+01	-3.78E+01	5.23E+01	0.0	4.59E+00
2s3s ¹ S - 2s3p ⁰ P	2.63E+00	-5.96E-03	1.32E+00	-2.51E-01	-3.41E-01	0.0
2s3s ¹ S - 2s3d ⁰ D	4.99E+00	1.95E-02	7.83E-01	3.89E-01	-5.31E-01	0.0
2s3s ¹ S - 2s3d ¹ D	6.76E+00	1.80E+00	-1.12E+00	1.13E+00	0.0	1.61E-02
2s3p ¹ P - 2s3p ⁰ P	1.77E-01	2.30E-01	3.36E+01	-6.41E+01	1.43E+01	0.0
2s3p ¹ P - 2s3d ⁰ D	2.54E+00	2.51E-02	3.17E+00	5.37E+00	-6.95E+00	0.0
2s3p ¹ P - 2s3d ¹ D	4.31E+00	3.75E+01	-7.87E+01	7.47E+01	0.0	2.27E+00
2s3p ³ P - 2s3d ⁰ D	2.37E+00	1.90E+02	-6.90E+02	7.81E+02	0.0	2.37E+00
2s3p ³ P - 2s3d ¹ D	4.14E+00	-4.54E-03	2.54E+00	2.56E+00	-3.48E+00	0.0
2s3d ³ D - 2s3d ¹ D	1.77E+00	-1.52E-02	1.92E+01	-1.06E+01	-8.95E+00	0.0
2s2p ³ P ₀ - 2p ² ³ P ₀	1.64E+01	6.65E-02	-3.53E-01	6.91E-01	-3.93E-01	0.0
2s2p ³ P ₀ - 2p ² ³ P ₁	1.64E+01	1.14E+00	-1.44E-01	3.97E-01	0.0	5.96E-01

	ΔE (eV)	a_1	a_2	a_3	a_4	a_5
$2s2p \ ^3P_0 - 2p^2 \ ^3P_2$	1.64E+01	1.05E-01	-5.08E-01	9.97E-01	-5.77E-01	0.0
$2s2p \ ^3P_0 - 2s3p \ ^3P_0$	6.20E+01	9.12E-02	3.42E-01	-8.11E-01	5.15E-01	0.0
$2s2p \ ^3P_0 - 2s3p \ ^3P_1$	6.20E+01	-2.78E-03	8.77E-02	-2.76E-01	2.66E-01	0.0
$2s2p \ ^3P_0 - 2s3p \ ^3P_2$	6.20E+01	2.23E-03	2.94E-01	-8.31E-01	6.31E-01	0.0
$2s2p \ ^3P_0 - 2s3d \ ^3D_1$	6.44E+01	-4.22E-01	1.16E+00	-4.96E-01	0.0	5.38E-01
$2s2p \ ^3P_0 - 2s3d \ ^3D_2$	6.44E+01	1.52E-02	-6.61E-03	-2.55E-02	8.47E-02	0.0
$2s2p \ ^3P_0 - 2s3d \ ^3D_3$	6.44E+01	3.85E-02	-7.45E-02	5.94E-02	3.14E-02	0.0
$2s2p \ ^3P_1 - 2p^2 \ ^3P_0$	1.64E+01	2.25E+00	-2.46E+00	1.66E+00	0.0	1.99E-01
$2s2p \ ^3P_1 - 2p^2 \ ^3P_1$	1.64E+01	1.69E+00	-1.57E+00	1.05E+00	0.0	1.49E-01
$2s2p \ ^3P_1 - 2p^2 \ ^3P_2$	1.64E+01	2.84E+00	-2.95E+00	1.99E+00	0.0	2.48E-01
$2s2p \ ^3P_1 - 2s3p \ ^3P_0$	6.20E+01	-5.64E-04	6.62E-02	-2.28E-01	2.37E-01	0.0
$2s2p \ ^3P_1 - 2s3p \ ^3P_1$	6.20E+01	1.27E-01	2.25E+00	-4.96E+00	3.15E+00	0.0
$2s2p \ ^3P_1 - 2s3p \ ^3P_2$	6.20E+01	1.23E-02	7.55E-01	-2.26E+00	1.80E+00	0.0
$2s2p \ ^3P_1 - 2s3d \ ^3D_1$	6.44E+01	4.21E-01	-5.42E-01	3.99E-01	0.0	1.35E-01
$2s2p \ ^3P_1 - 2s3d \ ^3D_2$	6.44E+01	1.20E+00	-1.39E+00	8.19E-01	0.0	4.03E-01
$2s2p \ ^3P_1 - 2s3d \ ^3D_3$	6.44E+01	3.04E-02	1.94E-01	-4.65E-01	4.46E-01	0.0
$2s2p \ ^3P_2 - 2p^2 \ ^3P_0$	1.64E+01	1.01E-01	-4.67E-01	8.93E-01	-5.06E-01	0.0

$\Delta E(\text{eV})$	a_1	a_2	a_3	a_4	a_5	
$2s2p \ ^3P_2 - 2p^2 \ ^3P_1$	1.64E+01	3.23E+00	-3.89E+00	2.58E+00	0.0	1.49E-01
$2s2p \ ^3P_2 - 2p^2 \ ^3P_2$	1.64E+01	9.61E+00	-1.18E+01	7.89E+00	0.0	4.64E-01
$2s2p \ ^3P_2 - 2s3p \ ^3P_0$	6.20E+01	-2.82E-03	2.53E-01	-6.79E-01	5.22E-01	0.0
$2s2p \ ^3P_2 - 2s3p \ ^3P_1$	6.20E+01	5.23E-03	7.47E-01	-2.19E+00	1.75E+00	0.0
$2s2p \ ^3P_2 - 2s3p \ ^3P_2$	6.20E+01	-5.09E-02	5.83E+00	-1.26E+01	7.99E+00	0.0
$2s2p \ ^3P_2 - 2s3d \ ^3D_1$	6.44E+01	1.23E-01	-2.76E-01	2.93E-01	0.0	5.36E-03
$2s2p \ ^3P_2 - 2s3d \ ^3D_2$	6.44E+01	6.46E-01	-1.02E+00	7.89E-01	0.0	8.05E-02
$2s2p \ ^3P_2 - 2s3d \ ^3D_3$	6.44E+01	2.38E+00	-2.31E+00	1.22E+00	0.0	4.51E-01
$2p^2 \ ^3P_0 - 2s3p \ ^3P_0$	4.56E+01	4.55E-01	-2.03E+00	2.80E+00	-1.20E+00	0.0
$2p^2 \ ^3P_0 - 2s3p \ ^3P_1$	4.56E+01	-3.60E-03	1.04E-01	-3.99E-01	4.21E-01	0.0
$2p^2 \ ^3P_0 - 2s3p \ ^3P_2$	4.56E+01	-3.49E-03	1.07E-01	-4.65E-01	4.91E-01	0.0
$2p^2 \ ^3P_0 - 2s3d \ ^3D_1$	4.80E+01	-1.36E-03	4.42E-02	-1.86E-01	2.32E-01	0.0
$2p^2 \ ^3P_0 - 2s3d \ ^3D_2$	4.80E+01	-2.88E-03	7.04E-02	-2.78E-01	3.21E-01	0.0
$2p^2 \ ^3P_0 - 2s3d \ ^3D_3$	4.80E+01	-1.46E-03	3.83E-02	-2.06E-01	2.56E-01	0.0
$2p^2 \ ^3P_1 - 2s3p \ ^3P_0$	4.56E+01	-2.50E-03	9.75E-02	-3.88E-01	4.16E-01	0.0
$2p^2 \ ^3P_1 - 2s3p \ ^3P_1$	4.56E+01	-6.90E-03	1.66E-01	-7.67E-01	8.78E-01	0.0
$2p^2 \ ^3P_1 - 2s3p \ ^3P_2$	4.56E+01	2.74E+00	-1.27E+01	1.77E+01	-7.28E+00	0.0

ΔE (eV)	a_1	a_2	a_3	a_4	a_5	
$2p^2 \ ^3P_1 - 2s3d \ ^3D_1$	4.80E+01	-5.91E-04	9.05E-02	-4.34E-01	5.57E-01	0.0
$2p^2 \ ^3P_1 - 2s3d \ ^3D_2$	4.80E+01	-8.18E-03	1.69E-01	-7.12E-01	8.65E-01	0.0
$2p^2 \ ^3P_1 - 2s3d \ ^3D_3$	4.80E+01	-4.95E-03	1.24E-01	-6.51E-01	8.55E-01	0.0
$2p^2 \ ^3P_2 - 2s3p \ ^3P_0$	4.56E+01	1.13E+00	-4.86E+00	6.28E+00	-2.40E+00	0.0
$2p^2 \ ^3P_2 - 2s3p \ ^3P_1$	4.56E+01	-2.52E-03	1.57E-01	-9.53E-01	1.22E+00	0.0
$2p^2 \ ^3P_2 - 2s3p \ ^3P_2$	4.56E+01	-1.77E-01	6.17E+00	-2.65E+00	2.88E+00	0.0
$2p^2 \ ^3P_2 - 2s3d \ ^3D_1$	4.80E+01	-1.37E-03	6.42E-02	-4.02E-01	5.47E-01	0.0
$2p^2 \ ^3P_2 - 2s3d \ ^3D_2$	4.80E+01	-3.05E-03	1.40E-01	-7.93E-01	1.08E+00	0.0
$2p^2 \ ^3P_2 - 2s3d \ ^3D_3$	4.80E+01	-5.14E-03	1.26E-01	-9.24E-01	1.56E+00	0.0
$2s3p \ ^3P_0 - 2s3d \ ^3D_1$	2.37E+00	2.50E+01	-1.57E+02	3.57E+02	-2.34E+02	0.0
$2s3p \ ^3P_0 - 2s3d \ ^3D_2$	2.37E+00	-1.17E-02	1.24E+00	2.52E-01	-1.46E+00	0.0
$2s3p \ ^3P_0 - 2s3d \ ^3D_3$	2.37E+00	2.29E-01	-8.81E-01	5.56E+00	-5.28E+00	0.0
$2s3p \ ^3P_1 - 2s3d \ ^3D_1$	2.37E+00	1.91E+01	-1.23E+02	2.83E+02	-1.86E+02	0.0
$2s3p \ ^3P_1 - 2s3d \ ^3D_2$	2.37E+00	4.35E+01	-1.49E+02	1.38E+02	0.0	1.77E+00
$2s3p \ ^3P_1 - 2s3d \ ^3D_3$	2.37E+00	1.55E+00	-1.52E+01	5.20E+01	-4.03E+01	0.0
$2s3p \ ^3P_2 - 2s3d \ ^3D_1$	2.37E+00	1.38E+00	-3.92E+00	5.33E+00	0.0	3.88E-02
$2s3p \ ^3P_2 - 2s3d \ ^3D_2$	2.37E+00	1.66E+01	-5.70E+01	5.48E+01	0.0	3.50E-01

$\Delta E(\text{eV})$	a_1	a_2	a_3	a_4	a_5	
$2s3p \ ^3P_2 - 2s3d \ ^3D_3$	$2.37E+00$	$7.70E+01$	$-2.41E+02$	$2.18E+02$	0.0	$1.98E+00$

	ΔE (eV)	b_1	b_2	b_3	b_4	b_5
2s2p 0P_0 - 2s2p 0P_1	0.00E+00	-6.47E+00	6.52E+01	-2.07E+02	1.94E+02	0.0
2s2p 0P_0 - 2s2p 0P_2	0.00E+00	-2.29E+00	-1.29E+01	2.46E+02	-6.49E+02	0.0
2s2p 0P_1 - 2s2p 0P_2	0.00E+00	-1.42E+01	1.83E+02	-7.65E+02	1.07E+03	0.0
2p ² 0P_0 - 2p ² 0P_1	0.00E+00	-2.13E+01	3.09E+02	-1.53E+03	2.53E+03	0.0
2p ² 0P_0 - 2p ² 0P_2	0.00E+00	-1.58E+01	2.23E+02	-1.10E+03	1.80E+03	0.0
2p ² 0P_1 - 2p ² 0P_2	0.00E+00	-2.98E+01	4.47E+02	-2.25E+03	3.75E+03	0.0
2s3p 0P_0 - 2s3p 0P_1	0.00E+00	-1.41E+01	1.58E+02	-5.84E+02	7.36E+02	0.0
2s3p 0P_0 - 2s3p 0P_2	0.00E+00	-1.20E+01	1.54E+02	-6.46E+02	9.08E+02	0.0
2s3p 0P_1 - 2s3p 0P_2	0.00E+00	-9.74E+00	1.21E+02	-4.58E+02	5.78E+02	0.0
2s3d 3D_1 - 2s3d 3D_2	0.00E+00	-1.96E+01	2.64E+02	-1.16E+03	1.69E+03	0.0
2s3d 3D_1 - 2s3d 3D_3	0.00E+00	-9.71E+00	9.16E+01	-2.17E+02	2.48E+01	0.0
2s3d 3D_2 - 2s3d 3D_3	0.00E+00	-1.86E+01	2.49E+02	-1.08E+03	1.56E+03	0.0

Explanation of Figures

Figure I. Line Intensity Ratios vs. Temperature

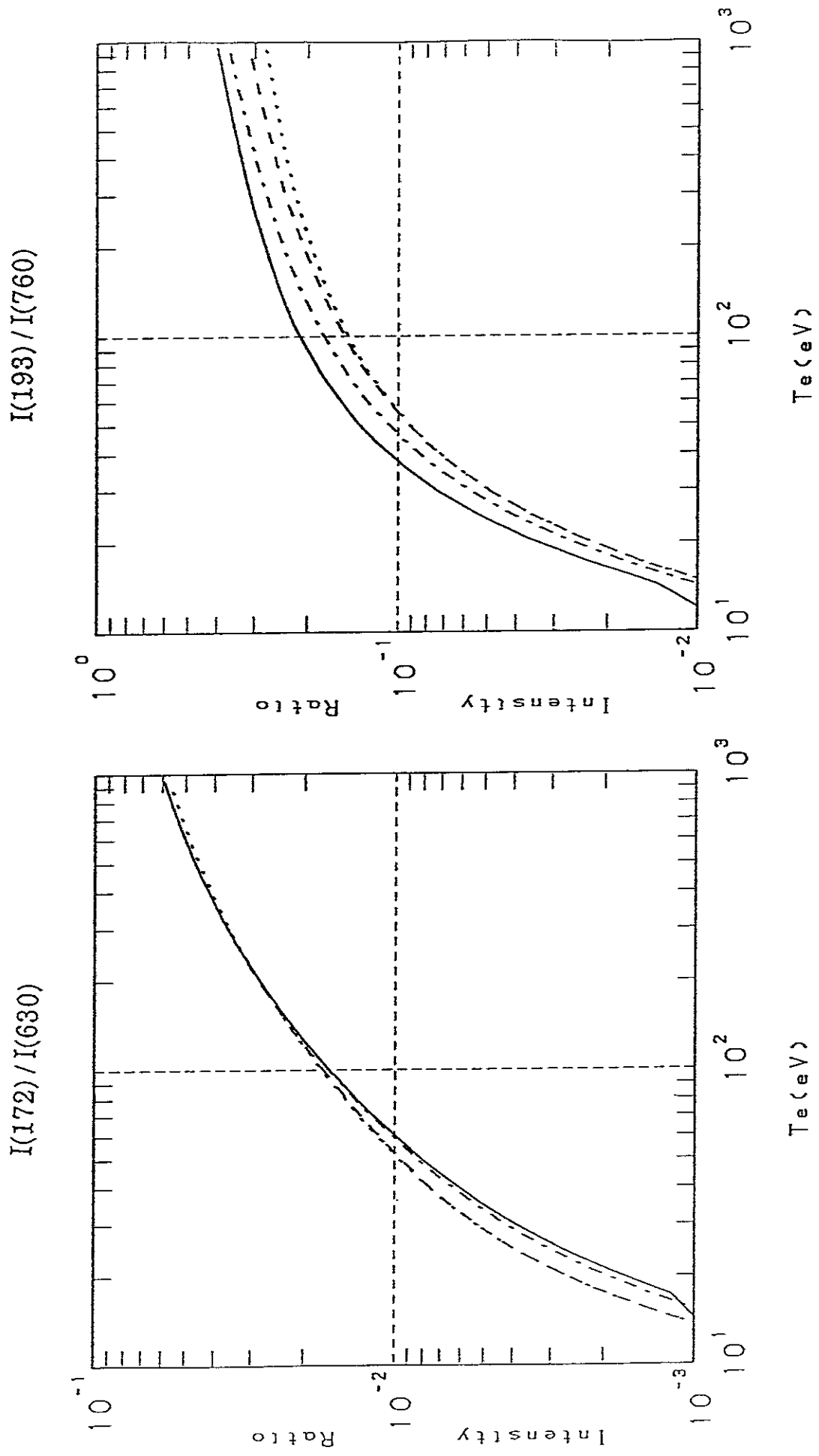
Ionization processes are included in the line intensity calculations. The curves shown are for electron densities $n_e = 10^9 \text{ cm}^{-3}$ (solid line), 10^{11} cm^{-3} (dash - dotted line) and 10^{13} cm^{-3} (dashed line) for $n(\text{OIV})=0$ and 10^{13} cm^{-3} assuming $n(\text{OIV}) = n(\text{OV})$ (dotted line). Plots are given for $I(172)/I(630)$, $I(193)/I(760)$, $I(220)/I(248)$, $I(215)/I(220)$, $I(215)/I(193)$ and $I(193)/I(220)$.

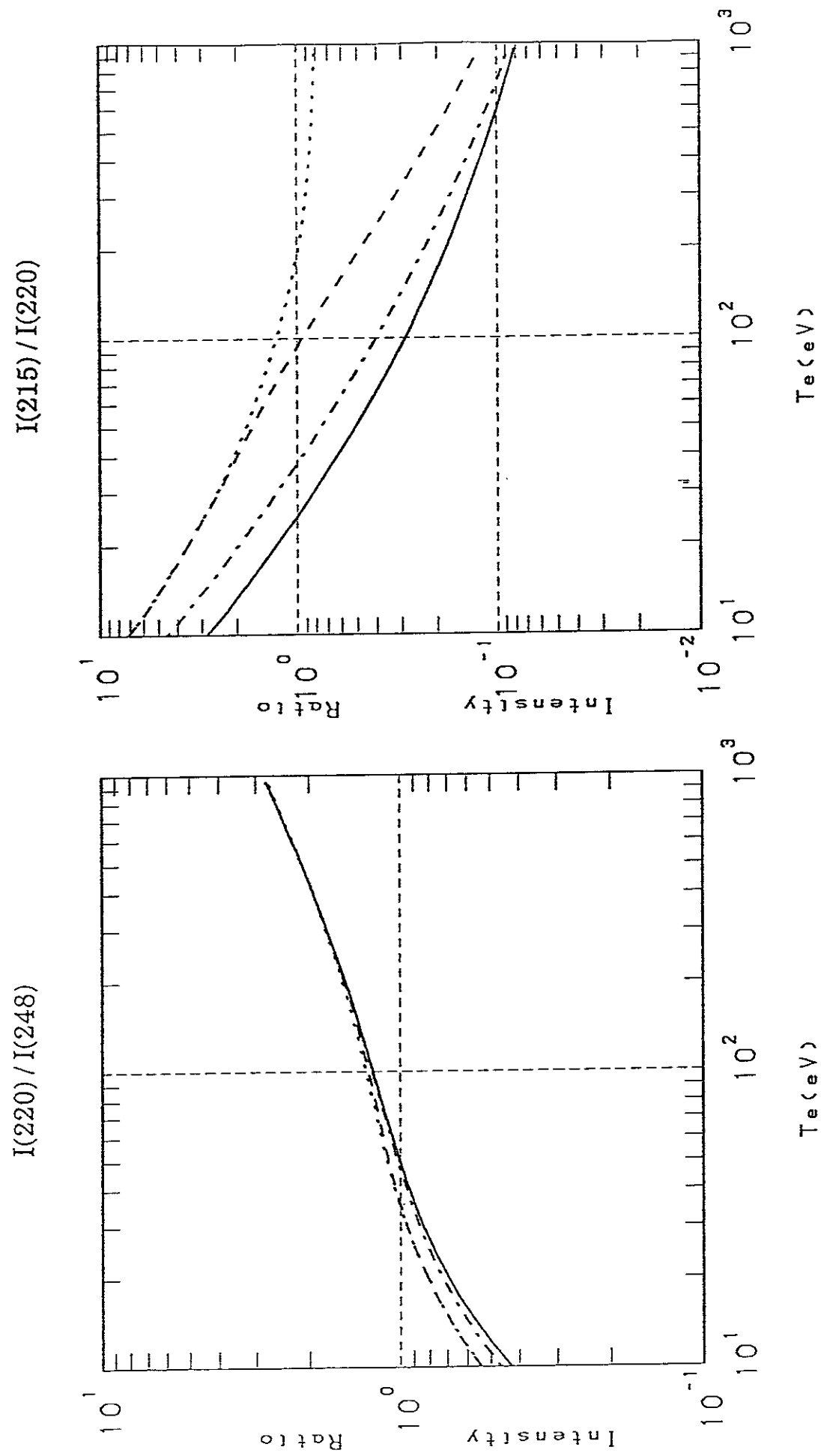
Figure II. Line Intensity Ratios vs. Density

Ionization processes are included in the line intensity calculations. The curves shown are for electron temperature $T_e = 20 \text{ eV}$ (solid line), 40 eV (dash - dotted line) and 100 eV (dashed line) for $n(\text{OIV})=0$ and 100eV assuming $n(\text{OIV}) = n(\text{OV})$ (dotted line). Plots are given for $I(220)/I(172)$ and $I(220)/I(248)$ in the singlet system and for the following cases involving the triplet system: $I(760)/I(630)$, $I(1218)/I(630)$, $I(193)/I(248)$, $I(193)/I(220)$, $I(215)/I(220)$, $I(193)/I(172)$, $I(215)/I(193)$, $I(271)/I(215)$, $I(2781.01)/I(193)$, $I(2781.01)/I(215)$, $I(760.45)/I(630)$ and $I(270.98)/I(215)$.

Ordinate	Line intensity ratio for the lines indicated at the top of the graph. Wavelengths (in angstrom) refer to transitions as indicated in Fig. 1 and Table 2 in the text. In the case of transitions involving triplets, truncation of the decimal in the wavelength indicates that line intensities for multiplets are summed.
Abscissa	Electron temperature T_e (in eV), or the electron density, n_e (in cm^{-3}).

Figure I





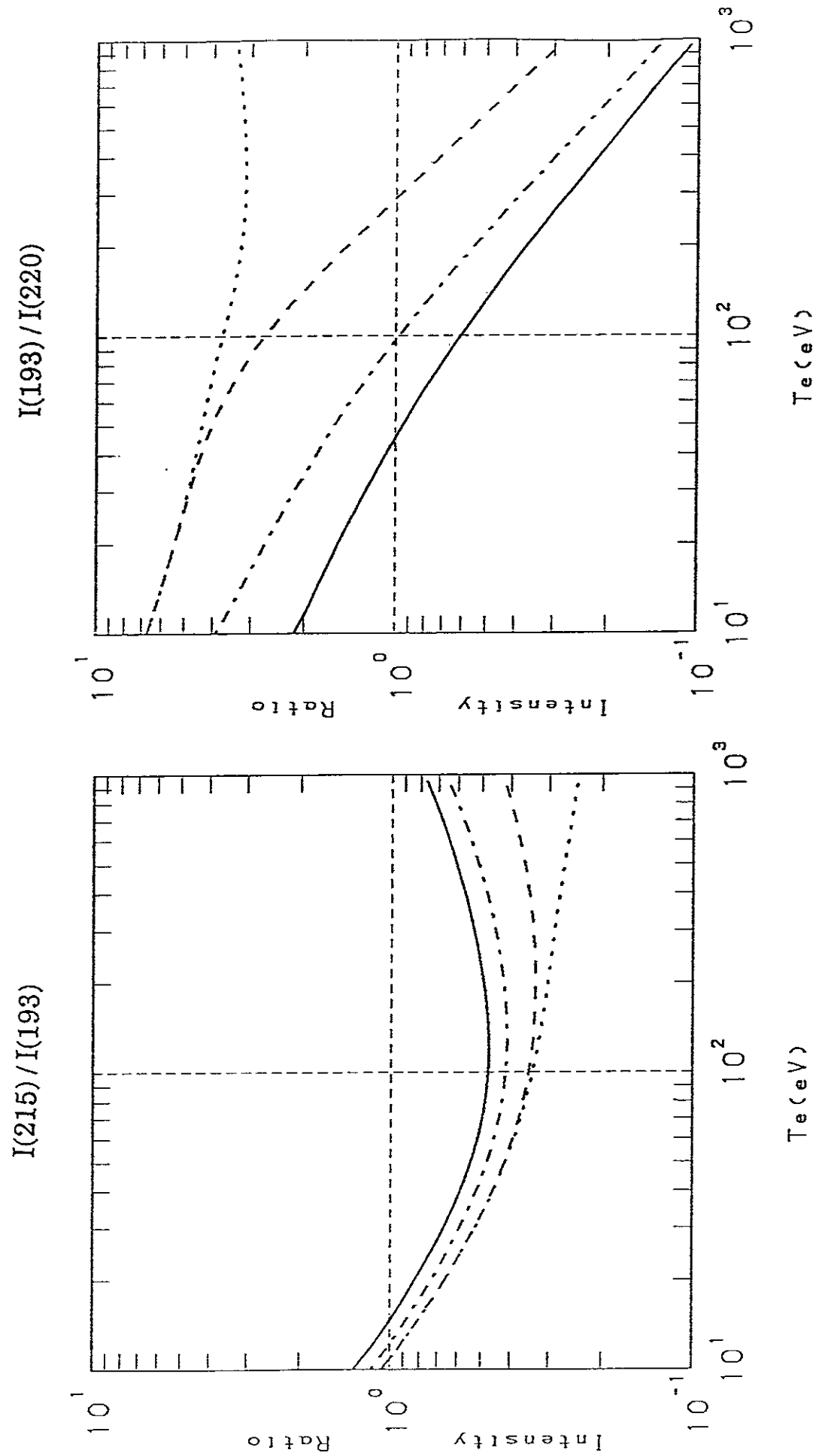
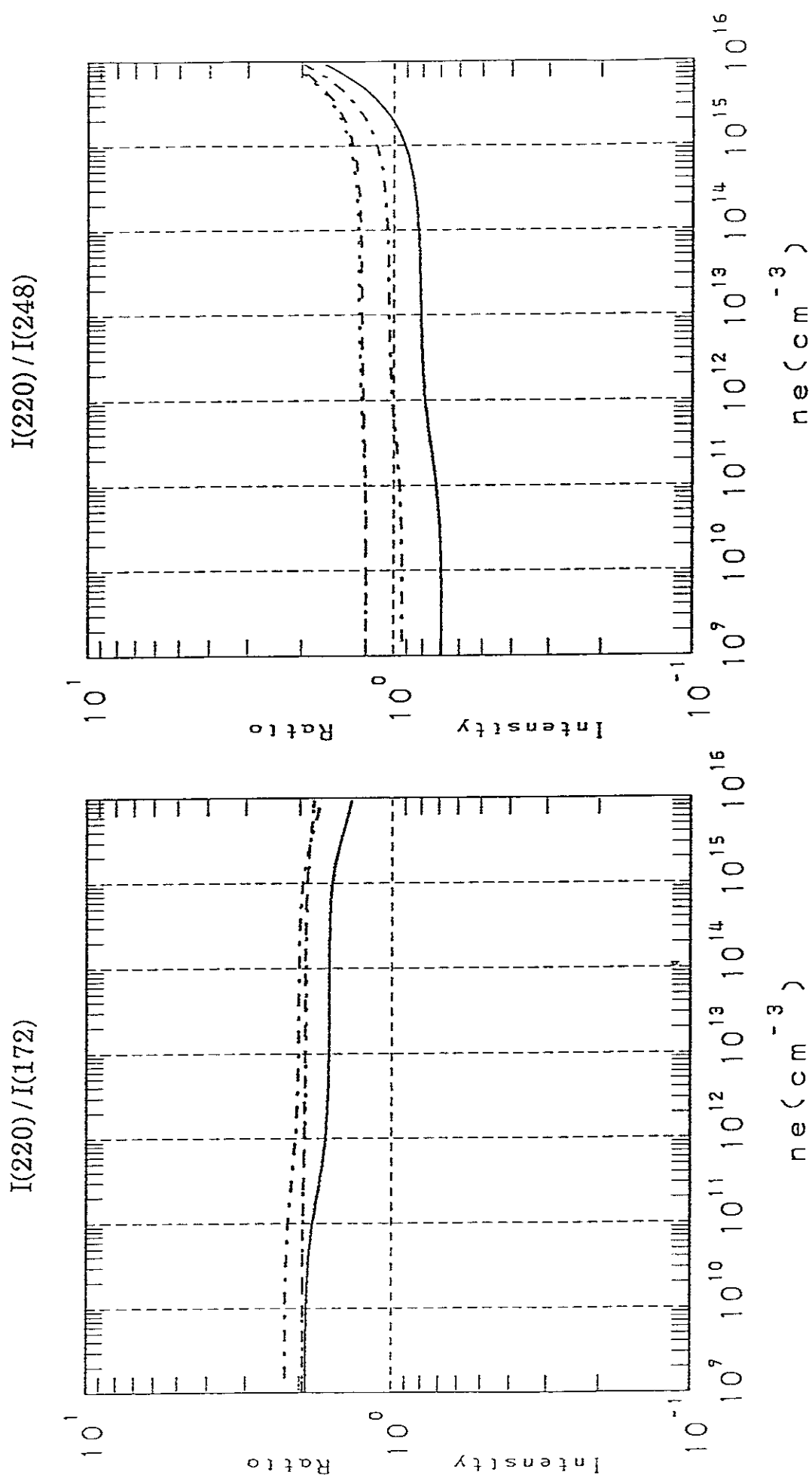
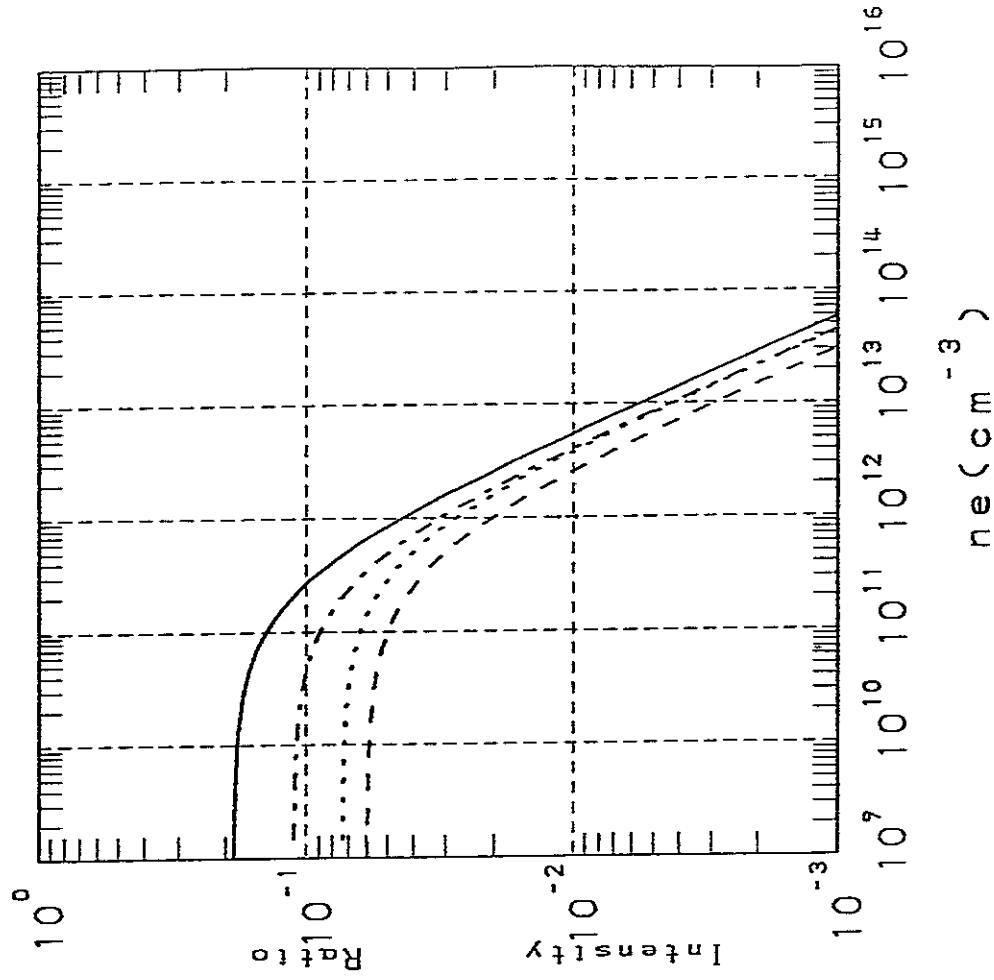


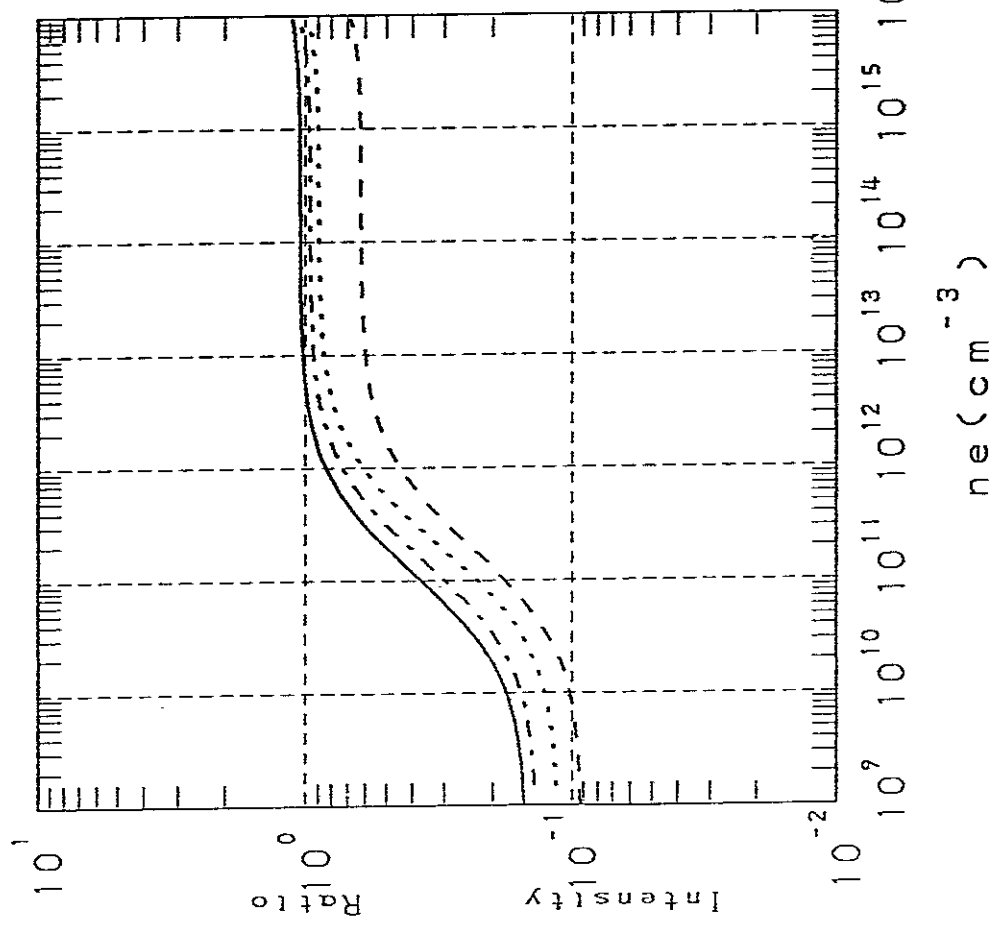
Figure II



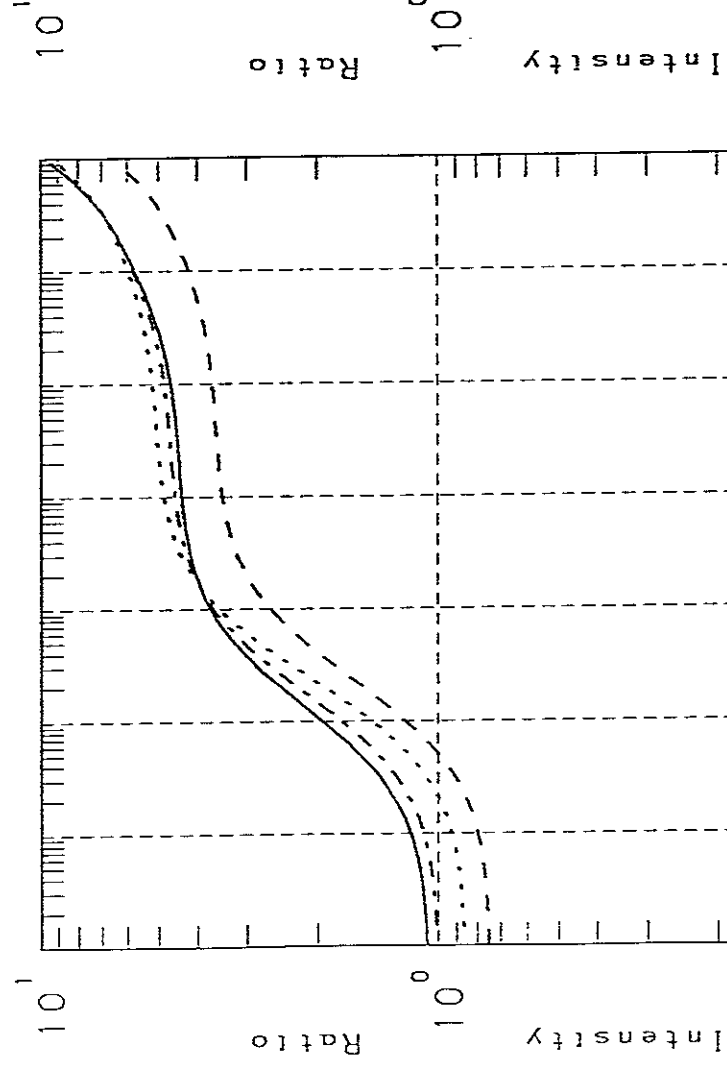
$I(1218) / I(630)$



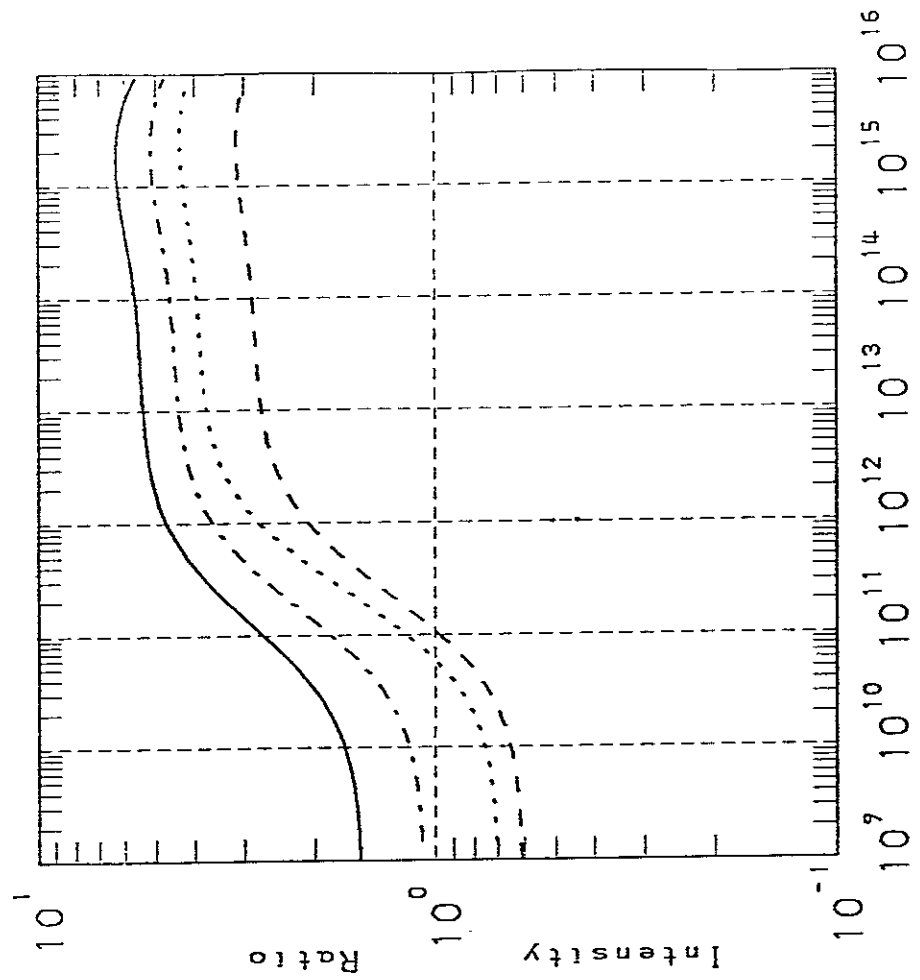
$I(760) / I(630)$

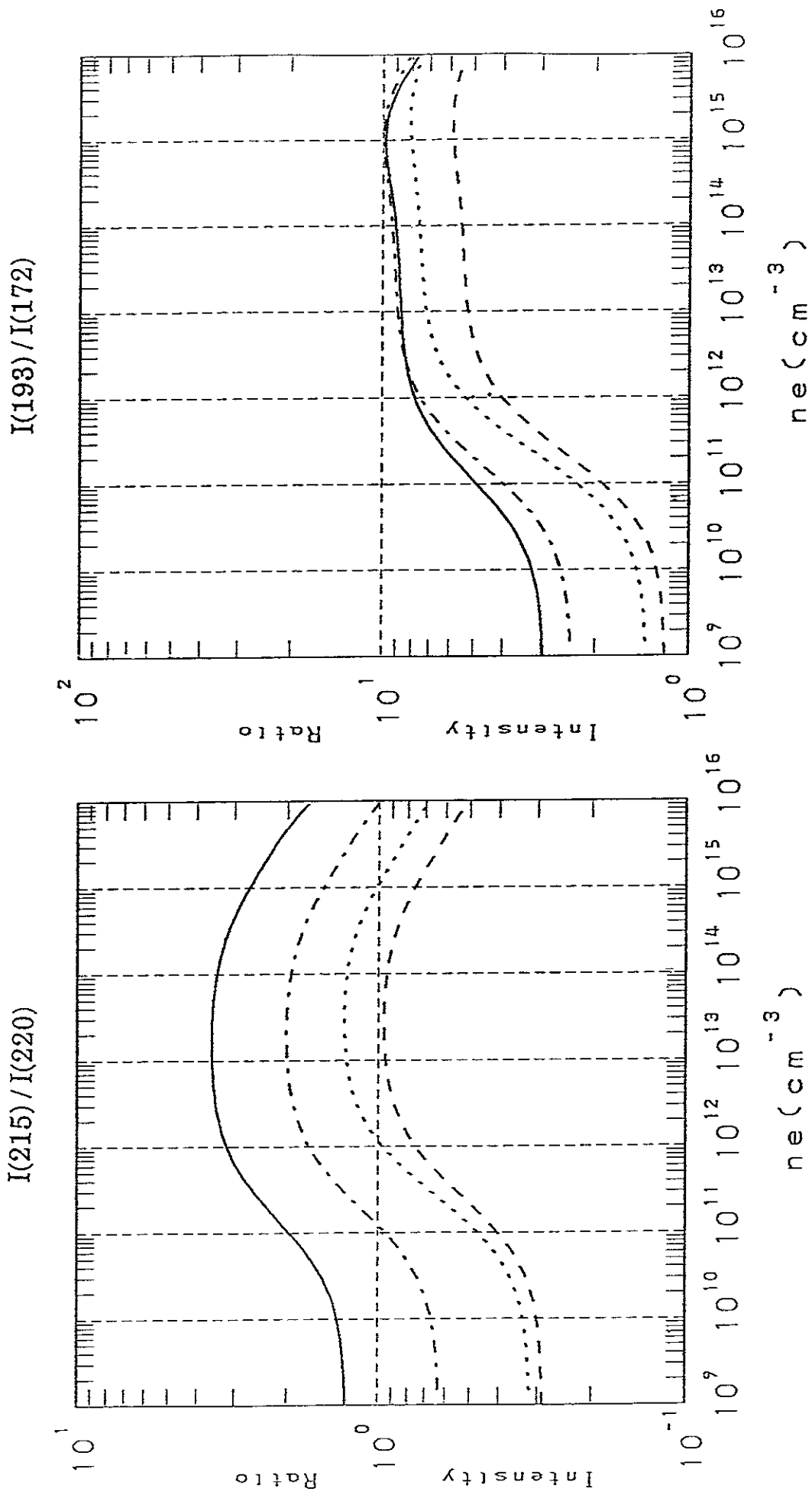


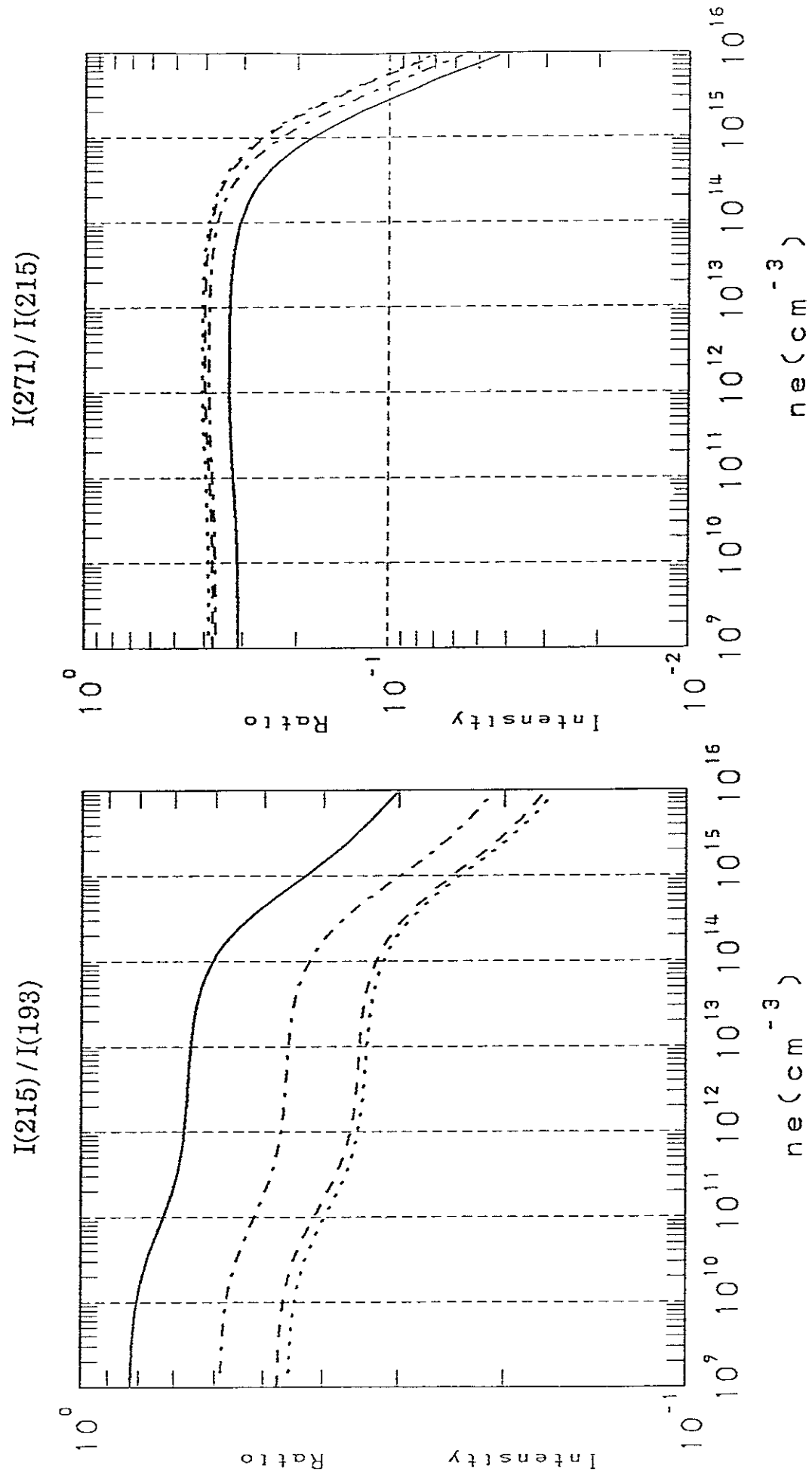
I(193) / I(248)

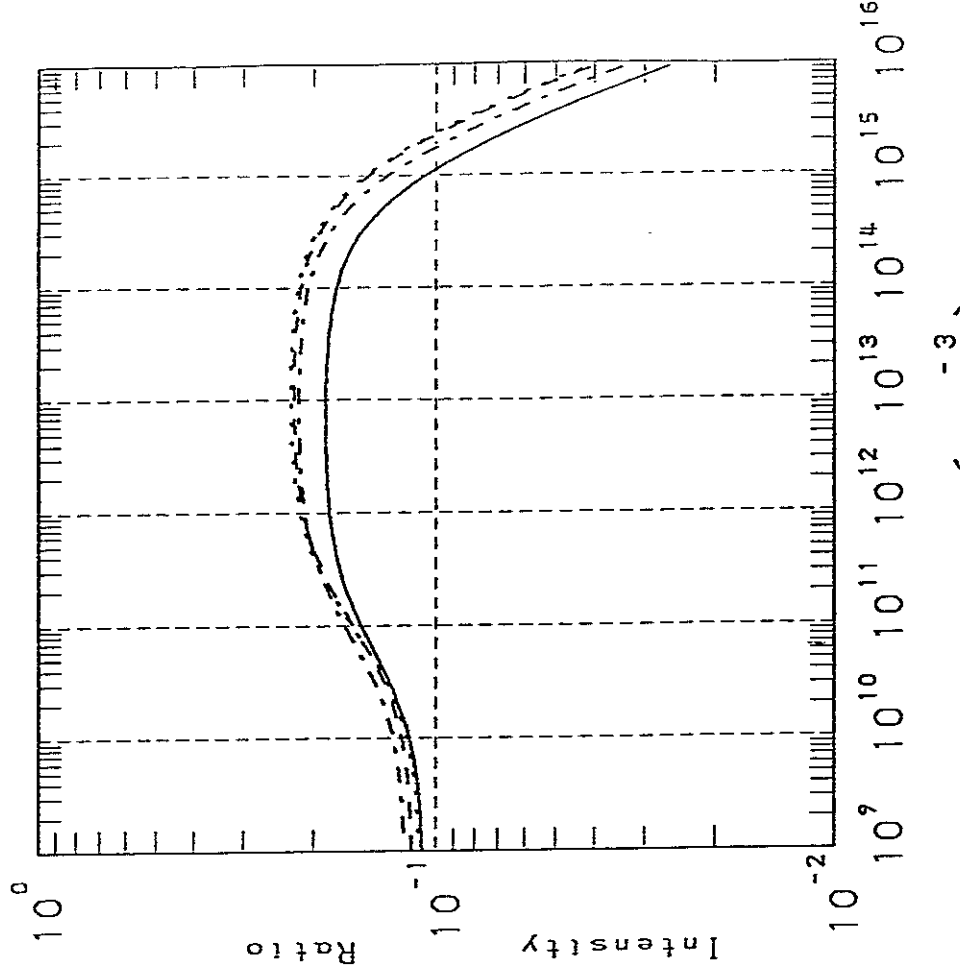
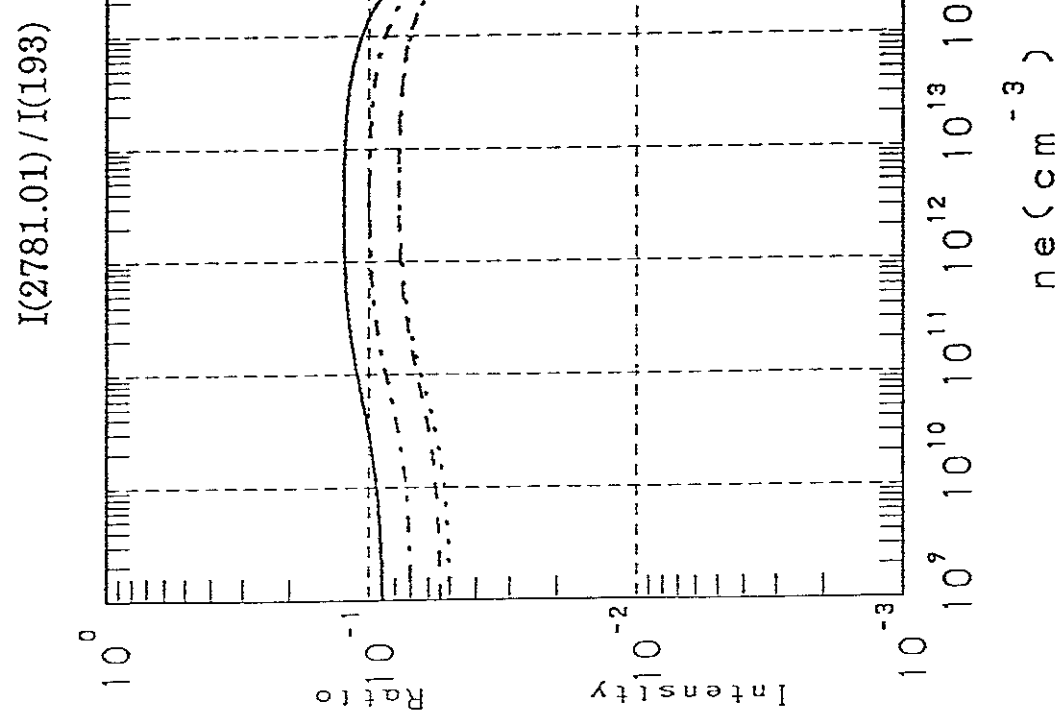


I(193) / I(220)









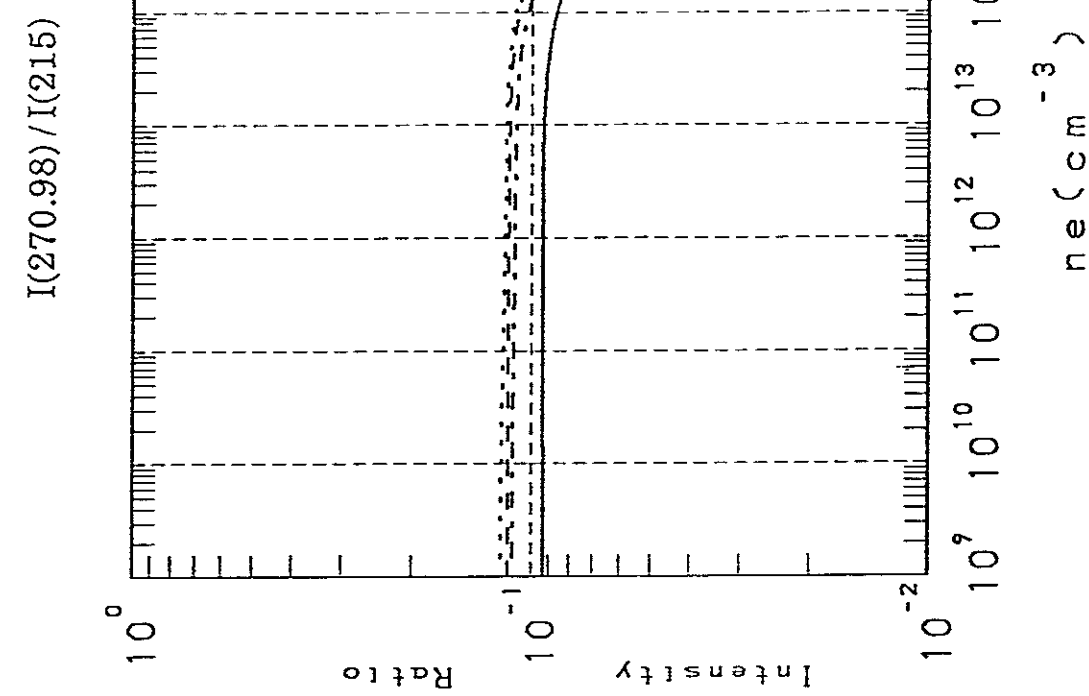
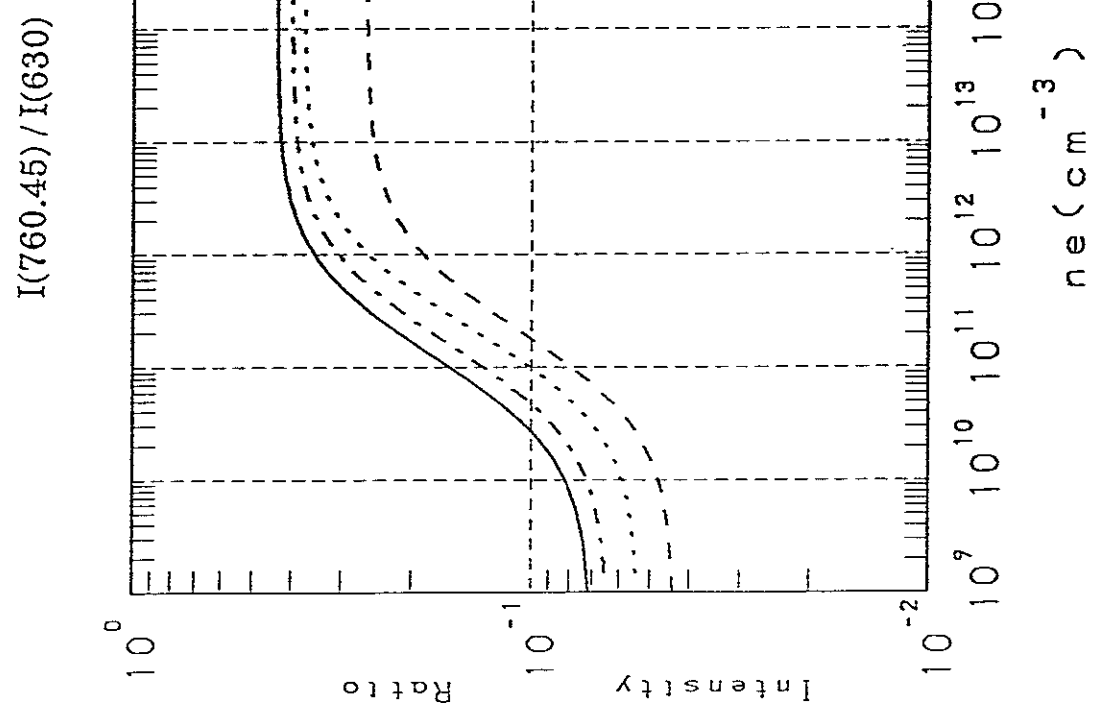
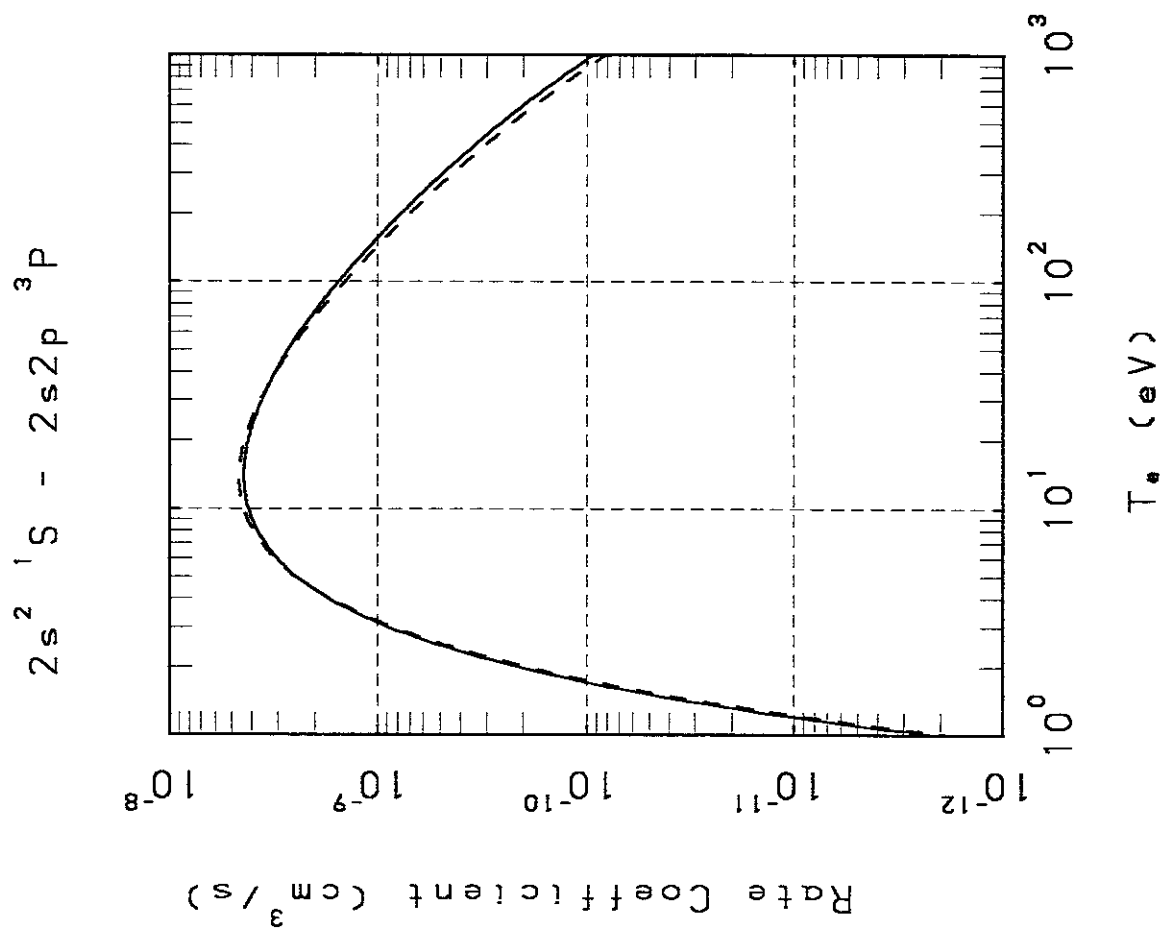
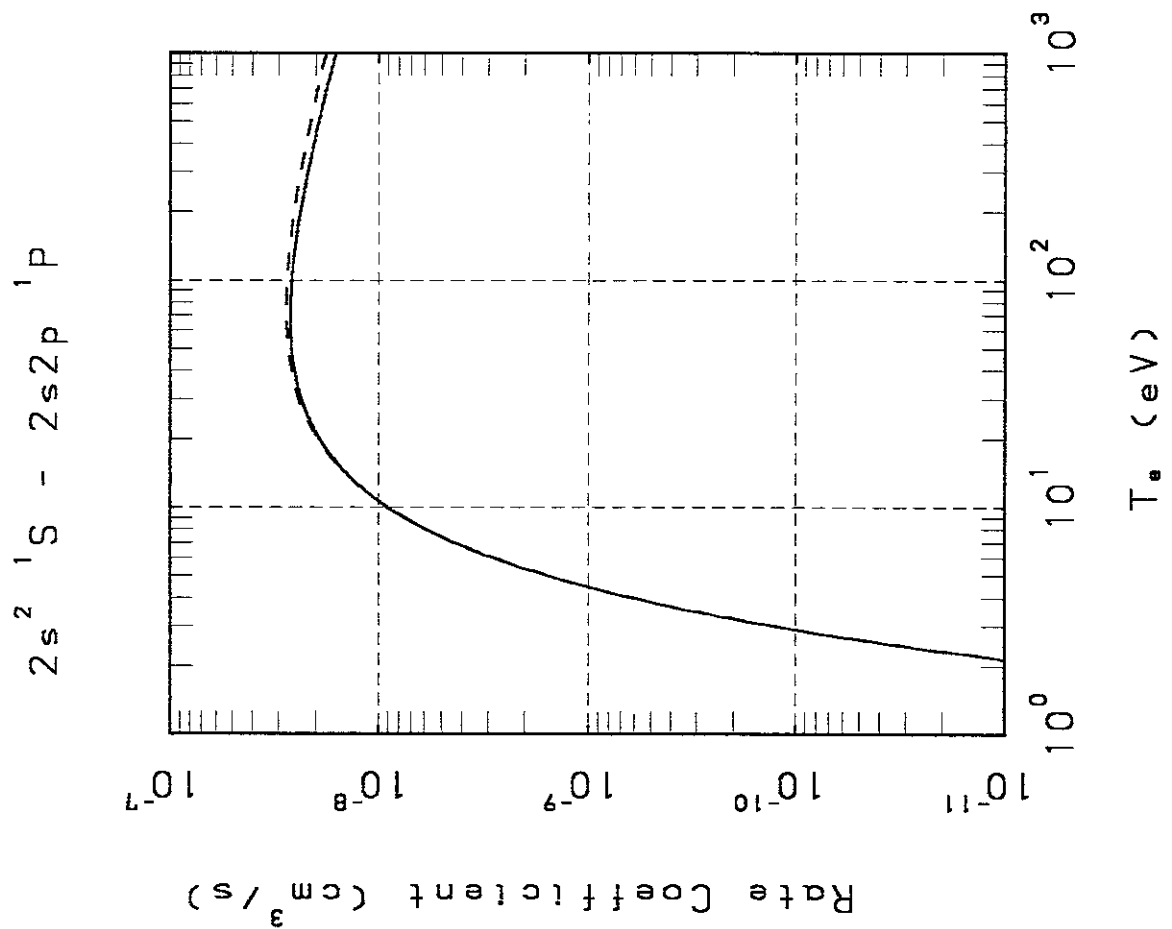
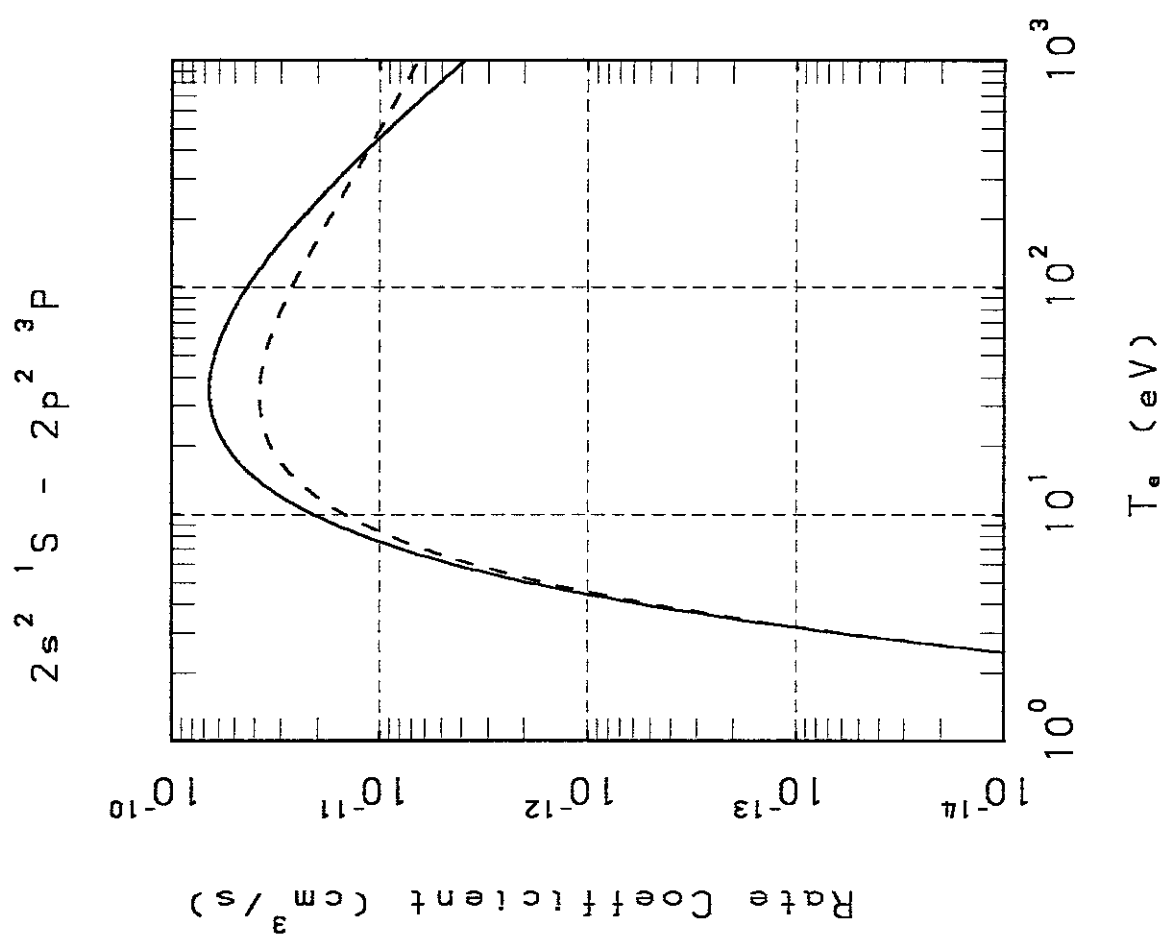
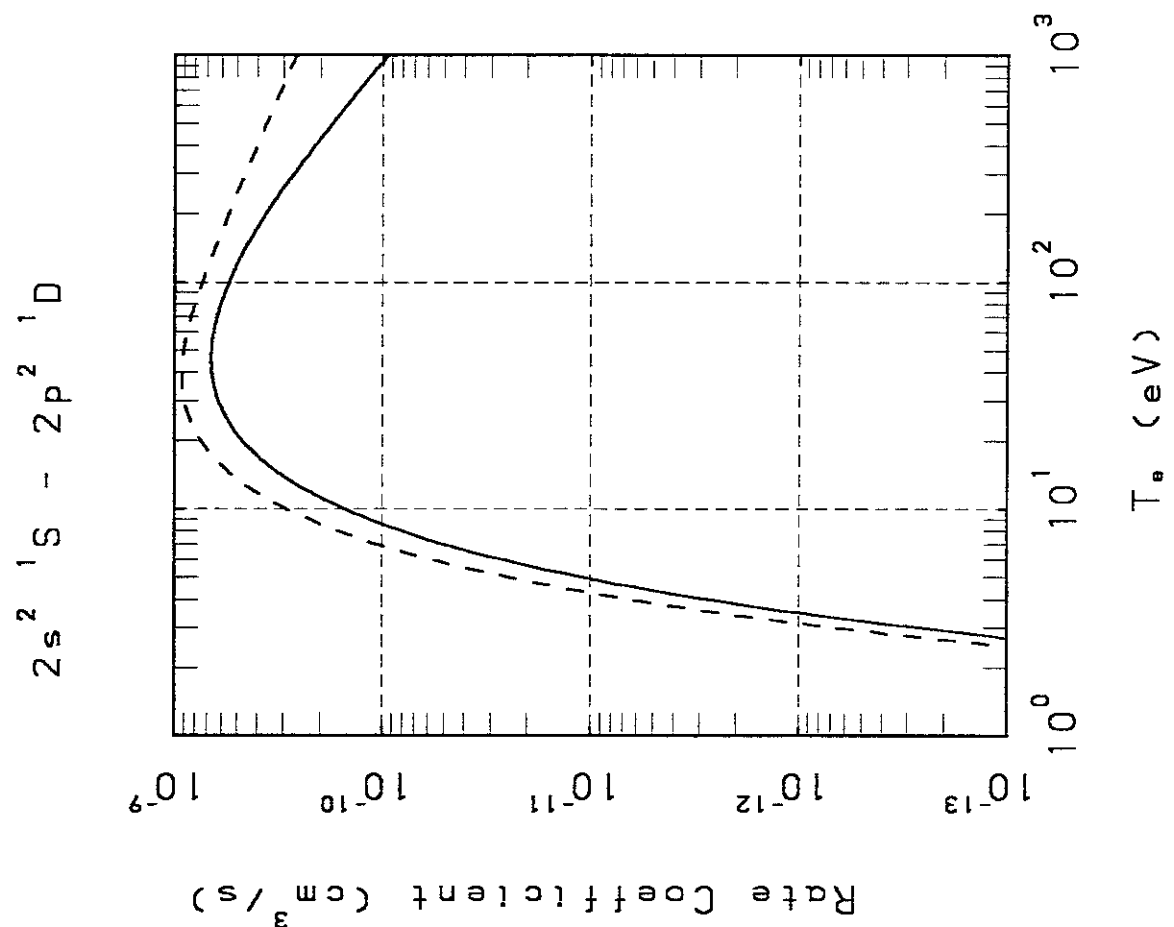
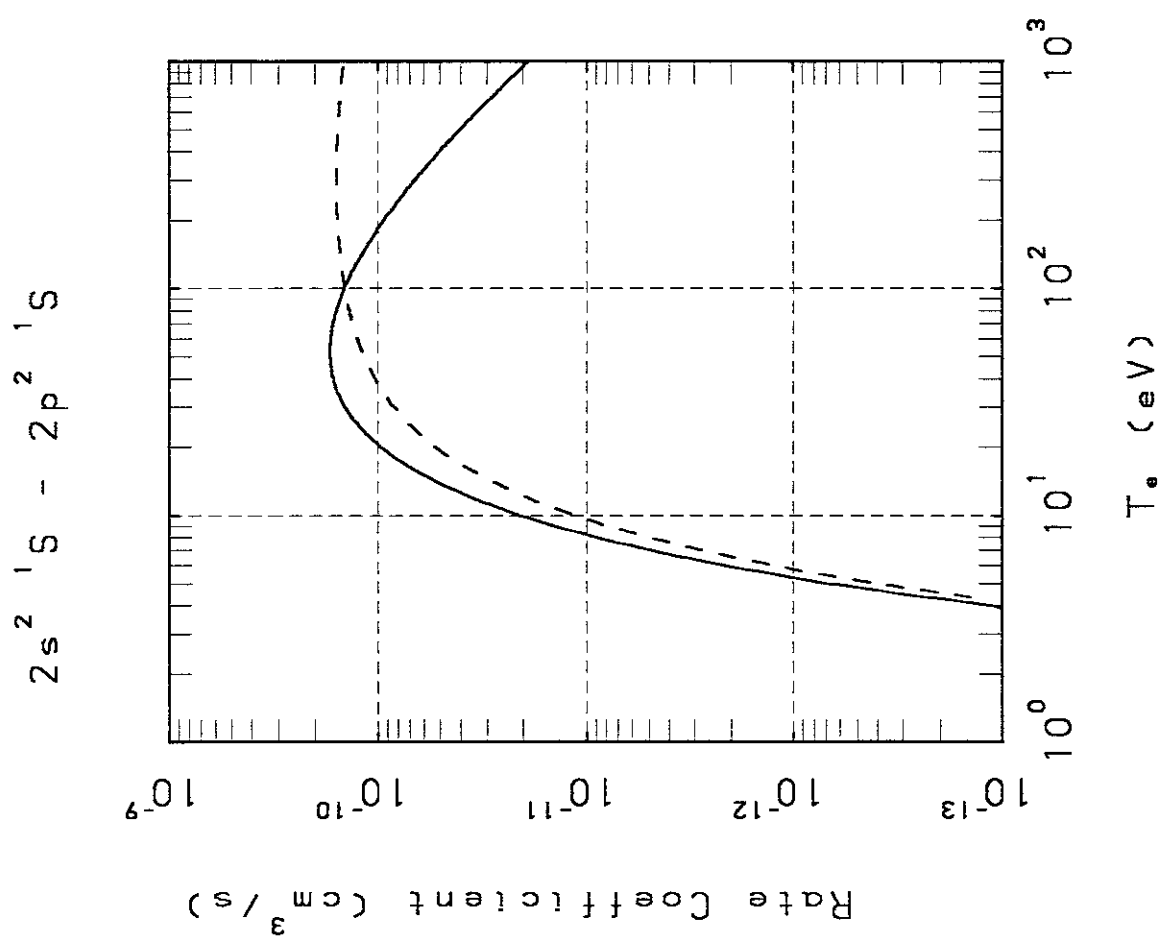
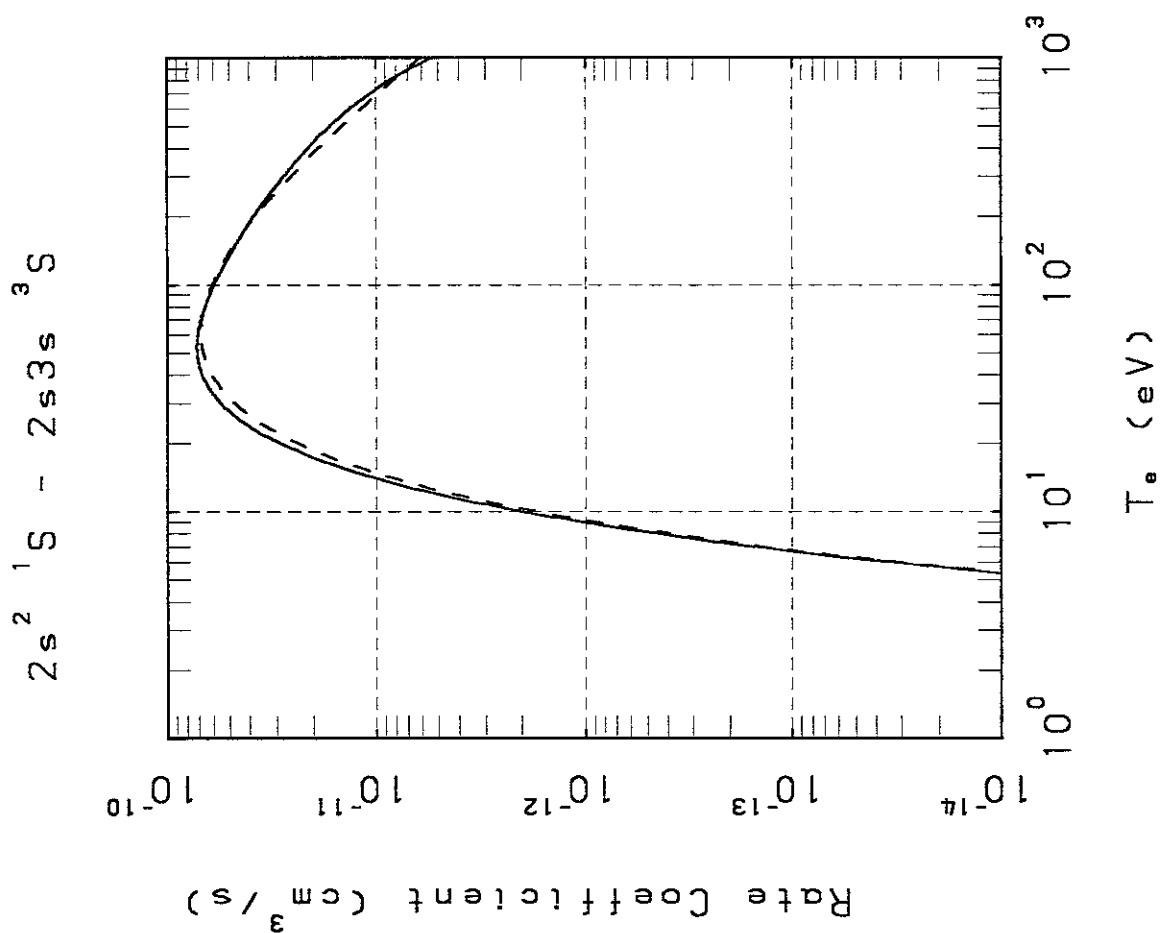


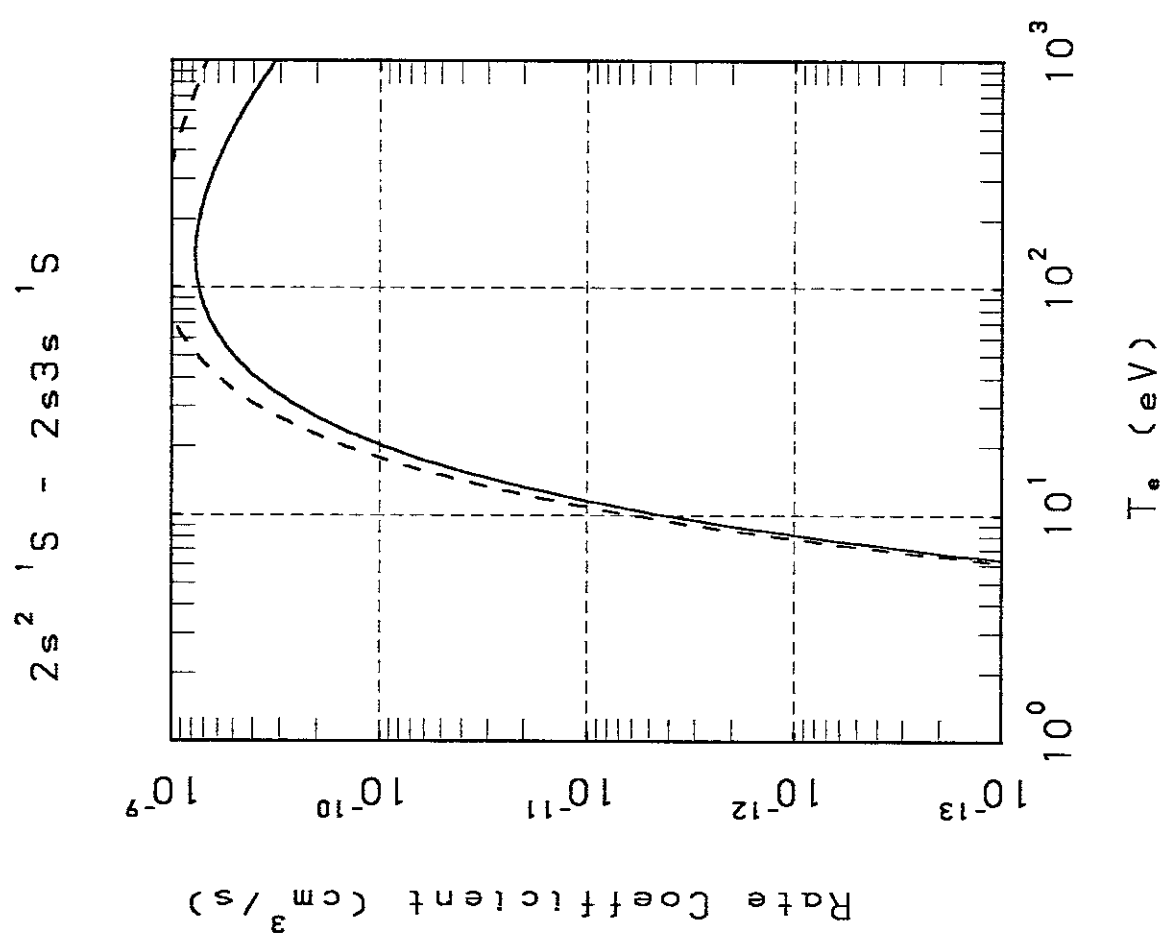
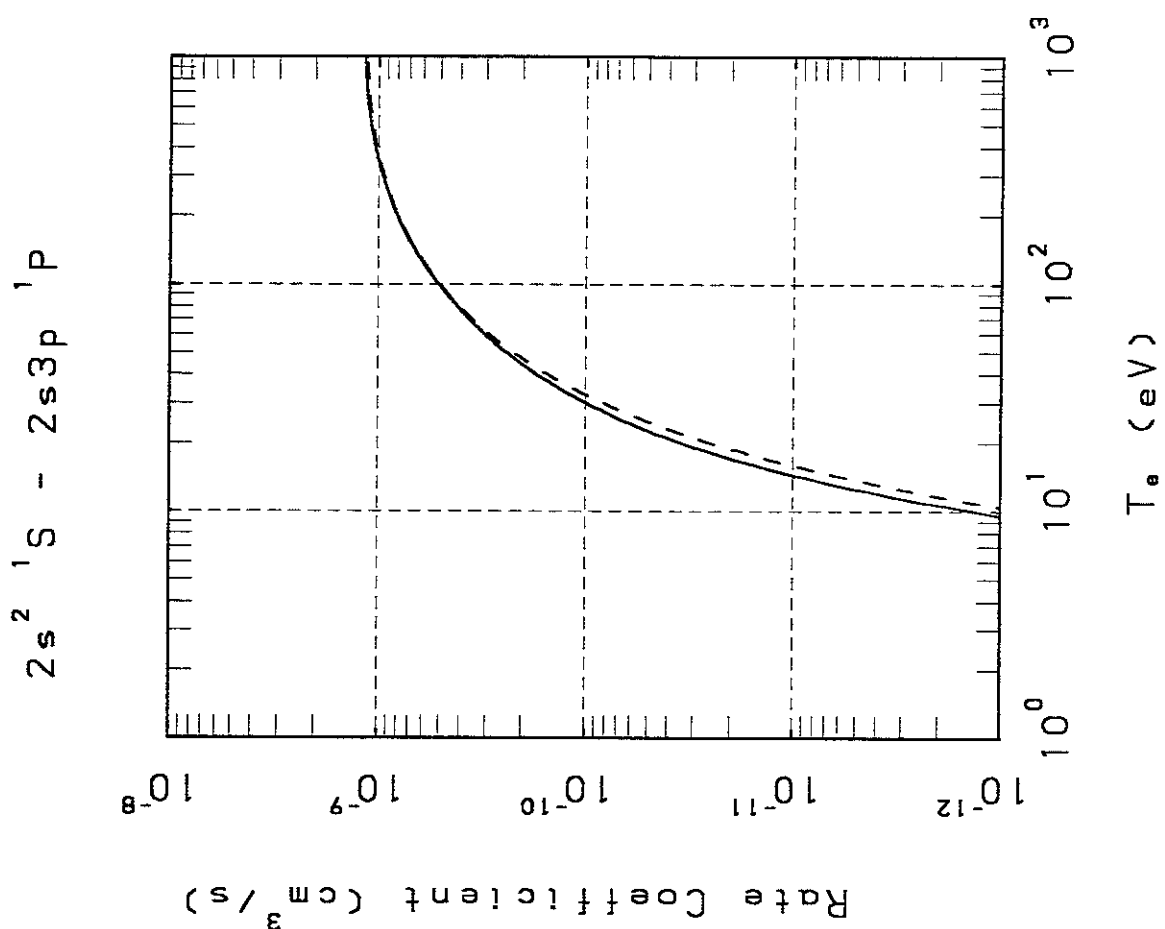
Figure III. Recommended Excitation Rate Coefficients

Excitation rate coefficients ($\text{cm}^3 \text{s}^{-1}$) are plotted against electron temperature T_e (eV). Transitions between energy terms are shown first, followed by transitions between the triplet fine structure levels. Dashed lines indicate values from Ref. 17. The initial and final states are given at the top of each figure using the same notation as that in Table I. ,

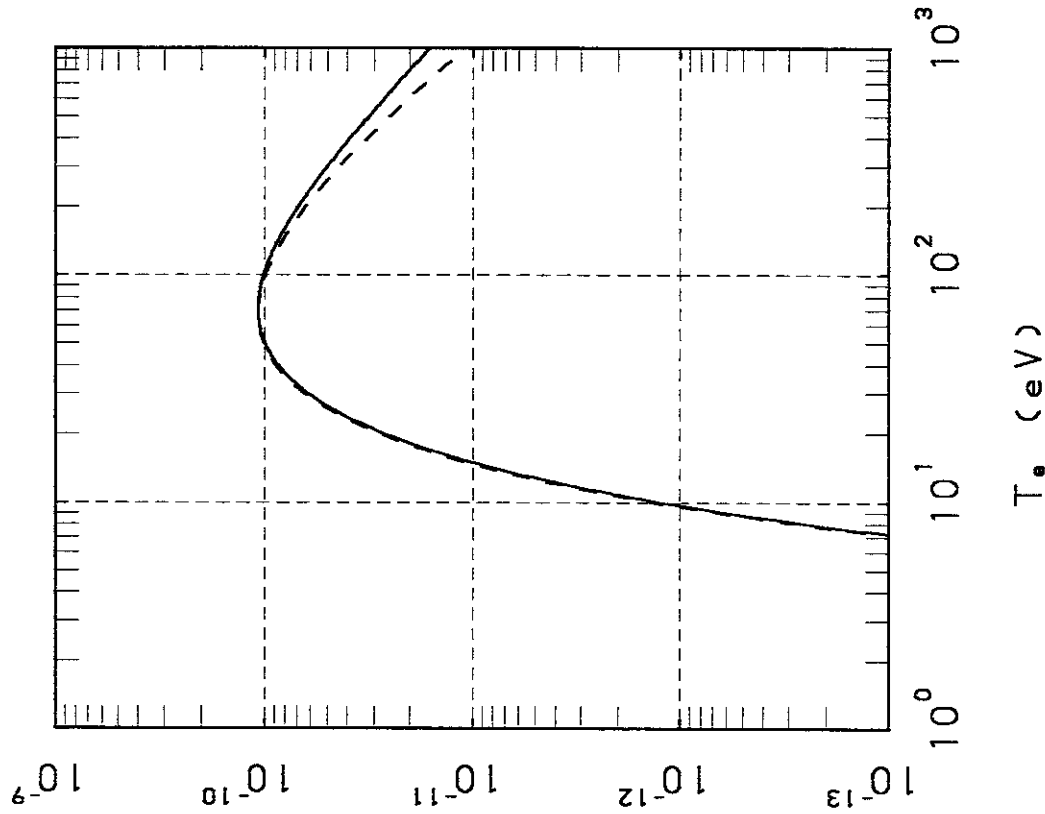




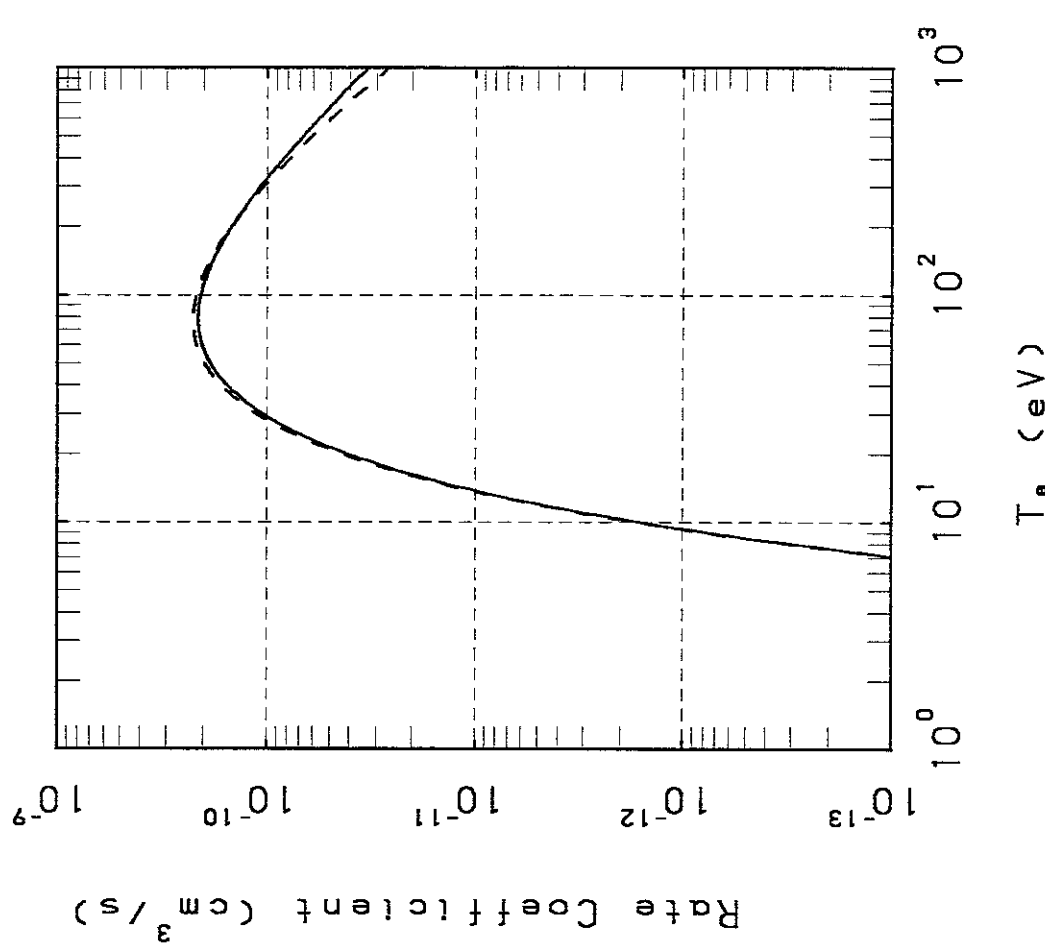




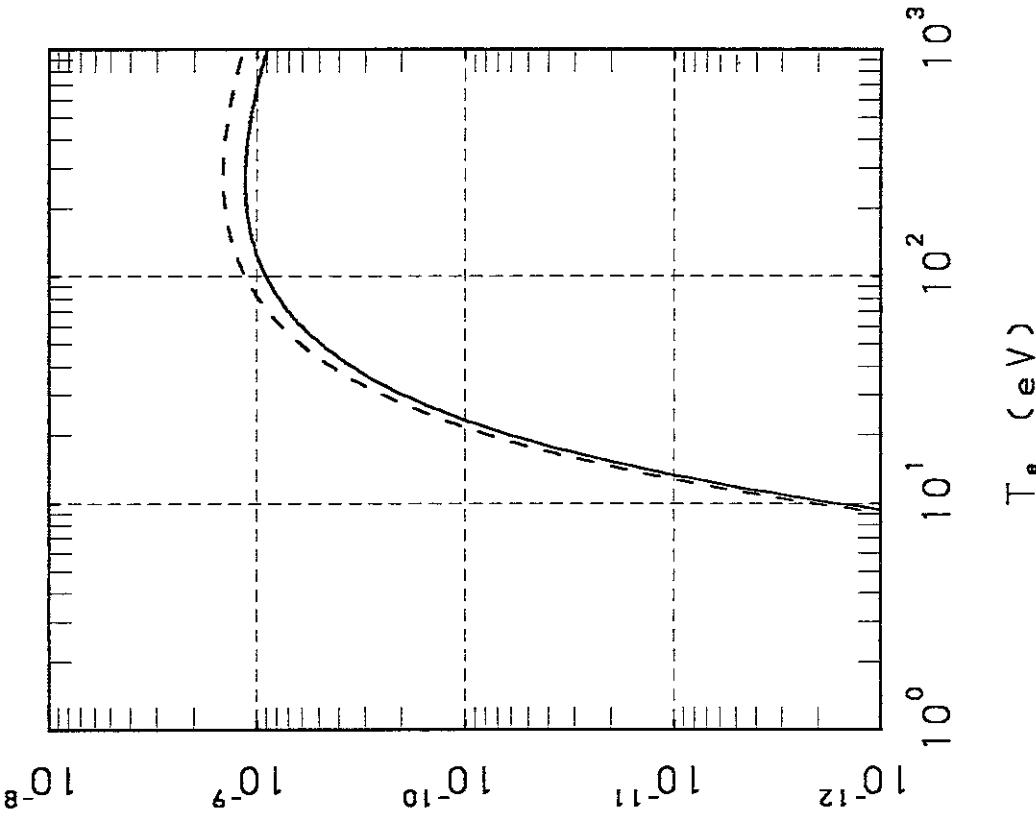
$2s^2 1S - 2s3p \ ^3P$



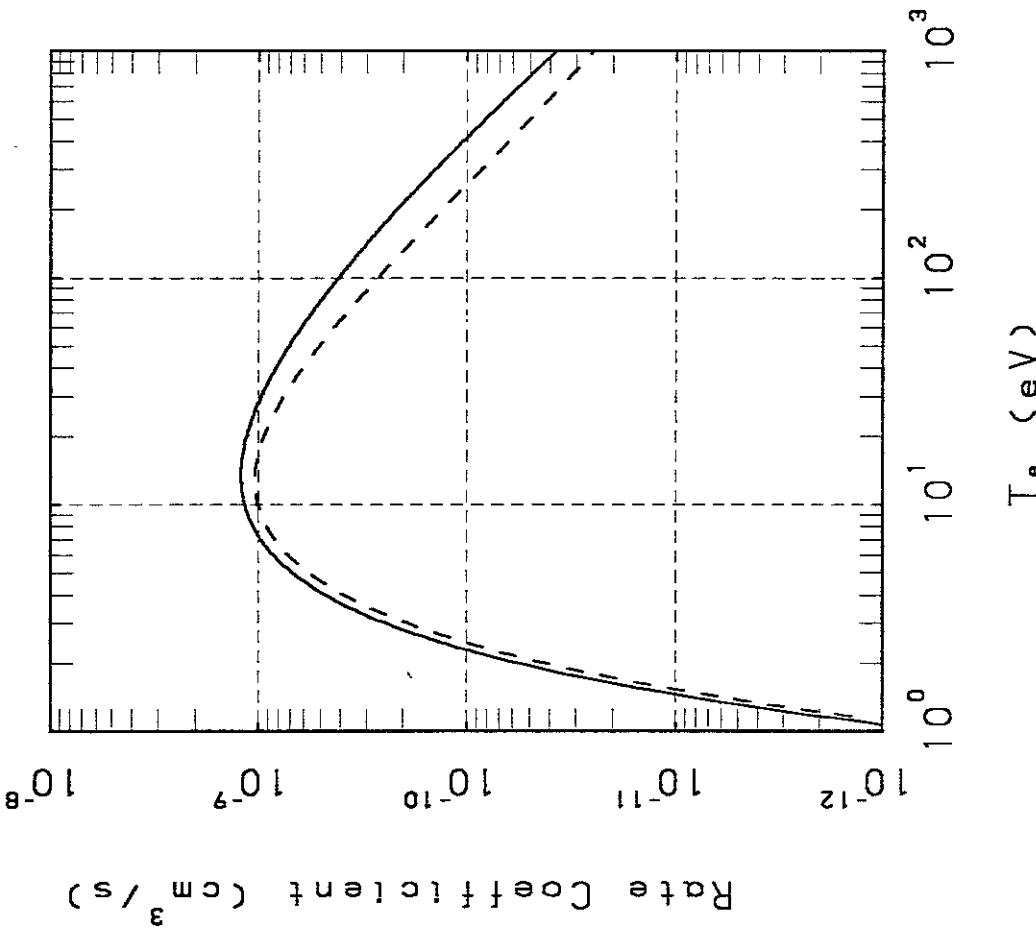
$2s^2 1S - 2s3d \ ^3D$



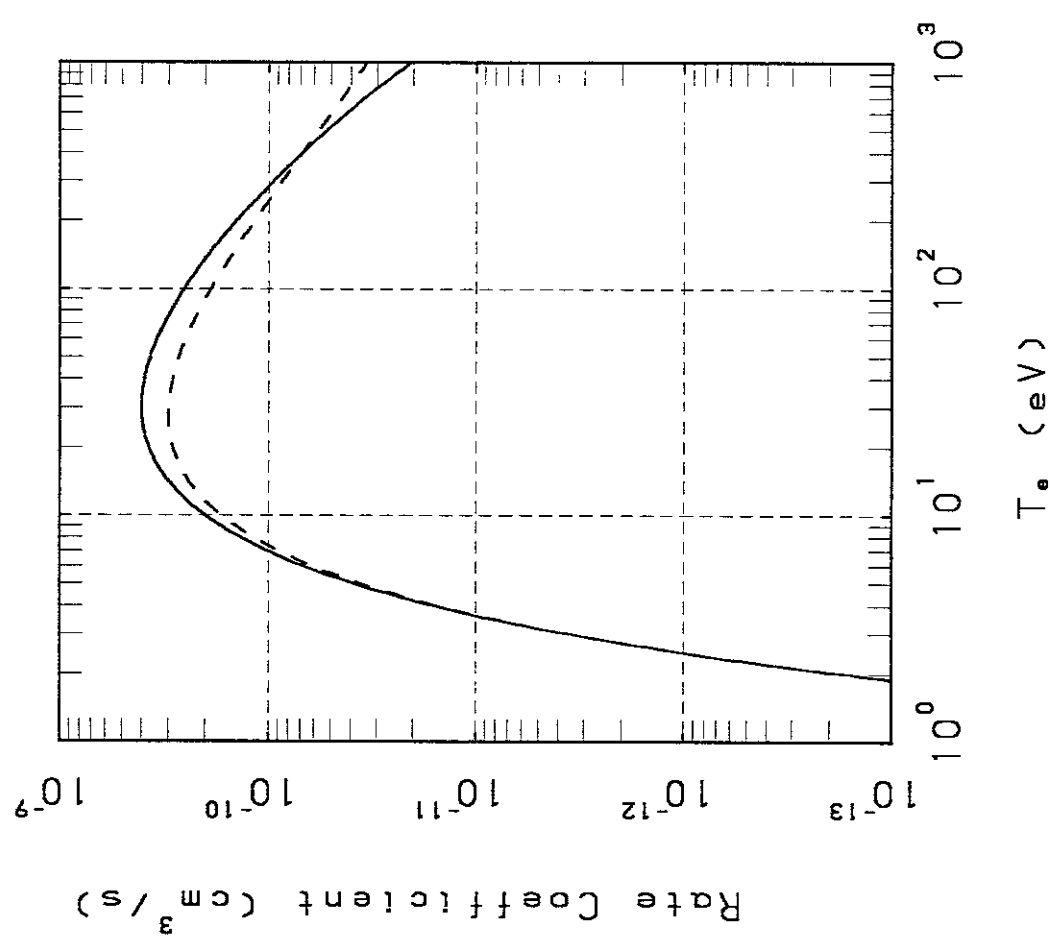
$2s^2 1S - 2s3p 1D$



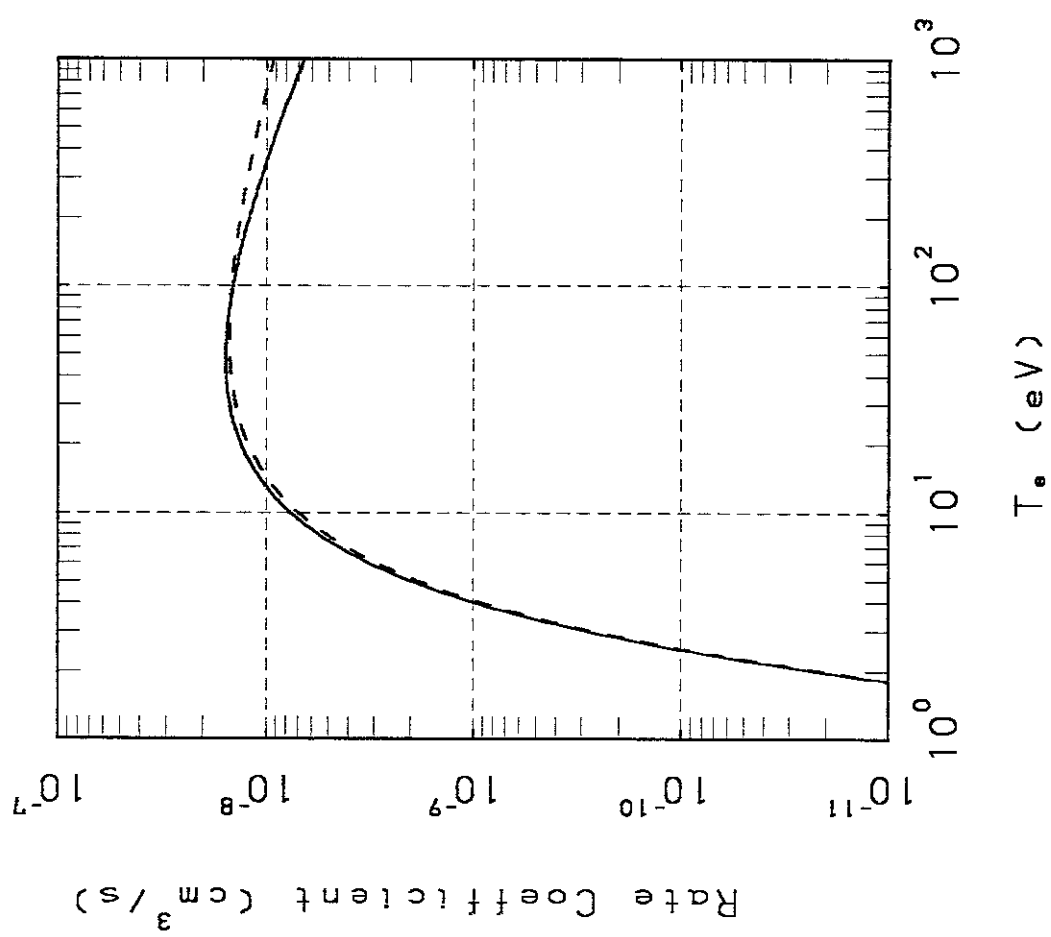
$2s2p 3P - 2s2p 1P$

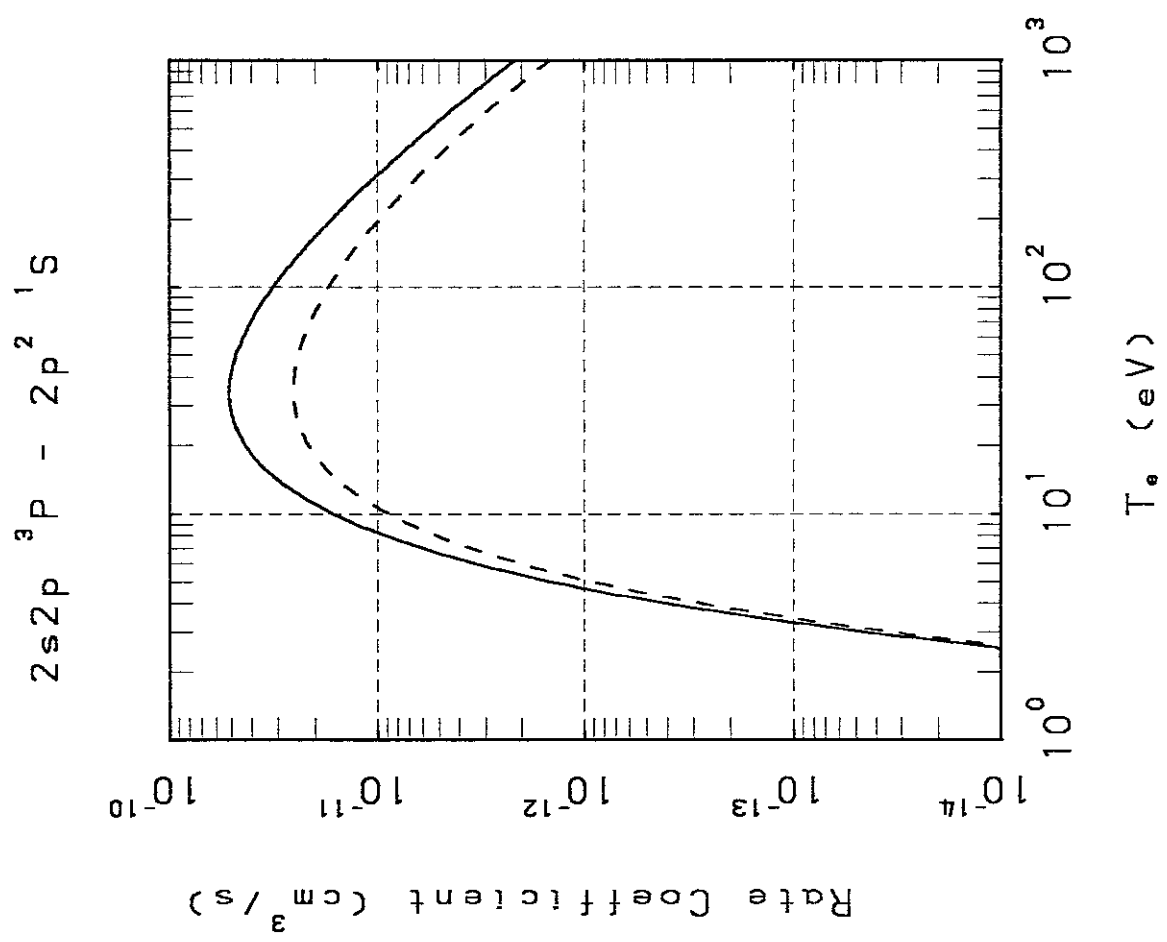
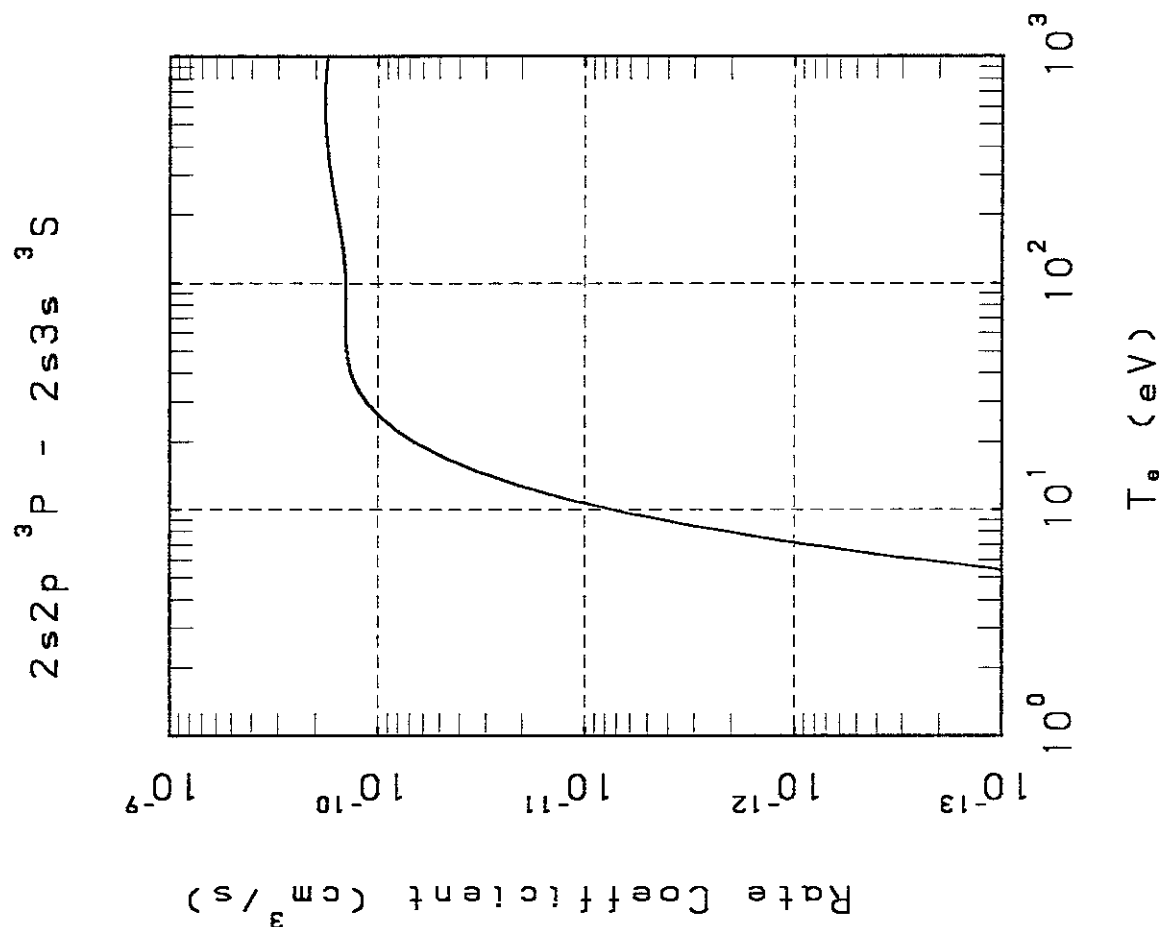


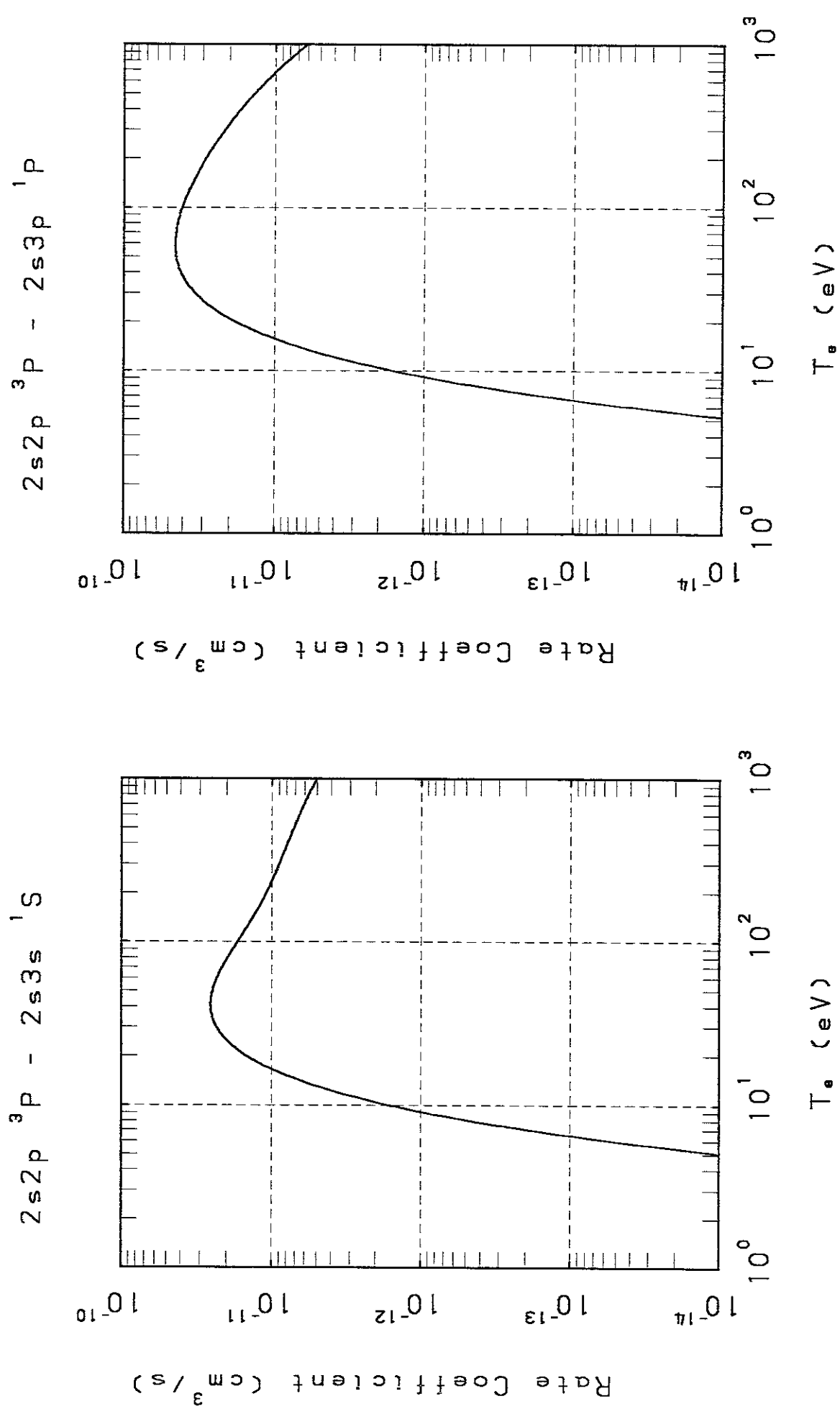
$2s\ 2p\ ^3P - 2p\ ^2D$

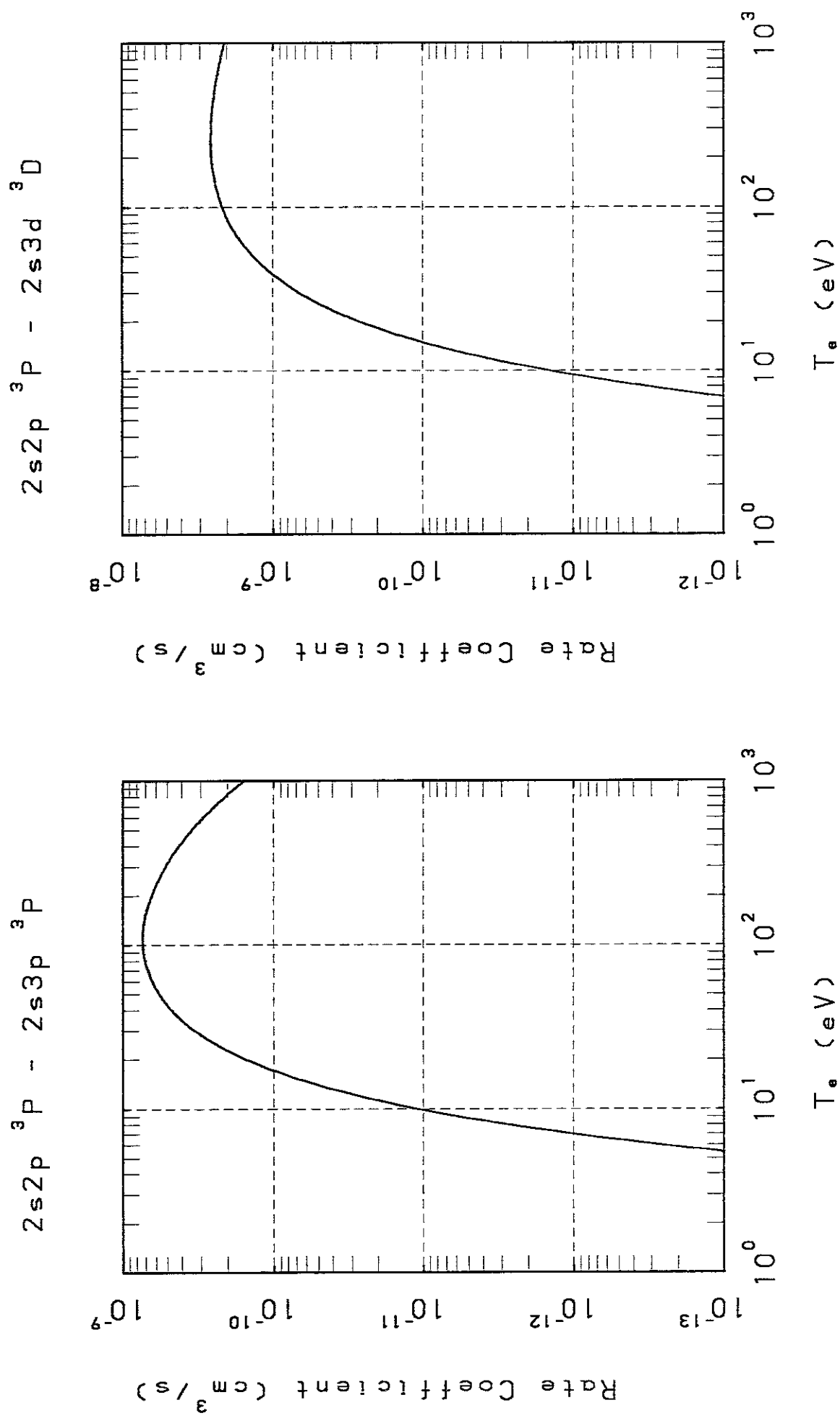


$2s\ 2p\ ^3P - 2p\ ^2P$

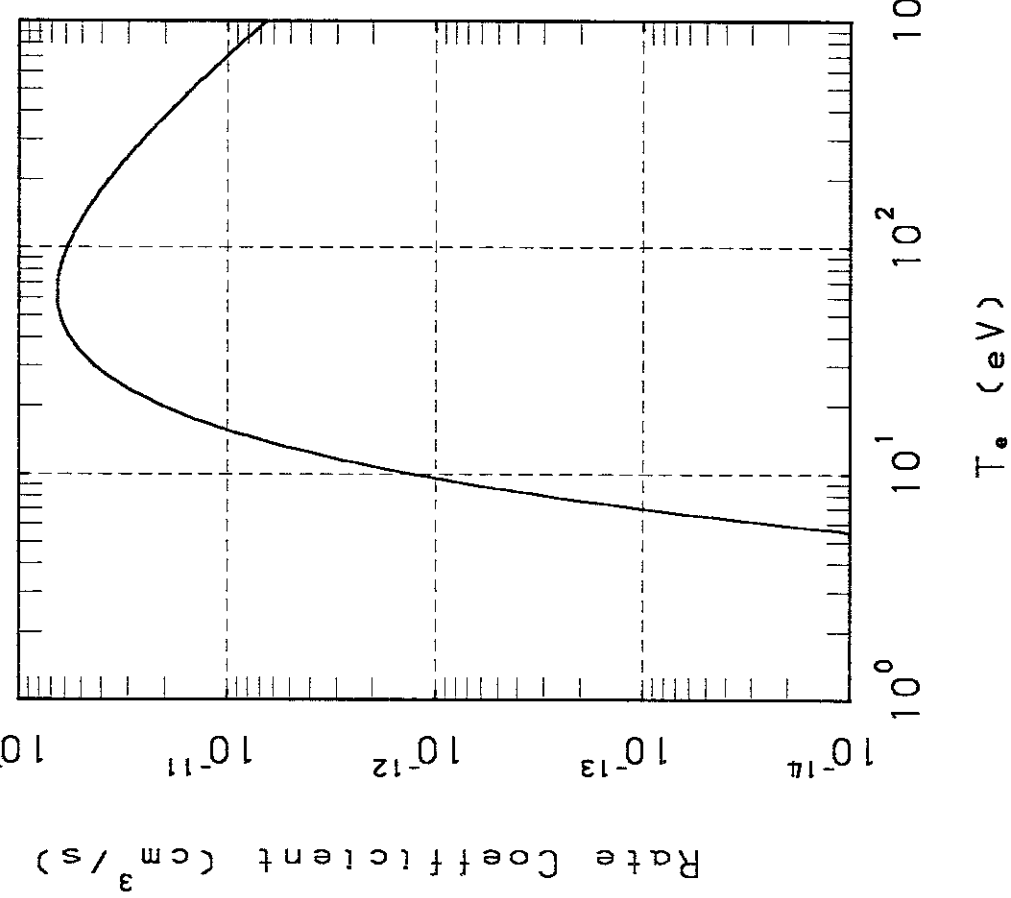




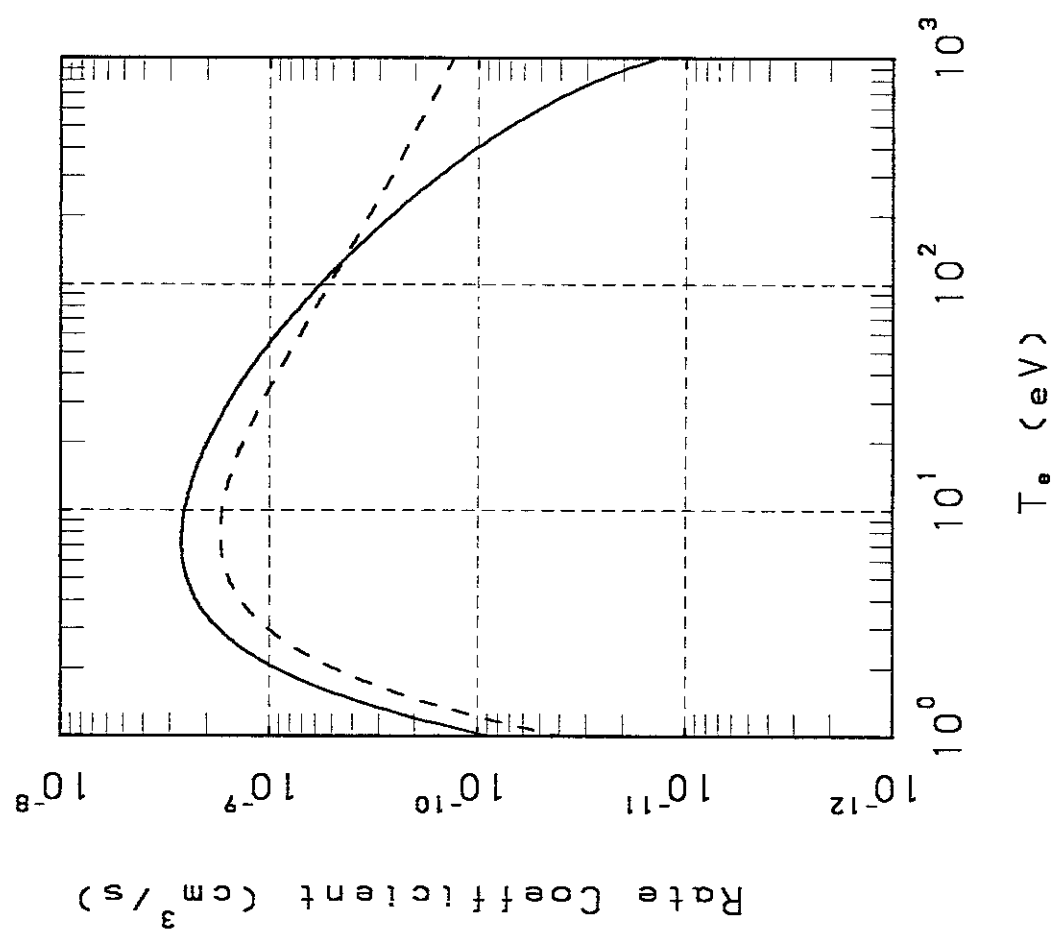


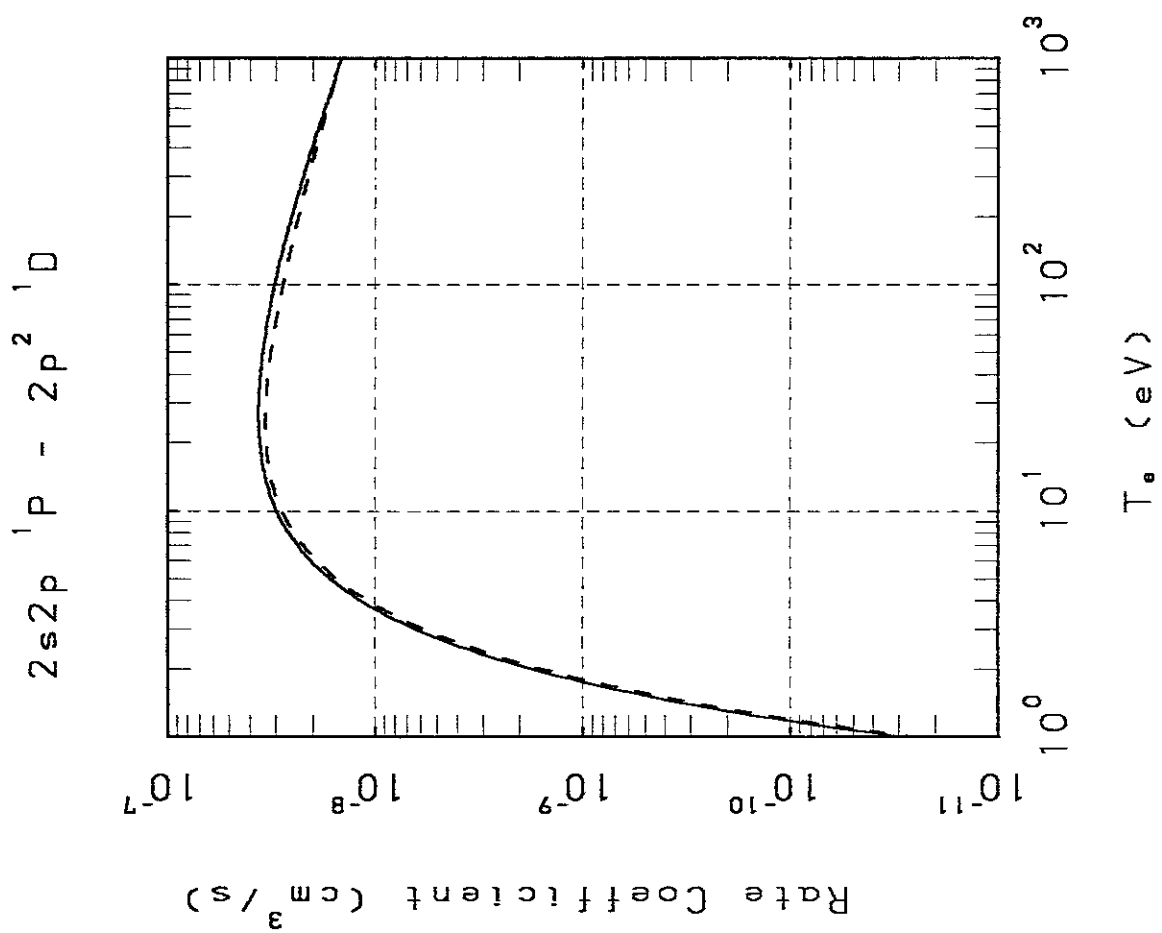
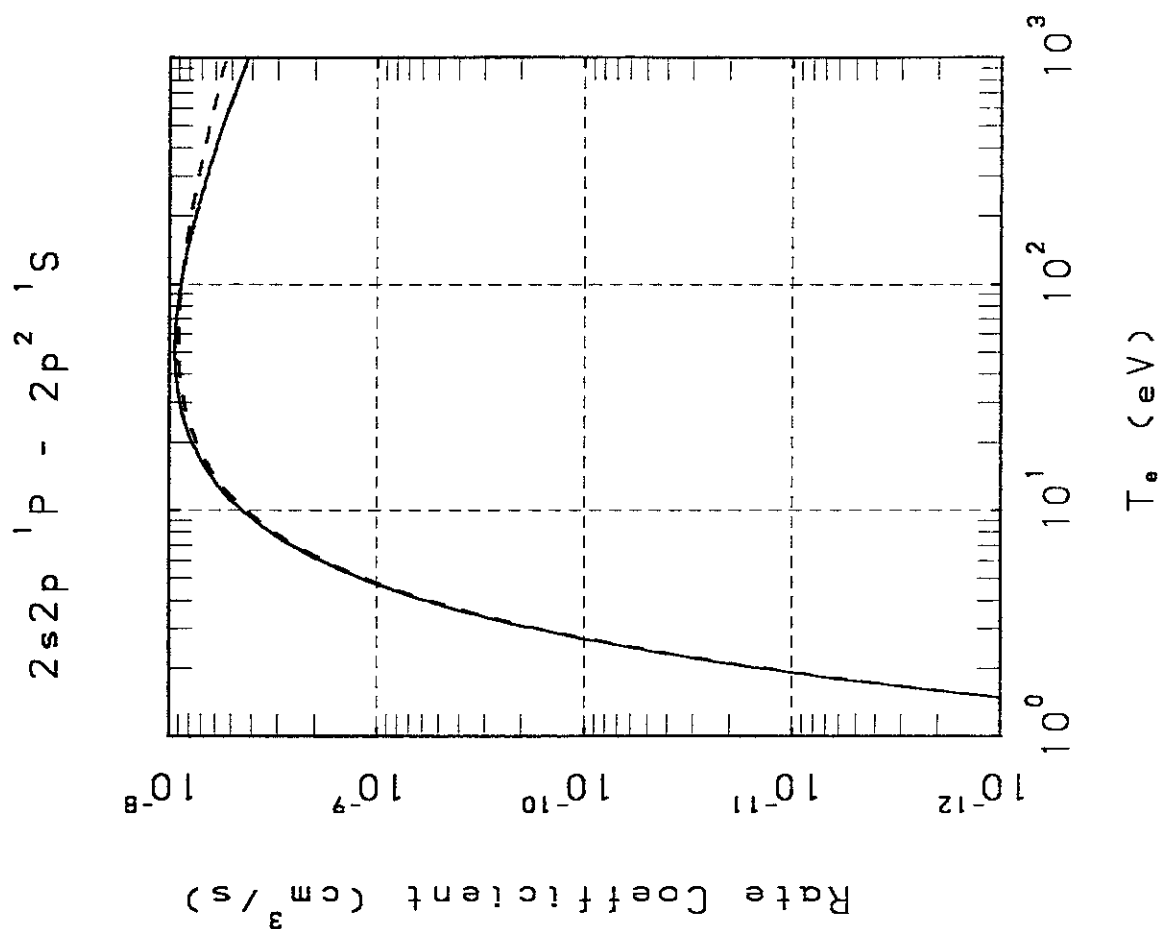


$2s2p^3P - 2s3p^1D$



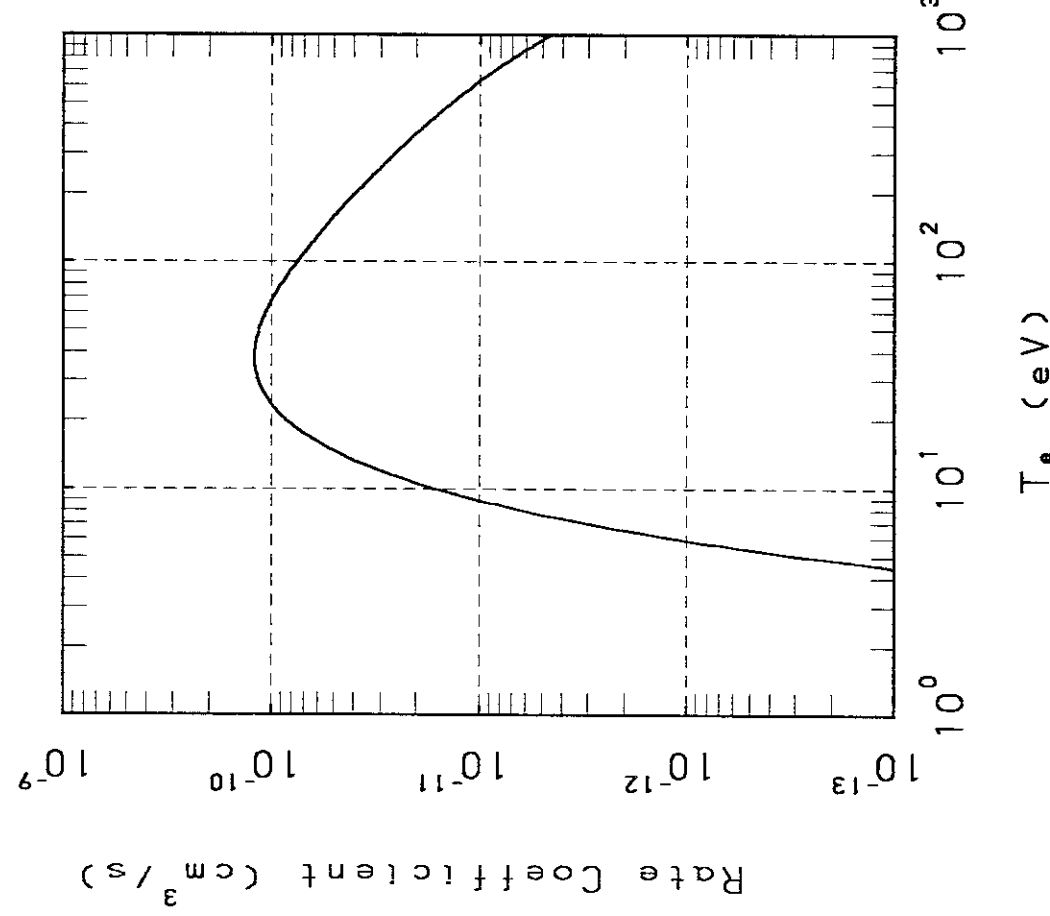
$2s2p^1P - 2p^2\ 3p$





$2s2p\ ^1P - 2s3s\ ^3S$

$2s2p\ ^1P - 2s3s\ ^1S$

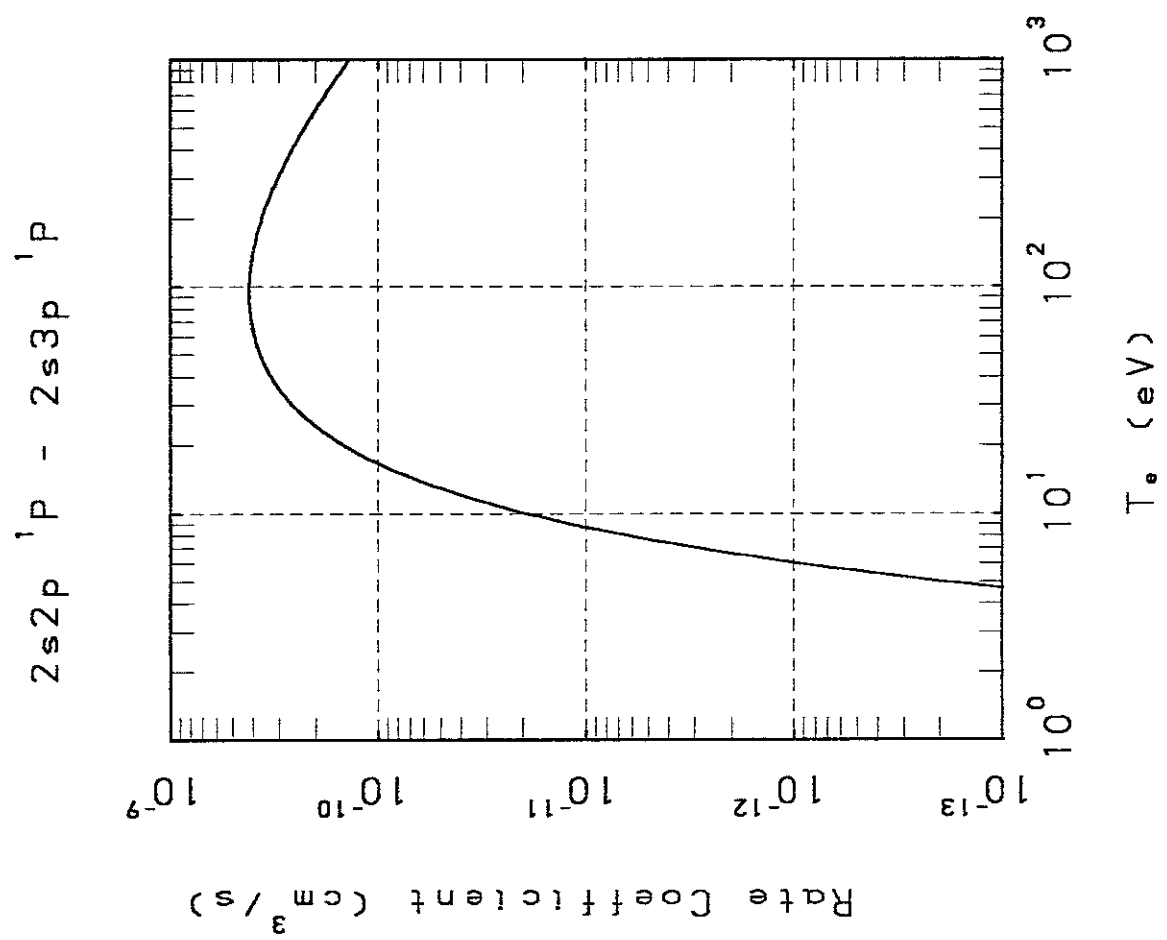
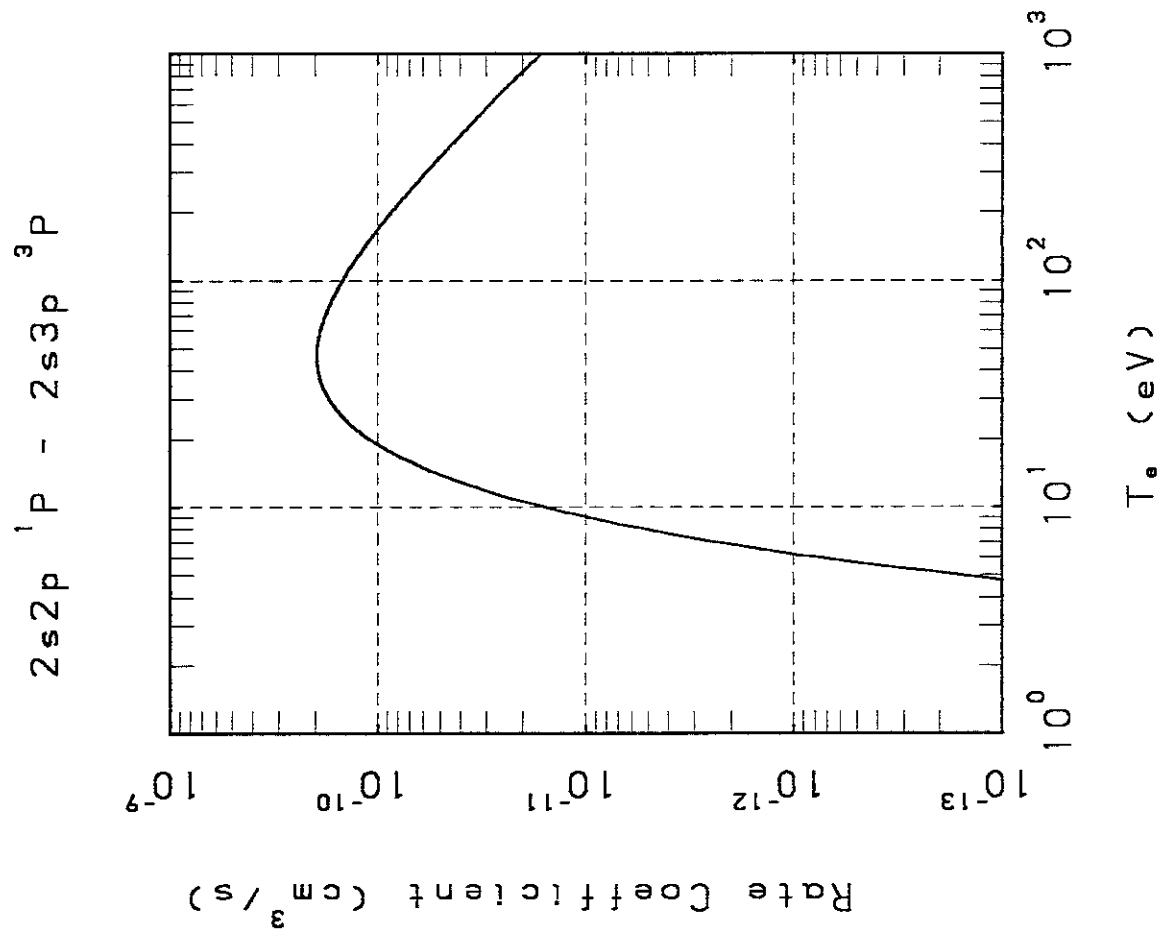


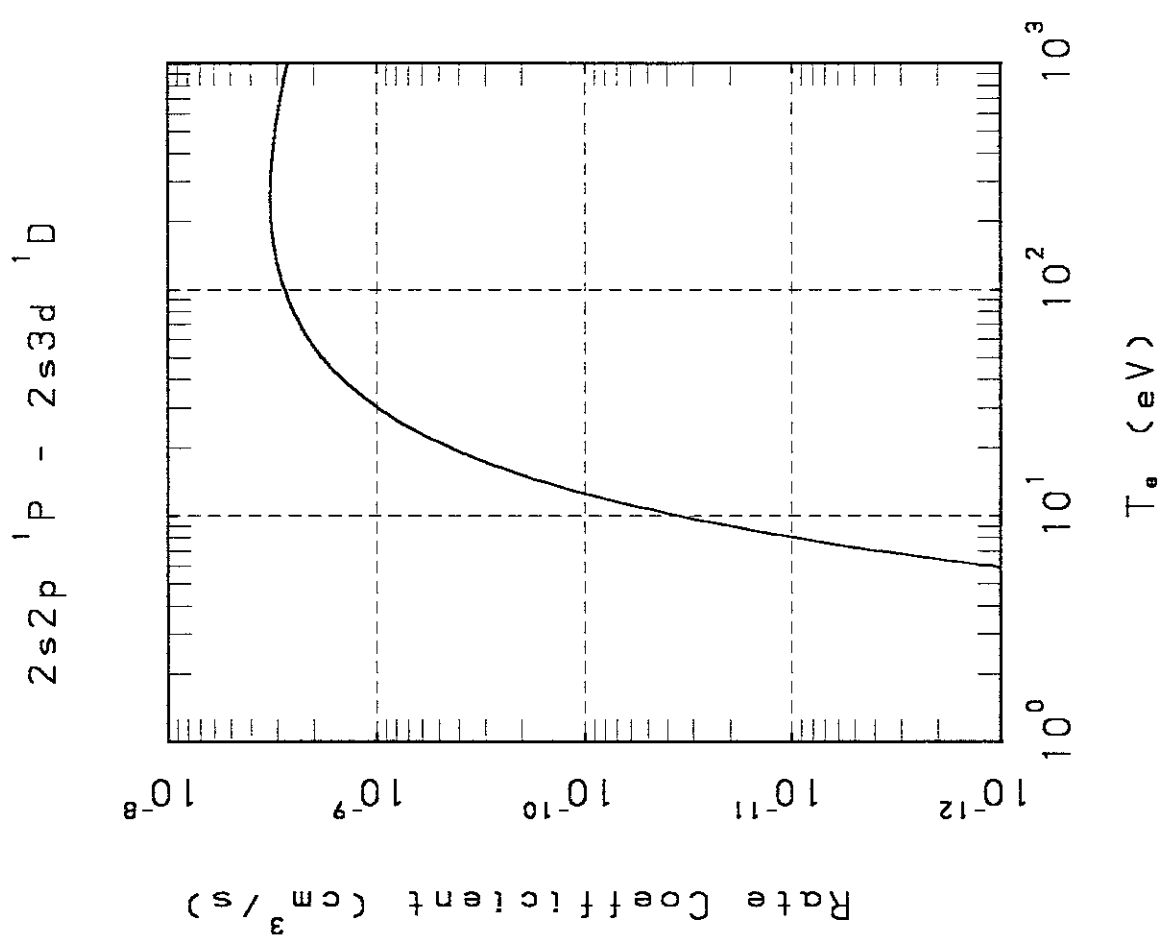
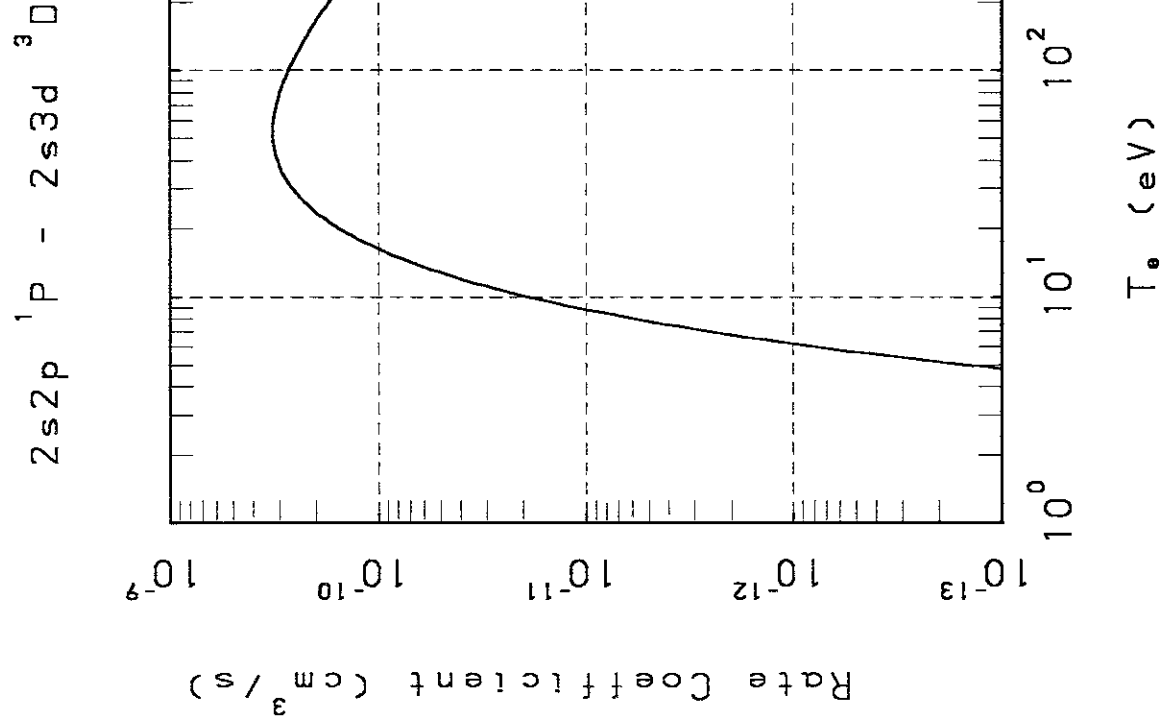
Rate Coefficient (cm^3/s)

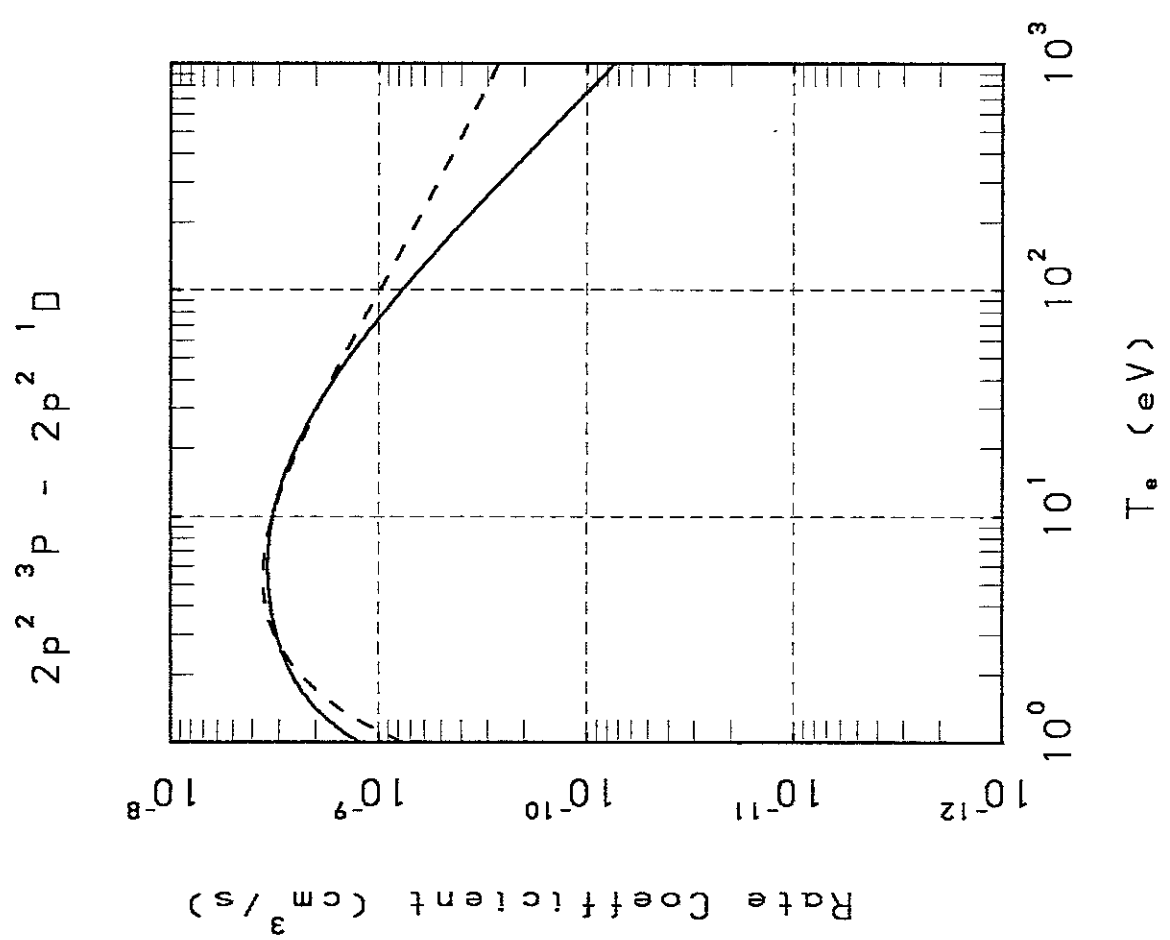
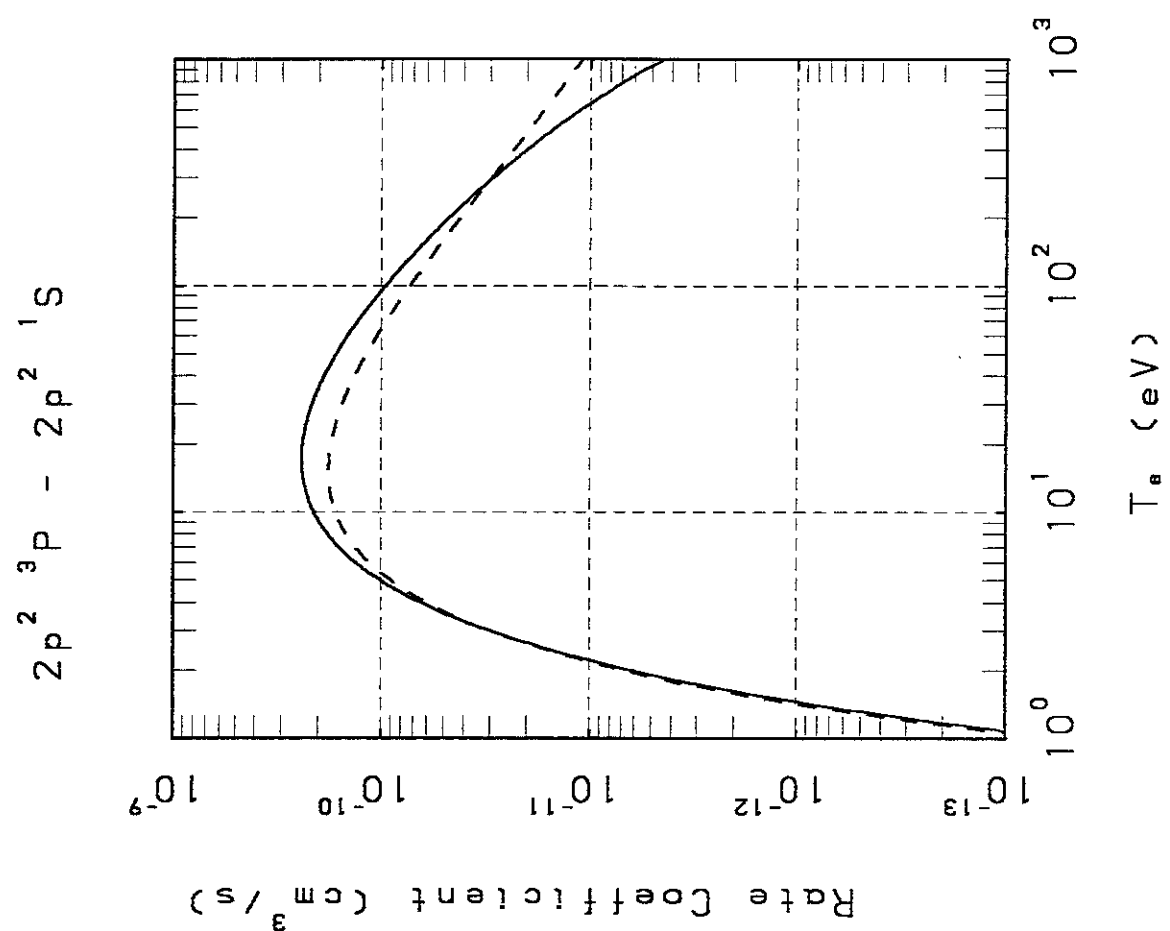
$10^{-13} \quad 10^{-12} \quad 10^{-11} \quad 10^{-10} \quad 10^{-9}$

T_e (eV)

$10^0 \quad 10^1 \quad 10^2 \quad 10^3$



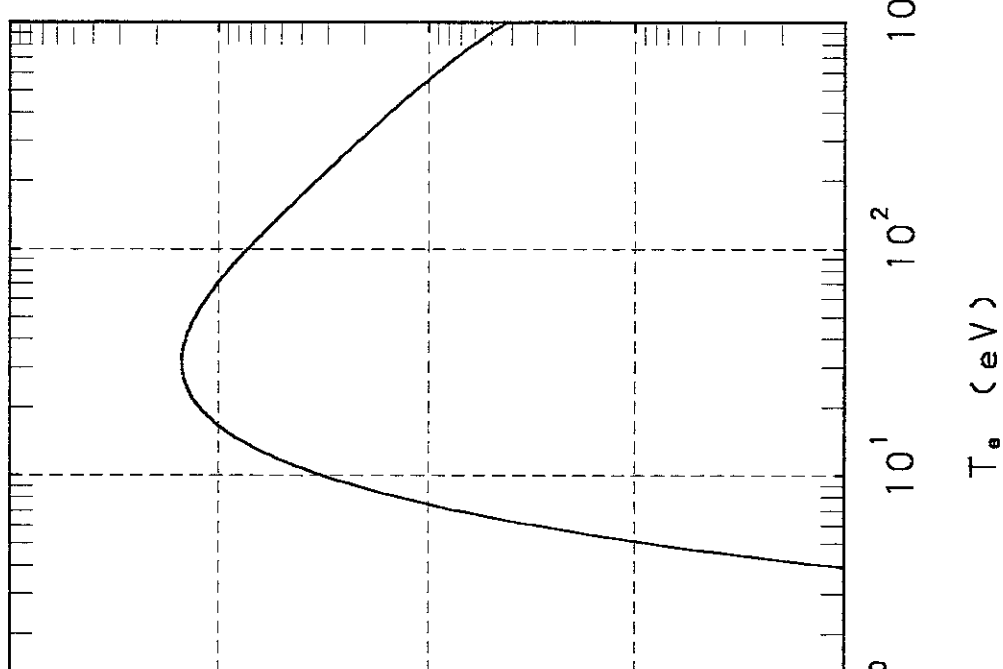




$2p^2 \ ^3P - 2s3s \ ^1S$

$10^{-14} \quad 10^{-13} \quad 10^{-12} \quad 10^{-11} \quad 10^{-10}$

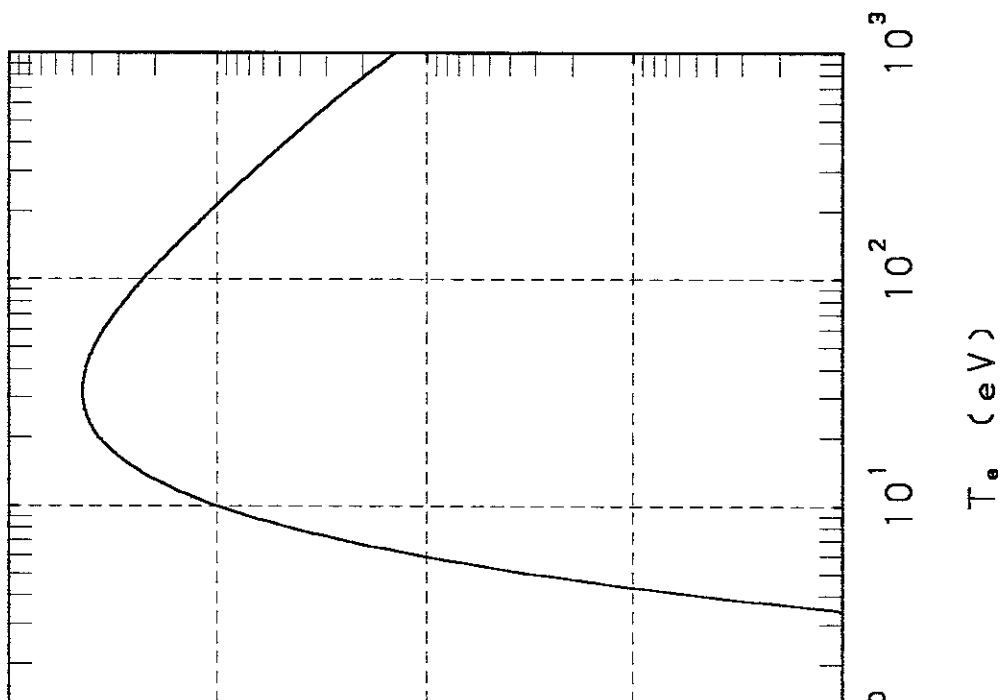
Rate Coefficient (cm^3/s)



$2p^2 \ ^3P - 2s3s \ ^3S$

$10^{-14} \quad 10^{-13} \quad 10^{-12} \quad 10^{-11} \quad 10^{-10}$

Rate Coefficient (cm^3/s)



$2p^2 \ ^3P - 2s3p \ ^3P$

10^{-9}

Rate Coefficient (cm^3/s)

$2p^2 \ ^3P - 2s3p \ ^1P$

10^{-14}

Rate Coefficient (cm^3/s)

$T_e \ (\text{eV})$

$10^0 \quad 10^1 \quad 10^2 \quad 10^3$

$2p^2 \ ^3P - 2s3p \ ^1P$

10^{-14}

Rate Coefficient (cm^3/s)

$T_e \ (\text{eV})$

$10^0 \quad 10^1 \quad 10^2 \quad 10^3$

$2p^2 \ ^3P - 2s3d \ ^1D$

10^{-14}

10^{-12}

10^{-11}

10^{-10}

Rate Coefficient (cm^3/s)

$10^0 \quad 10^1 \quad 10^2 \quad 10^3$

$T_e \ (\text{eV})$

$2p^2 \ ^3P - 2s3d \ ^3D$

10^{-9}

10^{-11}

10^{-13}

Rate Coefficient (cm^3/s)

$10^0 \quad 10^1 \quad 10^2 \quad 10^3$

$T_e \ (\text{eV})$

$2p^2 \ ^1D - 2s3s \ ^3S$

10^{-9}

10^{-10}

10^{-11}

10^{-12}

10^{-13}

Rate Coefficient (cm^3/s)

$10^0 \quad 10^1 \quad 10^2 \quad 10^3$

$T_e \ (\text{eV})$

$2p^2 \ ^1D - 2p^2 \ ^1S$

10^{-9}

10^{-10}

10^{-11}

10^{-12}

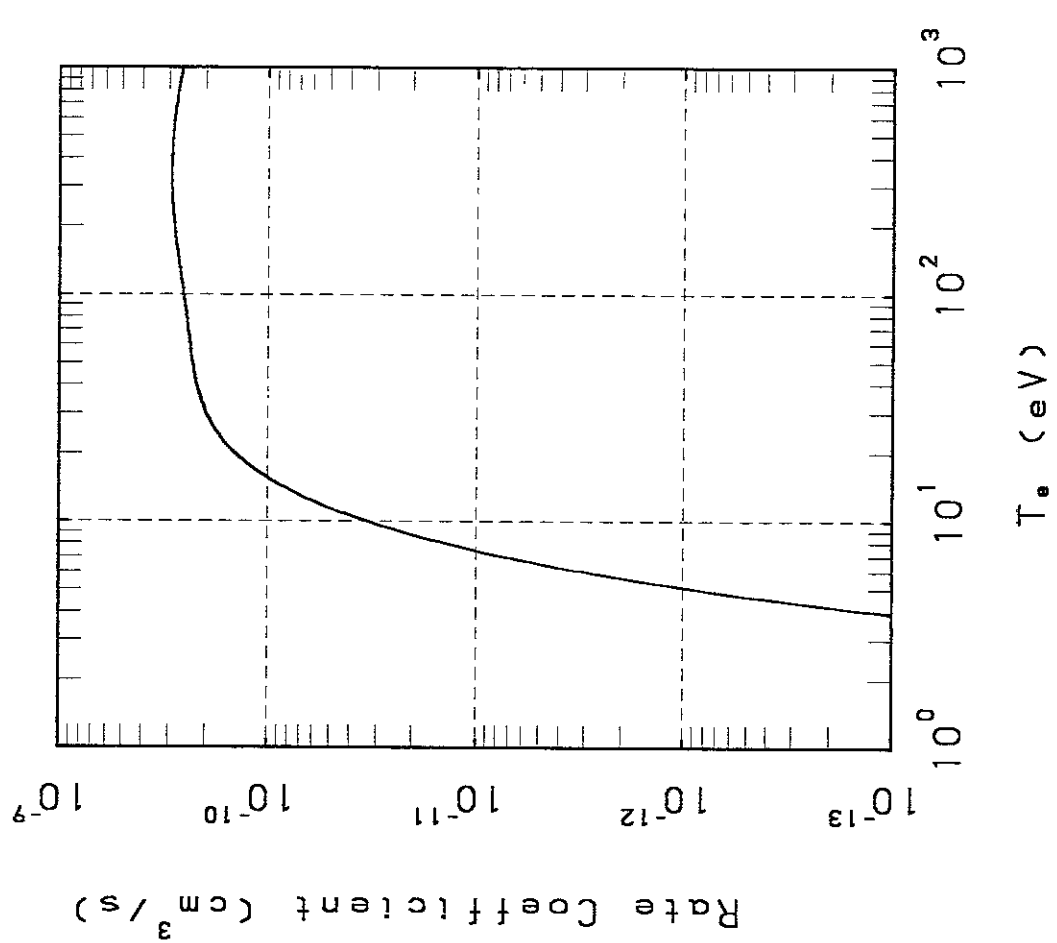
10^{-13}

Rate Coefficient (cm^3/s)

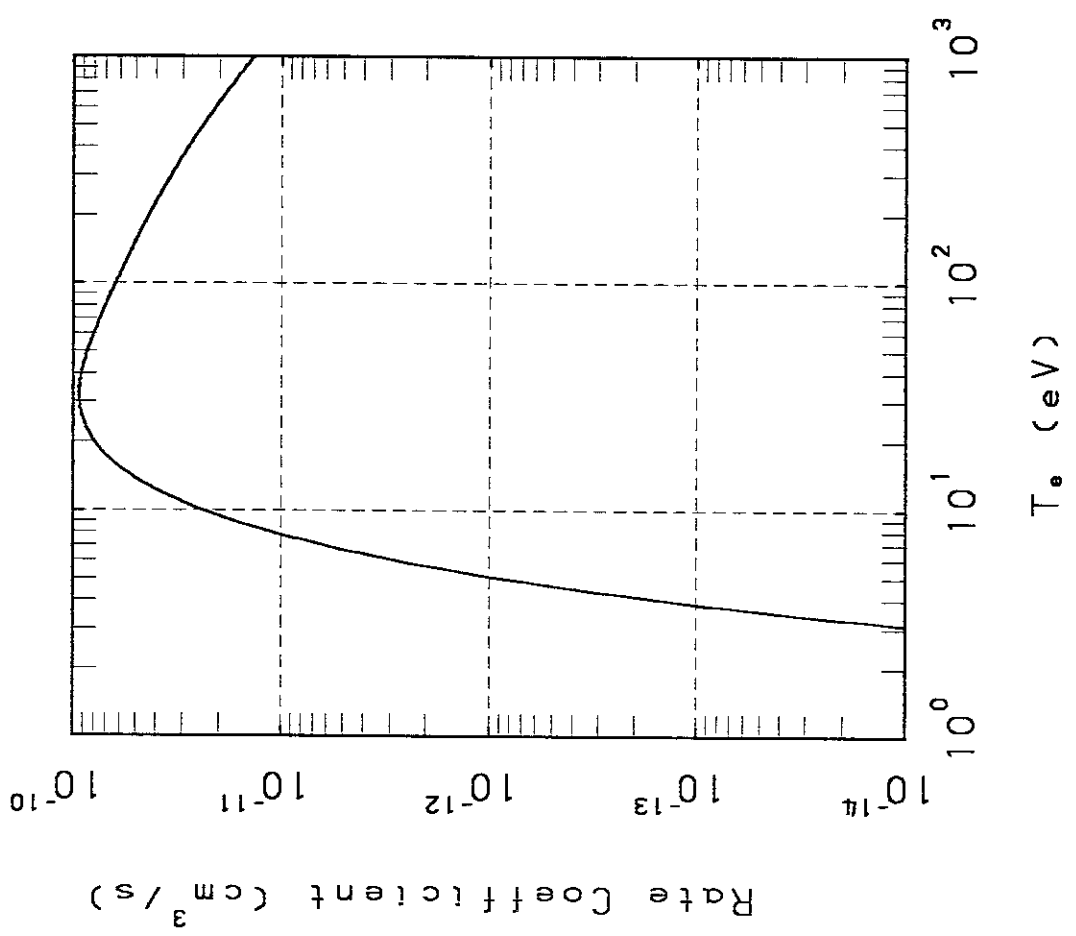
$10^0 \quad 10^1 \quad 10^2 \quad 10^3$

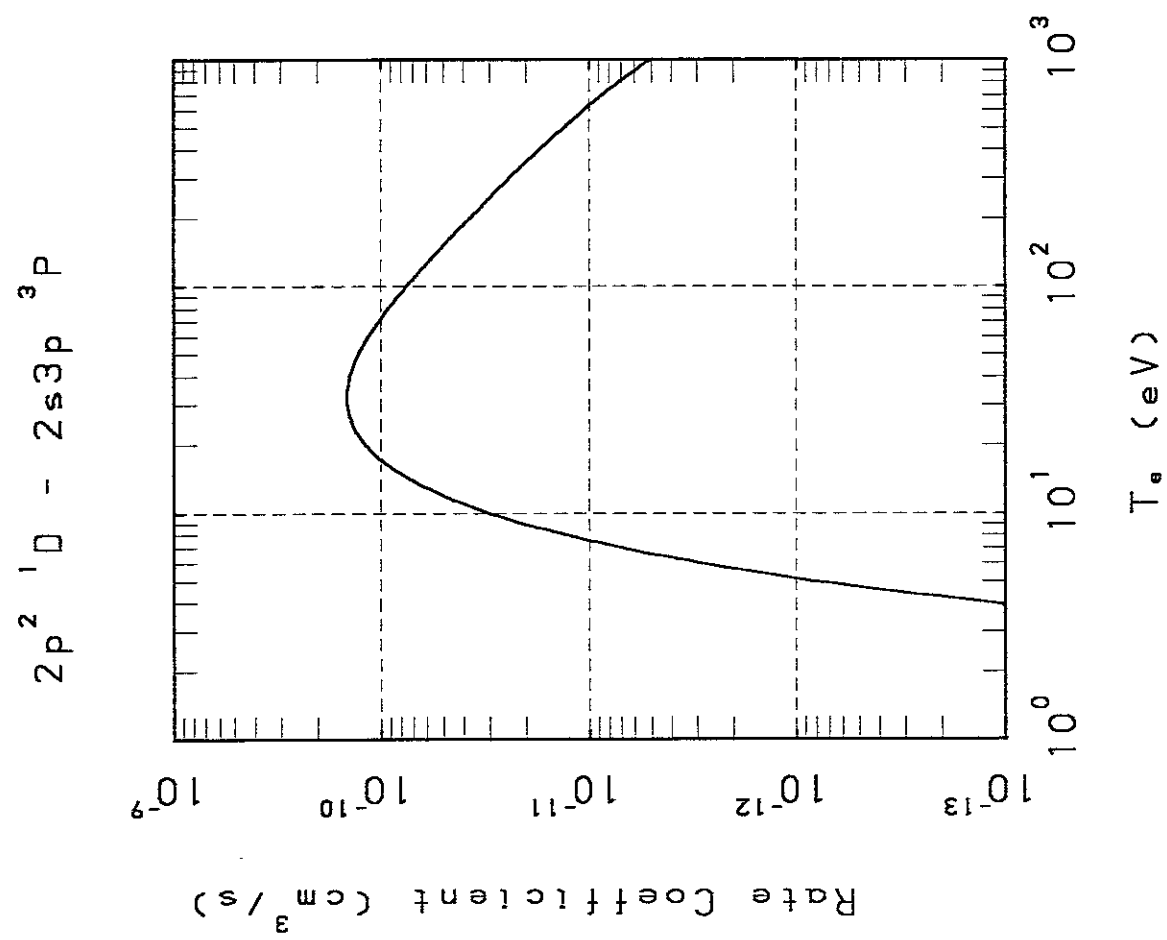
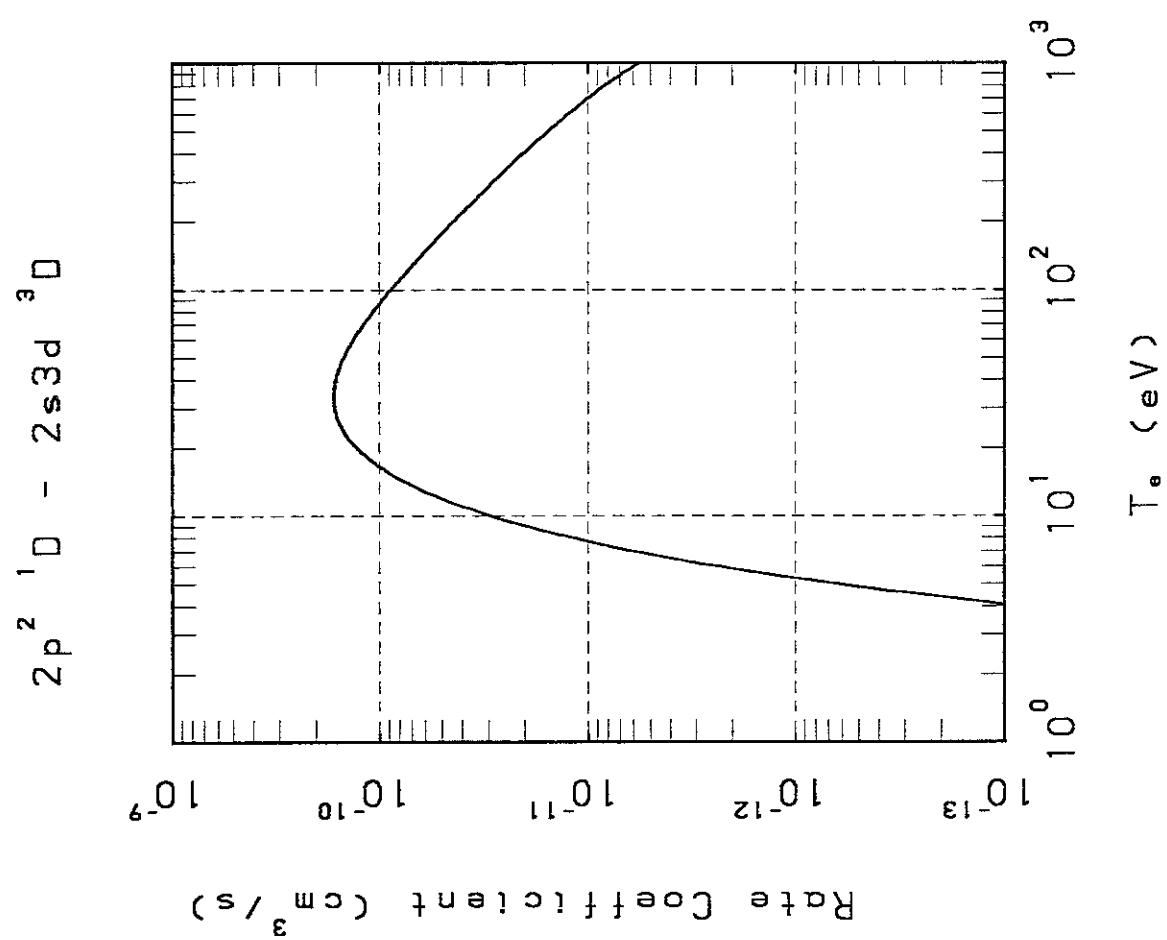
$T_e \ (\text{eV})$

$2p^2 \ ^1D - 2s3p \ ^1P$

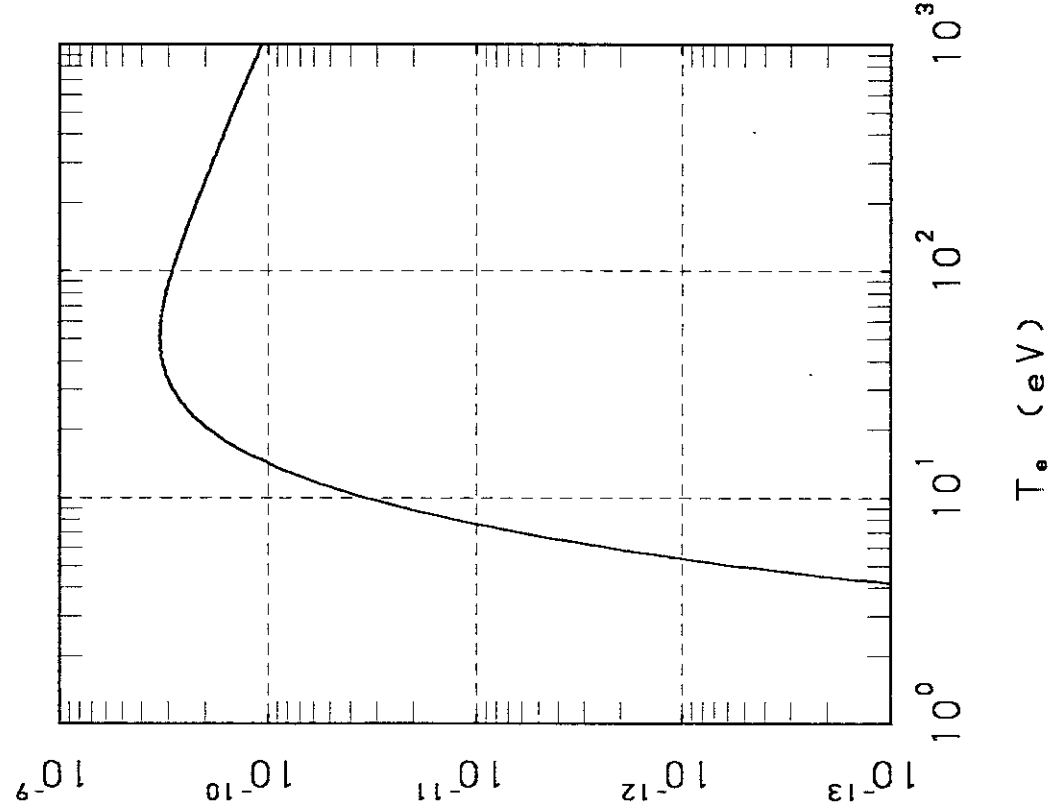


$2p^2 \ ^1D - 2s3s \ ^1S$

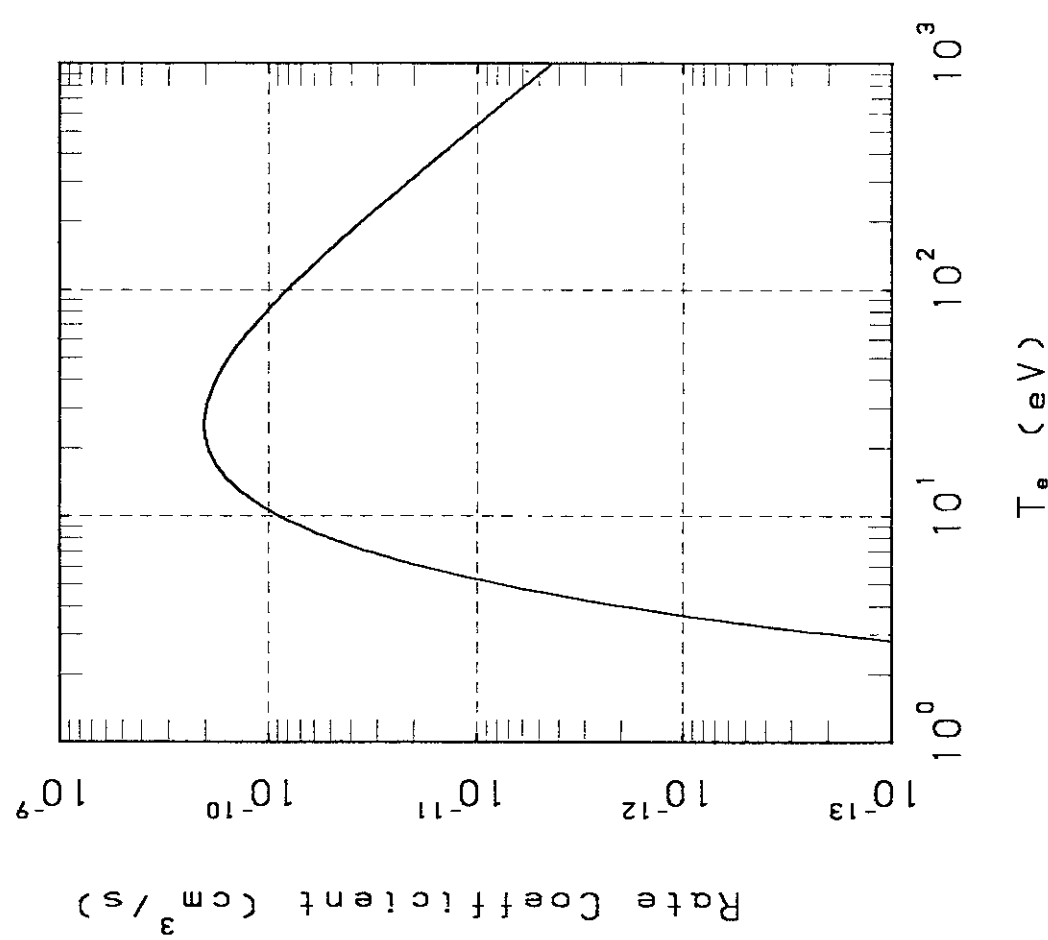


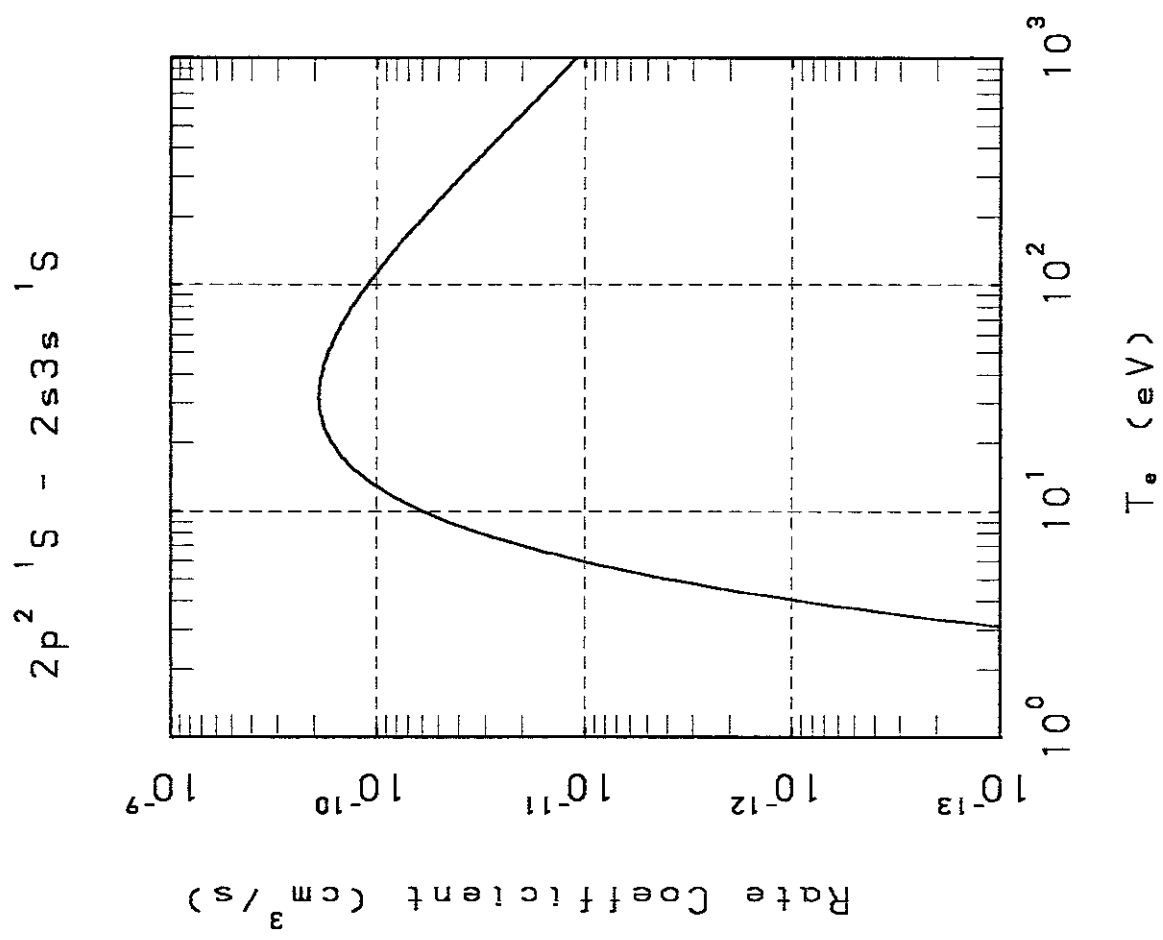
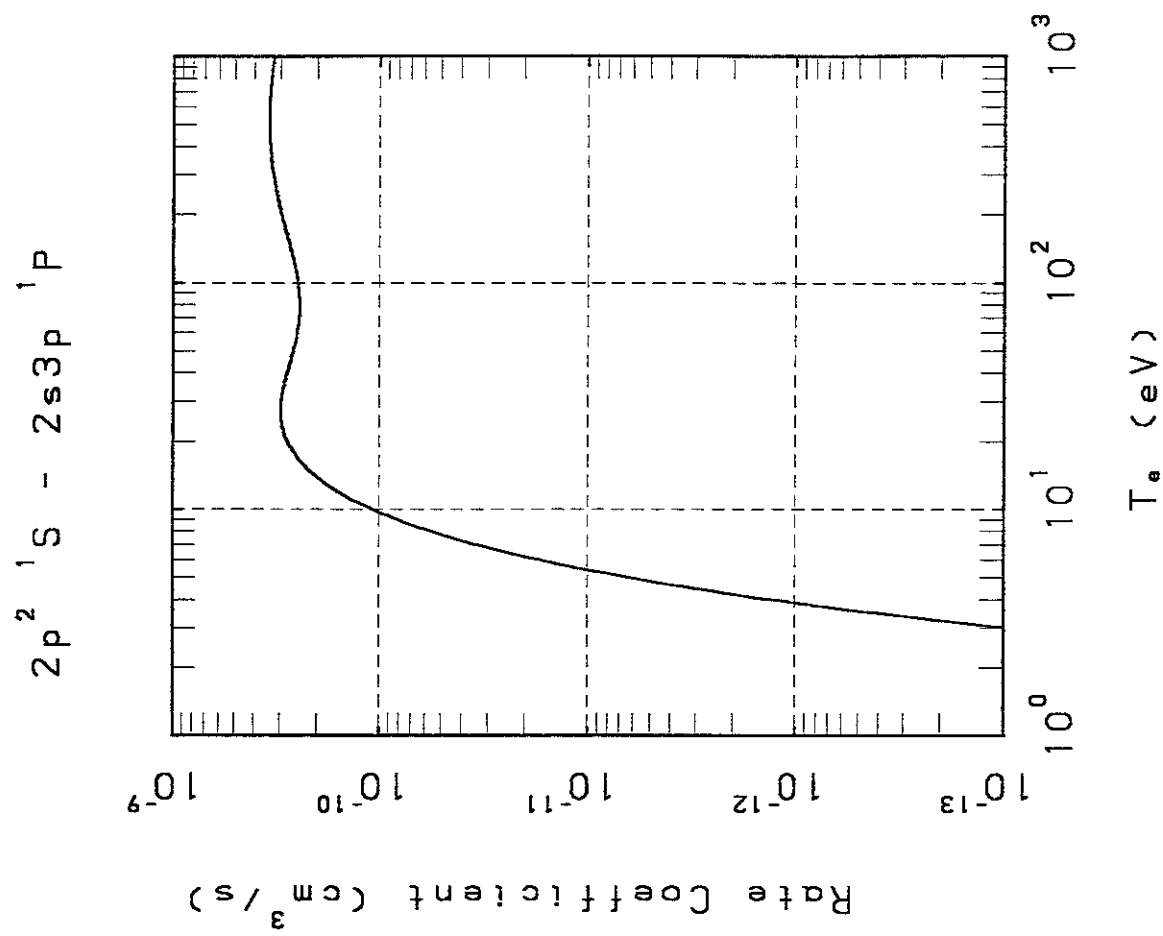


$2p^2 1D - 2s3d \quad ^1D$

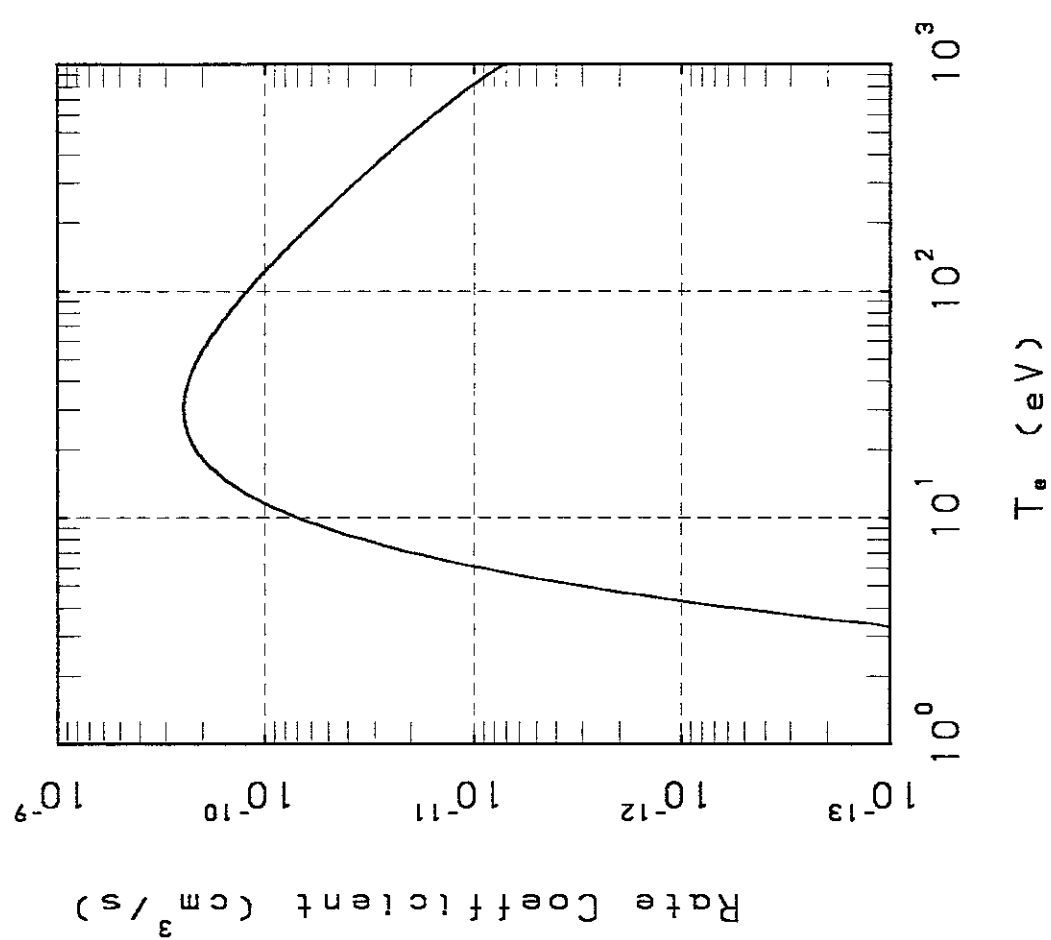


$2p^2 1S - 2s3s \quad ^3S$

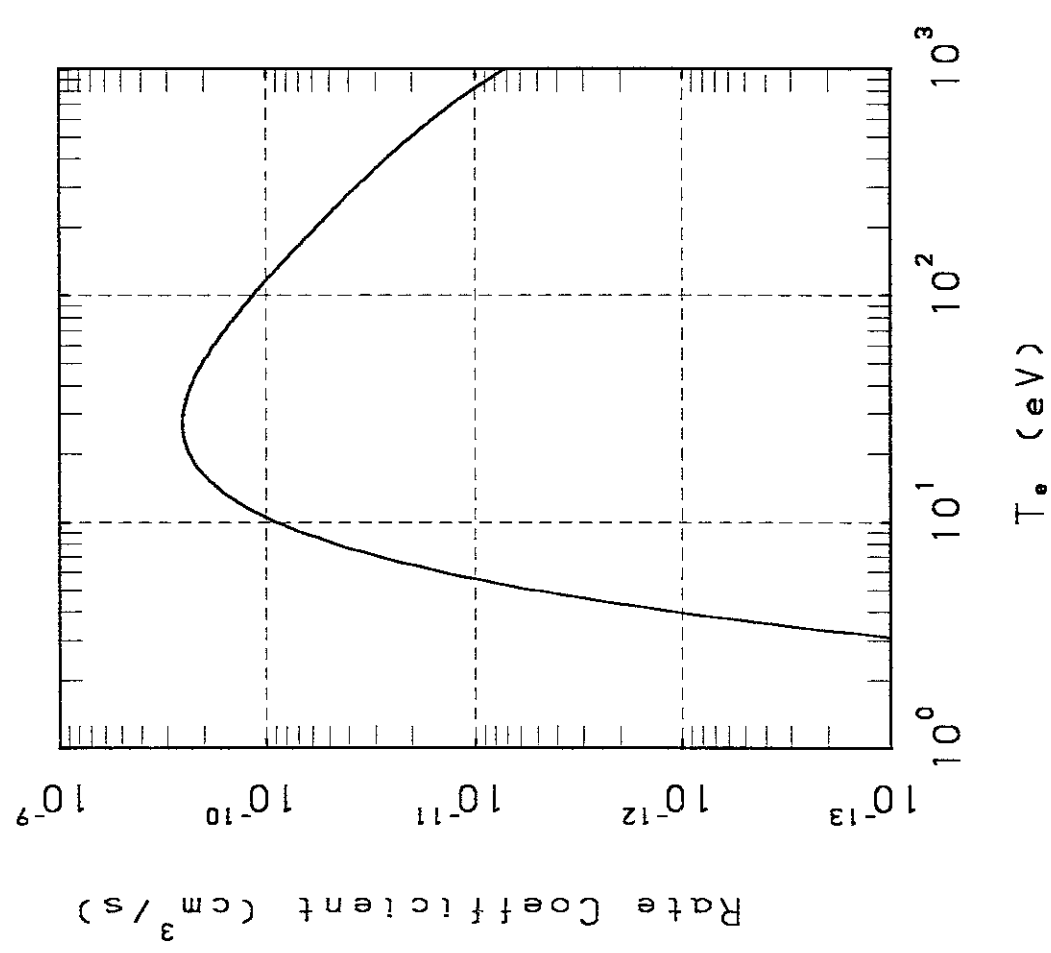


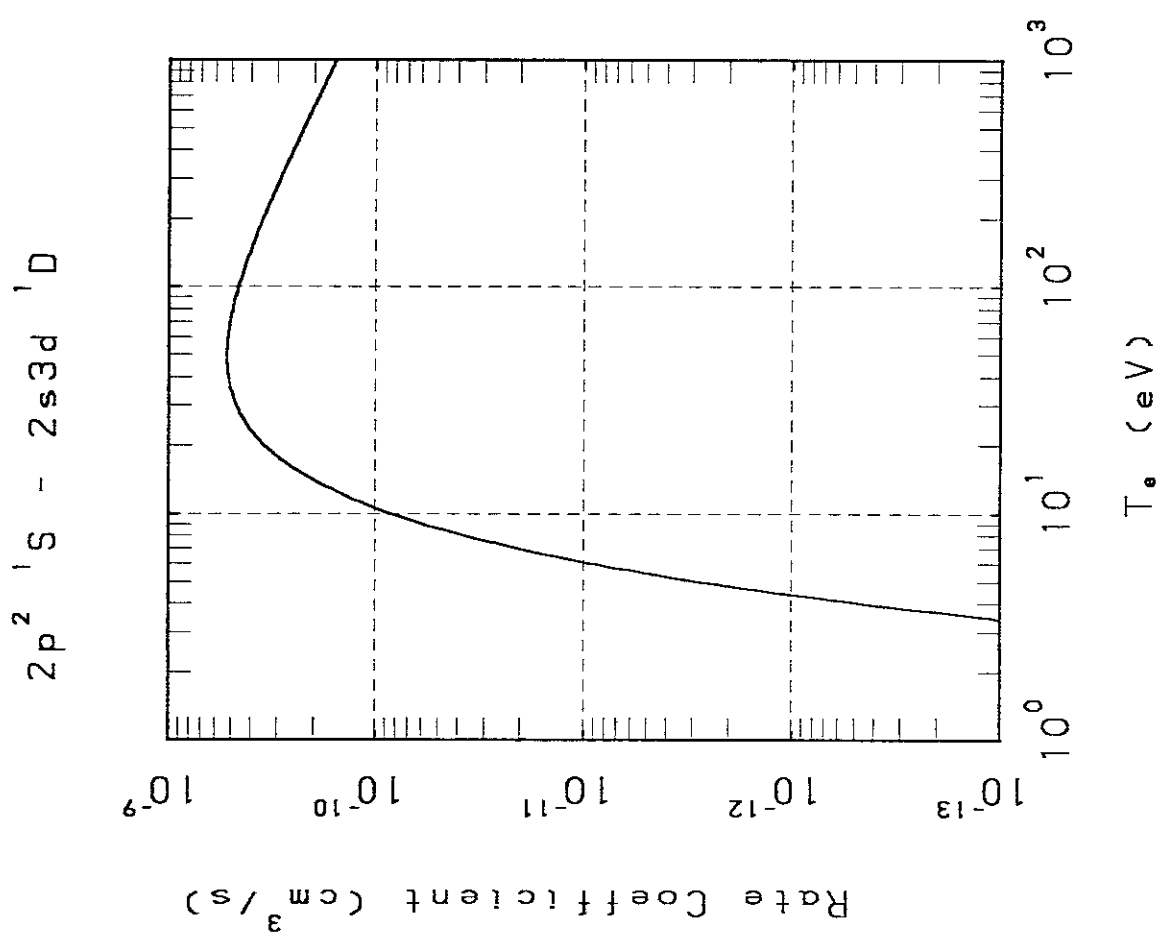
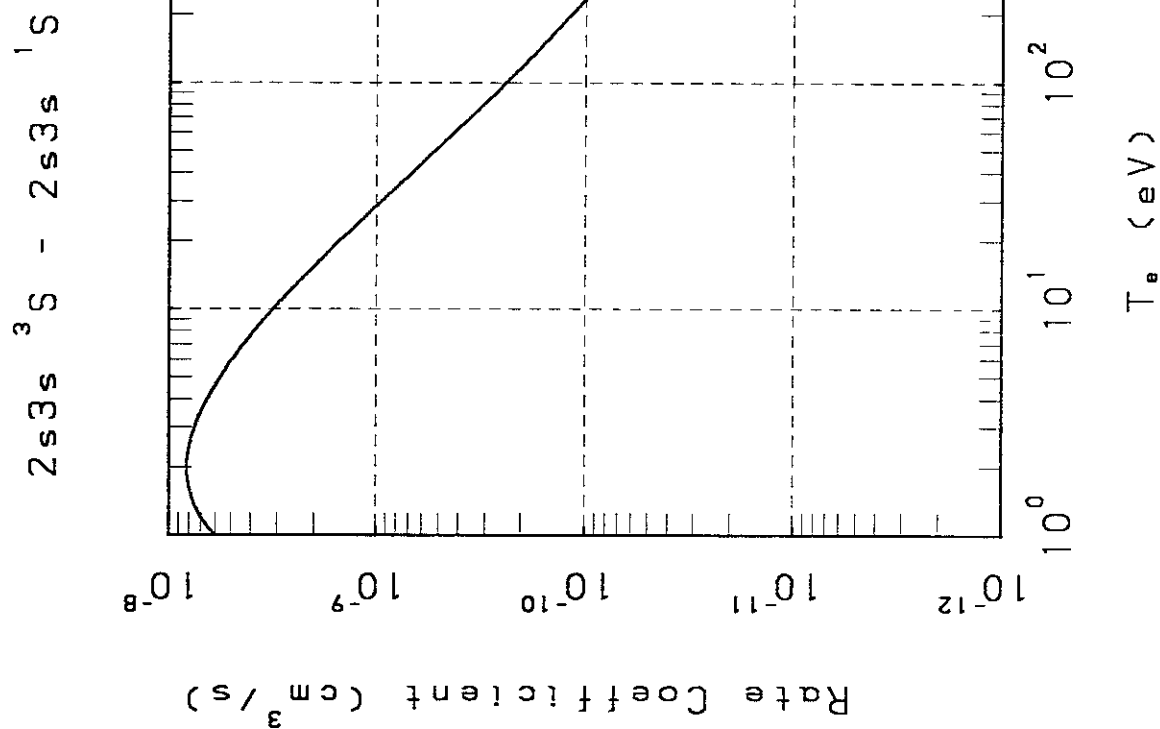


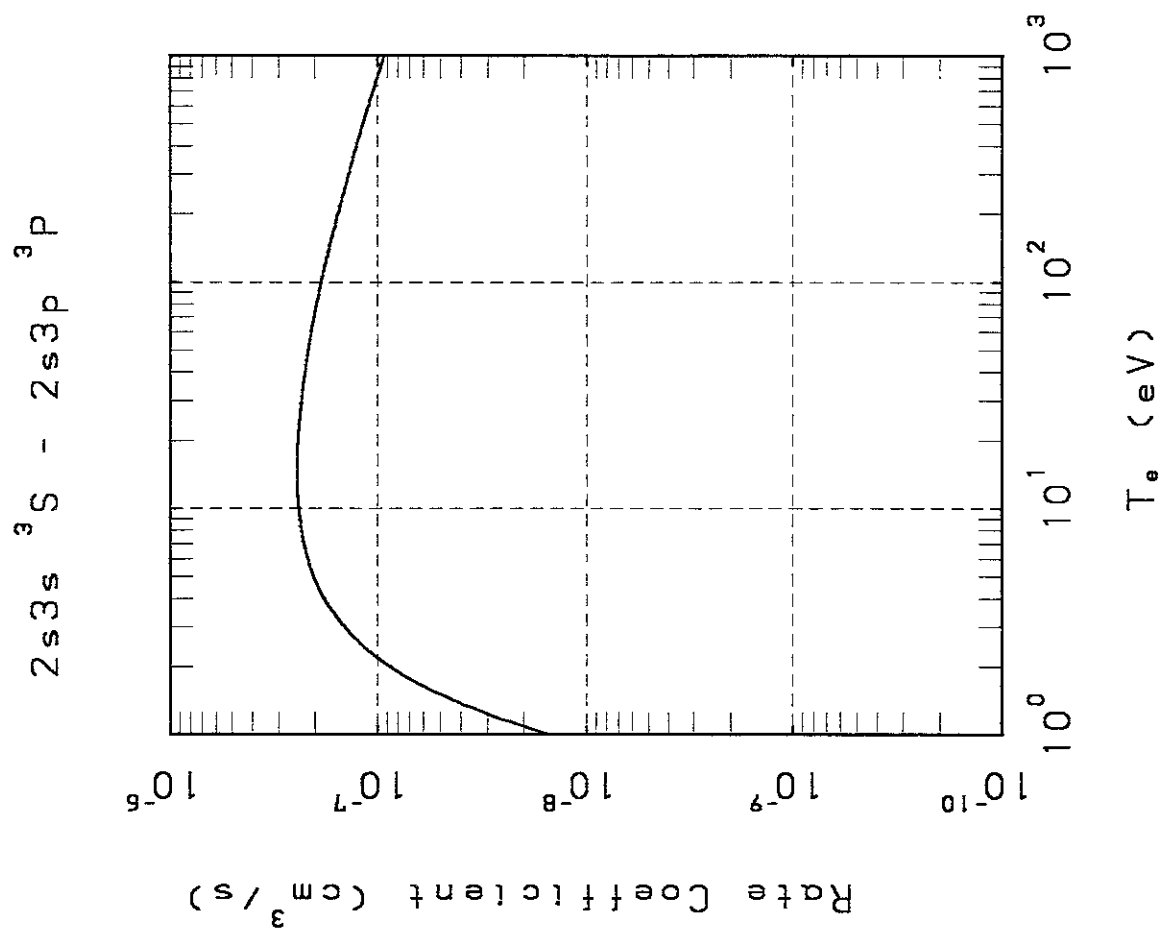
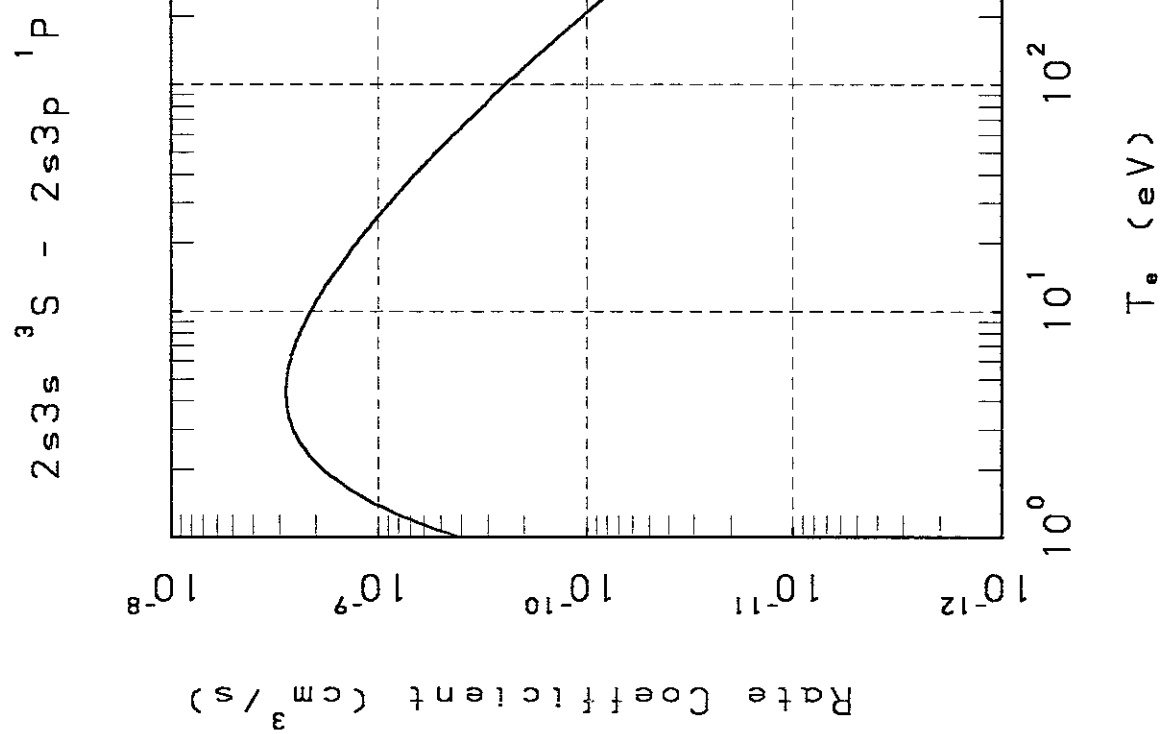
$2p^2 1S - 2s3d$ 3D



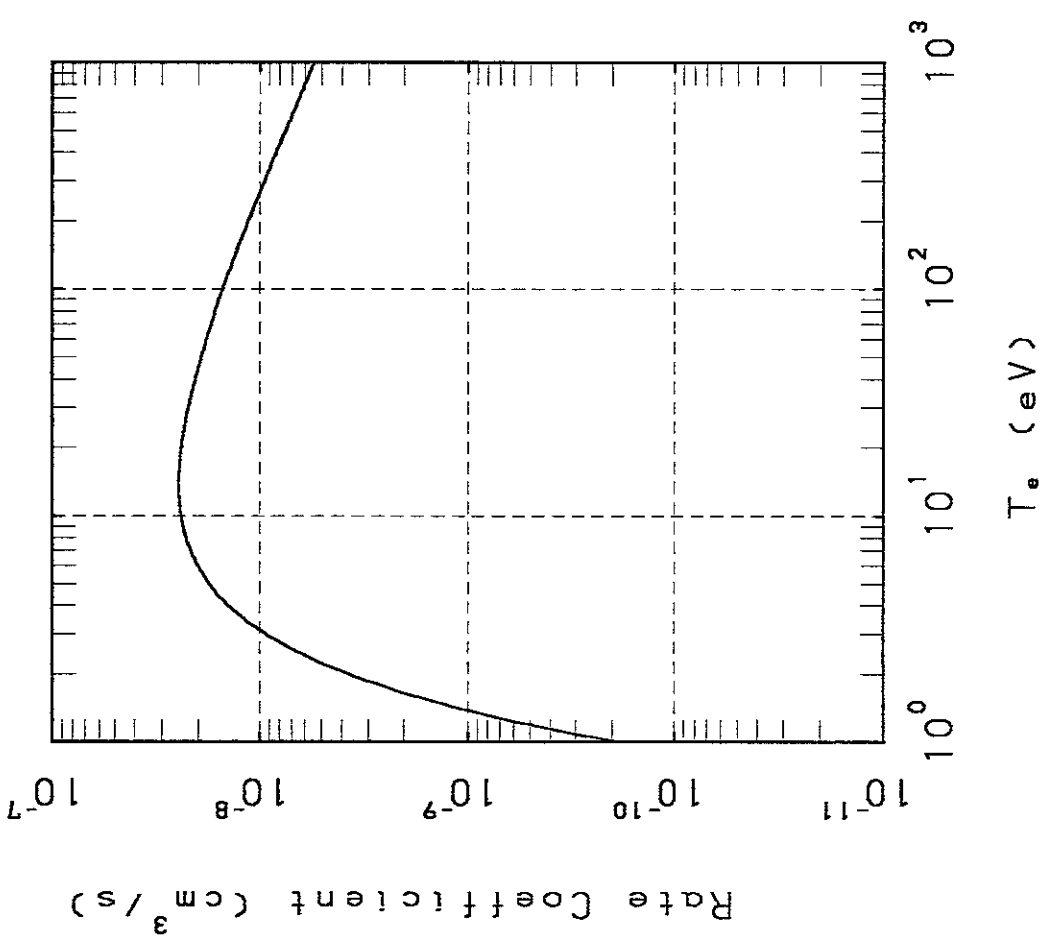
$2p^2 1S - 2s3p$ 3P



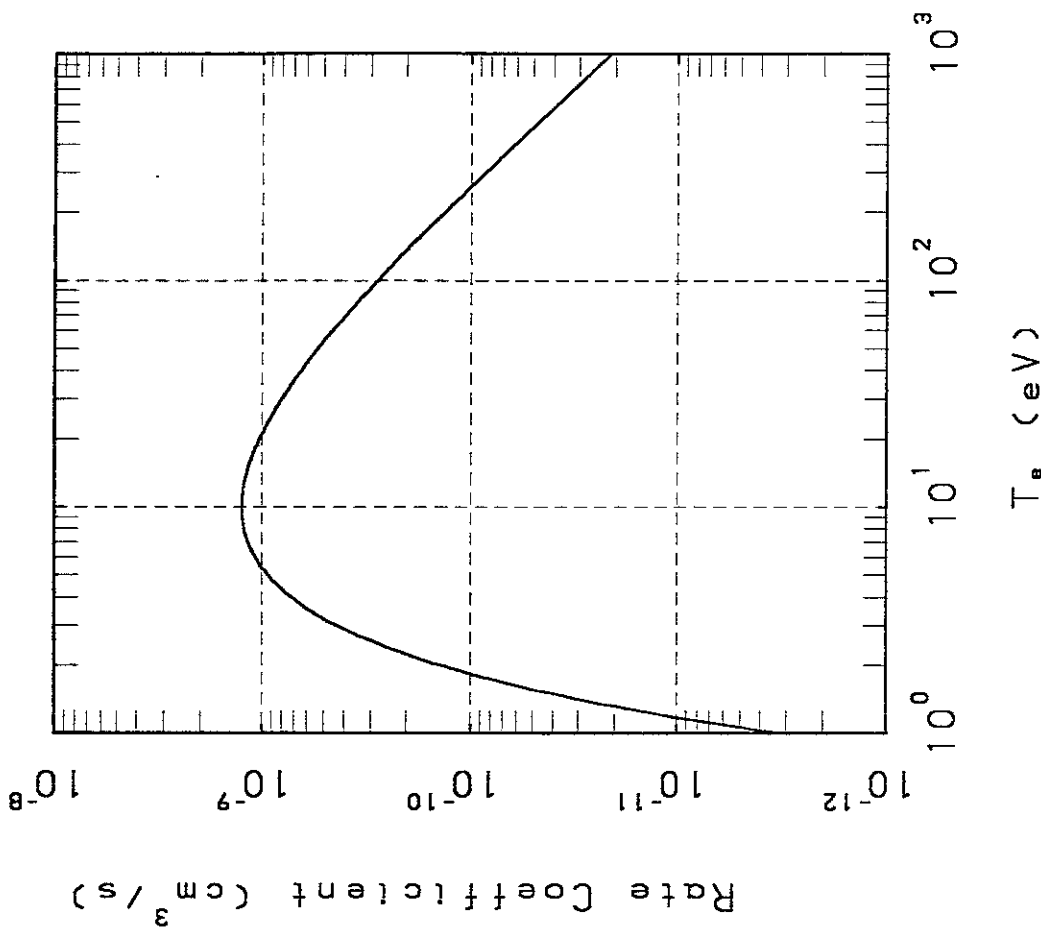




$2s3s\ ^3S - 2s3d\ ^3D$



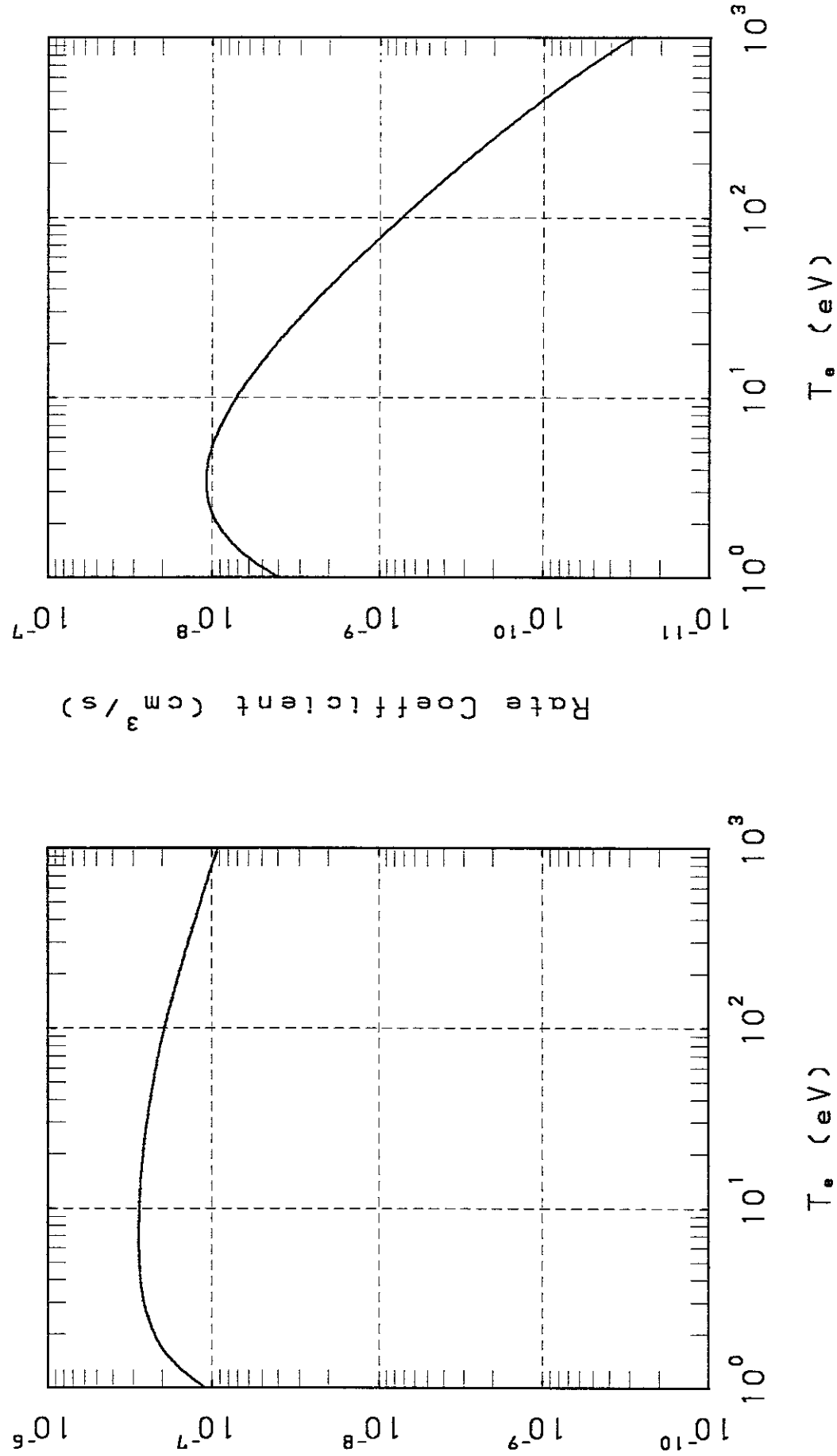
$2s3s\ ^3S - 2s3d\ ^1D$

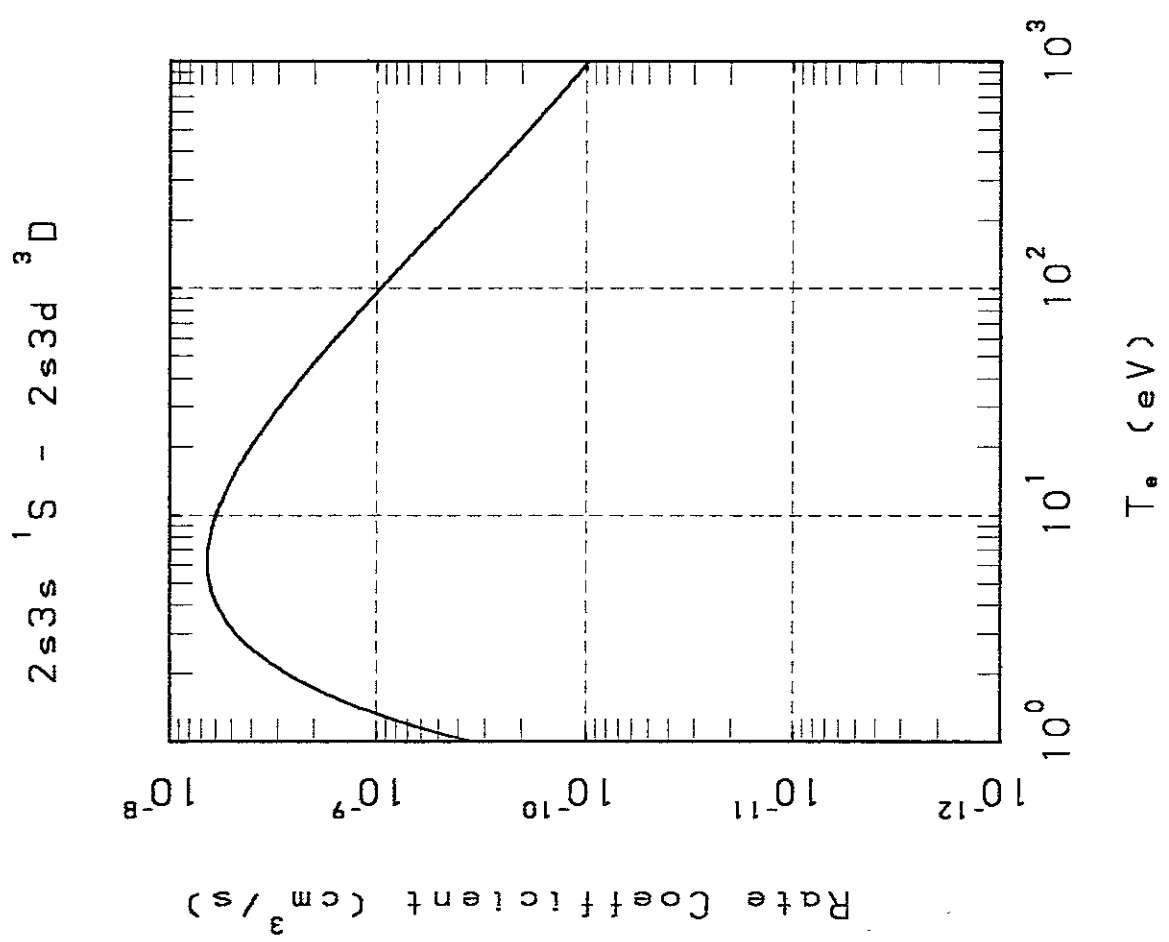
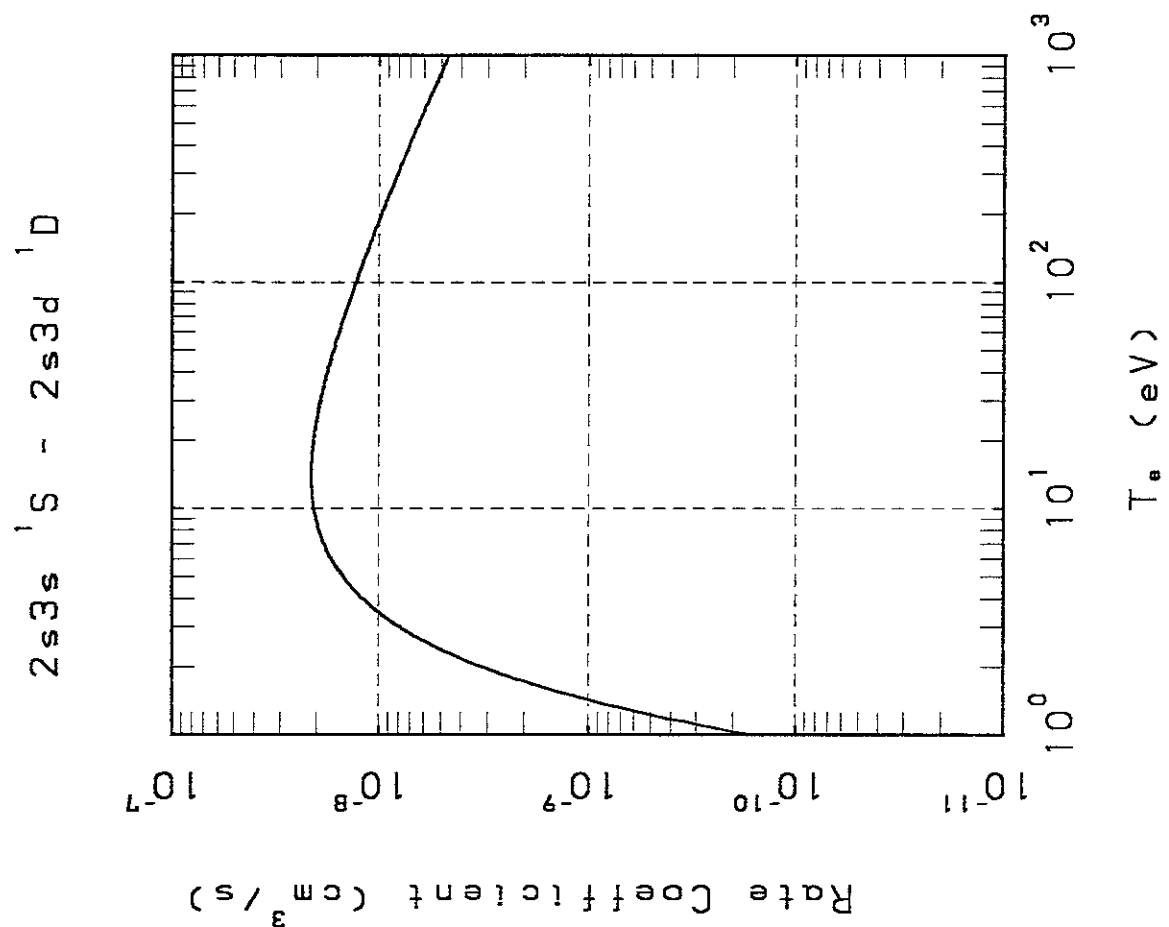


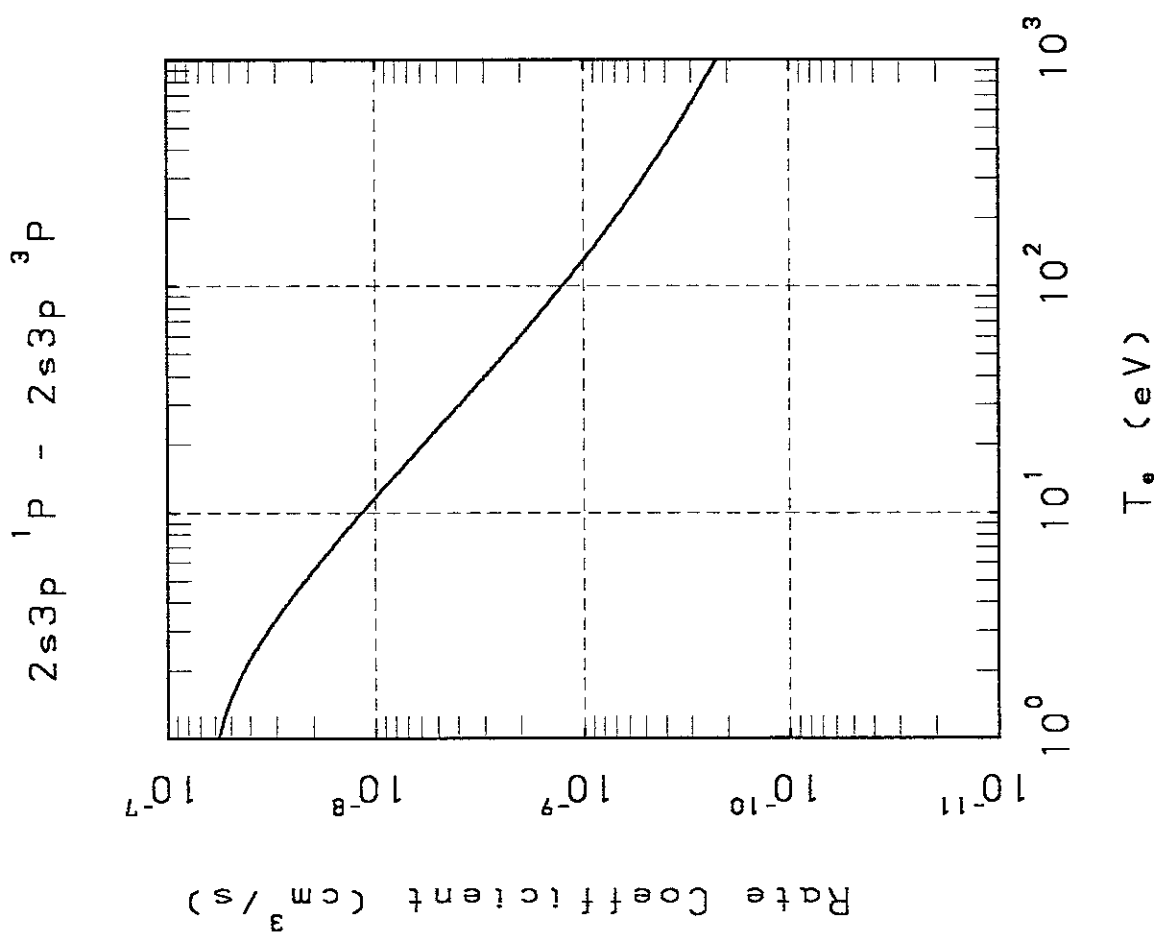
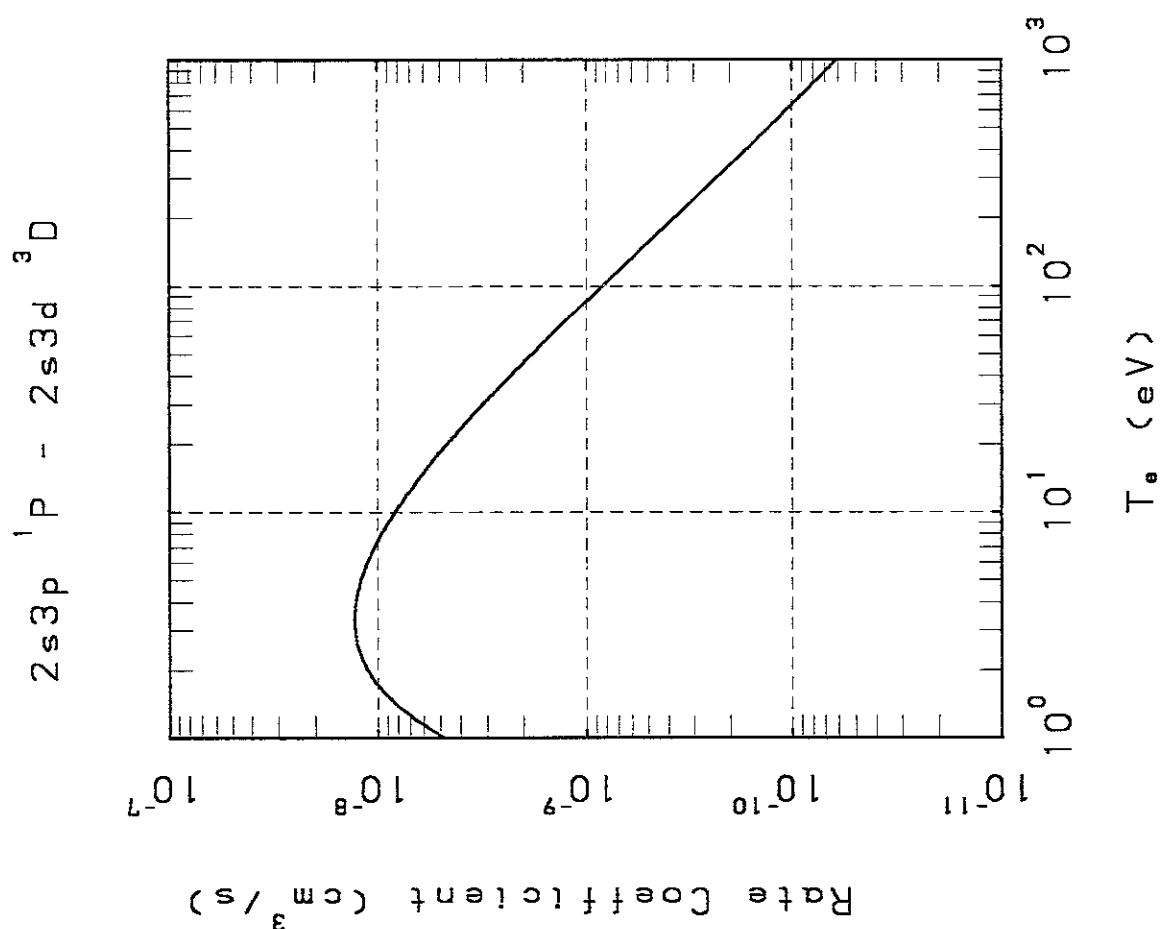
$2s3s\ 1S - 2s3p\ 1P$

Rate Coefficient (cm^3/s)

$2s3s\ 1S - 2s3p\ 3P$







$2s3p\ ^3P - 2s3d\ ^3D$

Rate Coefficient (cm^3/s)

$10^{-10} \quad 10^{-9} \quad 10^{-8} \quad 10^{-7} \quad 10^{-6}$

T_e (eV)

$10^0 \quad 10^1 \quad 10^2 \quad 10^3$

$2s3p\ ^1P - 2s3d\ ^1D$

Rate Coefficient (cm^3/s)

$10^{-10} \quad 10^{-9} \quad 10^{-8} \quad 10^{-7} \quad 10^{-6}$

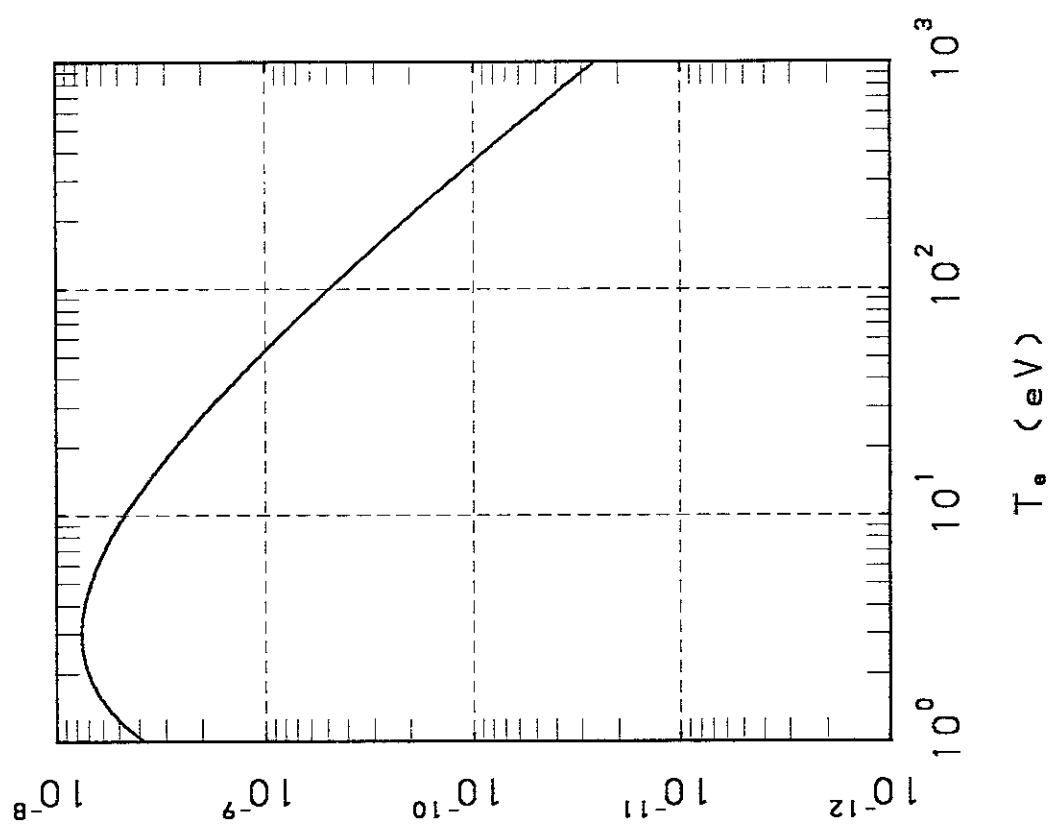
T_e (eV)

$10^0 \quad 10^1 \quad 10^2 \quad 10^3$

$2s3p\ ^3P - 2s3d\ ^1D$

Rate Coefficient (cm^3/s)

$2s3d\ ^3D - 2s3d\ ^1D$

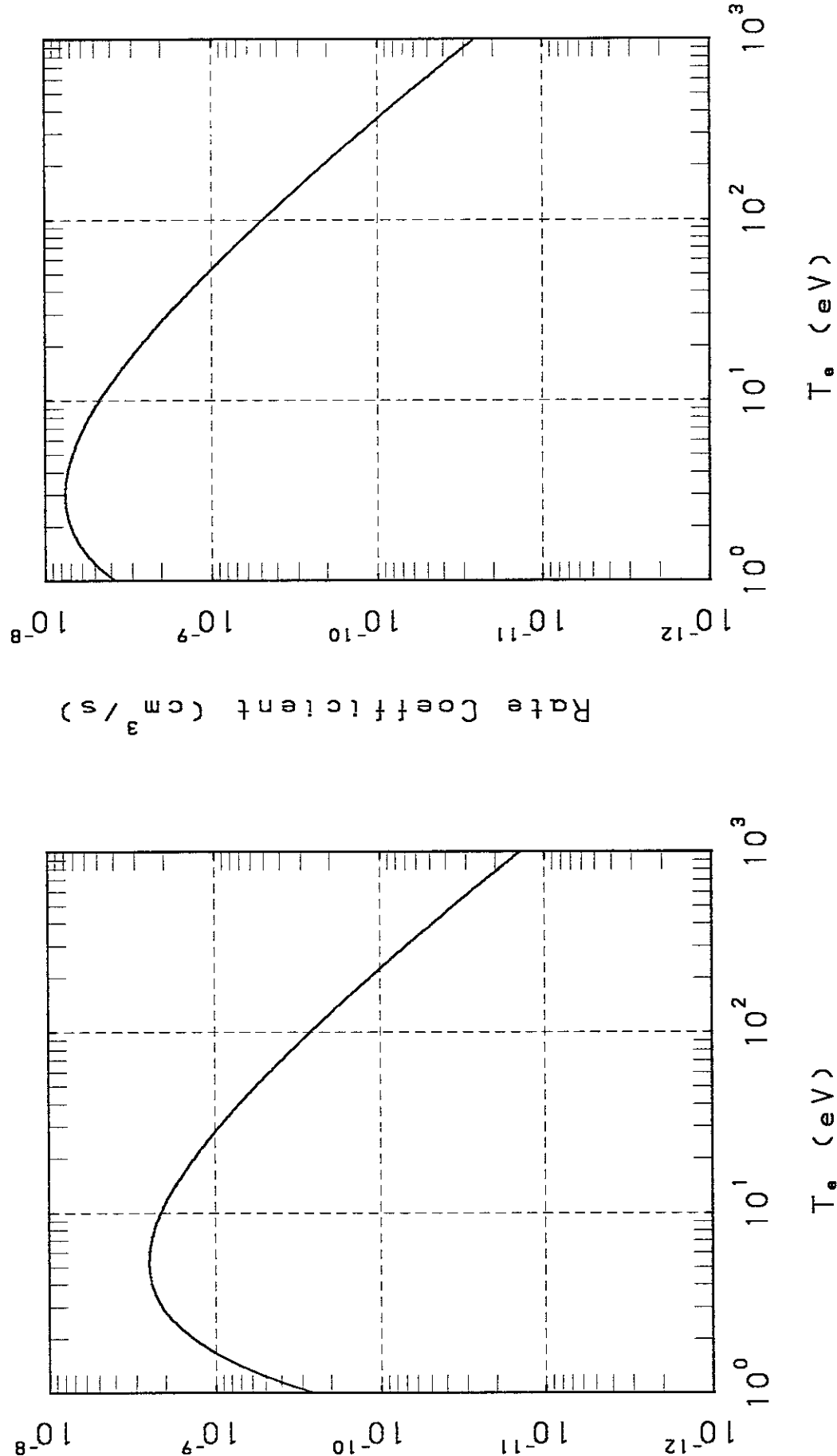


T_e (eV)

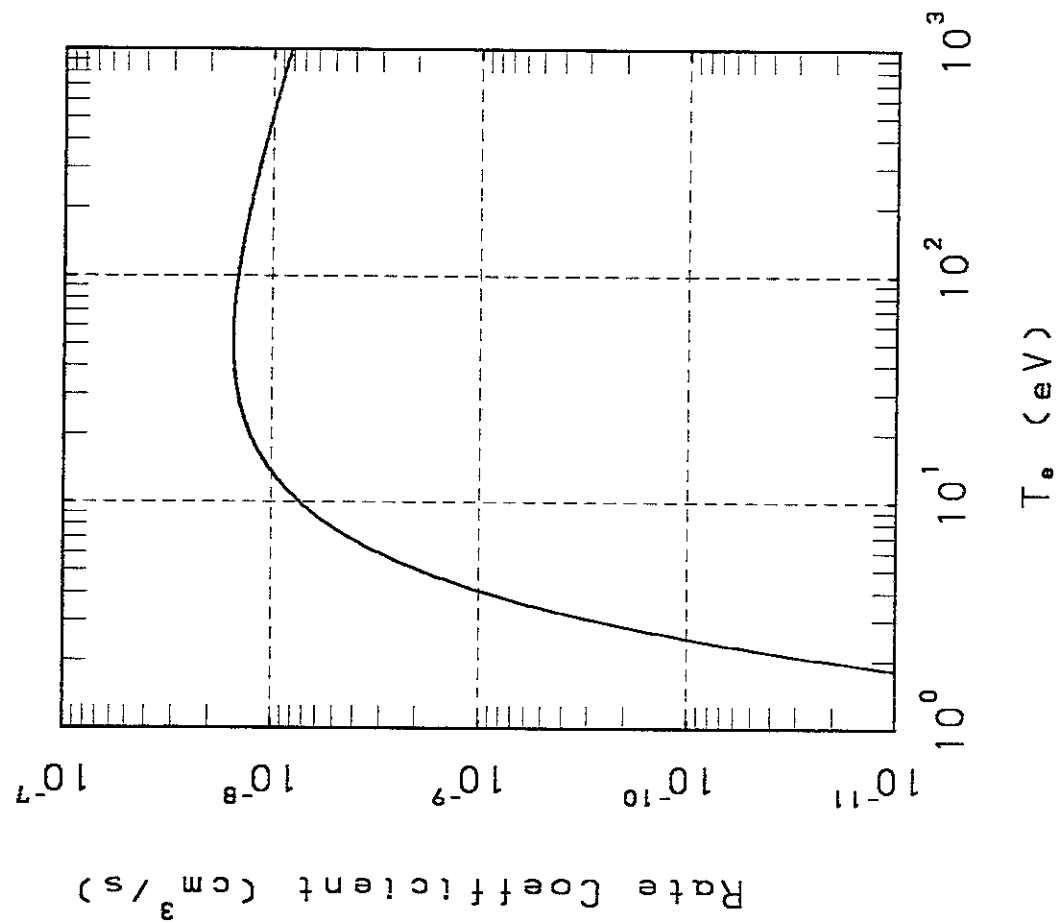
T_e (eV)

$2s3p\ ^3P - 2s3d\ ^1D$

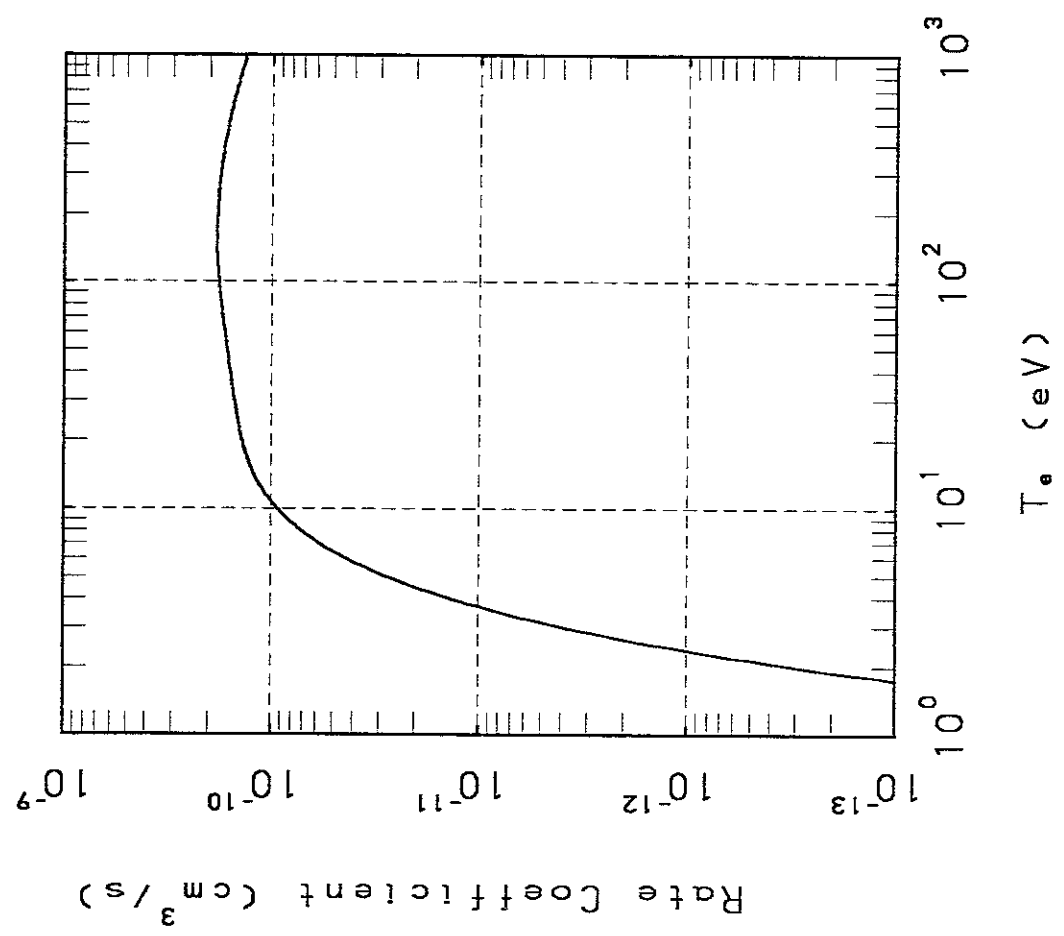
Rate Coefficient (cm^3/s)

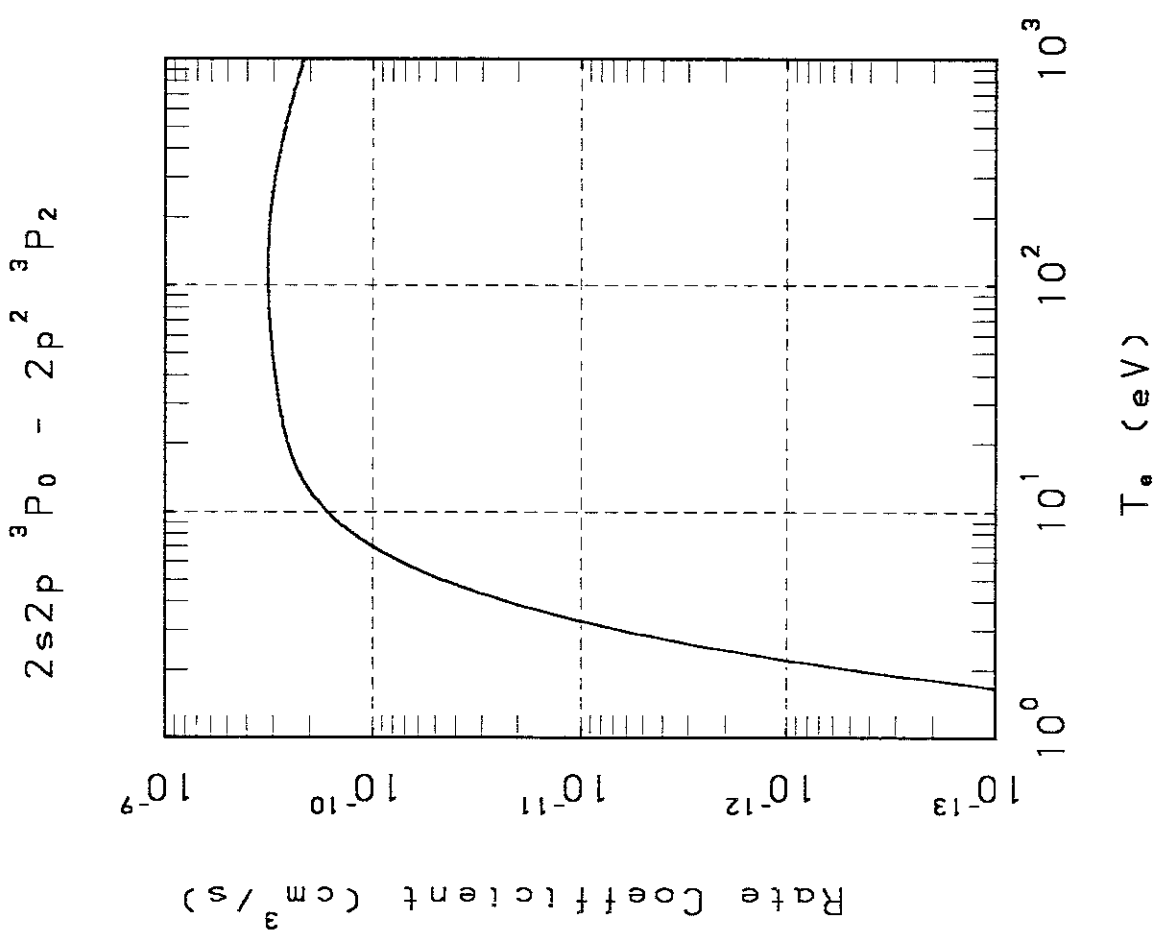
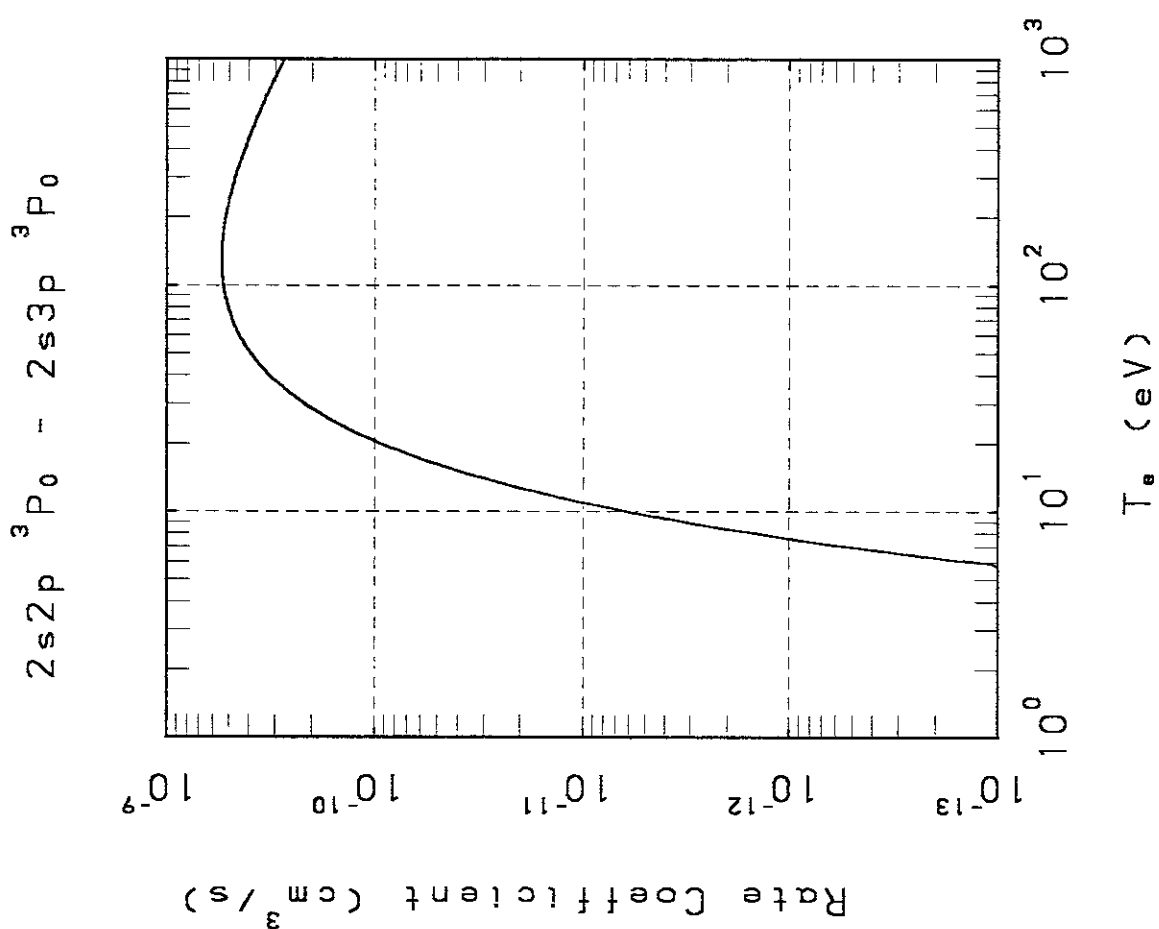


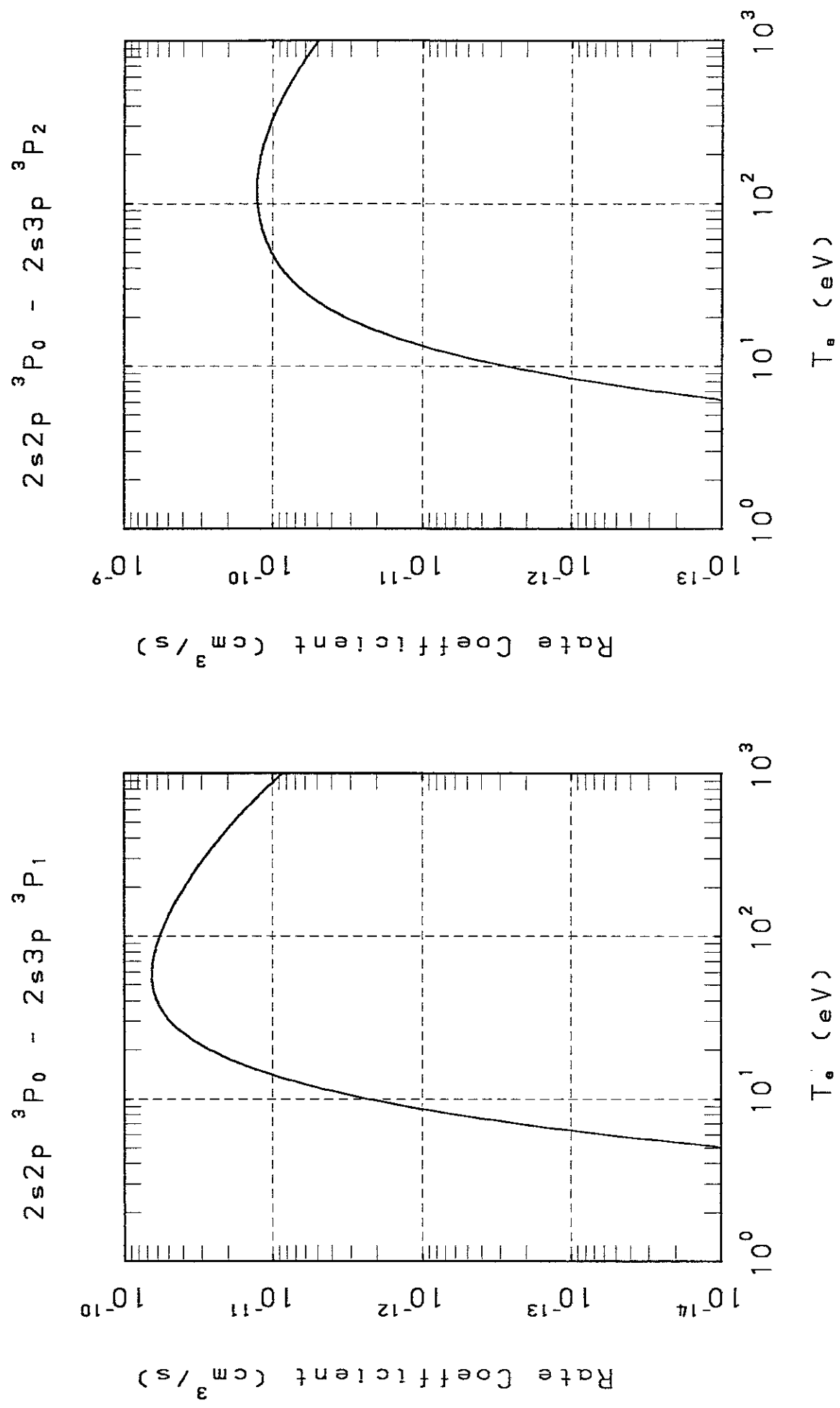
$2s\ 2p\ ^3P_0 - 2p^2\ ^3P_1$

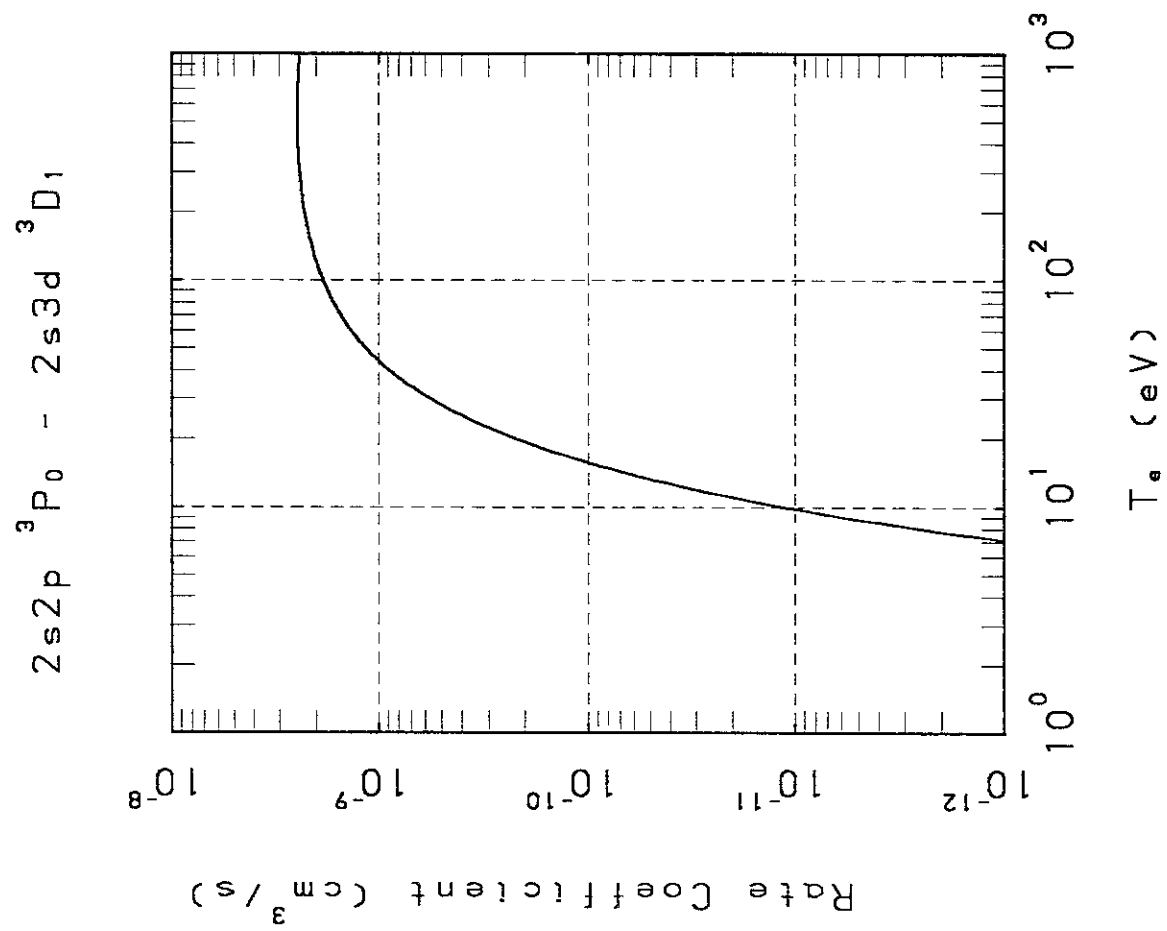
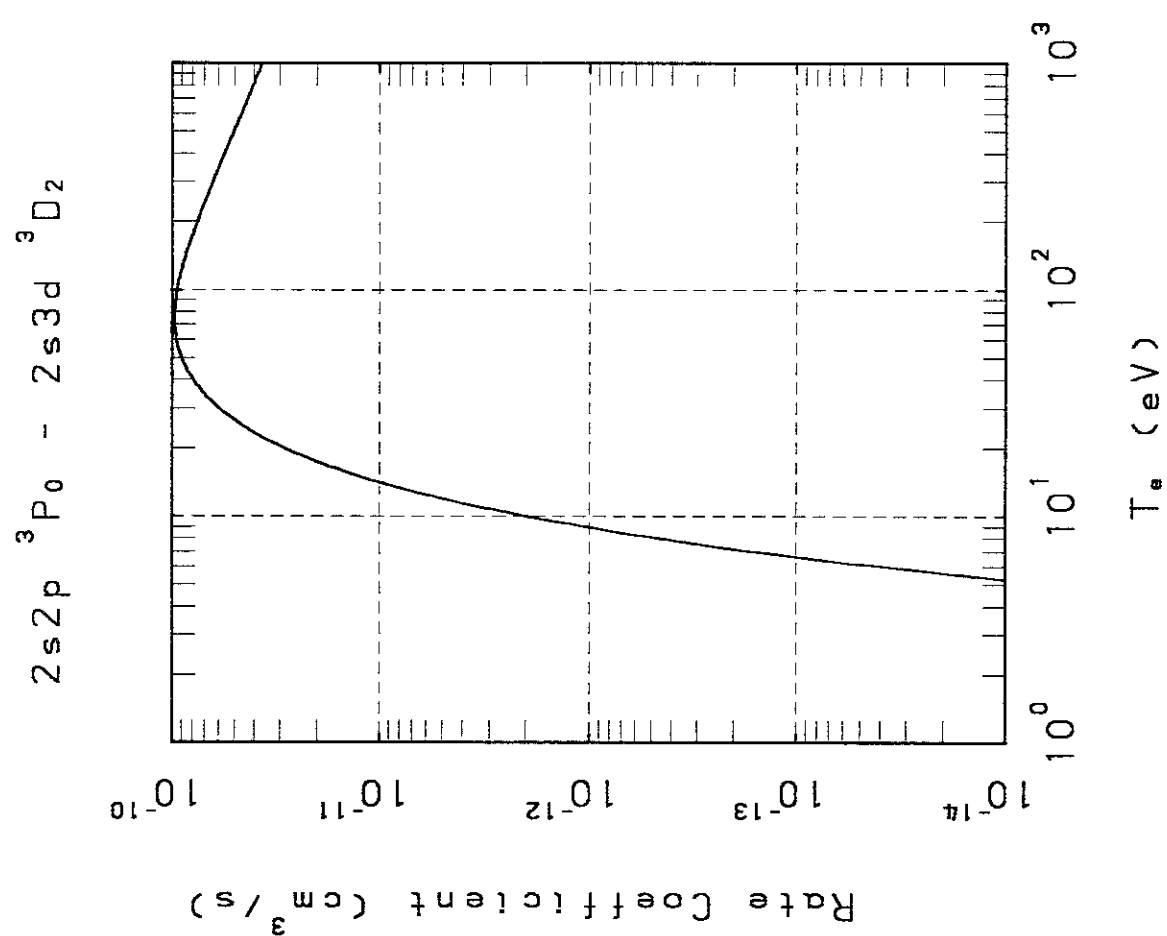


$2s\ 2p\ ^3P_0 - 2p^2\ ^3P_1$

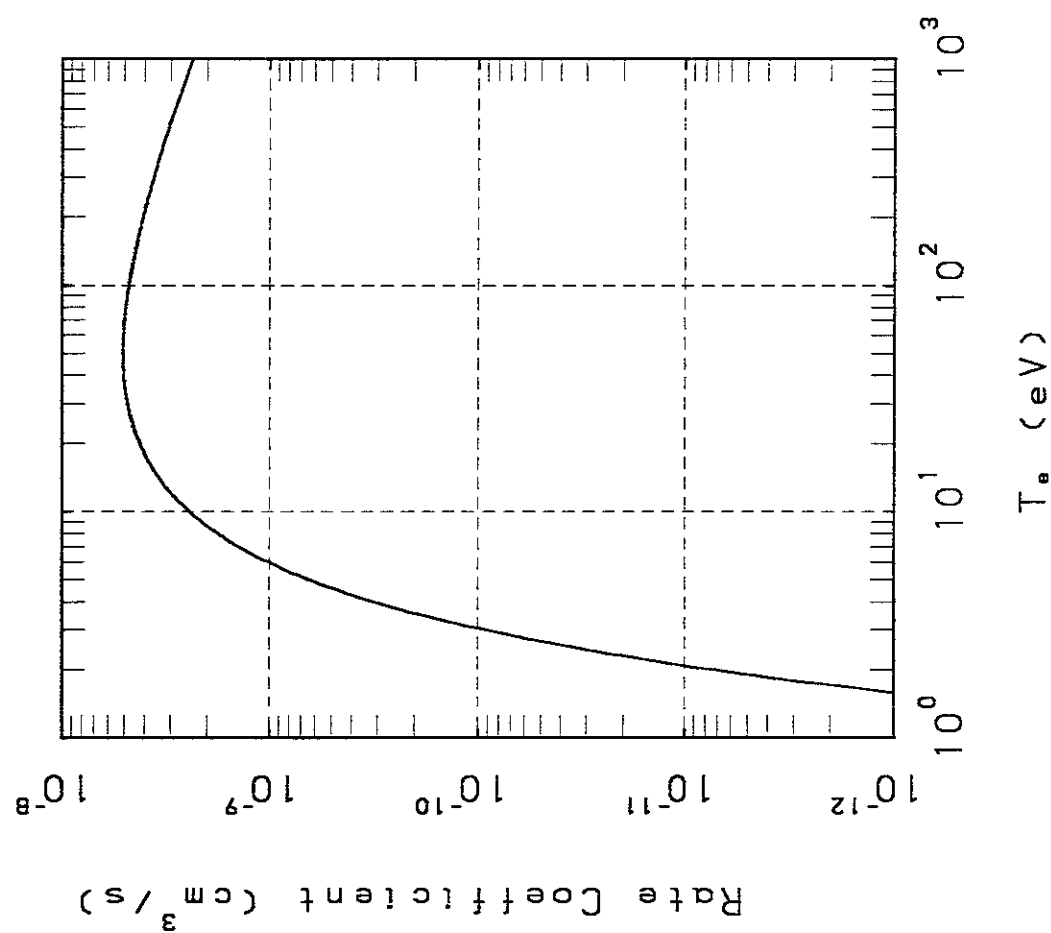




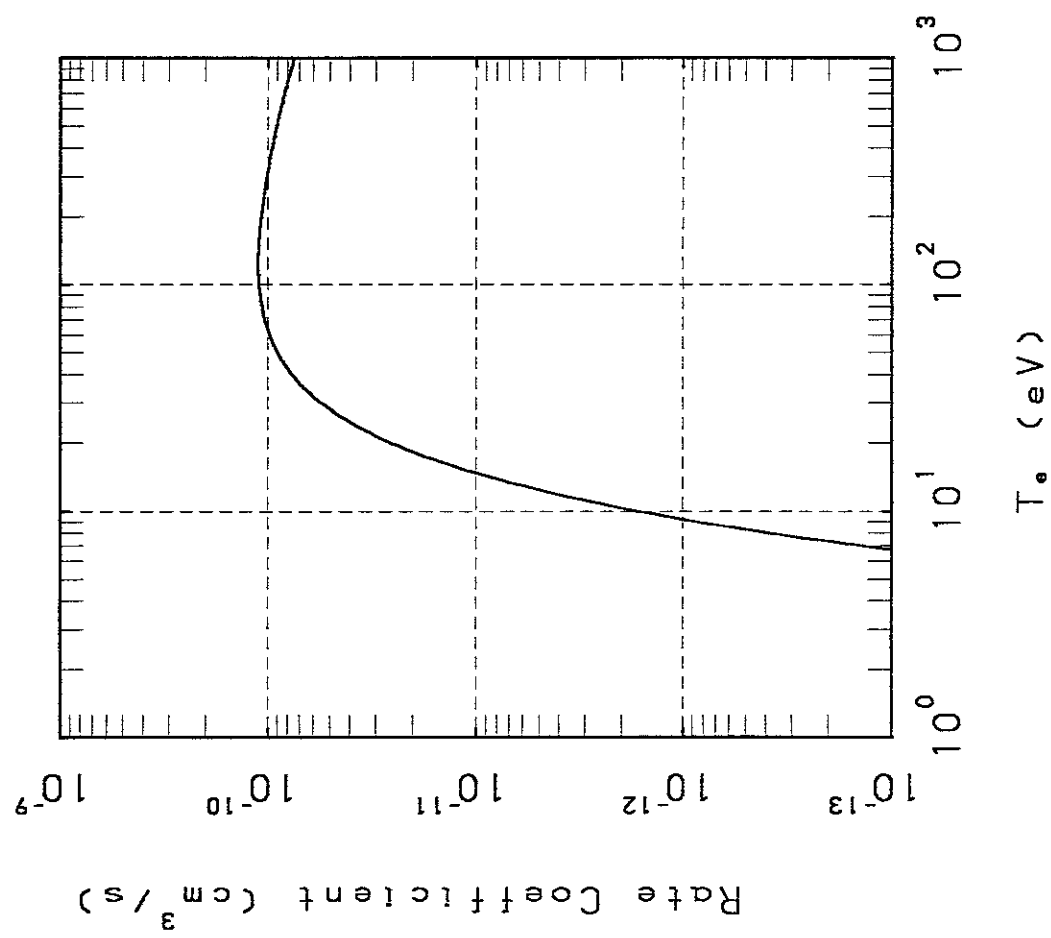




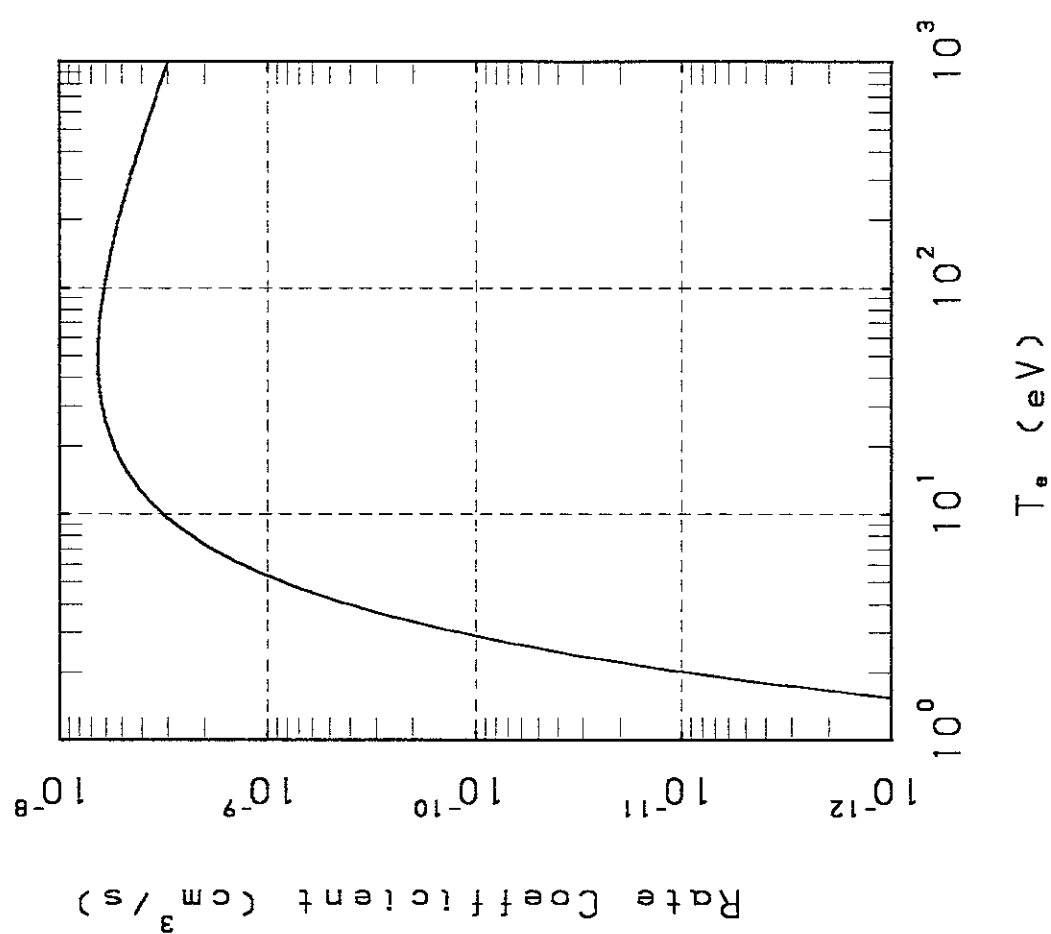
$2s2p\ ^3P_1 - 2p^2\ ^3P_0$



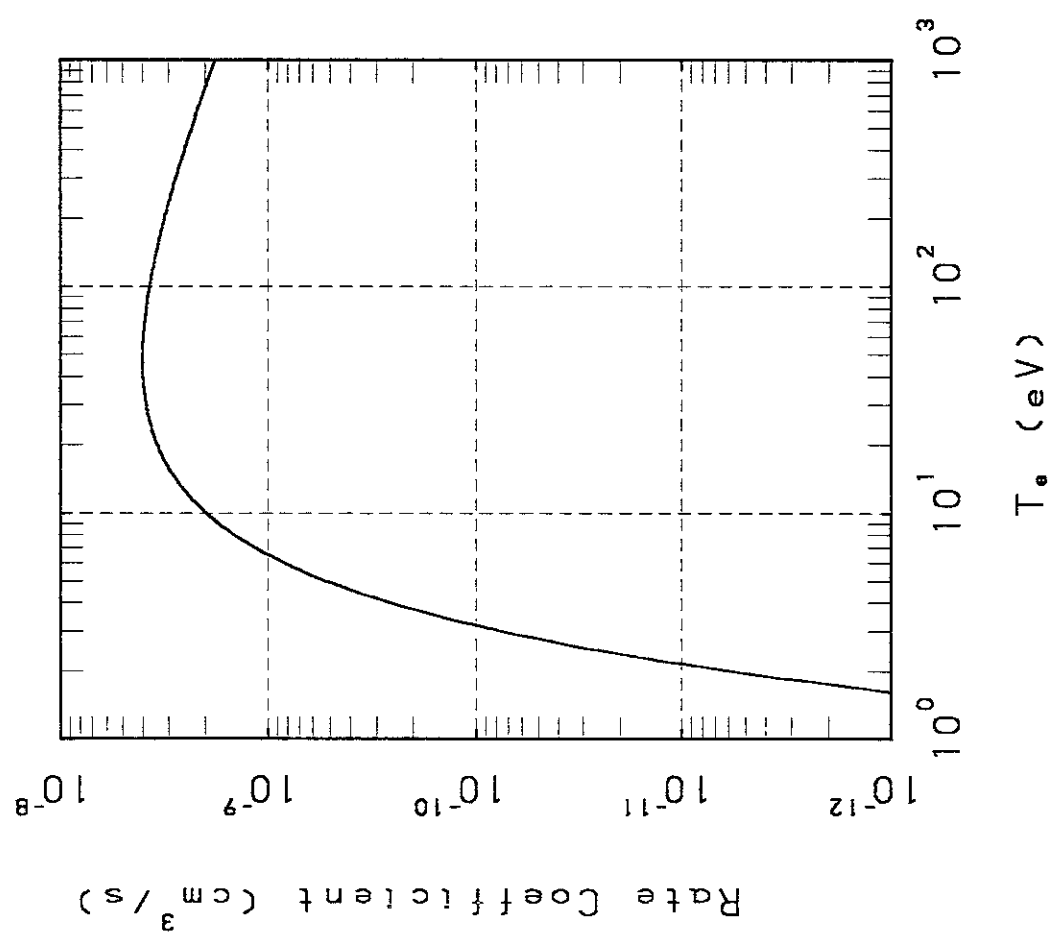
$2s2p\ ^3P_0 - 2s3d\ ^3D_3$

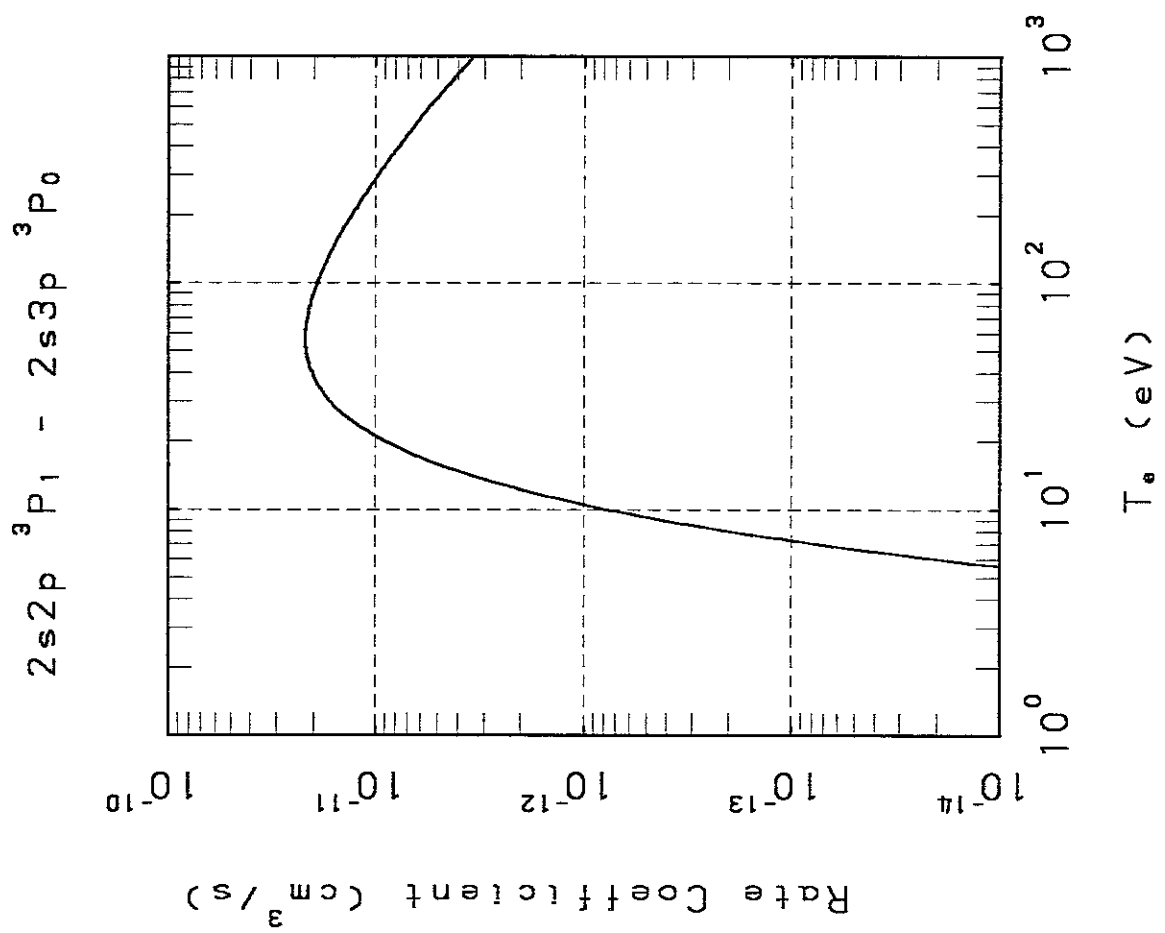
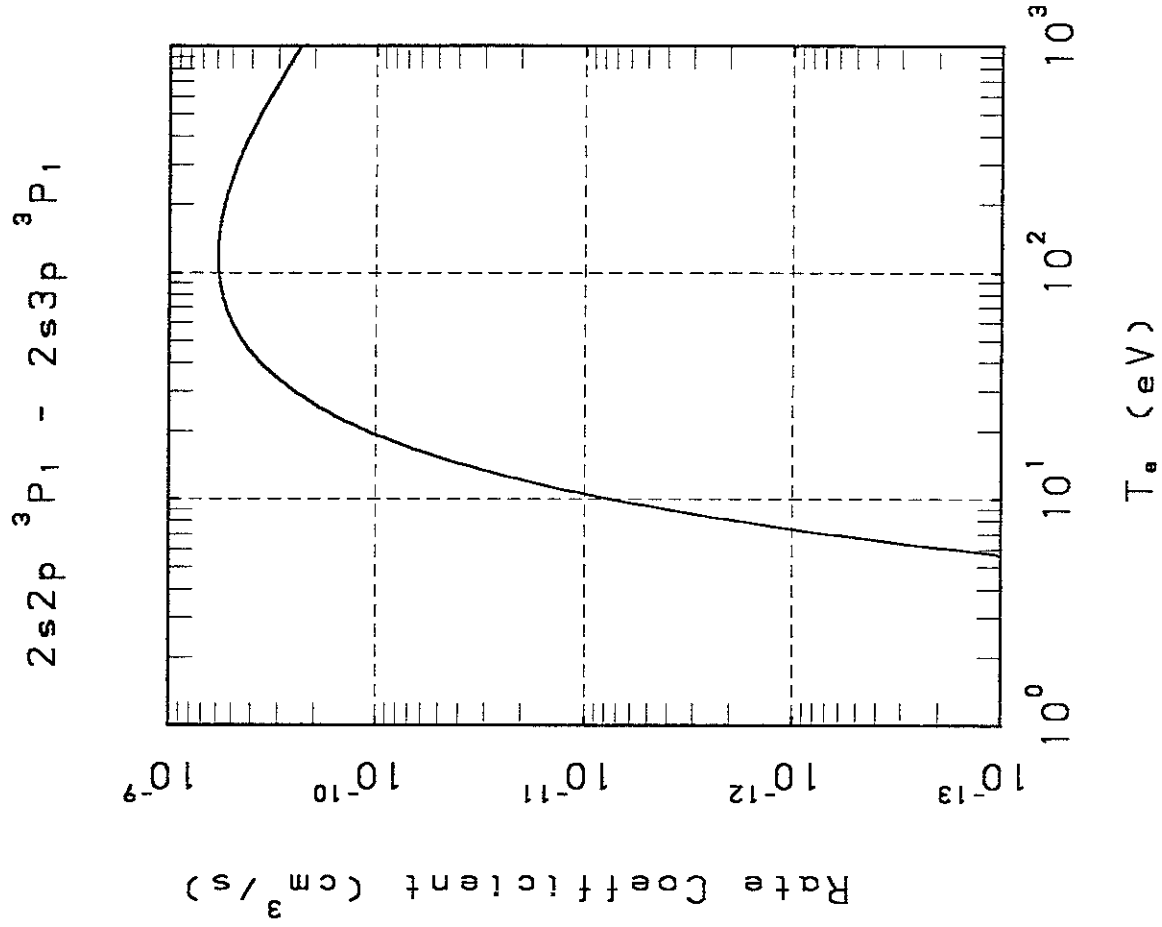


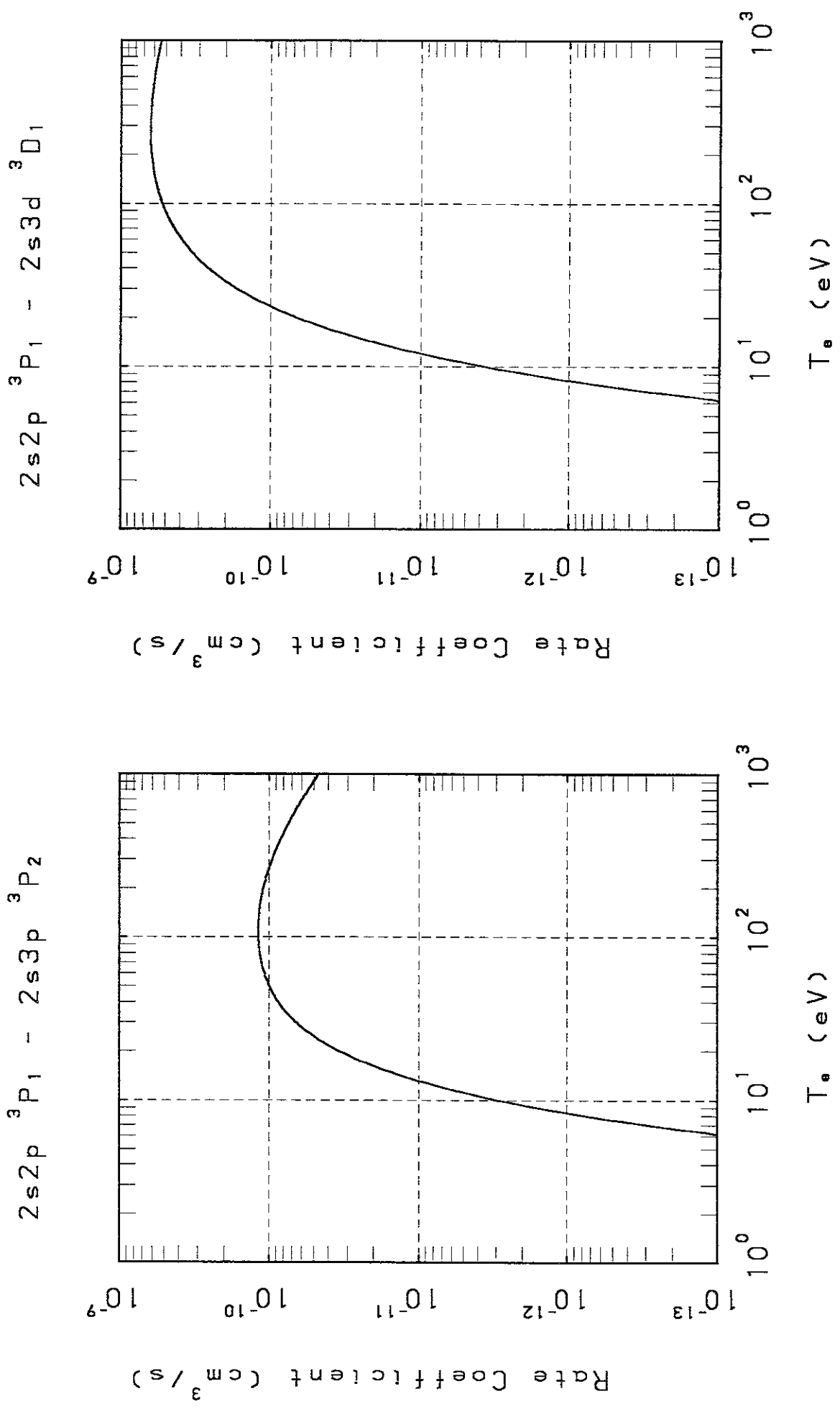
$2s\ 2p\ ^3P_1 - 2p^2\ ^3P_2$

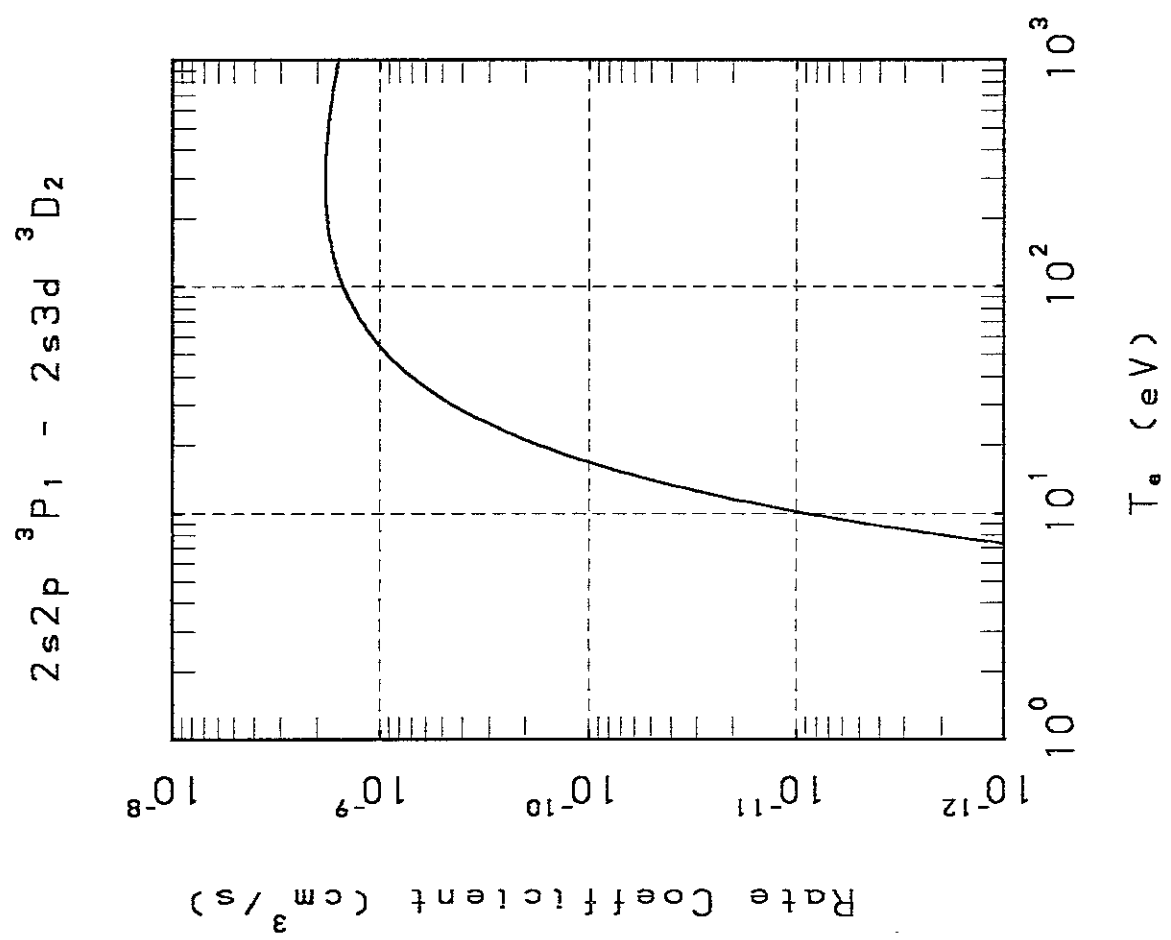
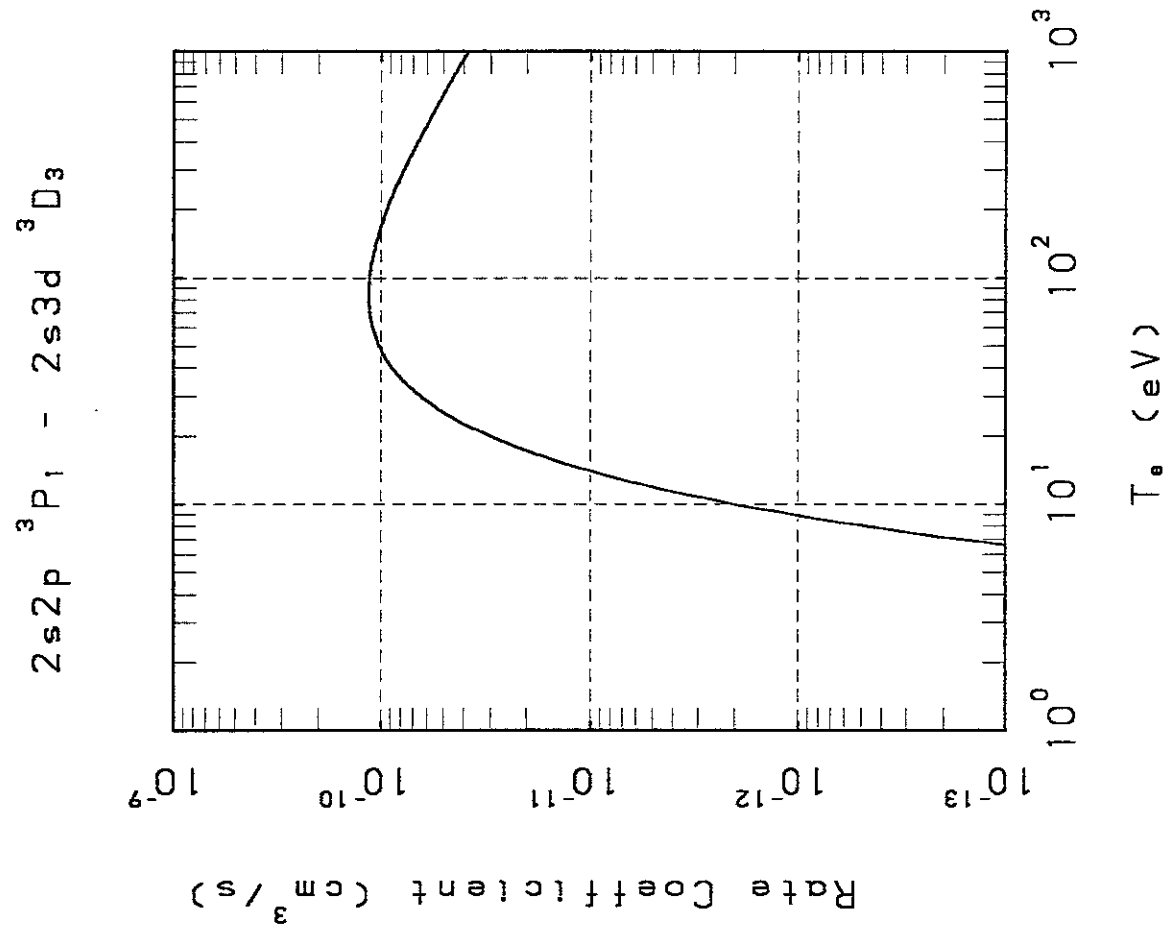


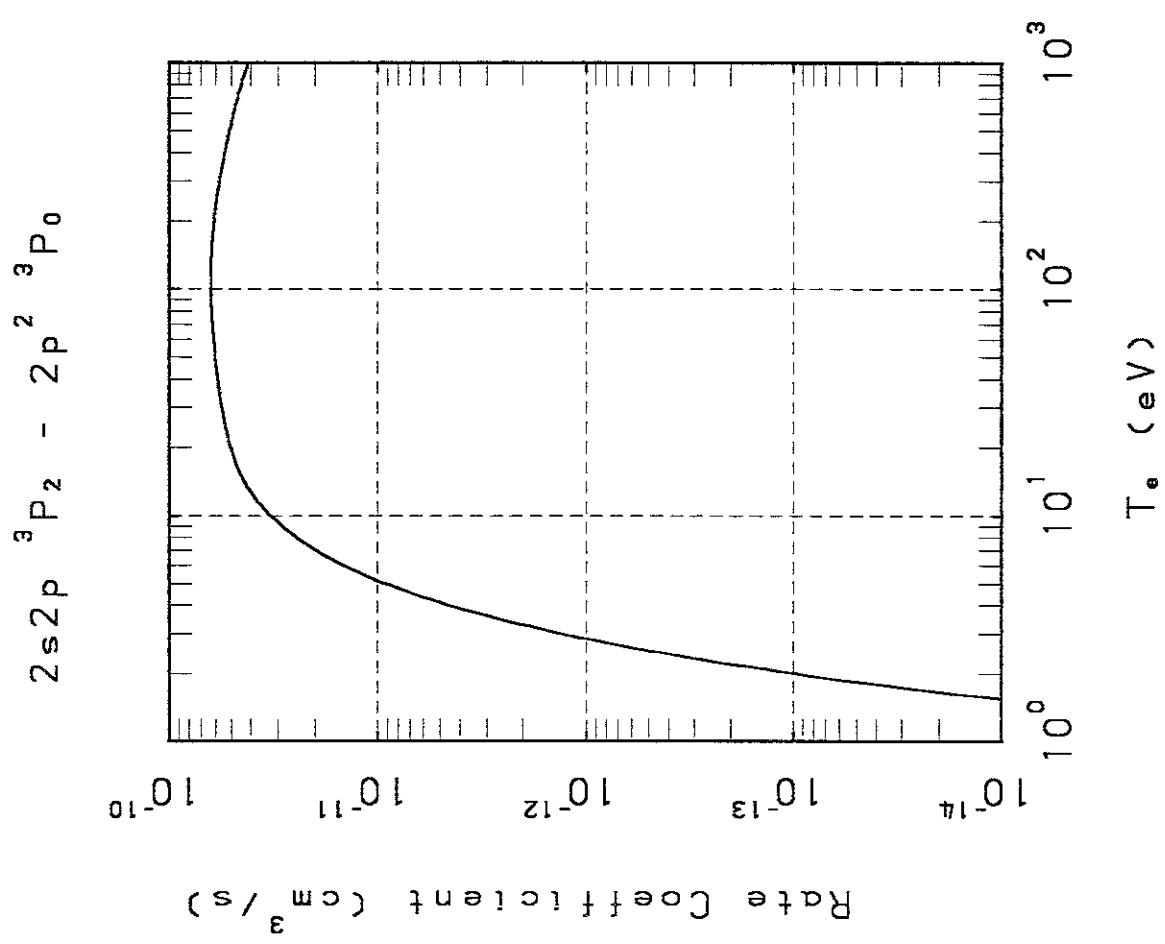
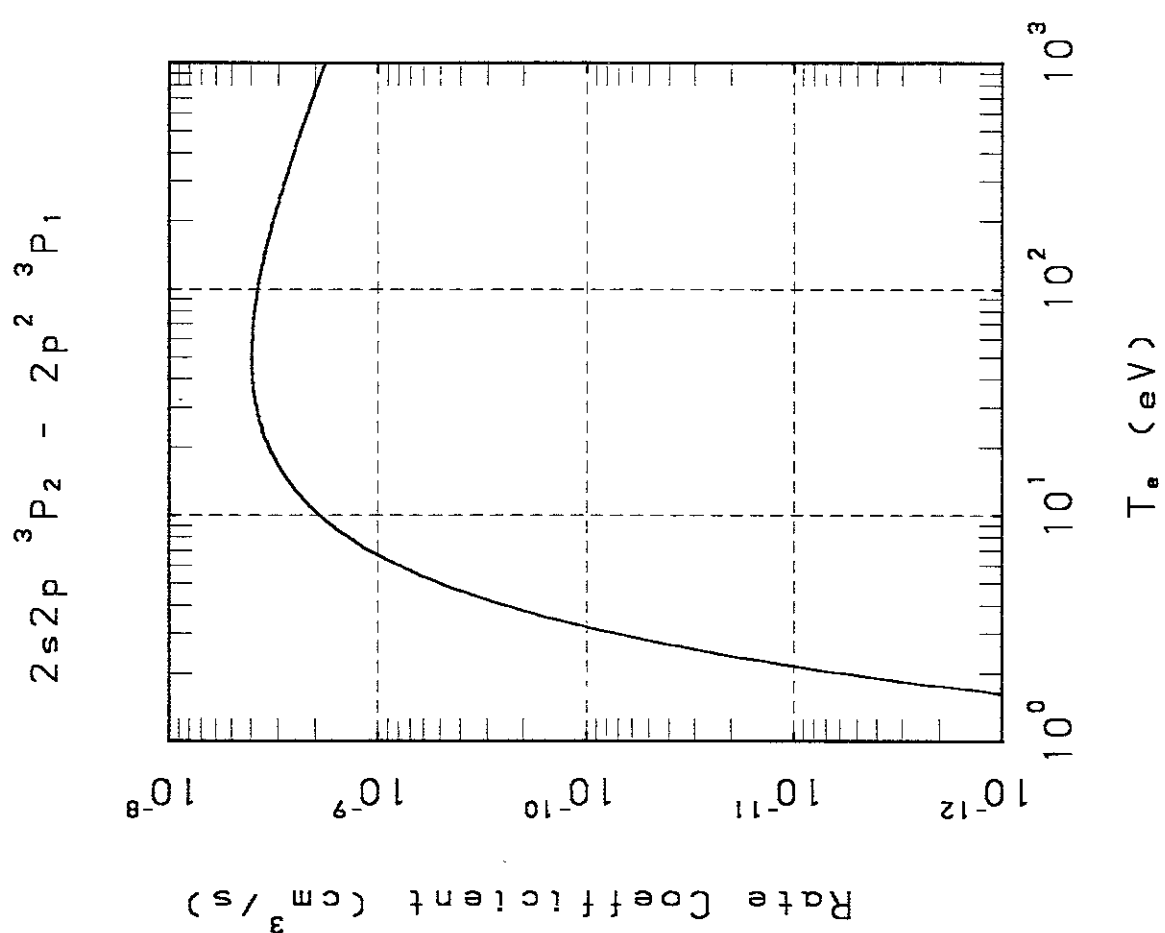
$2s\ 2p\ ^3P_1 - 2p^2\ ^3P_1$

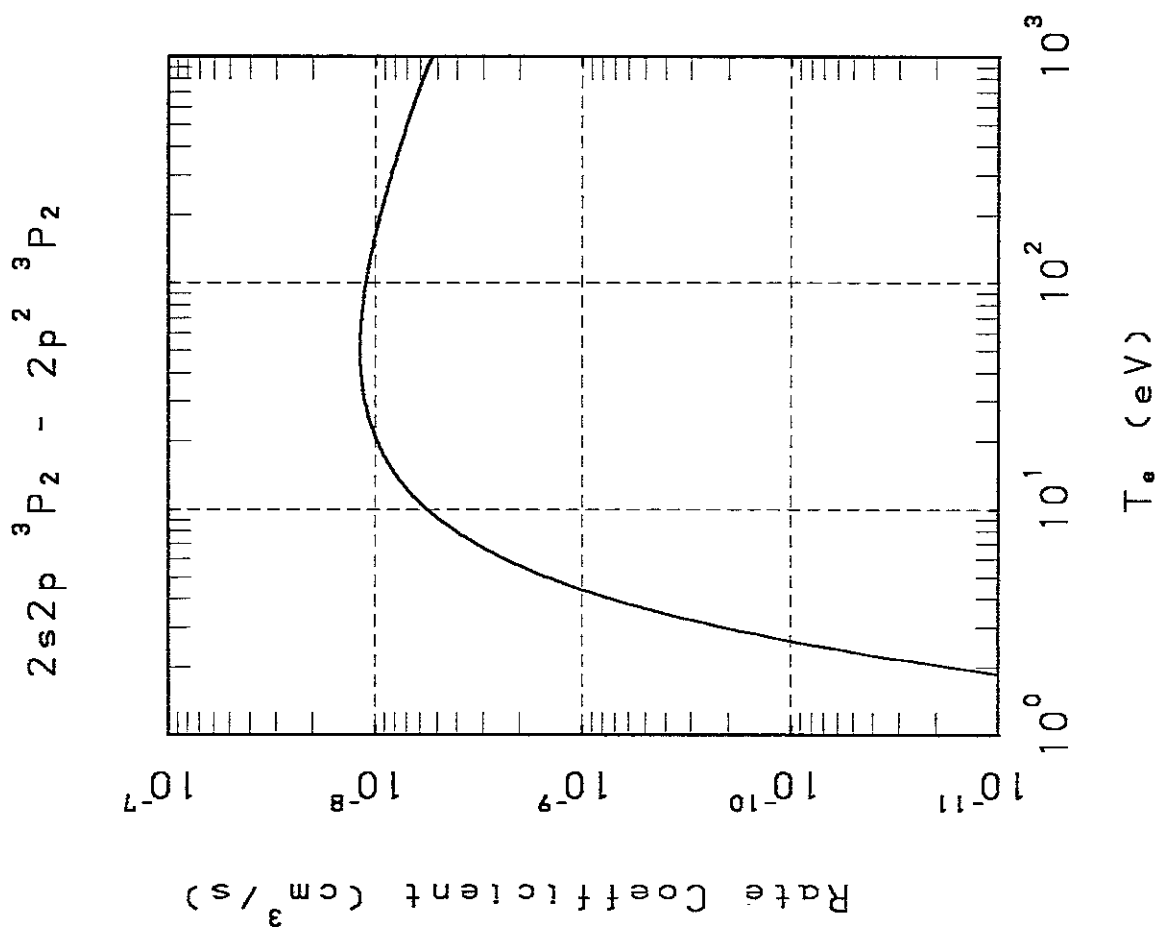
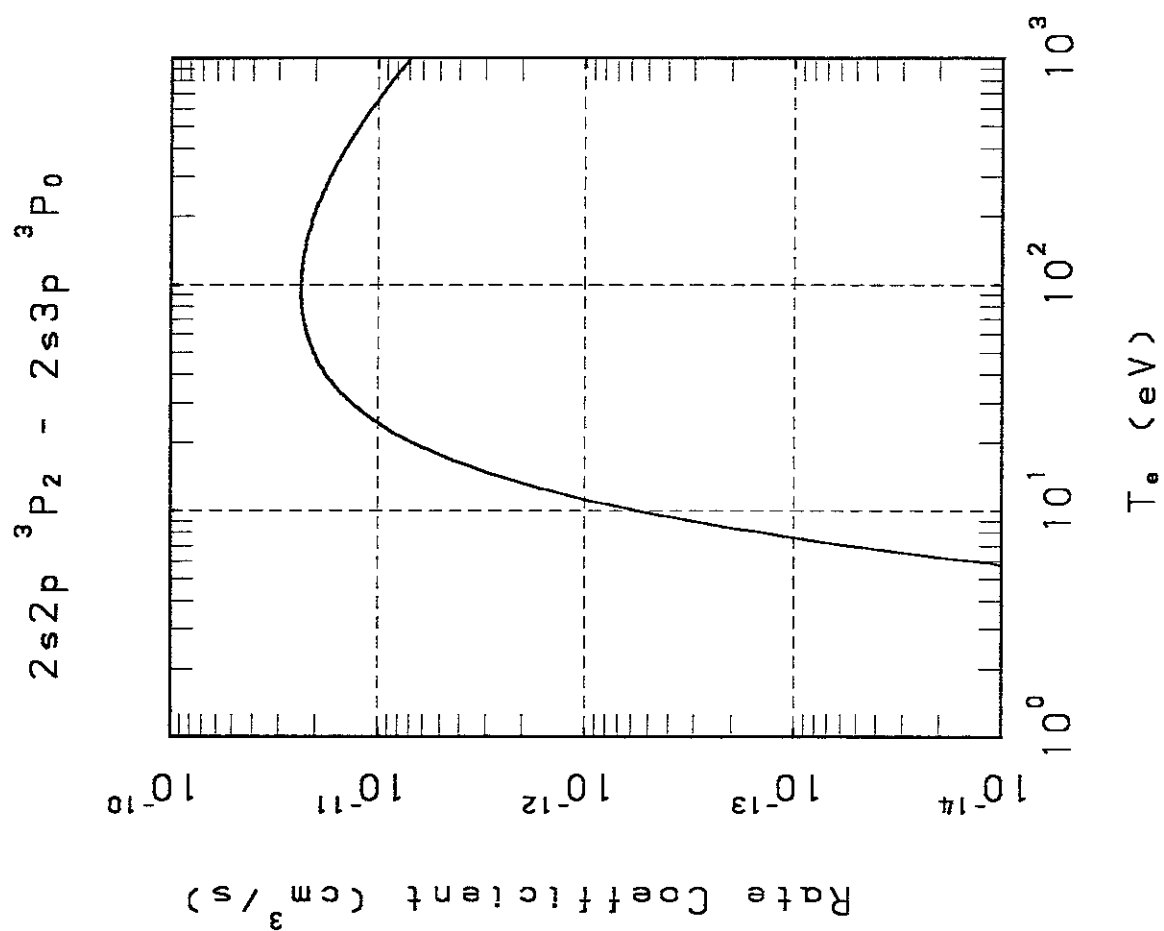


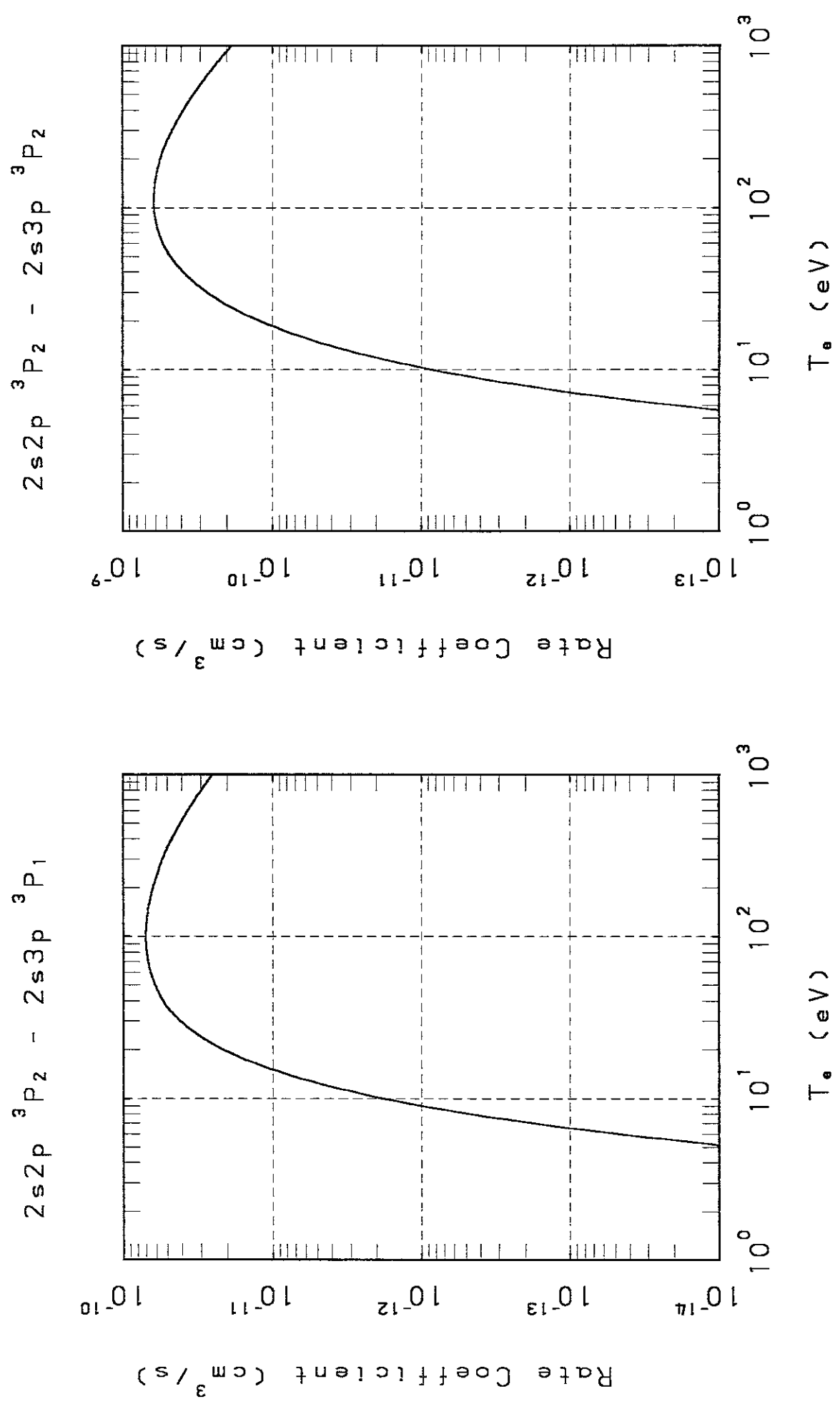


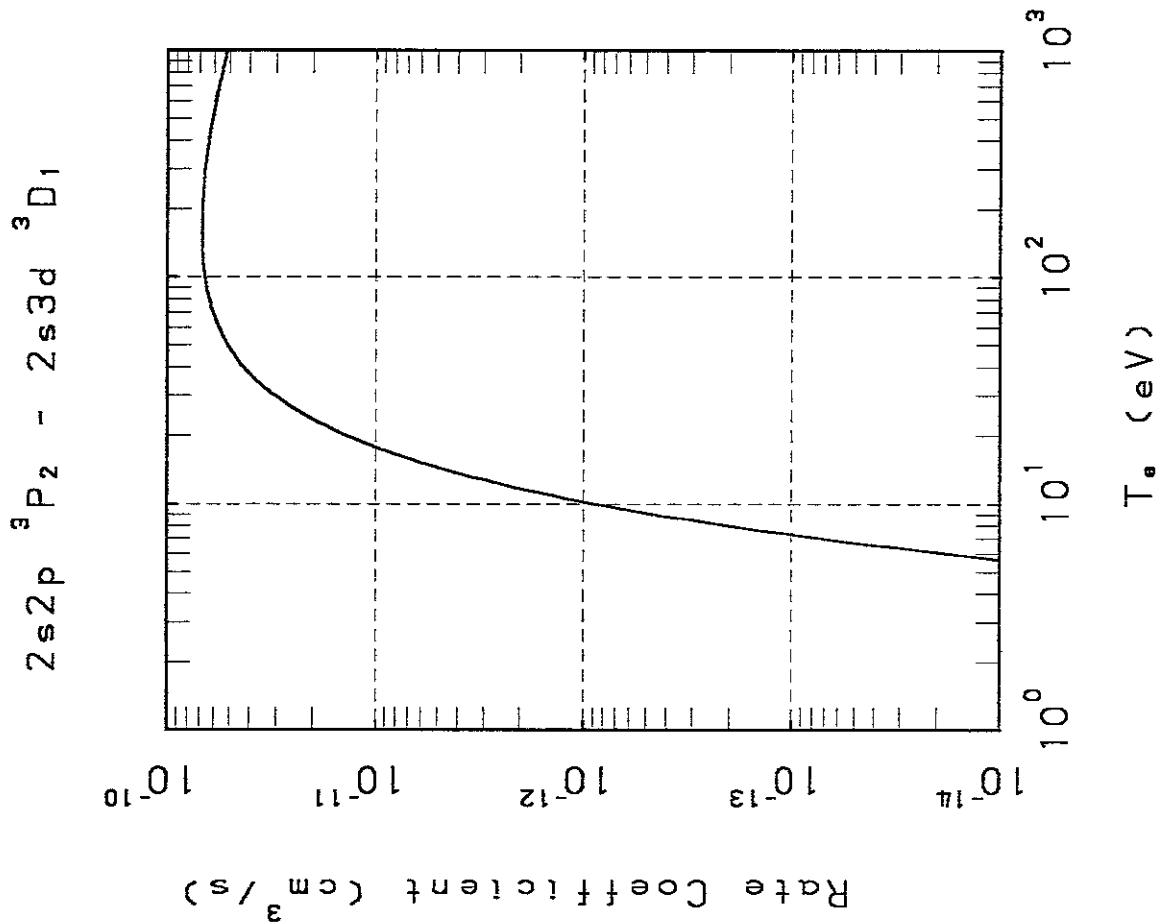
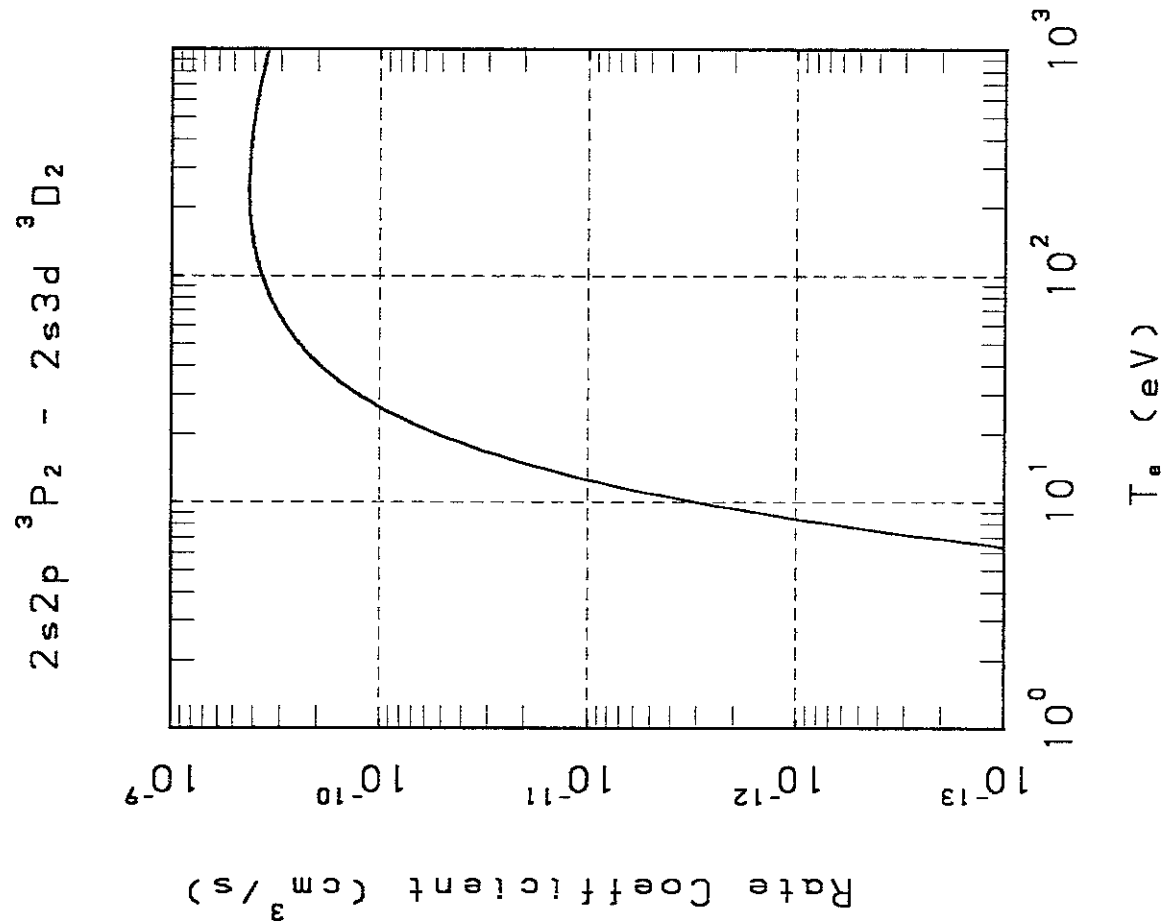


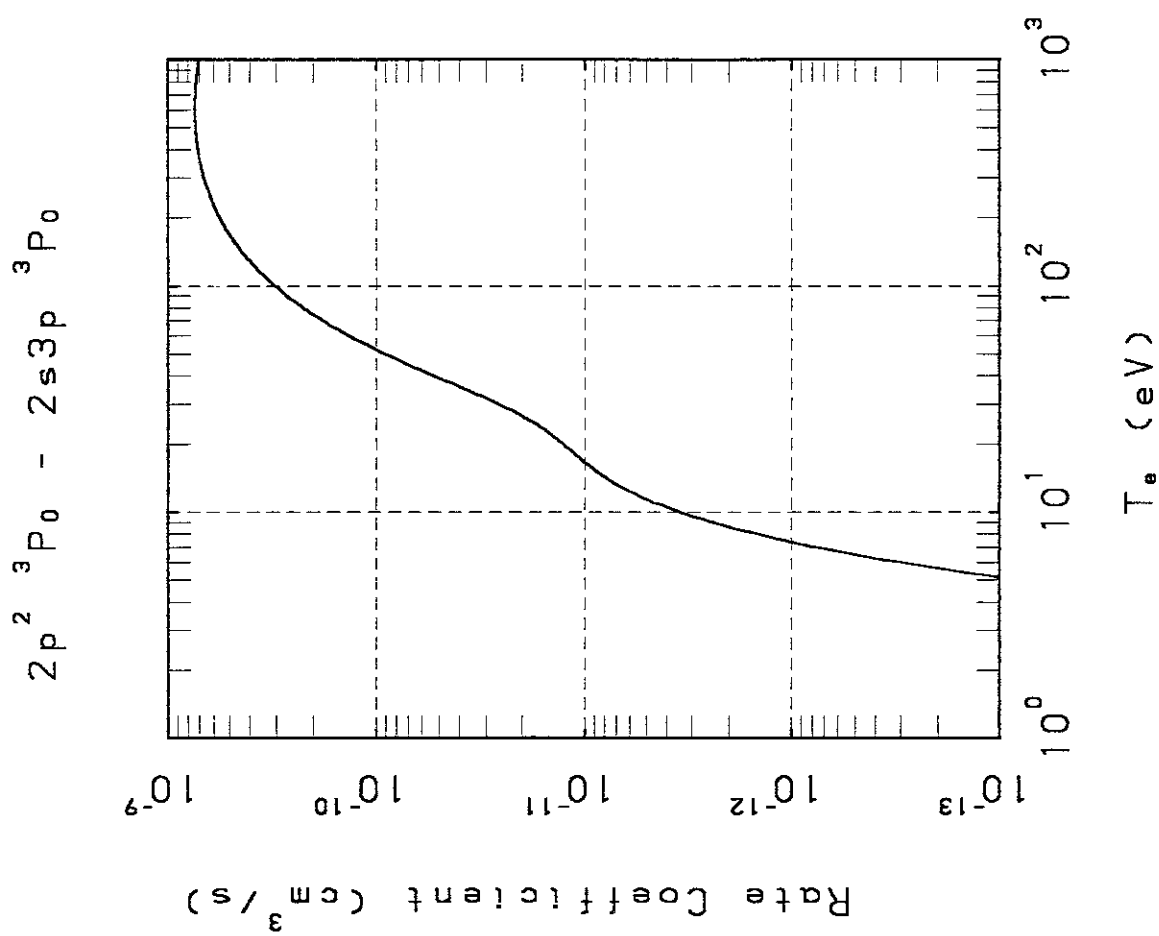
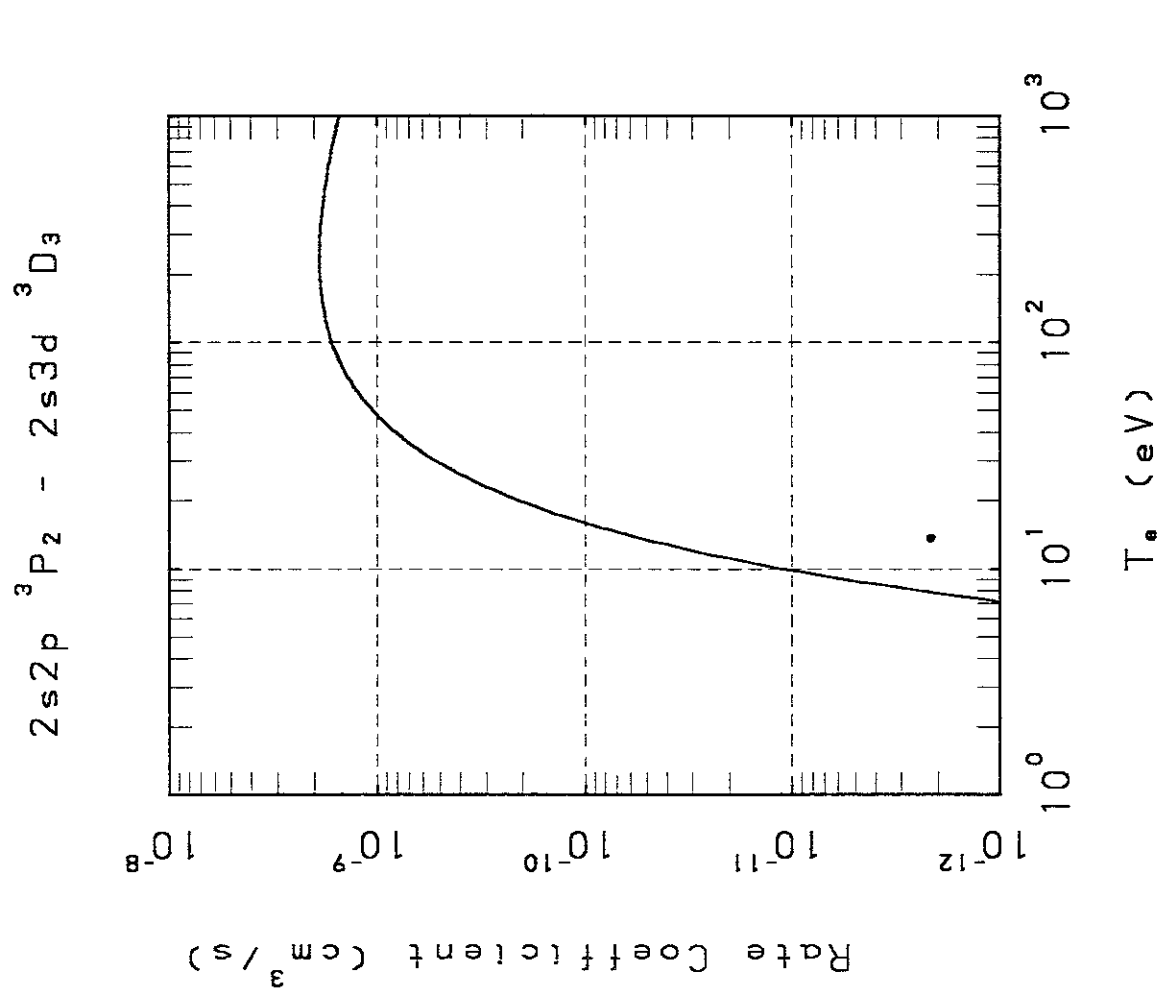


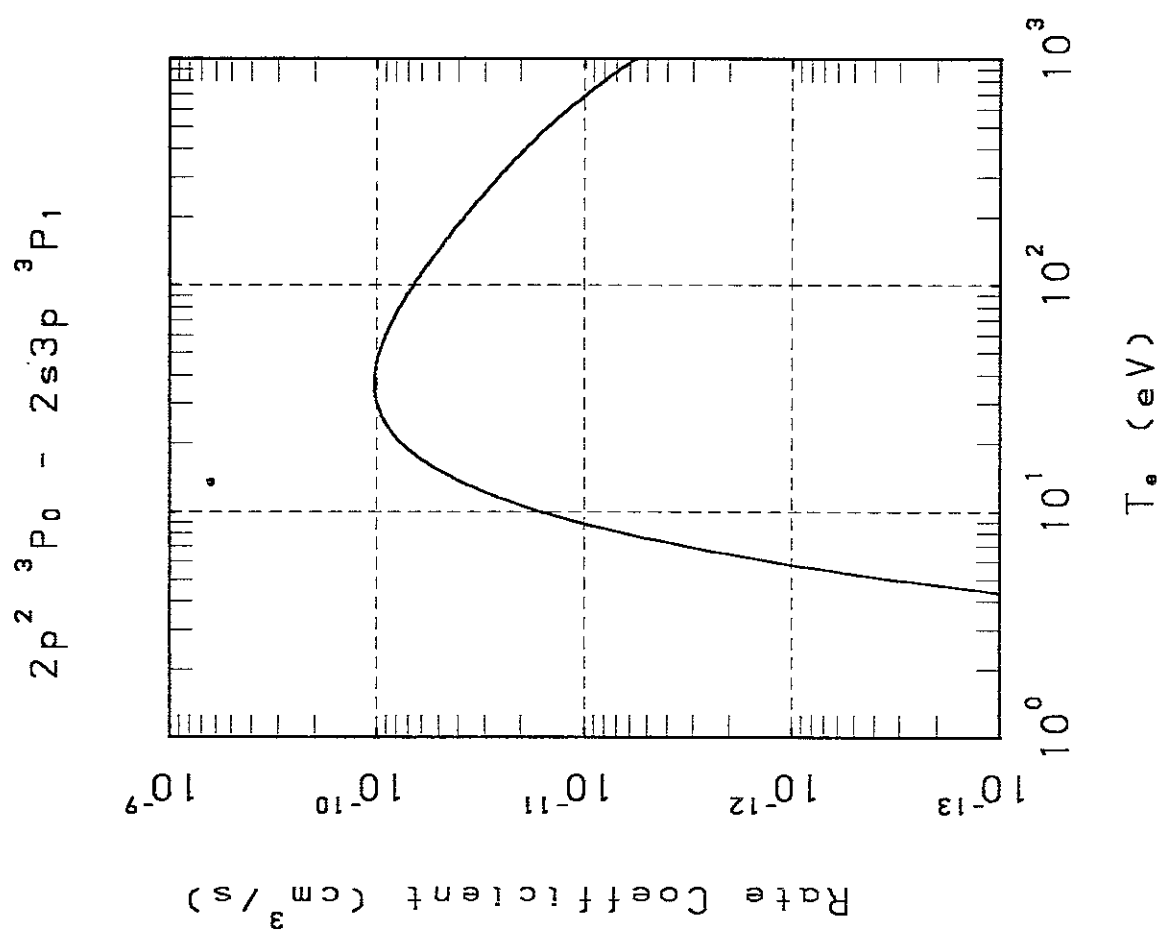
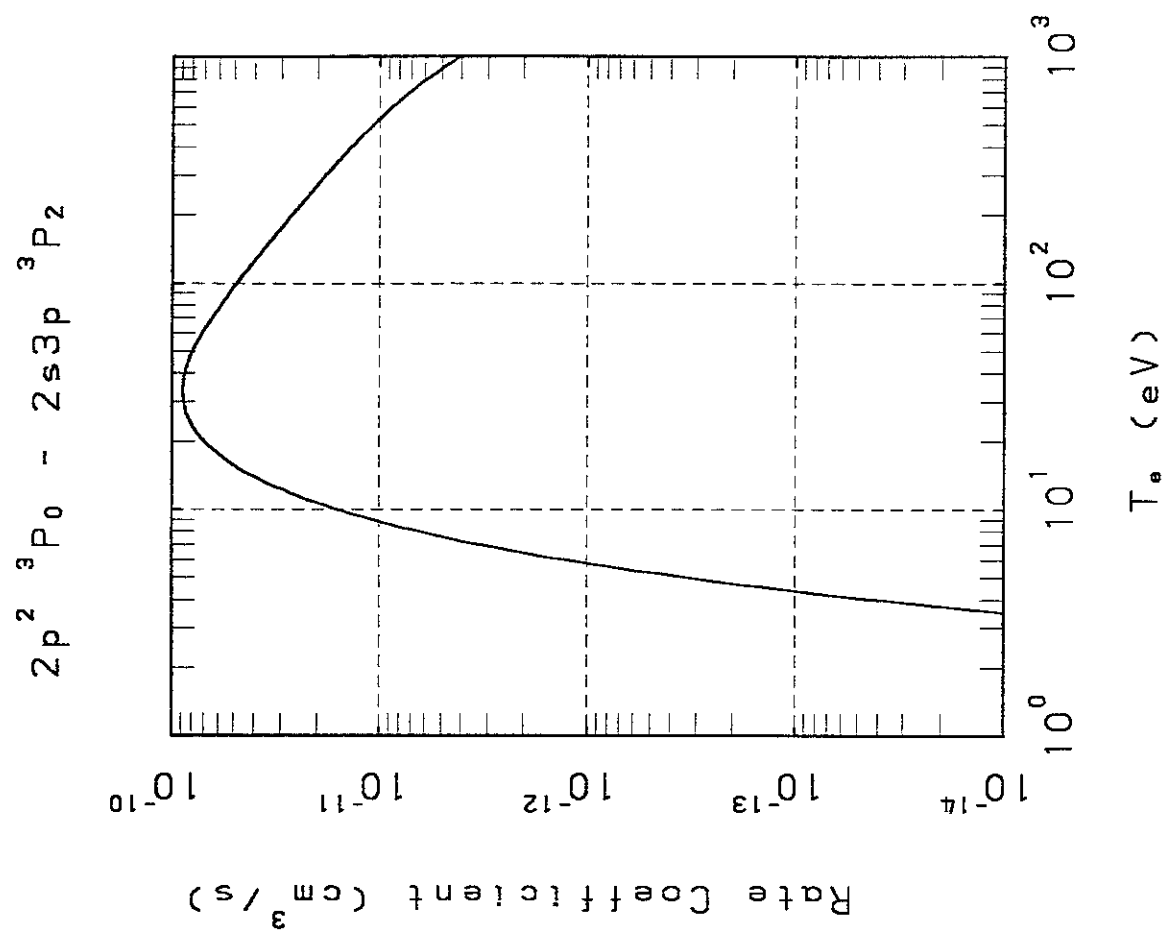


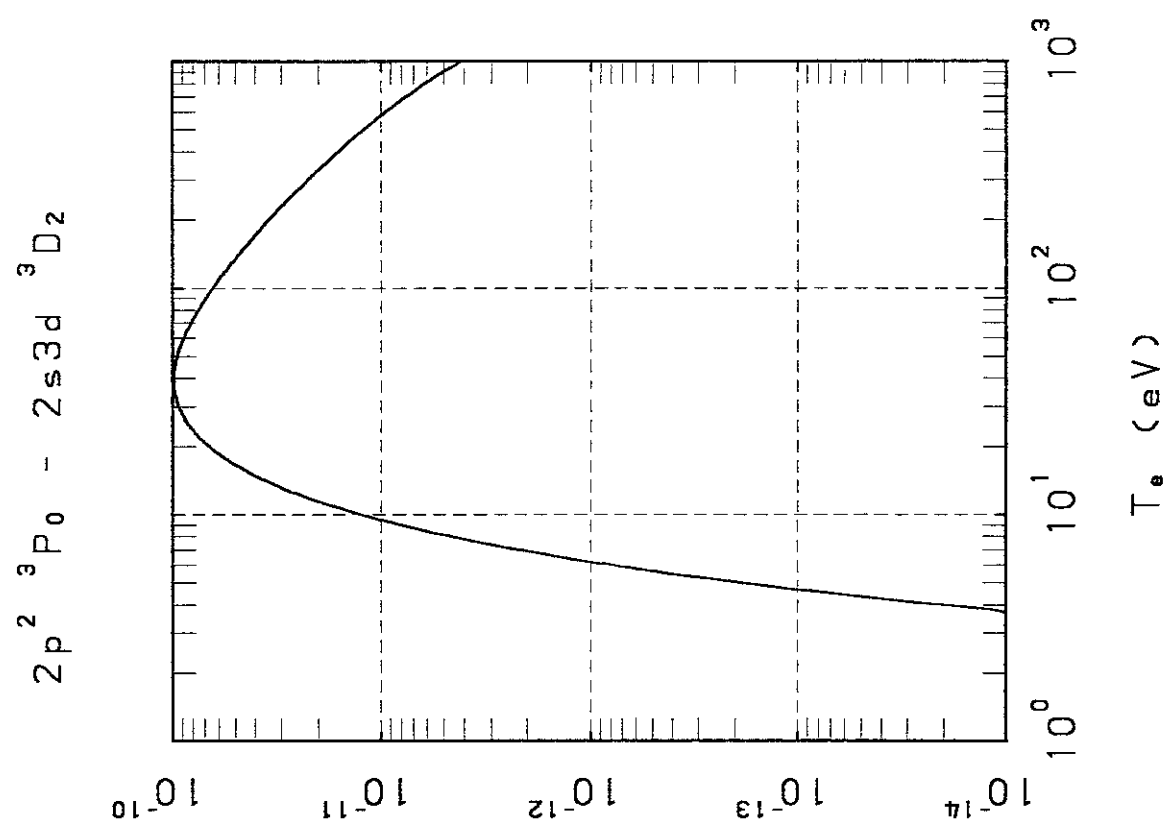
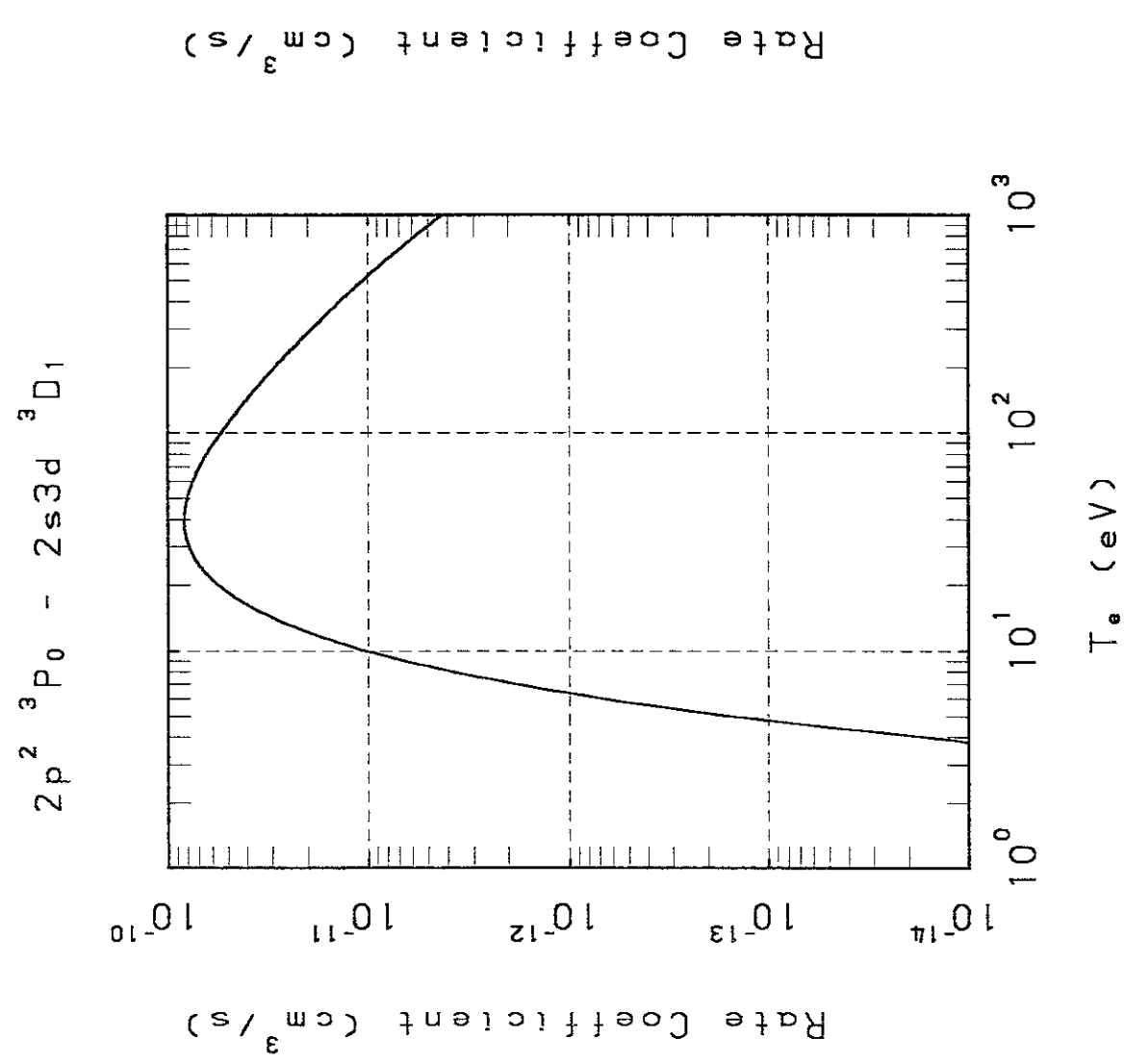


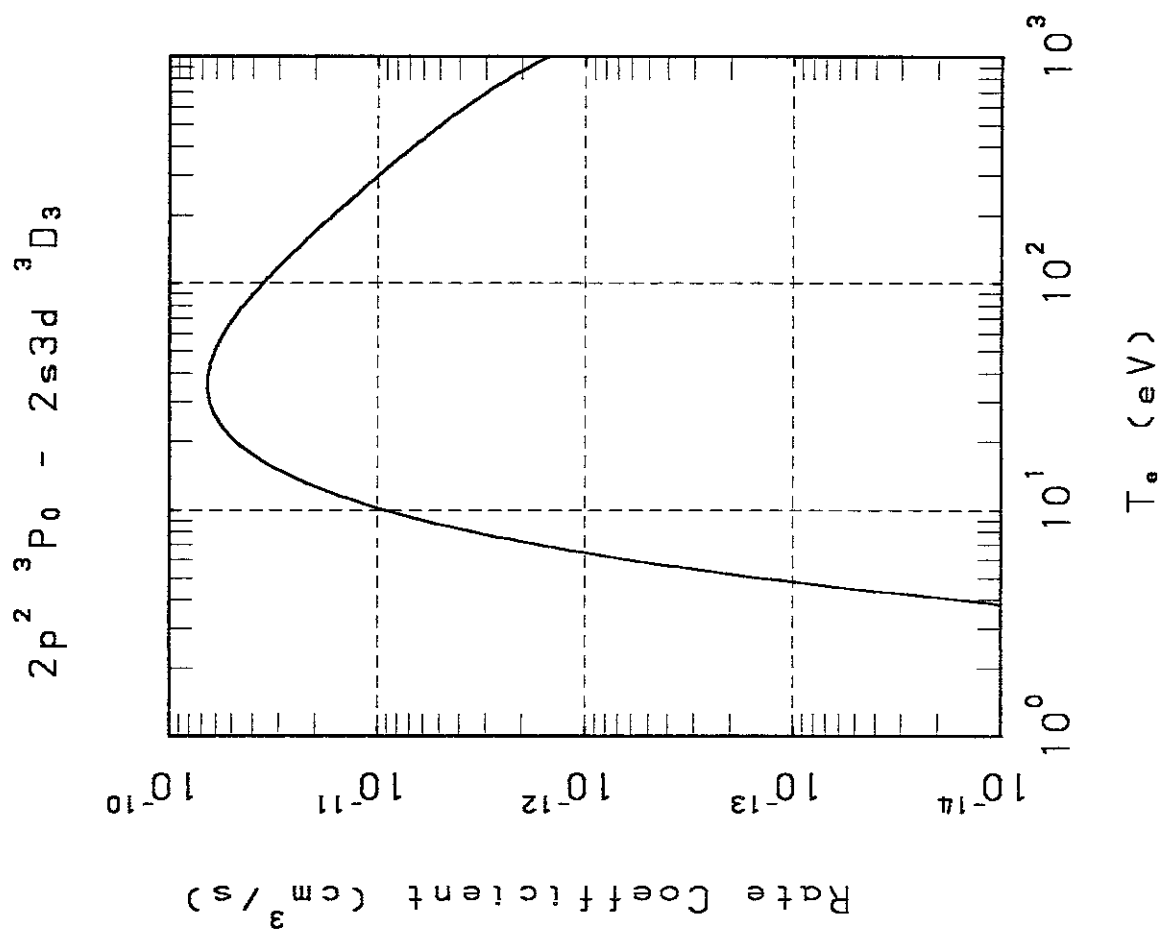
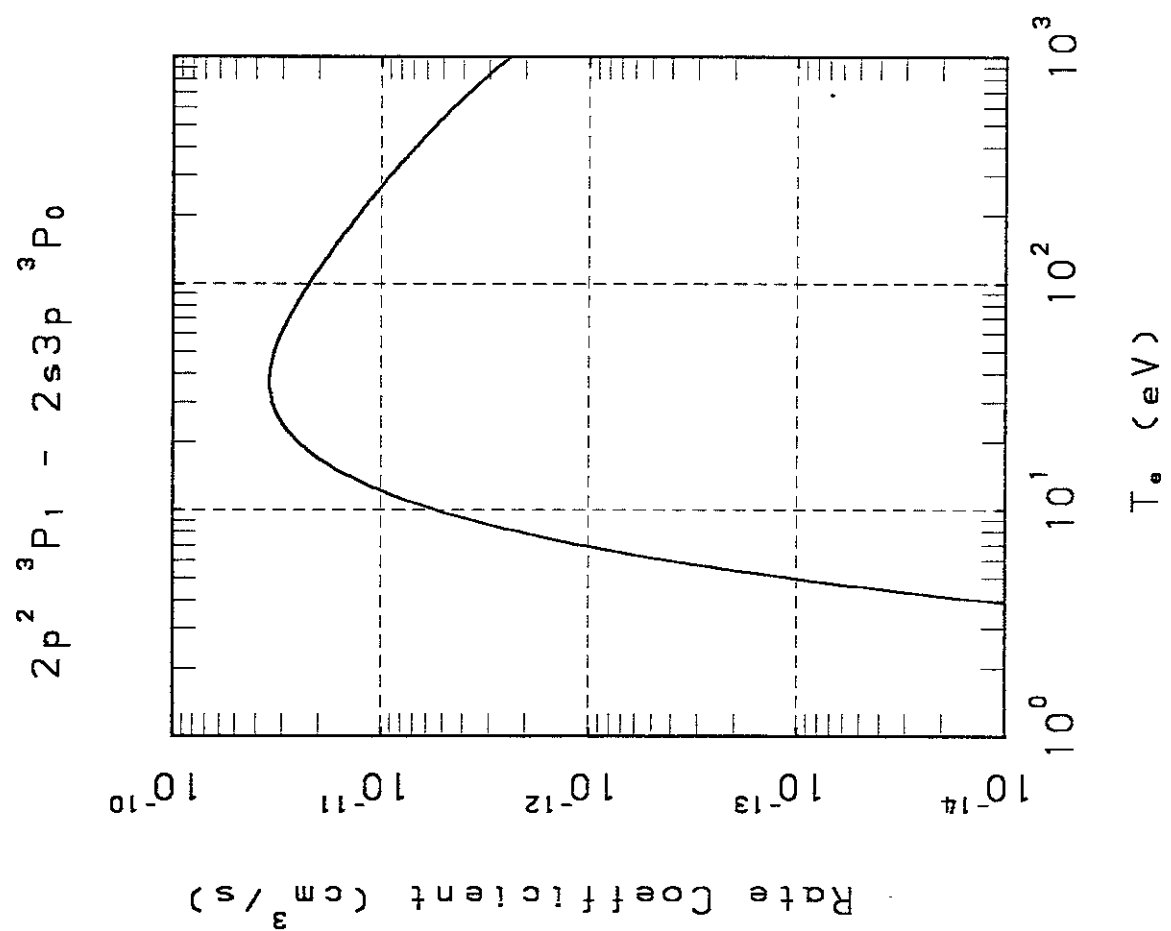


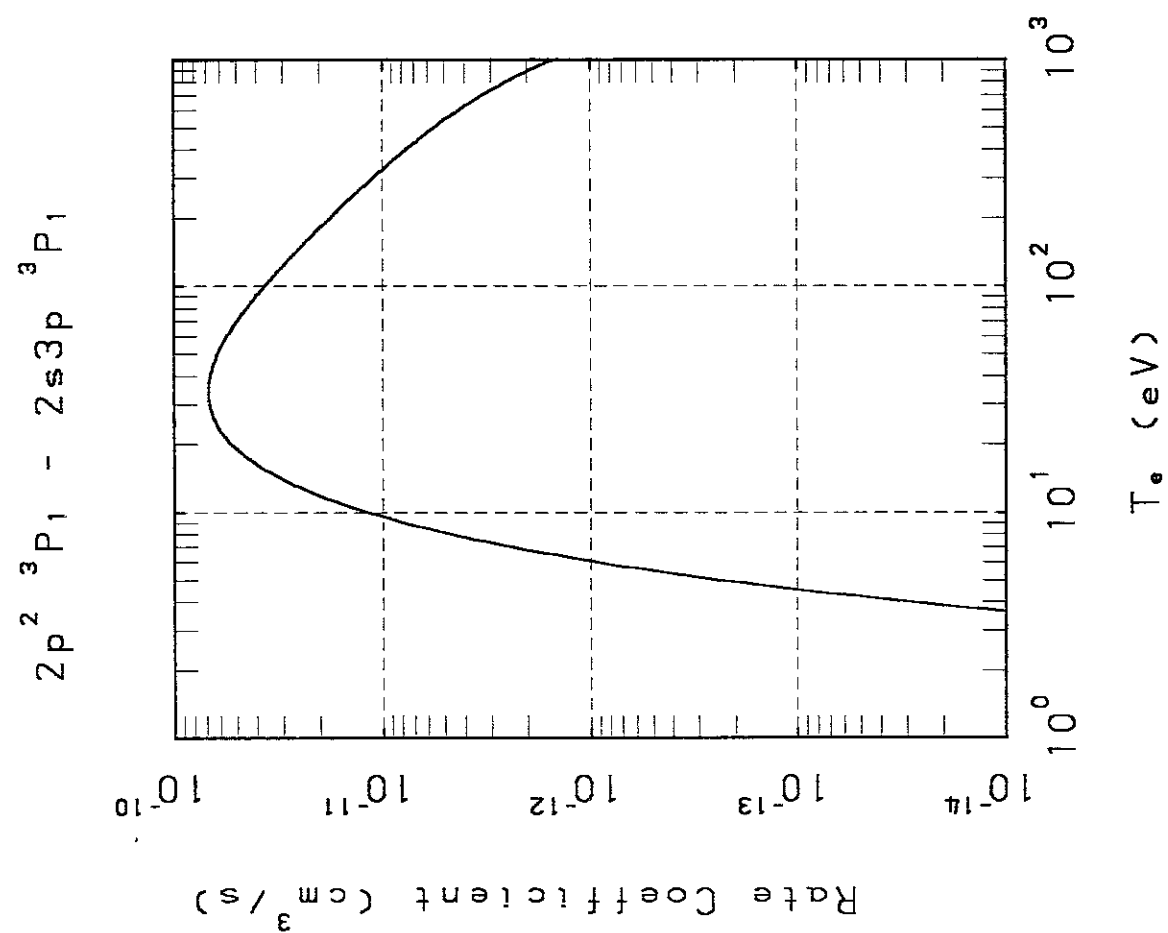
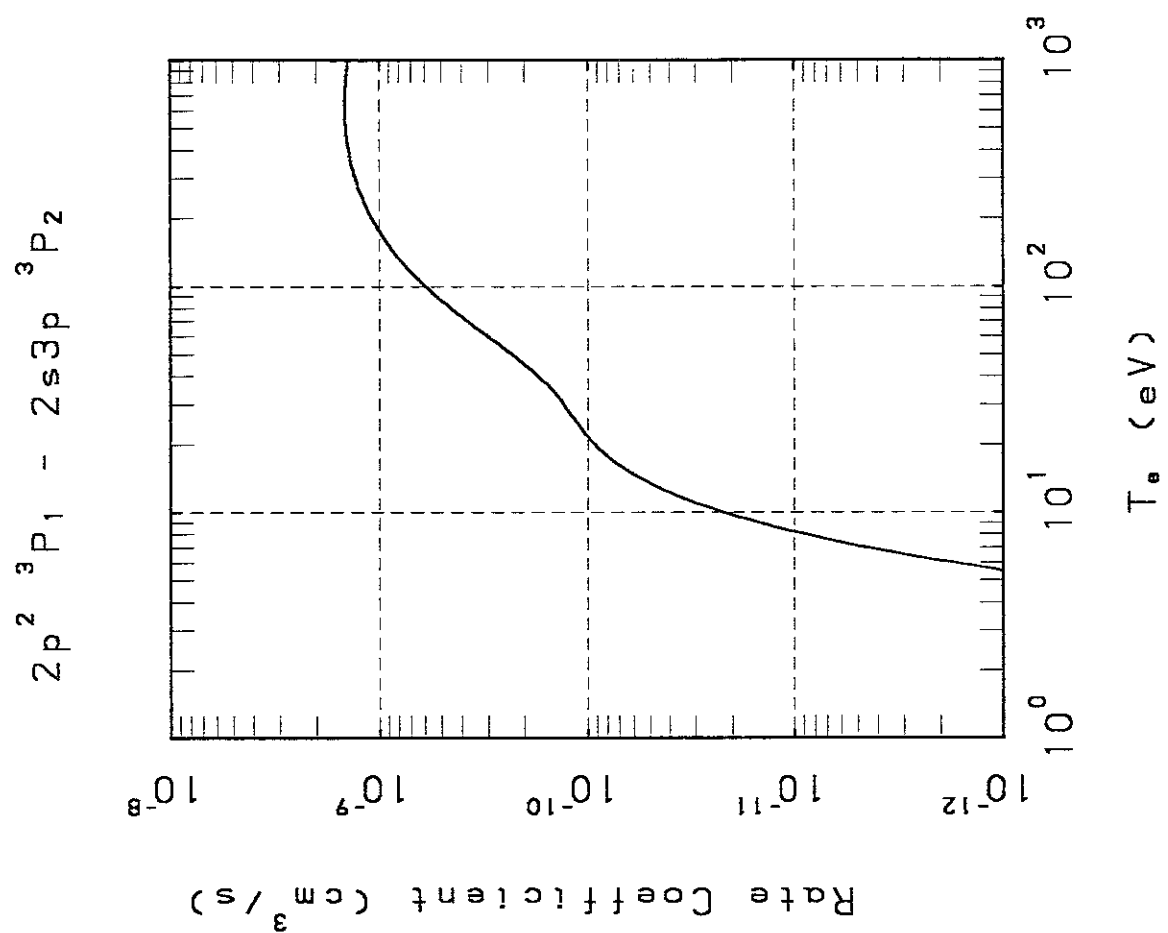


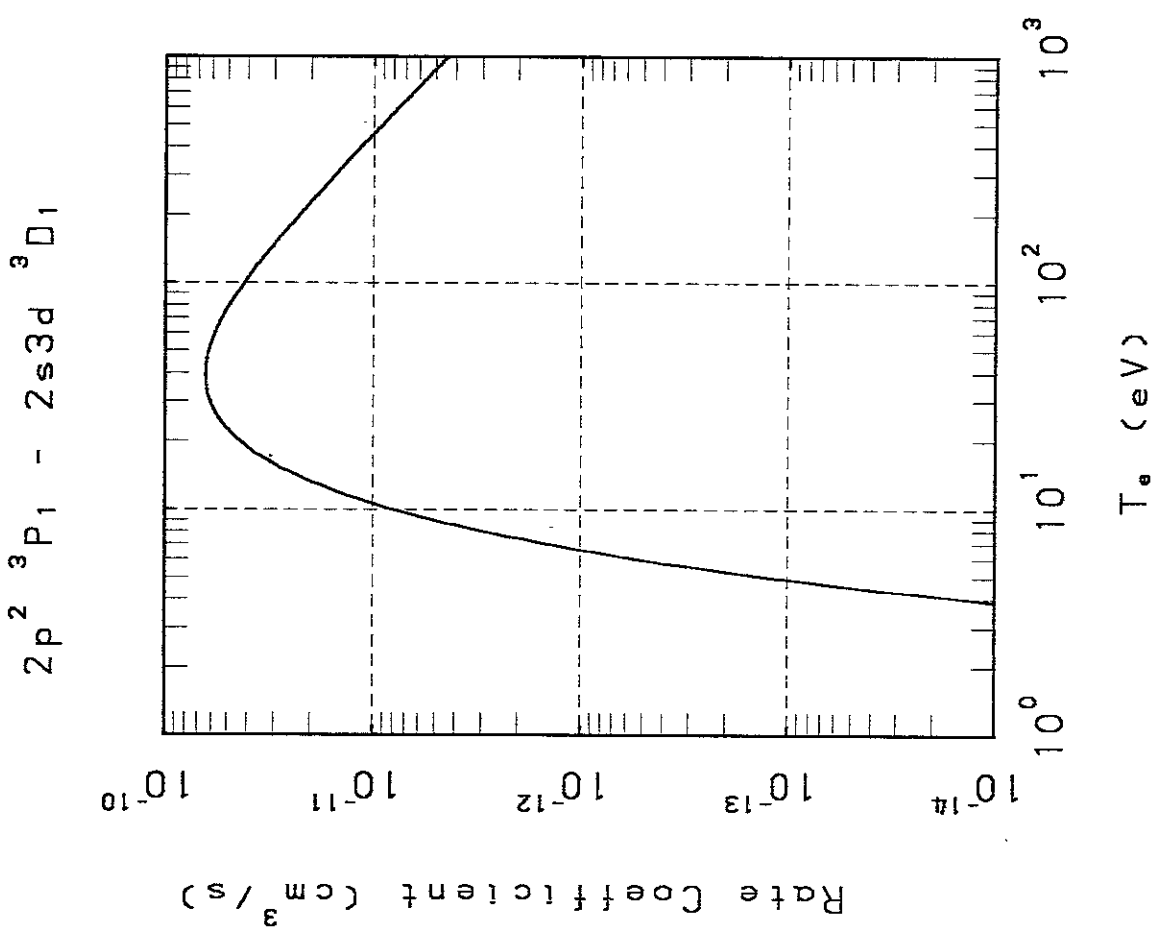
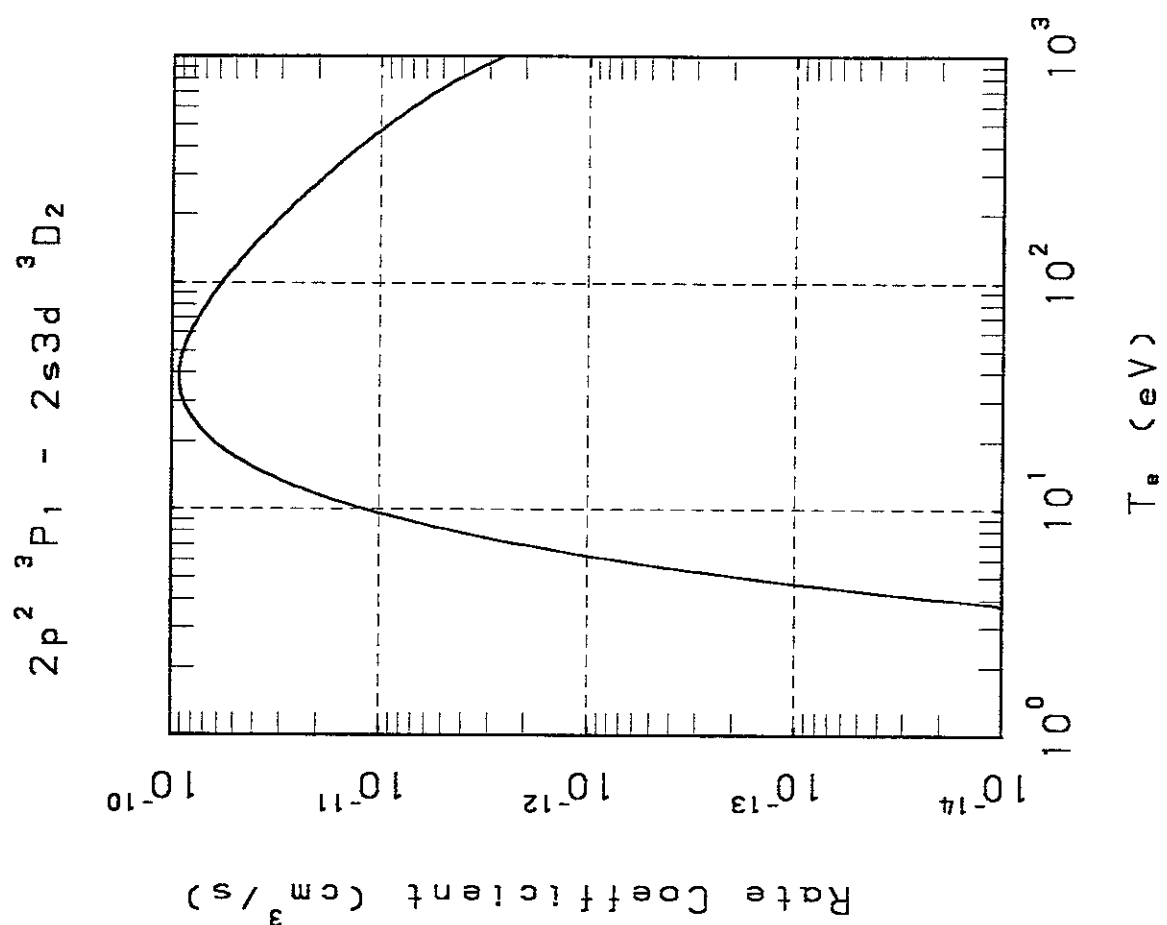


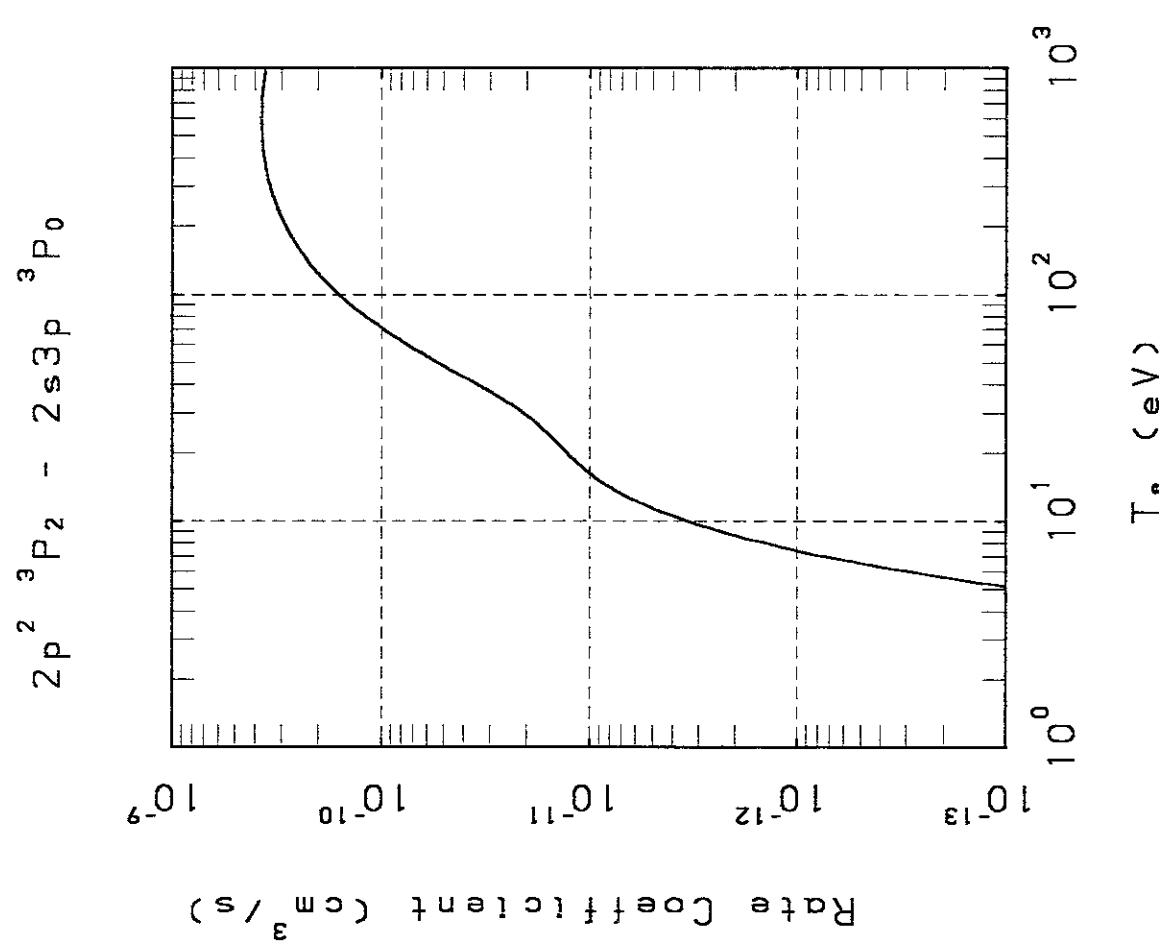
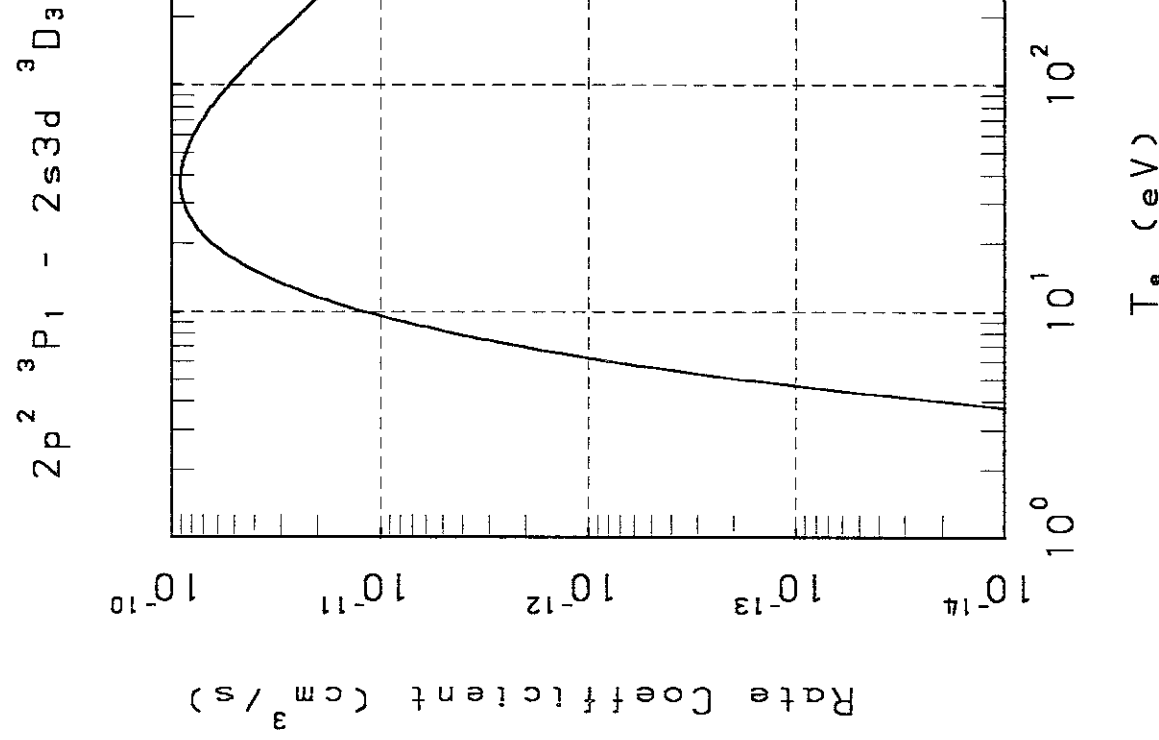


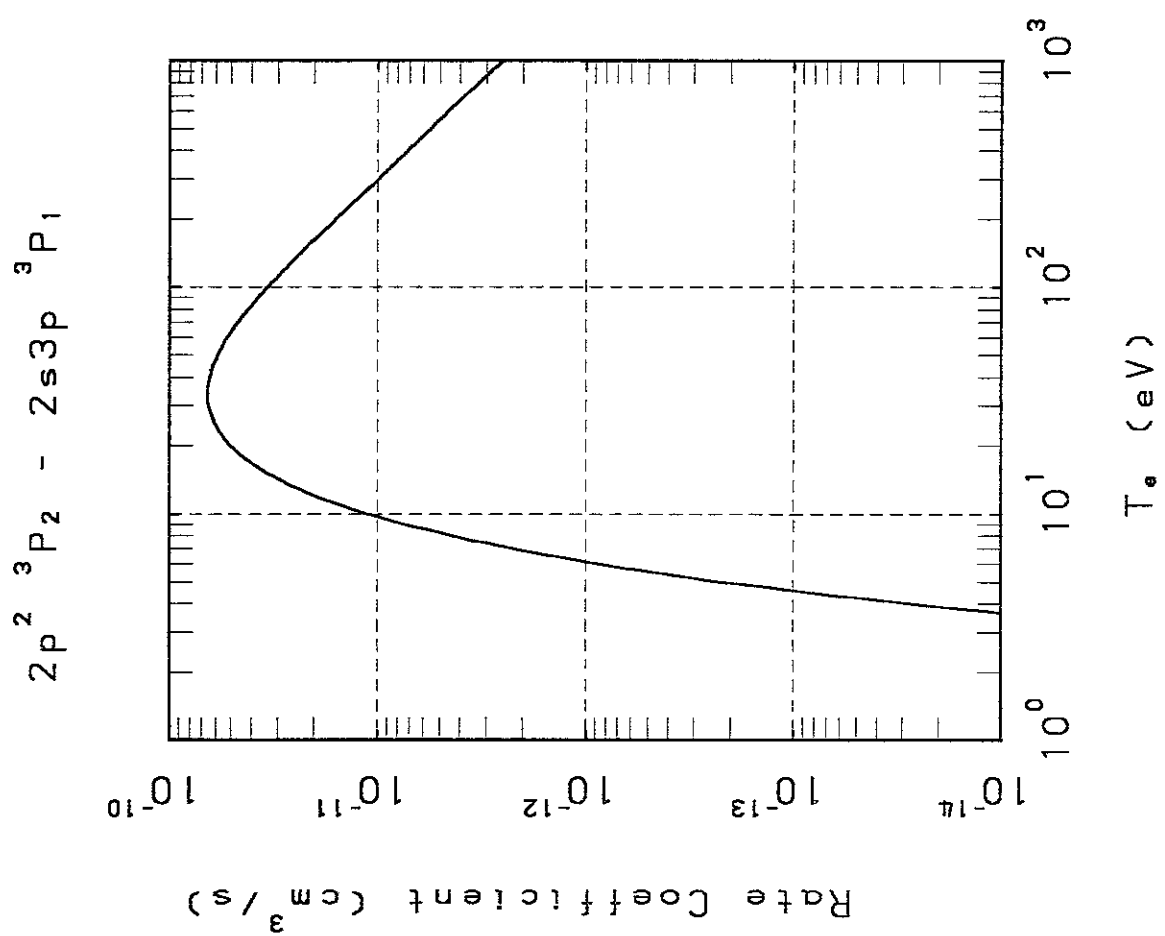
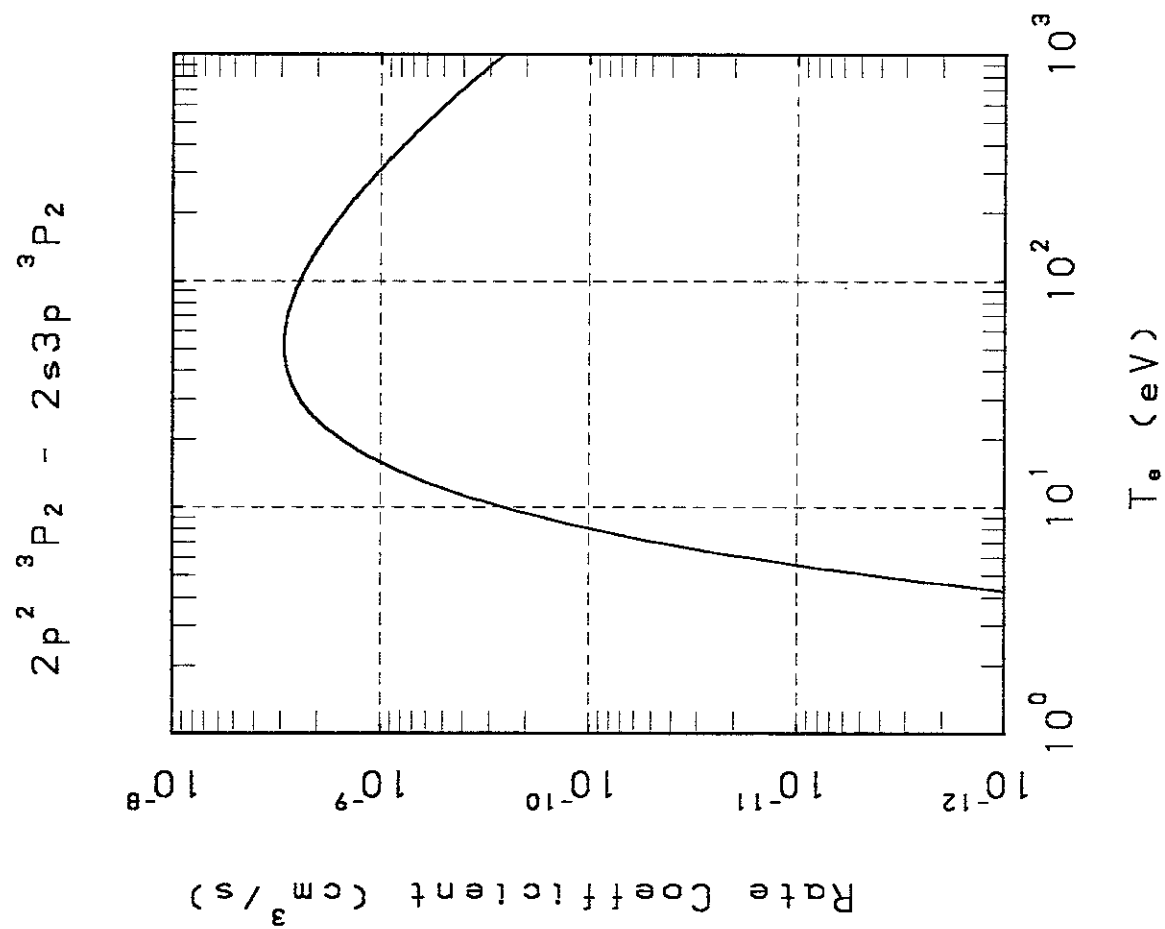


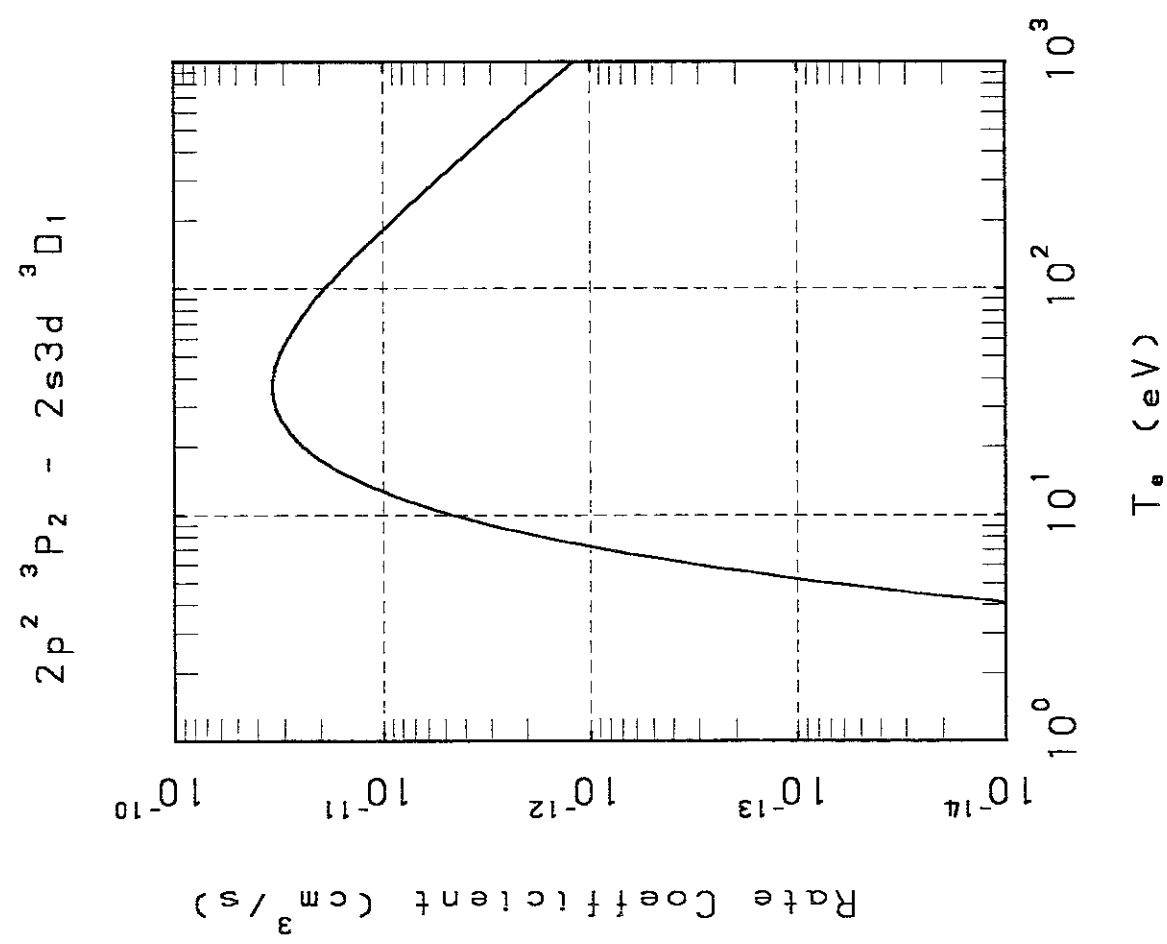
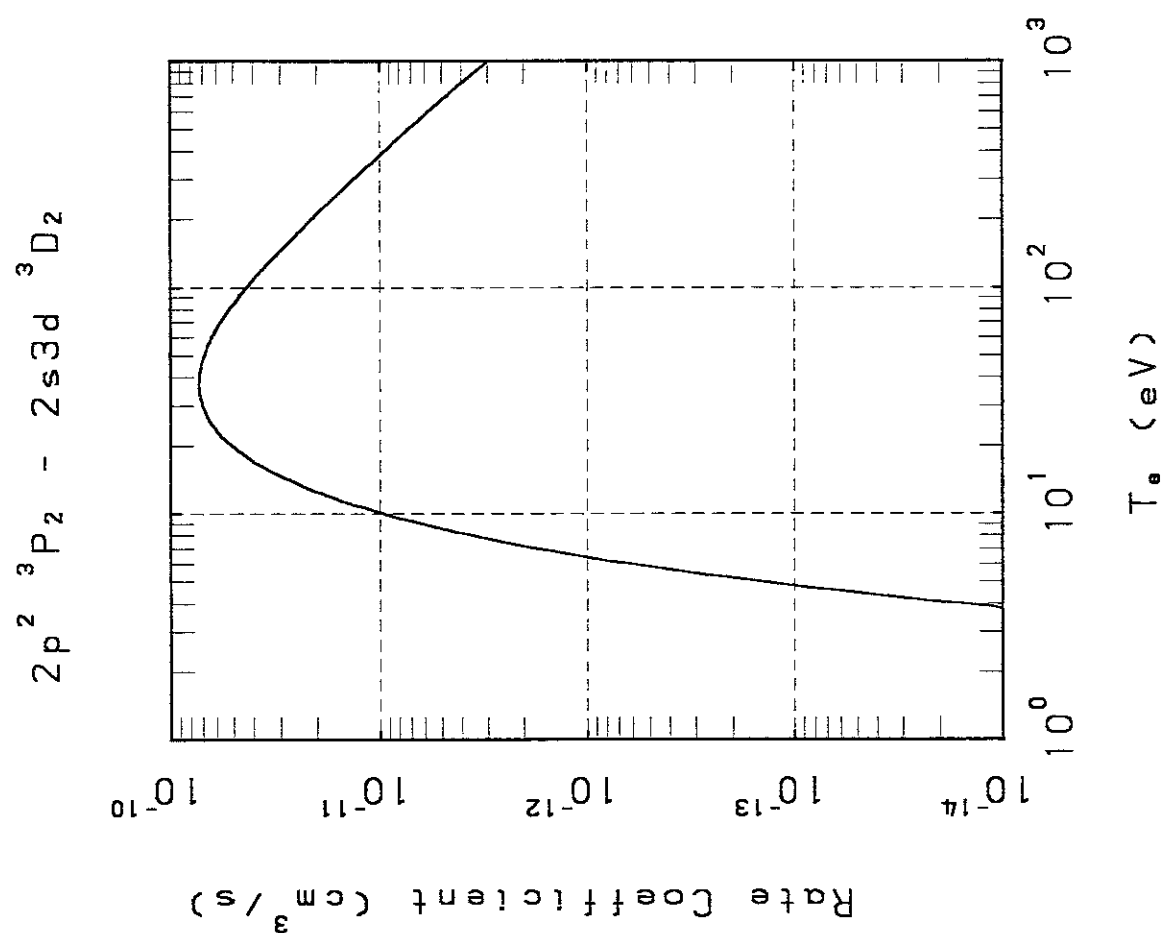


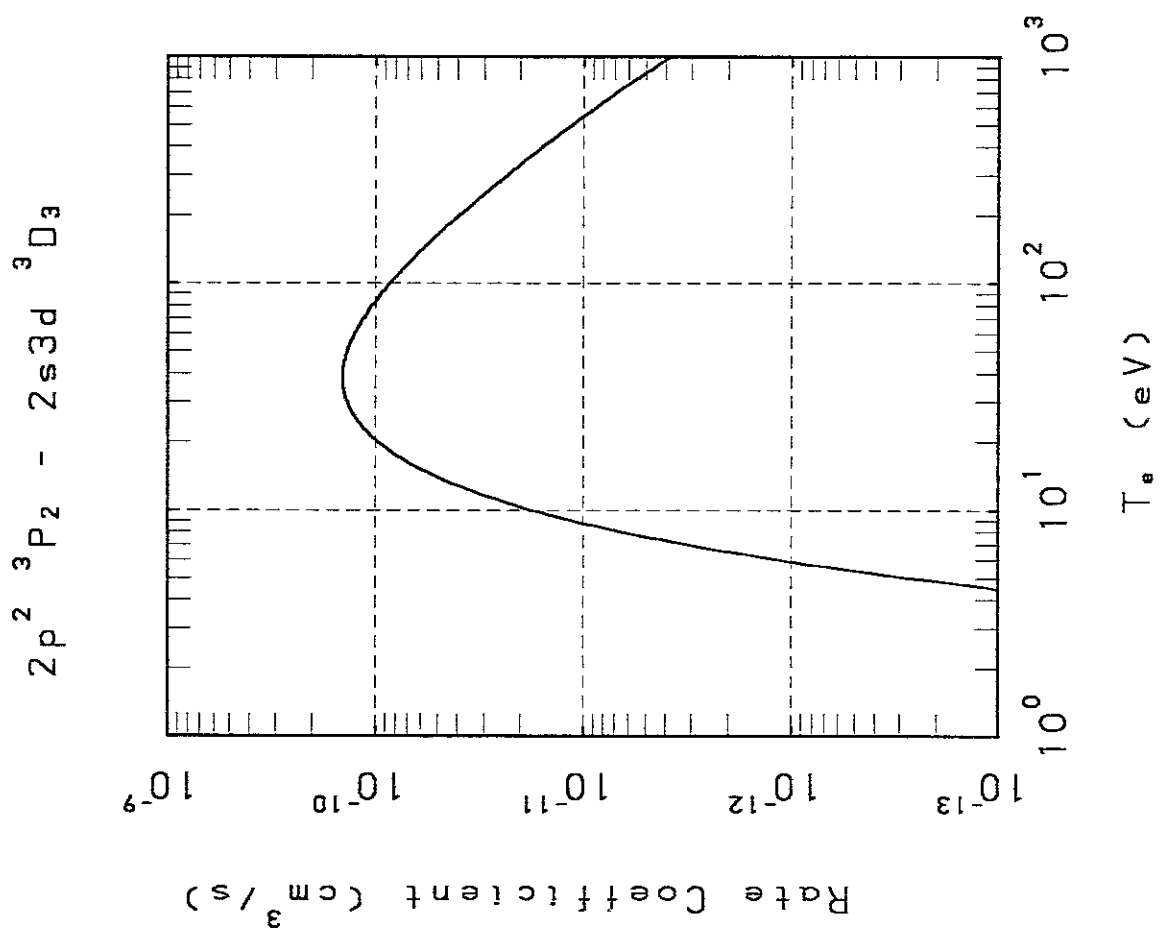
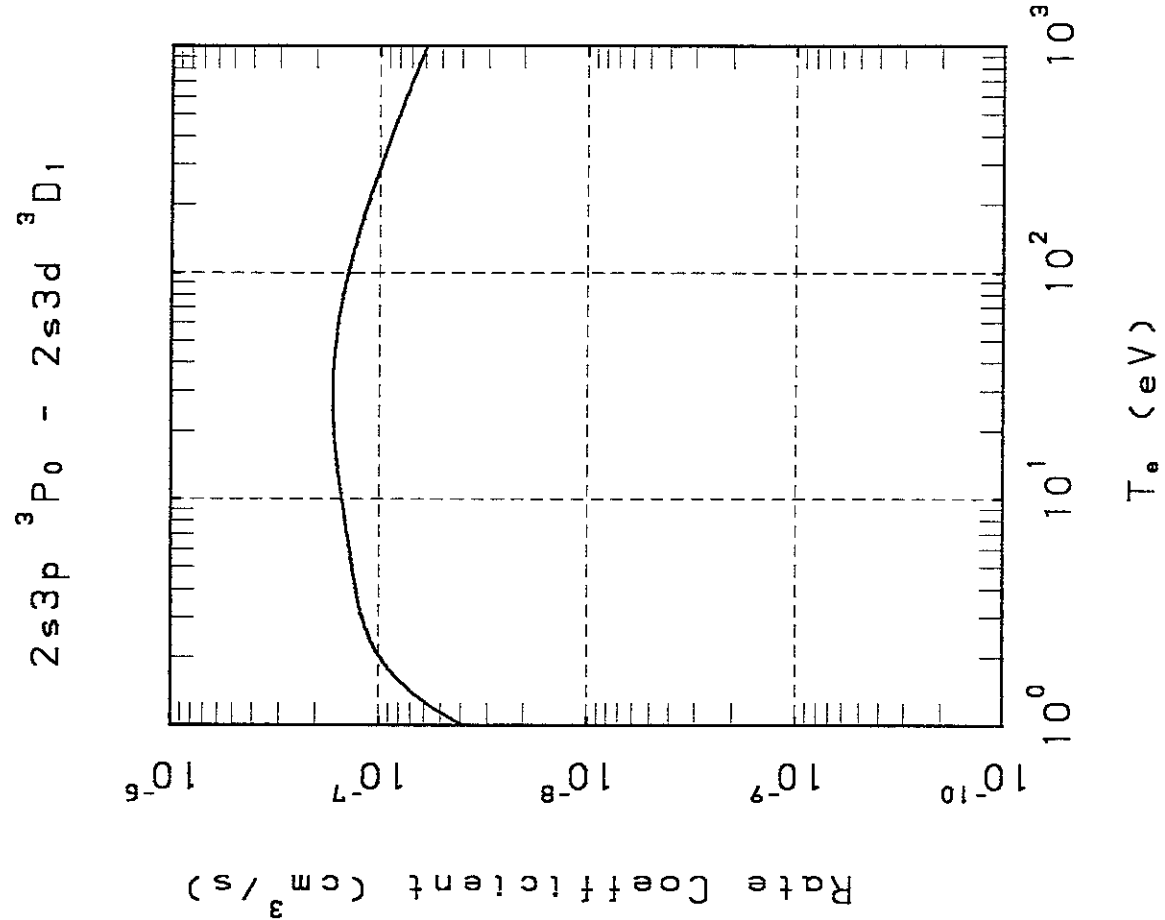




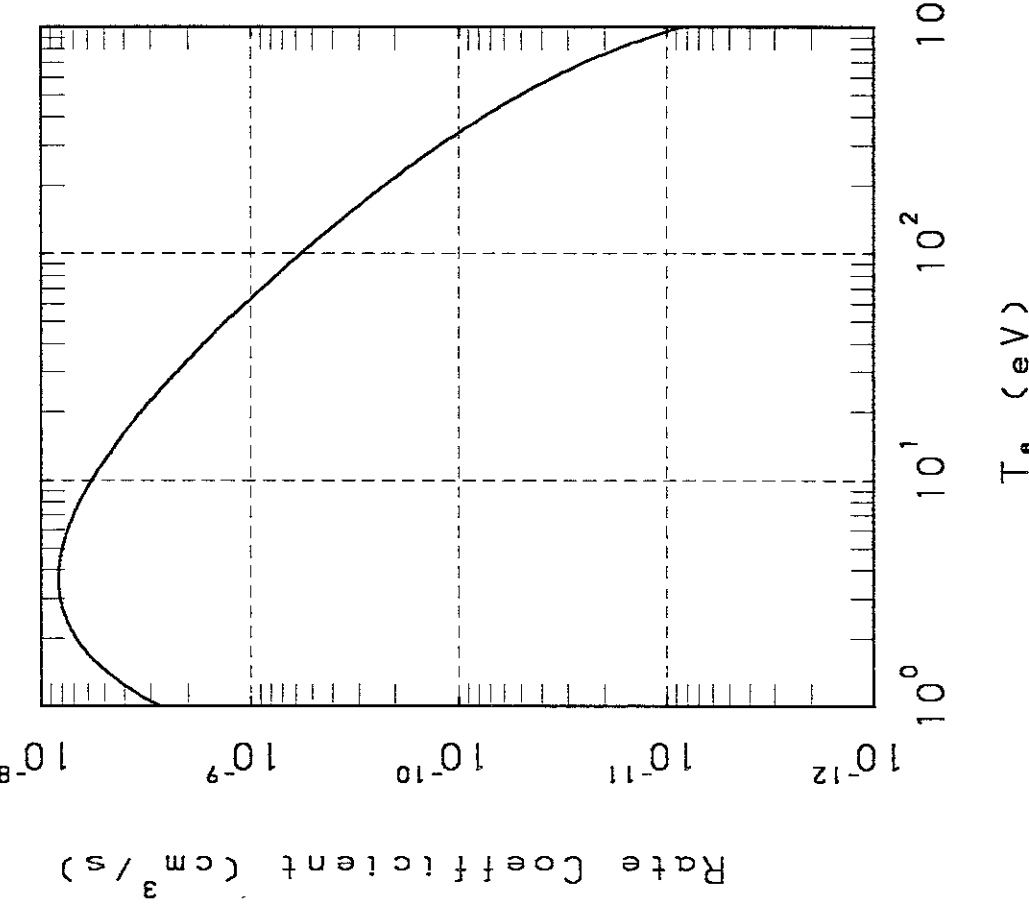




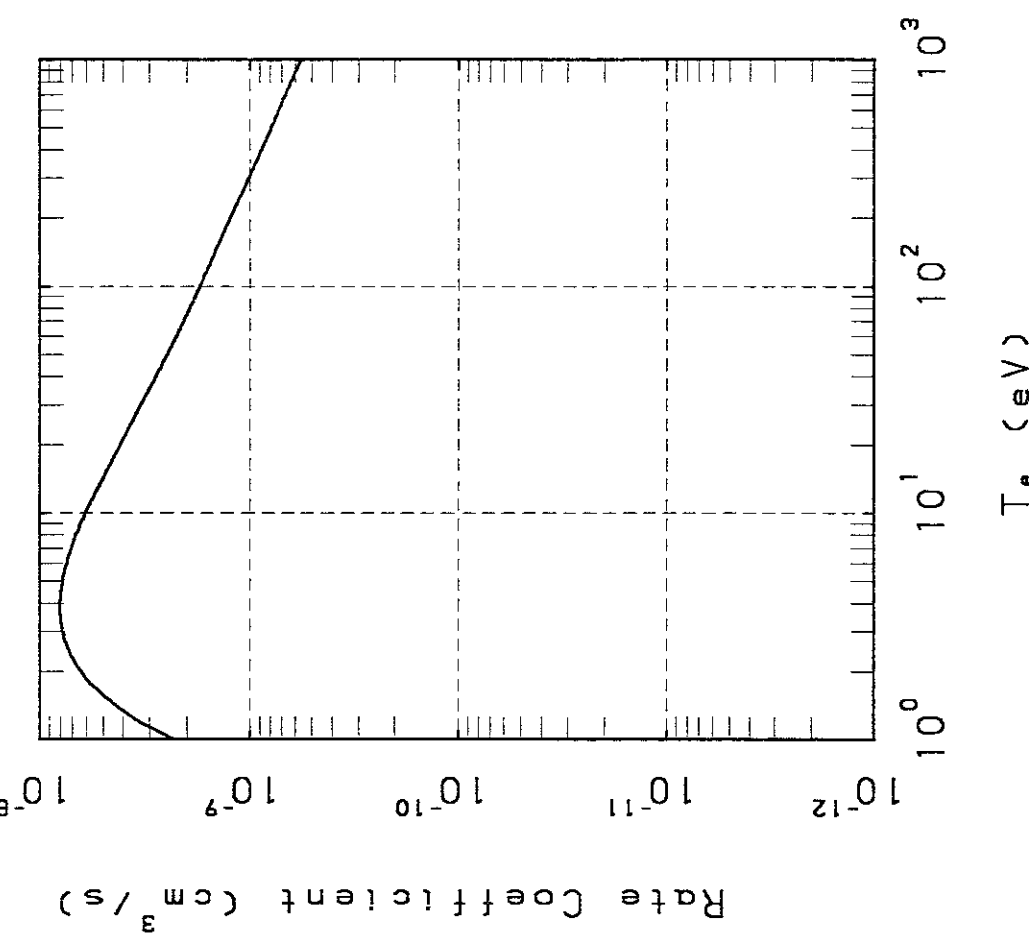




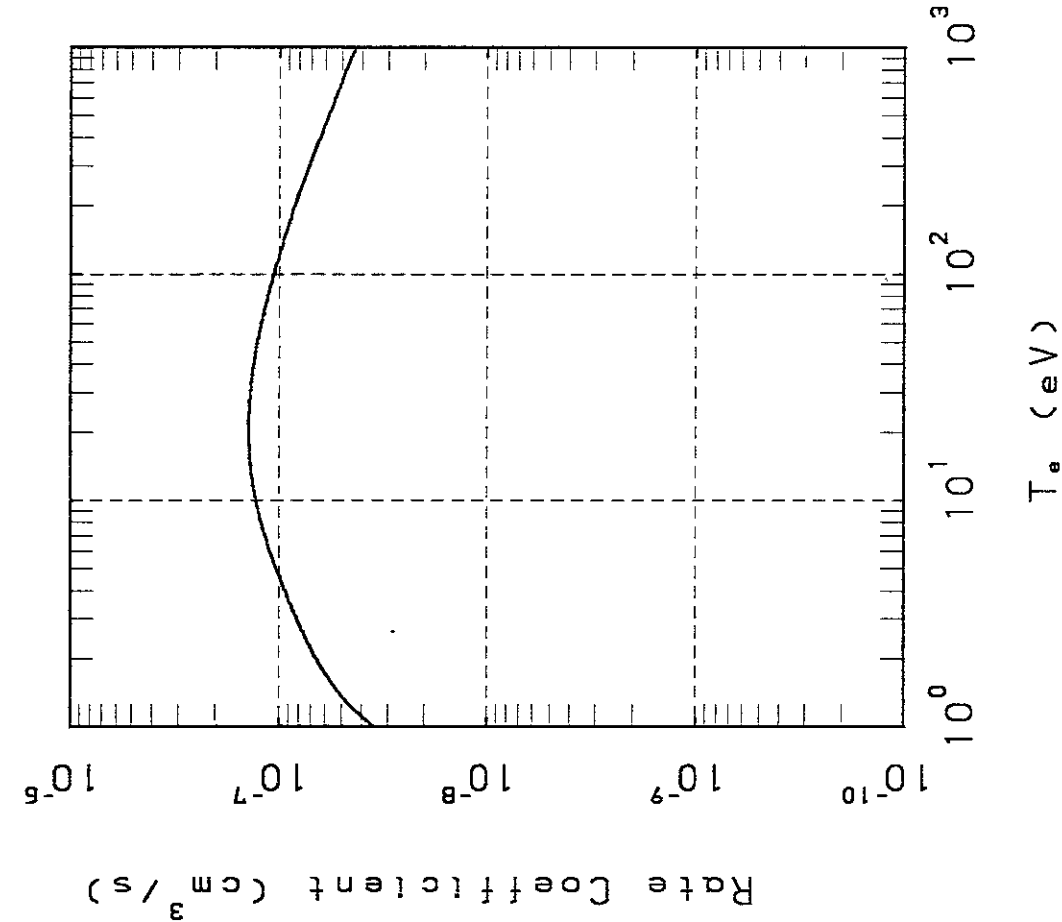
$2s3p\ ^3P_0 - 2s3d\ ^3D_2$



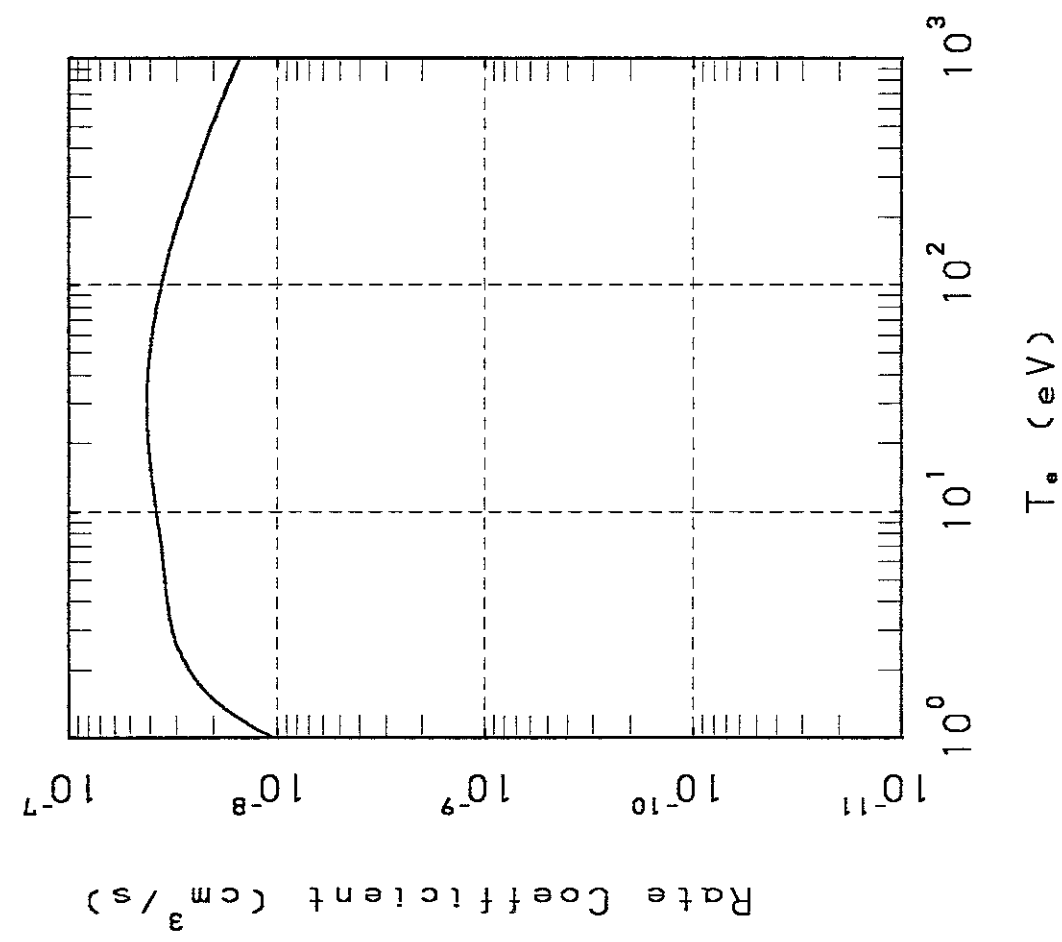
$2s3p\ ^3P_0 - 2s3d\ ^3D_3$



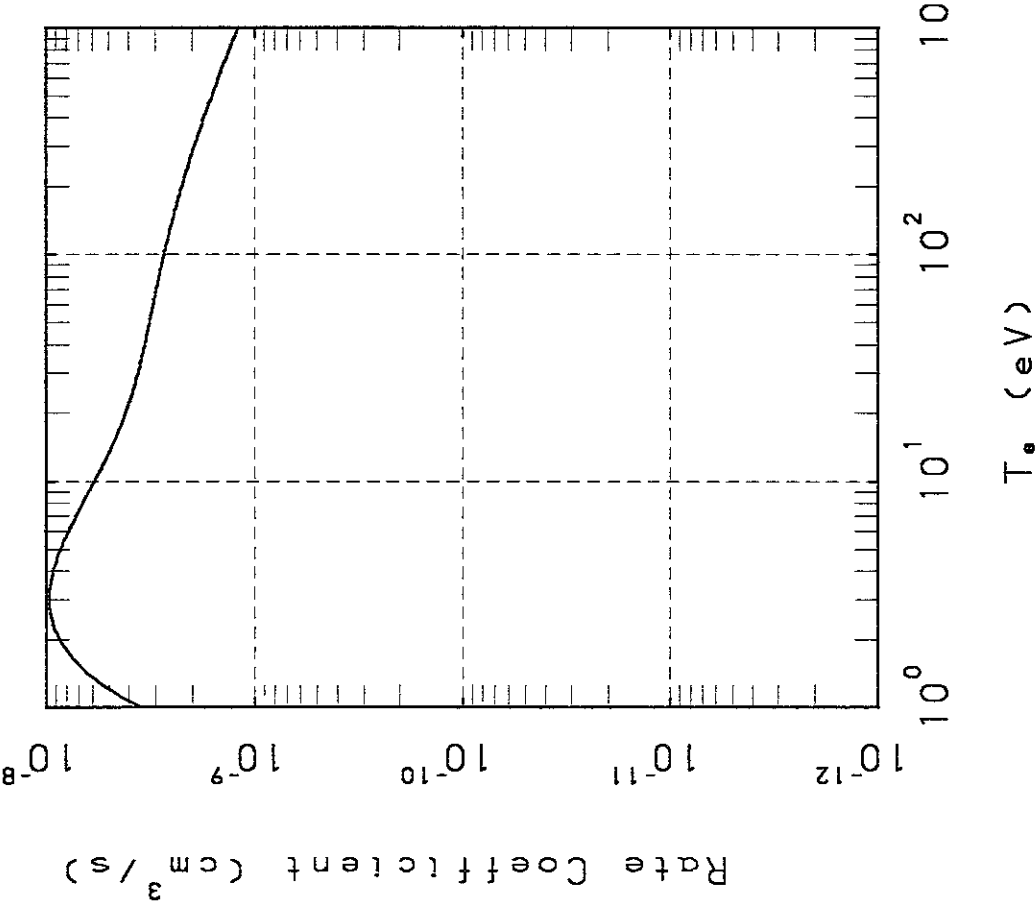
$2s3p\ ^3P_1 - 2s3d\ ^3D_2$



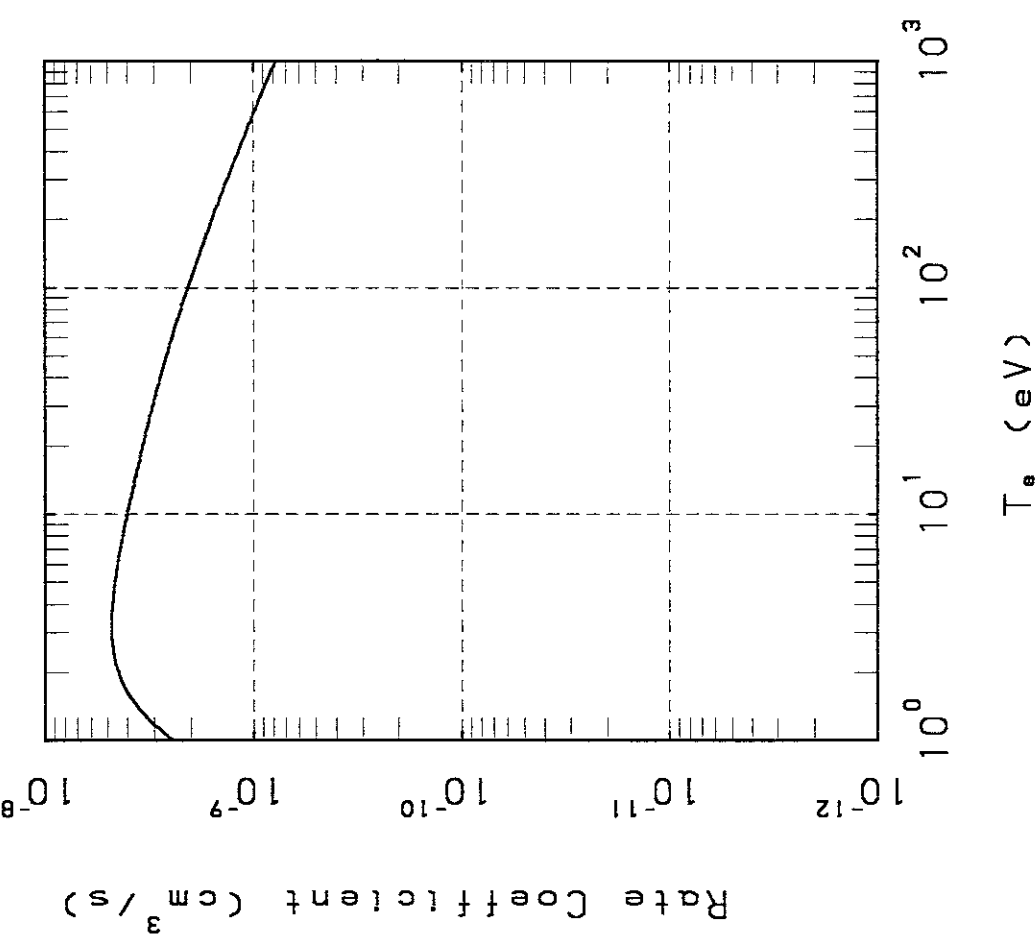
$2s3p\ ^3P_1 - 2s3d\ ^3D_1$

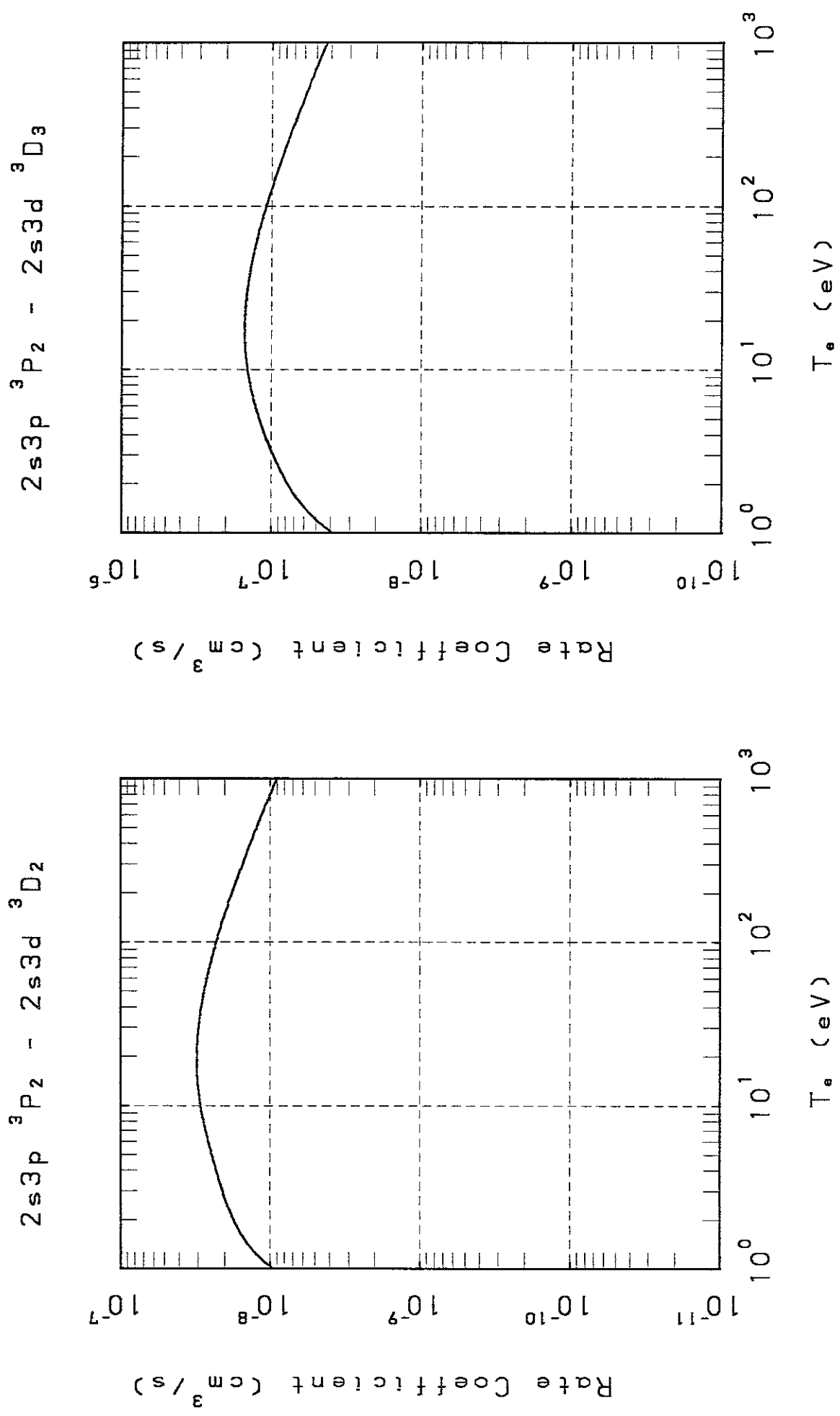


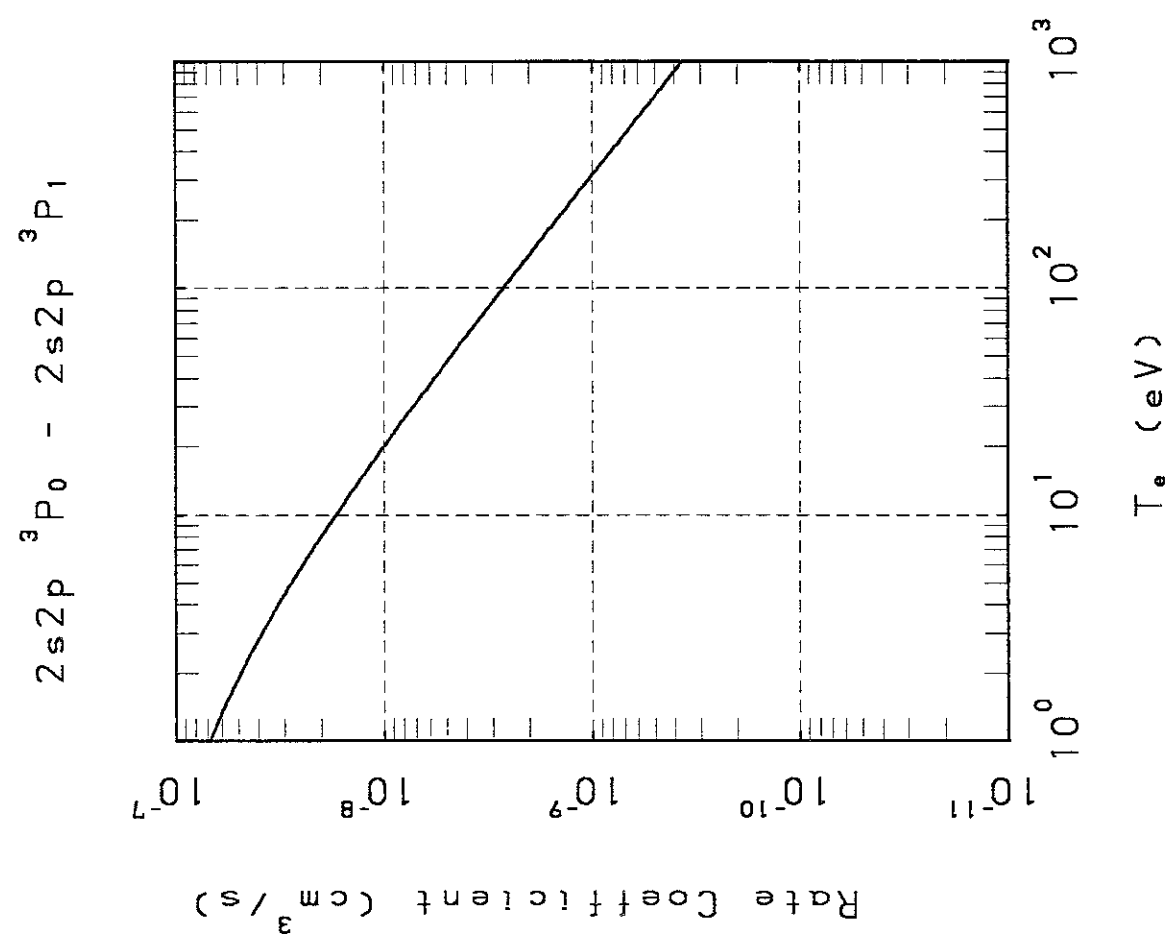
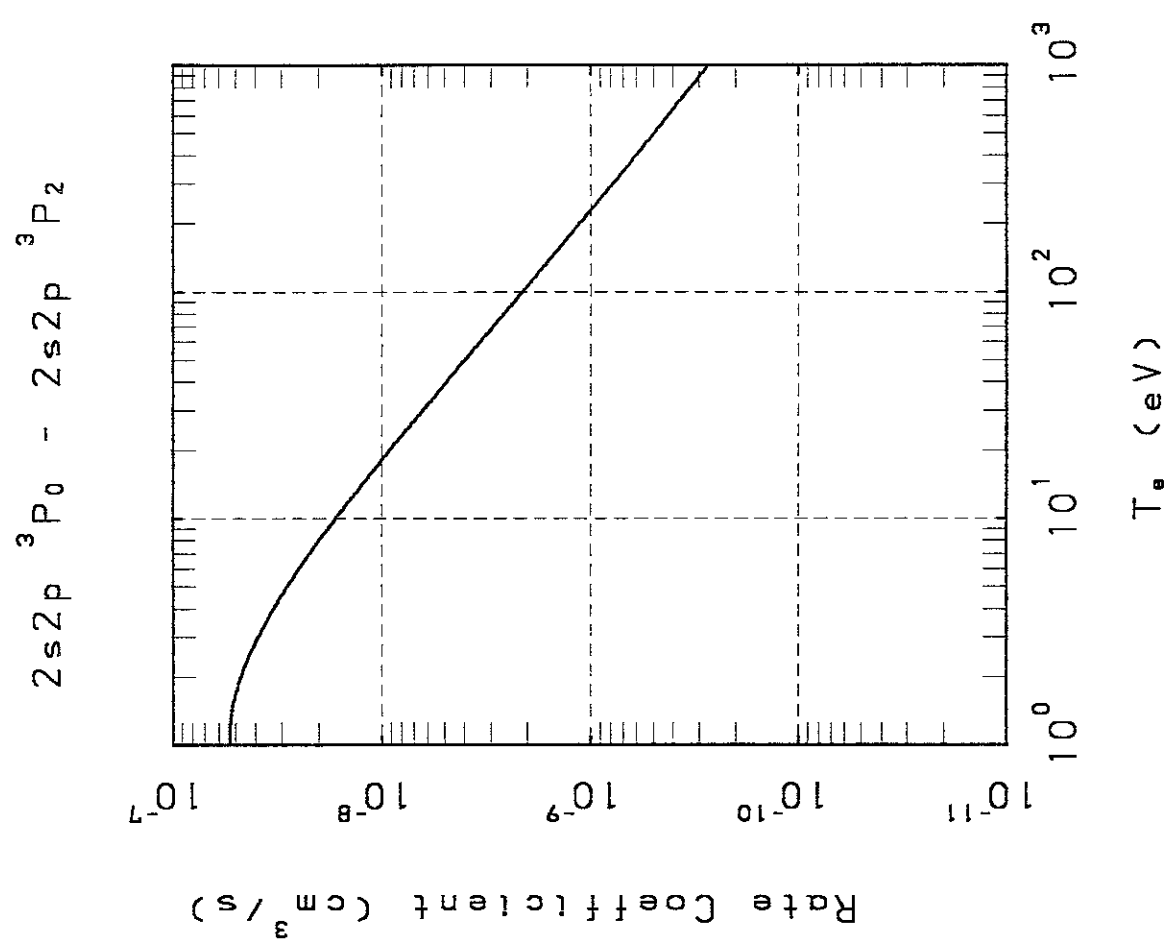
$2s3p\ ^3P_1 - 2s3d\ ^3D_3$

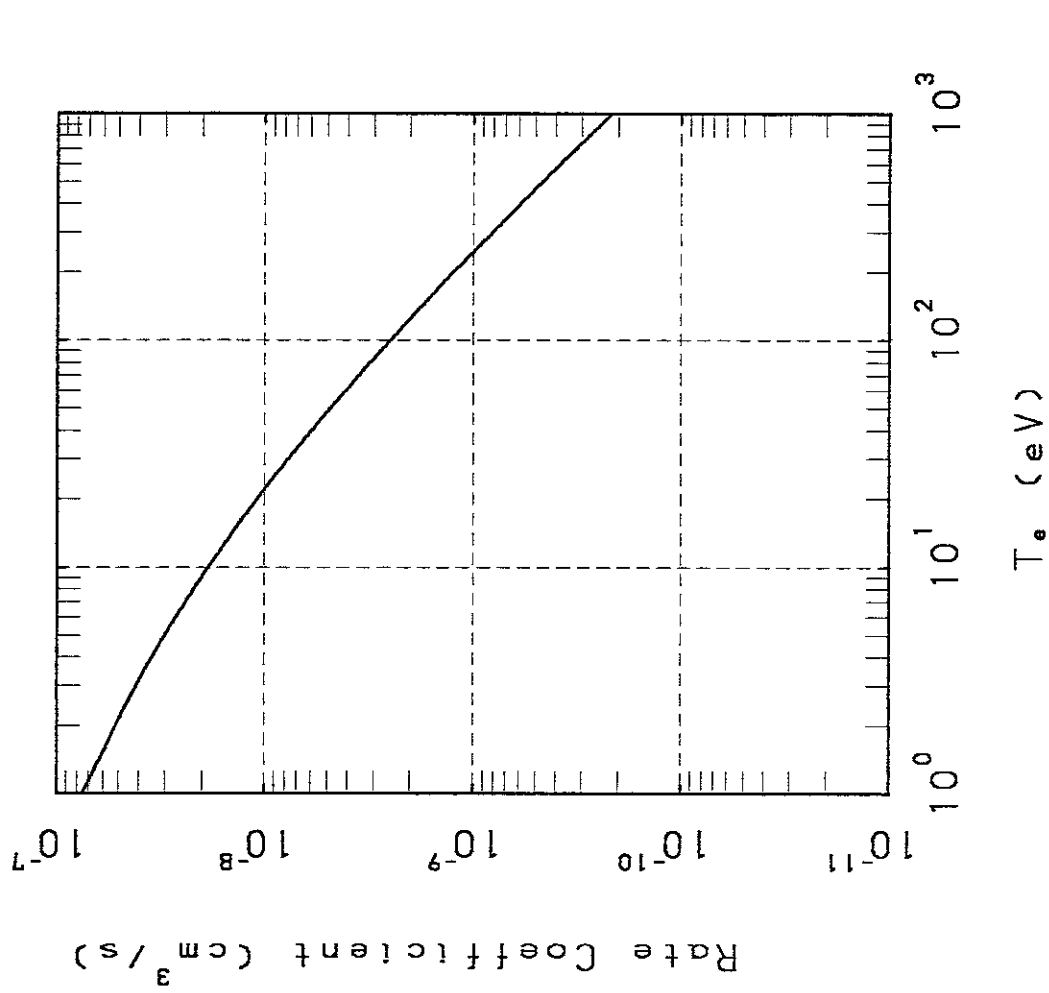
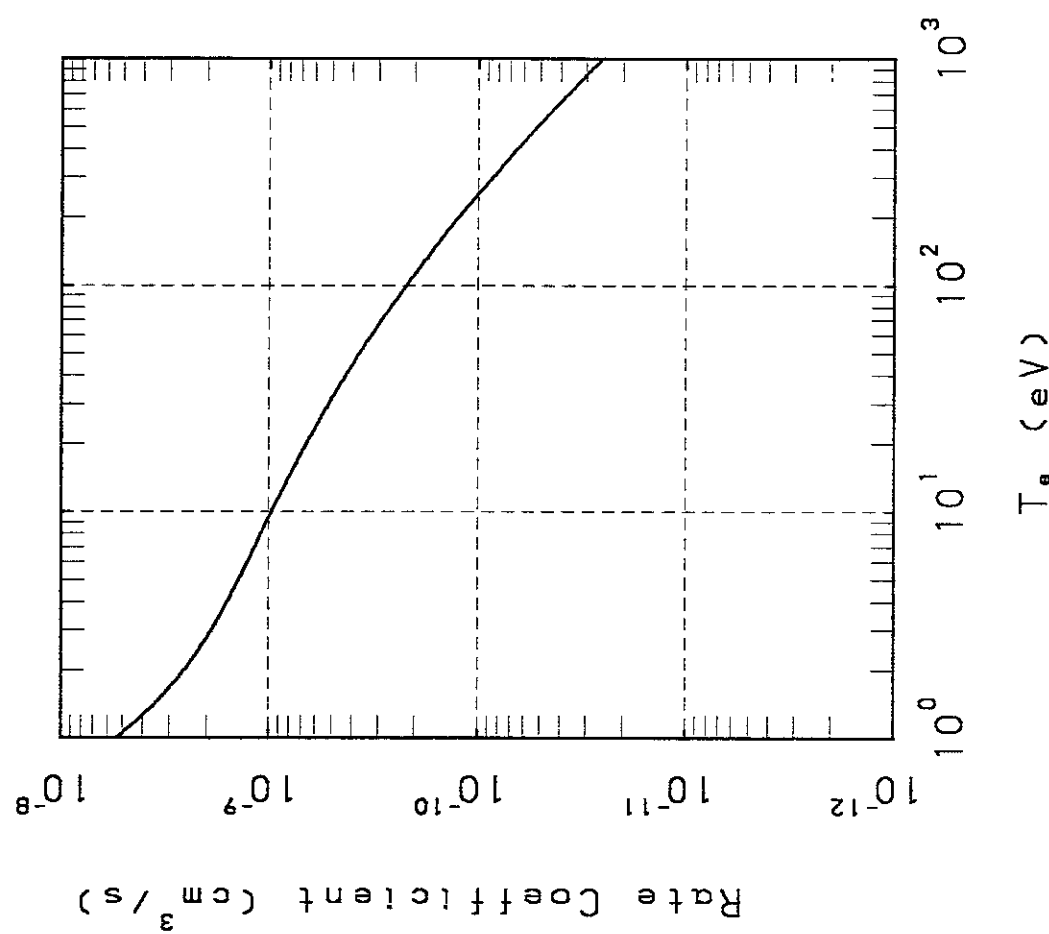


$2s3p\ ^3P_2 - 2s3d\ ^3D_1$

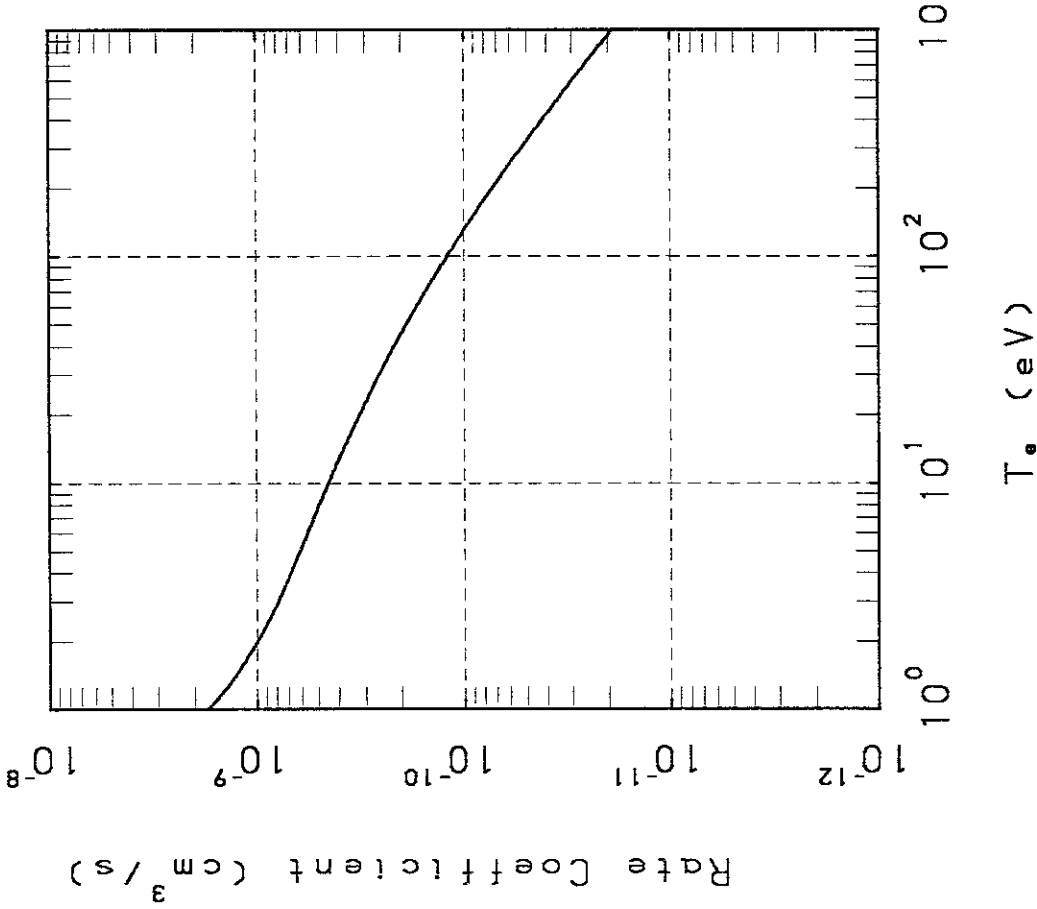






$2s2p\ ^3P_1 - 2s2p\ ^3P_2$  $2p^2\ ^3P_0 - 2p^2\ ^3P_1$ 

$2p^2\ 3P_0 - 2p^2\ 3P_2$



$2p^2\ 3P_1 - 2p^2\ 3P_2$

